



12-2015

## Is Quantitative Ultrasound a Valid Technique for Assessing Bone Quality in Deceased Infants?

Miriam Elizabeth Soto Martinez

*University of Tennessee - Knoxville*, [msoto@vols.utk.edu](mailto:msoto@vols.utk.edu)

Follow this and additional works at: [https://trace.tennessee.edu/utk\\_graddiss](https://trace.tennessee.edu/utk_graddiss)



Part of the [Biological and Physical Anthropology Commons](#)

---

### Recommended Citation

Soto Martinez, Miriam Elizabeth, "Is Quantitative Ultrasound a Valid Technique for Assessing Bone Quality in Deceased Infants?." PhD diss., University of Tennessee, 2015.

[https://trace.tennessee.edu/utk\\_graddiss/3555](https://trace.tennessee.edu/utk_graddiss/3555)

This Dissertation is brought to you for free and open access by the Graduate School at TRACE: Tennessee Research and Creative Exchange. It has been accepted for inclusion in Doctoral Dissertations by an authorized administrator of TRACE: Tennessee Research and Creative Exchange. For more information, please contact [trace@utk.edu](mailto:trace@utk.edu).

To the Graduate Council:

I am submitting herewith a dissertation written by Miriam Elizabeth Soto Martinez entitled "Is Quantitative Ultrasound a Valid Technique for Assessing Bone Quality in Deceased Infants?." I have examined the final electronic copy of this dissertation for form and content and recommend that it be accepted in partial fulfillment of the requirements for the degree of Doctor of Philosophy, with a major in Anthropology.

Amy Z. Mundorff, Major Professor

We have read this dissertation and recommend its acceptance:

Benjamin Auerbach, Kate Spradley, Darinka Mileusnic, Jennifer C. Love

Accepted for the Council:

Carolyn R. Hodges

Vice Provost and Dean of the Graduate School

(Original signatures are on file with official student records.)

# **Is Quantitative Ultrasound a Valid Technique for Assessing Bone Quality in Deceased Infants?**

**A Dissertation Presented for the  
Doctor of Philosophy  
Degree  
The University of Tennessee, Knoxville**

**Miriam Elizabeth Soto Martinez  
December 2015**

**Copyright © by Miriam E. Soto Martinez**  
**All rights reserved**

## **DEDICATION**

This dissertation is dedicated to my parents, Rita and Natividad Soto Jr, and my husband, Manuel Martinez. Your love, support, and encouragement gave me the strength to persevere during this arduous journey.

## ACKNOWLEDGEMENTS

There are a number of people I would like to acknowledge not only for their contributions to this research, but also for their guidance and help during my time as a graduate student. First, I would like to thank Dr. Jennifer C. Love. Dr. Love entrusted me with her project and allowed me to use the study as my dissertation research. As well as supervising this study, Dr. Love provided and continues to provide cherished guidance and advice. I would also like to thank my major professor, Dr. Amy Z. Mundorff. Dr. Mundorff provided me with advice and knowledge which enabled me to successfully complete my doctoral education and pursue my career goals. I would like to thank Dr. Kate M. Spradley for her support of this research and her highly valued input. Throughout my time as a graduate student, Dr. Spradley encouraged and supported my research interests. I consider these three women as my mentors, whose advice and guidance I will continue to seek in the future. I would also like to acknowledge my committee members Dr. Ben Auerbach and Dr. Darinka Mileusnic. Dr. Auerbach's expertise in biomechanics and statistics were a valuable contribution to this research. As a medical examiner, Dr. Mileusnic provided valuable insights into the applicability of this research for the medicolegal community.

This research would not have been possible without the assistance of Dr. Debra Kearney and Dr. John Hipp. Dr. Debra Kearney is a pathologist at Texas Children's Hospital. Dr. Kearney allowed me to collect data at Texas Children's Hospital. Dr. Hipp designed the custom program that calculated BMD estimates from x-ray attenuation values. Dr. Hipp's clear explanations of the program and underlying calculations were invaluable. Additionally, the funding provided by the Texas Center for the Judiciary- Children's Justice Act was vital for this research. This project would not have been realized without funding from the CJA.

I would like to acknowledge the contributions of my colleagues Dr. Deborrah C. Pinto and Dr. Christian M. Crowder. Dr. Pinto provided valuable input throughout this study and during the writing process. Over the past year, I have benefitted from Dr. Crowder's expertise in bone biology. Discussions with Dr. Crowder regarding the results of this study were extremely helpful in the interpretation of results.

Finally, I want to acknowledge the contributions of my and family. I want to thank my parents for being supportive throughout my time as a graduate student and never doubting my

capabilities. I want to thank my husband, Manuel Martinez. You held my hand from the beginning and you never let go. You have been my source of strength more times than I can count. Lastly, but definitely not least, I would like to thank my friends/colleagues, Angela Dautartas and Shauna McNulty. I acknowledge you with my family because that is exactly what I consider you both. Getting through this marathon would not have been possible without your day to day support and friendship. I hope you know how much I appreciate and value both of you.

## ABSTRACT

There is no quantitative method for evaluating infant bone quality that is non-invasive, portable, brief in scan duration, and does not use ionizing radiation. This study investigates the relationship between components of infant bone quality and a measure of quantitative ultrasound (QUS), speed of sound (SOS), to provide insight into the validity of QUS as a diagnostic tool for evaluating infant bone quality. The study sample was comprised of 78 infants between the age of 30 weeks estimated gestational age and 12 postnatal months receiving an autopsy at the Harris County Institute of Forensic Sciences and Texas Children's Hospital. Bone SOS measurements, costochondral rib and iliac crest samples, and radiographs of the forearm and leg were prospectively collected over a 9-month period. Demographic information, medical history, autopsy findings, and investigator reports were collected and used to identify chronic illness. Qualitative radiographic evaluation, bone mineral density (BMD), and tibial measurements were obtained from radiographs.

Results indicated that SOS measures aspects of bone quality related to bone macrostructure. Prematurity and chronic illness were significantly associated in the current study sample and their detrimental effects could not be separated. Prematurity and, possibly, chronic illness significantly influenced SOS through their adverse effects on growth and bone health. BMD was not significantly associated with tibial or body size measurements, but this may have been due to the small area of bone used to estimate BMD. Although SOS and BMD were not significantly correlated, both showed a postnatal decline and subsequent increase at greater ages. Chronically ill infants had significantly lower BMD and greater qualitative radiographic evaluation scores than infants without chronic illness.

Assessing bone quality is complex due to the multitude of factors which compose it. QUS remains a highly promising technology for evaluating infant bone quality, but it cannot be definitively concluded that QUS is a valid technique for evaluating infant bone quality based on this research alone. Research comparing SOS to finer-grained measurements of aspects of bone quality are necessary before the validity of QUS as a diagnostic tool for evaluating infant bone quality and strength can be determined.



# TABLE OF CONTENTS

<b>Chapter 1 : Introduction .....</b>	<b>1</b>
<b>Chapter 2 : Literature Review.....</b>	<b>8</b>
Introduction.....	8
Bone Biology .....	9
Nutrition and other Prenatal Factors Affecting Skeletal Development .....	36
Mineral Homeostasis .....	39
Disease and Bone.....	48
Basic Bone Biomechanics.....	64
Bone Histology .....	69
Imaging Methods for Assessing Bone Quality .....	73
Summary.....	84
<b>Chapter 3 : Materials and Methods .....</b>	<b>85</b>
Infant Injury Database.....	85
Study Sample .....	88
Methods.....	89
Summary.....	106
<b>Chapter 4 : Results.....</b>	<b>108</b>
Introduction.....	108
Descriptive Analyses .....	109
Association between Growth-Related Changes in Size and Age-Related Changes in SOS and BMD .....	153
Association between Traumatic Injury, Health, and Bone Health.....	181
Association between Chronic Illness, Growth, and Bone Health.....	183
Association between Skeletal Maturity at Birth, Body Size, Tibial Structure, and Bone Health .....	185

Relationships between Measures of Bone Quality .....	194
Summary .....	196
<b>Chapter 5 : Discussion .....</b>	<b>199</b>
Introduction.....	199
Association between Growth-Related Changes in Size and Age-Related Changes in SOS and BMD .....	199
Association between Traumatic Injury, Health, and Bone Health.....	212
Association between Chronic Illness, Growth, and Bone Health.....	213
Association between Skeletal Maturity at Birth, Body Size, Tibial Structure, and Bone Health .....	220
Relationships between Measures of Bone Quality .....	227
Limitations .....	231
<b>Chapter 6 : Conclusions and Recommendations .....</b>	<b>235</b>
<b>References .....</b>	<b>243</b>
<b>Appendices.....</b>	<b>273</b>
<b>Vita .....</b>	<b>311</b>

## LIST OF TABLES

Table 4-1. The demographic breakdown of the study sample by race, sex, median chronological age, and term-corrected chronological age. ....	110
Table 4-2. Age (months) frequencies by chronological age and term-corrected age. ....	110
Table 4-3. Description of infants with chronic illness. ....	113
Table 4-4. Frequency of study sample cases by Manner of Death classification. ....	118
Table 4-5. Frequency of study sample cases by Cause of Death category. ....	119
Table 4-6. Frequency of study sample cases by presence/absence of traumatic injury. ....	120
Table 4-7. Models summaries for regression analyses predicting tibial measurements from age. Tibial length is the dependent variable in model 1. Tibial midshaft diameter is the dependent variable in Model 2. Medullary cavity diameter is the dependent variable in Model 3. Cortical thickness is the dependent variable in Model 4. Cortical Index is the dependent variable of Model 5. ....	122
Table 4-8. Results of regression analyses of cross-sectional measurements and age, with chronically ill infants excluded. Tibial length is the dependent variable in model 1. Tibial midshaft diameter is the dependent variable in model 2. Medullary cavity diameter is the dependent variable in model 3. Cortical thickness is the dependent variable in Model 4. Cortical Index is the dependent variable of Model 5. ....	131
Table 4-9. Results of regression analyses of cross-sectional measurements and age, with premature infants excluded. Tibial length is the dependent variable in Model 1. Tibial midshaft diameter is the dependent variable in Model 2. Medullary cavity diameter is the dependent variable in Model 3. Cortical thickness is the dependent variable in Model 4. Cortical Index is the dependent variable of Model 5. ....	132
Table 4-10. Model summary for two-way ANOVA predicting cortical thickness using sex, age, and sex*age. ....	141
Table 4-11. <i>LSD</i> post hoc comparisons between racial groups with tibial midshaft diameter as the dependent variable and chronically ill infants excluded from analyses. ....	147
Table 4-12. <i>LSD</i> post hoc comparisons between racial groups with sex as the dependent variable (Males = 1) and chronically ill infants excluded from analyses. ....	147
Table 4-13. <i>LSD</i> post hoc comparisons between racial groups with BMD as the dependent variable. ....	152
Table 4-14. Results of regression analyses with SOS as the dependent variable. Model 1 predicts mean SOS using the age variables. Model 2 predicts mean SOS from the age variables with premature infants excluded from the analysis. ....	159
Table 4-15. <i>LSD</i> post hoc comparisons of SOS group means by age in months. ....	162
Table 4-16. <i>LSD</i> post hoc comparisons of SOS group means by age in months with premature infants excluded. ....	168
Table 4-17. Model summary for regression analysis of premature infant data with SOS as the dependent variable and using age as the predictor variable. ....	171
Table 4-18. Model summaries of regression analyses with SOS as the dependent variable. ....	173
Table 4-19. Model summaries for regression analyses with SOS as the dependent variable and chronically ill infants excluded from analyses. ....	175
Table 4-20. Model summary of regression analysis predicting BMD using cortical index. ....	177
Table 4-21. Model summaries of regression analyses with SOS as the dependent variable, age as a covariate, and tibial measurements as independent variables. ....	178

Table 4-22. Model summaries for regression analyses with SOS as the dependent variable and premature infants excluded from analyses.....	179
Table 4-23. Summary of multiple regression results with SOS as the dependent variable.....	180
Table 4-24. Summary of multiple regression results with SOS as the dependent variable and chronically ill infants excluded from the analysis. ....	181
Table 4-25. Summary of multiple regression results with SOS as the dependent variable and premature infants excluded from the analysis. ....	182
Table 4-26. Model summaries of regression analyses with age as a covariate and chronic illness as the predictor variable. Tibial length is the dependent variable in model 1. Tibial midshaft diameter is the dependent variable in model 2. Cortical thickness is the dependent variable in Model 3. ....	185
Table 4-27. Model summaries of regression analyses with age as a covariate and prematurity as the predictor variable. Tibial length is the dependent variable in Model 1. Tibial midshaft diameter is the dependent variable in Model 2. Medullary cavity diameter is the dependent variable in Model 3. Cortical thickness is the dependent variable in Model 4. ....	191
Table 4-28. Results of simple linear regression analysis with BMD as the dependent variable and birthweight as the predictor. ....	191
Table 4-29. Model summaries of regression analyses using the age variables as covariates and birthweight (Model 1), and EGA (Model 2) to predict SOS. ....	193
Table 4-30. Model summaries of regression analyses using the age variables as covariates and birthweight (Model 1), and EGA (Model 2) to predict SOS, excluding chronically ill infants.....	194
Table 5-1. Illustration of the age-related changes in tibial measurements and SOS during the first year of life. ....	201
Table A- 1. Demographic and autopsy findings of each infant in the study sample. ....	285
Table A- 2. Chronic illness and autopsy classifications .....	288
Table A- 3. Description of infants with traumatic injuries. ....	293
Table A- 4. Qualitative Radiographic Evaluation Results.....	293
Table A- 5. Description of infants with abnormally mineralized bone on radiographs. ....	294
Table A- 6. Descriptive statistics of bone measurements, BMD, and SOS data. ....	295
Table A- 7. Data associated with chronically ill infants. ....	295
Table A- 8. Results of Qualitative Radiographic Evaluation for each infant. ....	296
Table A- 9. Results of Qualitative Histological Evaluation of the costochondral rib section for each infant. ....	299
Table A- 10. Results of Qualitative Histological Evaluation of the iliac crest section for each infant. ....	303
Table A- 11. Body size, growth percentiles, and tibia measurements for each infant.....	306
Table A- 12. SOS and BMD measurements for each infants. ....	309

## LIST OF FIGURES

Figure 3-1. Setup for obtaining radiographs. ....	90
Figure 3-2. Radiograph of right forearm in anatomic position with spherical density phantoms alongside. ....	91
Figure 3-3. Radiograph of left leg with spherical density phantoms alongside.....	91
Figure 3-4. a. Plot of image intensity values by spatial coordinates of the pixels in the image. Note that the plot of image intensity values has two peaks. Each peak corresponds to image intensity values obtained from the medial and lateral cortical walls. The valley between the two peaks represents image intensity values obtained from the medullary cavity. b. Radiograph of leg with green highlighted area representing the location where image intensity values were obtained for the plot (a).....	94
Figure 3-5. Setting the scale in ImageJ. Plot profile of the image intensity values is shown at the bottom of the figure. Red arrows on the plot profile indicate half-maximum intensity points along plot profile line.....	95
Figure 3-6. Obtaining cross-sectional measurements of the tibia in ImageJ. Measurement results of the tibial length, midshaft diameter and medullary cavity diameter are shown in the upper right hand corner of the figure. Plot profile of the image intensity values across the entire midshaft is shown in the lower right hand corner of the figure. Note that the plot profile line has two peaks. Red arrows point to the portion of the plot profile line (outer slopes) generated from image intensity values associated with the periosteal surface of the tibial midshaft. Blue arrows point to the portion of the plot profile line (inner slopes) generated from image intensity values associated with the endocortical surface of the tibial midshaft. ....	97
Figure 3-7: a. Costochondral junction of left 4 <sup>th</sup> rib (area marked in red) or other available rib taken for qualitative histological evaluation. b. Bone sample excised from mid-point of iliac crest (area marked in red) for qualitative histological evaluation.....	99
Figure 4-1. Sex distribution of the study sample. ....	111
Figure 4-2. Race distribution of the study sample. ....	111
Figure 4-3. Sex distribution of the study sample by race. ....	112
Figure 4-4. Distribution of study sample by estimated gestational age (EGA). One case with unknown EGA is excluded from the plot. ....	114
Figure 4-5. Distribution of study sample by length for age percentile. ....	116
Figure 4-6. Distribution of study sample by weight for age percentile. ....	117
Figure 4-7. Distribution of study sample by weight for length percentile. Weight for length could not be calculated for two cases and were excluded from the above plot. ....	118
Figure 4-8. Scatter plot of tibial length by chronological age in months. Black regression line is fitted to total sample. Dark blue regression line is fitted to data from infants without chronic illness. Light blue regression line is fitted to data from infants with chronic illness. ....	123
Figure 4-9. Scatter plot of tibial midshaft diameter by chronological age in months. Black regression line is fitted to total sample. Dark blue regression line is fitted to data from infants without chronic illness. Light blue regression line is fitted to data from infants with chronic illness. ....	124
Figure 4-10. Scatter plot of medullary cavity diameter by chronological age in months. Black regression line is fitted to total sample. Dark blue regression line is fitted to data from	

infants without chronic illness. Light blue regression line is fitted to data from infants with chronic illness. ....	125
Figure 4-11. Scatter plot of cortical thickness by chronological age in months. Black regression line is fitted to total sample. Dark blue regression line is fitted to data from infants without chronic illness. Light blue regression line is fitted to data from infants with chronic illness. ....	127
Figure 4-12. Scatter plot of cortical index by chronological age in months. Black regression line is fitted to total sample. Dark blue regression line is fitted to data from infants without chronic illness. Light blue regression line is fitted to data from infants with chronic illness. ....	128
Figure 4-13. Scatter plot of tibial length by chronological age in months. Black regression line is fitted to total sample. Dark blue regression line is fitted to data from term infants. Light blue regression line is fitted to data from premature infants. ....	133
Figure 4-14. Scatter plot of tibial midshaft diameter by chronological age in months. Black regression line is fitted to total sample. Dark blue regression line is fitted to data from term infants. Light blue regression line is fitted to data from premature infants. ....	134
Figure 4-15. Scatter plot of medullary cavity diameter by chronological age in months. Black regression line is fitted to total sample. Dark blue regression line is fitted to data from term infants. Light blue regression line is fitted to data from premature infants. ....	135
Figure 4-16. Scatter plot of cortical thickness by chronological age in months. Black regression line is fitted to total sample. Dark blue regression line is fitted to data from term infants. Light blue regression line is fitted to data from premature infants. ....	136
Figure 4-17. Scatter plot of cortical index by chronological age in months. Black regression line is fitted to total sample. Dark blue regression line is fitted to data from term infants. Light blue regression line is fitted to data from premature infants. ....	137
Figure 4-18. Plot of tibial length by age and sex. ....	139
Figure 4-19. Plot of tibial midshaft diameter by age and sex. ....	140
Figure 4-20. Plot of medullary cavity diameter by age and sex. ....	141
Figure 4-21. Plot of cortical thickness by age and sex. ....	142
Figure 4-22. Plot of cortical index by age and sex. ....	143
Figure 4-23. Plot of tibial length by age and sex with chronically ill infants excluded. ....	145
Figure 4-24. Distribution of average SOS readings. Dark blue represents SOS data from term born infants and light blue represents data from premature infants. ....	150
Figure 4-25. Box and whisker plot of BMD by chronological age in months with chronically ill infants excluded. ....	156
Figure 4-26. Box and whisker plot of BMD distributed by chronological age in months and sex, chronically ill infants excluded. Dark blue boxes represent data from female infants and are located to the left of gridlines representing age and light blue boxes represent data from male infants and are located to the right of gridlines representing age. The dark blue circle is a female outlier (Case ID # 159). ....	157
Figure 4-27. Box and whisker plot of SOS by chronological age in months. ....	160
Figure 4-28. Plot of SOS readings against age in months with a Lowess-smoothed regression line. Dark blue circles represent SOS readings from term born infants. Light blue circles represent SOS readings from premature infants. ....	161
Figure 4-29. Box and whisker plot of SOS by chronological age in months with premature infants excluded. The circles represent outliers. Case ID # 204 is a trauma case. Case ID #	

152 was a chronically ill infant. There was nothing remarkable in the case history of Case ID # 189. ....	166
Figure 4-30. Plot of SOS readings against age in months with a separate Lowess-smoothed regression lines for premature and term infants. Dark blue circles with dark blue dashed Lowess-smoothed regression line represent SOS data from term born infants. Light blue circles with light blue dashed Lowess-smoothed regression line represent SOS data from premature infants. ....	171
Figure 4-31. Distribution of BMD data differentiating between infants with and without chronic illness. Dark blue represents BMD data from infants without chronic illness and light blue represents data from chronically ill infants.....	186
Figure 4-32. Distribution of BMD values with qualitative radiographic score specified. Dark blue represents cases classified as normally mineralized on radiographs. Light blue represents cases classified as indeterminately or slightly demineralized on radiographs. Purple represents cases classified as abnormally mineralized on radiographs. ....	195
Figure A- 1. Data recorded for each infant in the Infant Injury Database and associated variable definitions. ....	282
Figure A-2. Page 1 of form completed by TCH pathologist for each decedent. ....	283
Figure A-3. Page 2 of form completed by TCH pathologist for each decedent .....	284
Figure A-4. Qualitative radiography evaluation score form.....	291
Figure A-5. Qualitative histological evaluation score form.....	292

## CHAPTER 1 : INTRODUCTION

In infants, the finding of multiple skeletal fractures without a reasonable and/or consistent injury history, and in the presence of normal bone, is considered suspicious for non-accidental injury (i.e. child abuse) (Harris County Institute of Forensic Sciences 2014; Kemp et al. 2008; Ravichandiran et al. 2010; Worlock et al. 1986). In 2013, Texas Children's Hospital (TCH) evaluated 1,416 patients for abuse and neglect, 504 of these cases were evaluations for physical abuse (M. Donaruma-Kwoh, M.D., personal communication, November 22, 2014). Approximately 60-65% of the abuse and neglect evaluations have positive findings for abuse or neglect. Harris County Institute of Forensic Sciences (HCIFS) investigated the death of 143 child fatalities (0-4 years of age) of which 24 were classified as homicide (Harris County Institute of Forensic Sciences 2014). On a state level, the Texas Department of Family and Protective Services reported a total of 11,734 cases of confirmed physical abuse and 119,991 cases of unconfirmed risk for child abuse/neglect (Department of Family and Protective Services 2014). Bone fragility is the most common used legal defense during adjudication of child abuse cases. However, there is no quantitative method for evaluating infant bone quality. The previously mentioned statistics highlight the need for a quantitative method for the evaluation of bone quality in infants at risk for physical abuse. Such a method could provide substantiated medical evidence for child abuse case adjudication, or equally as important, help prevent false accusations of physical abuse. Infants affected by chronic illness, heritable, and/or metabolic disease are at higher risk of skeletal fragility. The cause of skeletal fractures in these infants may be interpreted incorrectly as non-accidental injury (Kemp 2008; Paterson 2009; Scherl 2006). In both the medical examiner and clinical setting, the assessment of bone fragility may be pivotal in the diagnosis or exclusion of non-accidental injury as the cause of trauma. An incorrect diagnosis or exclusion of child abuse has devastating long-term effects for families. Research that aids the physician in making the correct diagnosis is an important contribution.

Radiographic evaluation, a qualitative method, is often used to assess bone mineral density (BMD). However, qualitative radiographic evaluation is unreliable due to the substantial amount of bone loss that must occur before the reduction can be detected on radiographs and the large degree of inter-observer variation associated with the method (Allgrove 2009; Ardran 1951; Brooke and Lucas 1985; Epstein et al. 1986; Miller and Hangartner 1999; Shore and Poznanski



1999). In a study of 26 infants diagnosed with fragile bones, bone density was classified as normal according to qualitative radiographic evaluation (Miller and Hangartner 1999).

Quantitative evaluation of bone mineral density is helpful for the assessment of bone fragility, but has limitations. Techniques, like dual-energy x-ray (DXA) and computed tomography (CT), used to measure bone mineral density are costly, possibly require sedation, use ionizing radiation, and have not been validated for infants (Adams and Bishop 2009; Chen et al. 2004; Glüer 2009; Koo et al. 2008; Rack et al. 2012; Shore and Poznanski 1999; Teitelbaum et al. 2006). Magnetic resonance imaging (MRI) does not use ionizing radiation, but is not feasible for the sole purpose of evaluating BMD due to cost, relatively long scan times, and lack of pediatric standards (Ward et al. 2007). A non-invasive, quantitative method for the assessment of bone fragility that is portable, brief in scan duration, and does not expose the patient to ionizing radiation has yet to be developed and validated. Currently, pediatricians, forensic pathologists and forensic anthropologists have no quantitative method for evaluating infant bone fragility that is feasible for use in all infants, regardless of circumstance. Quantitative ultrasound (QUS) has been marketed as a technique that measures infant bone quality by measuring speed of sound (SOS). However, it remains unclear what aspects of bone quality are measured by SOS. The purpose of this research is to evaluate components of infant bone quality that are measured by SOS in order to determine if QUS is valid technique for measuring infant bone quality.

Preliminary data on the use of QUS for the assessment of bone fragility in pediatric patients are promising (Ahmad et al. 2010; Chen et al. 2012; Gonnelli et al. 2004; Litmanovitz et al. 2003; Littner et al. 2005; McDevitt et al. 2005; Nemet et al. 2001; Pereda et al. 2003; Rack et al. 2012; Ritschl et al. 2005; Rubinacci et al. 2003; Tomlinson et al. 2006). Bone speed of sound (SOS), a QUS measurement, is influenced by bone properties which also influence DXA measurements of BMD. Studies indicate that bone SOS is correlated with BMD, bone elasticity, cortical thickness, trabecular microarchitecture, and fatigue damage (Foldes et al. 1995; Greenfield et al. 1981; Guglielmi et al. 2009; Kaufman and Einhorn 1993; Lee et al. 1997; Njeh et al. 1997; Prevrhal et al. 2001). Research also indicates that SOS is correlated with bone strength (Bouxsein et al. 1995; Nicholson et al. 1997; Njeh et al. 2001) and is consistent with the claim that SOS measures bone quality (Koo et al. 2008; McDevitt et al. 2005; Pereda et al. 2003; Ritschl et al. 2005; Rubinacci et al. 2003). QUS has advantages over other methods used to assess bone fragility.

QUS does not use ionizing radiation, scan duration is brief, and the device is portable (Chen et al. 2012; Fricke et al. 2005). In premature infants, significant correlation was found between SOS and BMD values measured by DXA (Ahmad et al. 2010). In adults, QUS is already considered a reliable technology for osteoporosis screening (Bauer et al. 1997; Bouxsein et al. 1999; Hans et al. 1996; Huang et al. 1998; Ross et al. 1995; Thompson et al. 1998).

Although preliminary data are promising, most infant studies using QUS to assess bone quality are limited to preterm and term infants during the immediate neonatal period and preterm infant at term-corrected age (Ahmad et al. 2010; Altuncu et al. 2007; Chen et al. 2012; Gonnelli et al. 2004; Litmanovitz et al. 2003; Littner et al. 2004a; Littner et al. 2003; Littner et al. 2005; McDevitt et al. 2005; Nemet et al. 2001; Pereda et al. 2003; Rack et al. 2012; Rigo and De Curtis 2006; Ritschl et al. 2005; Rubinacci et al. 2003; Tomlinson et al. 2006; Wright et al. 1987; Yiallourides et al. 2004). Longitudinal studies have also been limited to preterm or very low birthweight infants. Other limitations of longitudinal studies include small sample sizes and inconsistent measurement intervals (Gonnelli et al. 2004; Litmanovitz et al. 2003; Litmanovitz et al. 2004; McDevitt et al. 2007; Mercy et al. 2007; Rack et al. 2012; Ritschl et al. 2005; Tansug et al. 2011; Tomlinson et al. 2006). Additionally, age-specific data for the first year of life are lacking and no threshold has been established for normal and abnormal SOS readings. Research in this area is necessary to investigate whether QUS is a valid diagnostic tool for the assessment of bone quality in the infant population. The current study is the first step in addressing this knowledge gap.

This study addresses three primary questions, listed below.

1. Is QUS a valid tool for evaluating bone quality in infants?
2. Can SOS be used to differentiate between infants with poor bone quality and infants with normal bone quality?
3. If QUS is a valid method for evaluation bone health in infants, can a threshold for normal bone SOS values in infants be identified?

To determine whether QUS can be used as a diagnostic tool, a prospective study was designed in which SOS measurements were compared to other indicators of overall health, bone health, and bone strength. Over a 9 month period, every infant between the age of 30 weeks estimated

gestational age (EGA) and 12 postnatal months that received an autopsy at HCIFS or TCH was included in the study. These populations were chosen because the hospital population consists of infants with well-documented, chronic illness and the medical examiner population consists of infants that were relatively healthy prior to death and chronically ill infants. QUS was used to obtain SOS measurements at a site on the anterior leg that approximated the midshaft of the tibia. Digital radiographs of the leg and forearm were collected for qualitative radiographic evaluation and to calculate BMD estimates from units of x-ray attenuation. Leg radiographs were also used to obtain tibial measurements (length, midshaft diameter, medullary cavity diameter, cortical thickness, and cortical index). BMD and cross-sectional measurements of the tibia served as proxies for bone strength. Additionally, data pertaining to demographics, medical history, family medical history, autopsy findings, and law enforcement/investigator reports were collected from each infant. Each infant's medical history and autopsy findings were used to determine the presence/absence of chronic illness.

The relationships between SOS and other bone health indicators were investigated by building associations. The pattern of growth-related changes in tibial structure was related to age-related changes in BMD and SOS. This was done to evaluate the similarity between relationships and establish whether SOS captured similar differences as BMD and qualitative radiographic analysis. The association between traumatic injury and indicators of bone health were evaluated to assess whether there were significant differences in bone quality between infants with and without traumatic injury. The effects of chronic illness and skeletal maturity at birth on growth were examined to establish whether these factors had significant detrimental effects on growth in the current study sample. These findings were then compared with SOS and BMD readings between chronically ill and premature infants. Differences in qualitative radiographic evaluation results based on prematurity and chronic illness were also assessed. Finally, direct comparisons between methods of evaluating infant bone quality were conducted.

Various univariate statistics were used to test the following specific hypotheses.

1. Growth-related changes in tibial structure and body size are significantly associated with each other, and both are significantly associated with age-related changes in BMD and SOS, which is reflected by the following sub-hypotheses.

- a. Age-related changes in tibial measurements are positively associated with variables related to body size and growth percentiles.
  - b. BMD and SOS are significantly related to age.
  - c. BMD and SOS have positive relationships with variables associated with body size and growth percentiles.
  - d. BMD and SOS are significantly related to tibial structure.
    - BMD and SOS have negative relationships with medullary cavity diameter.
    - BMD and SOS have positive relationships with cortical thickness and cortical index.
2. The presence of traumatic injury is not associated with indicators of overall health, body size, or bone health.
3. Chronic illness is negatively associated with growth and bone health, which is reflected by the following sub-hypotheses.
- a. Variables related to body size are negatively associated with chronic illness.
  - b. Tibial growth is negatively associated with chronic illness.
    - Tibial length, cortical thickness, midshaft diameter, and cortical index are negatively associated with chronic illness.
    - Medullary cavity diameter is positively associated with chronic illness.
  - c. Chronic illness is significantly related to qualitative and quantitative measures of infant bone health.
    - Qualitative radiographic evaluation scores are positively associated with chronic illness.
    - BMD and SOS have negative relationships with chronic illness.
4. Skeletal maturity at birth is positively associated with body size, bone size, and bone health, which is reflected by the following sub-hypotheses.
- a. Skeletal maturity at birth is significantly related to body size.
    - Body size is positively associated with EGA and birthweight, and negatively associated with prematurity.
  - b. Skeletal maturity at birth is significantly related to tibial measurements.
    - Tibial length and cross-sectional measurements are positively associated with birthweight and EGA, and negatively associated with prematurity.

- c. Skeletal maturity at birth is significantly related to qualitative and quantitative measures of infant bone health.
  - BMD and SOS have positive relationships with EGA and birthweight, and negative relationships with prematurity.
  - Qualitative radiographic score has a positive relationship with prematurity.
5. The methods used to assess infant bone quality are significantly associated with one another, which are reflected by the following sub-hypotheses.
  - a. BMD has a negative relationship with qualitative radiographic score.
  - b. SOS has a significant positive relationship with BMD.
  - c. SOS has a negative relationship with qualitative radiographic score.

The analyses used to test these hypotheses include Analysis of Variance (ANOVA), linear regression, and non-parametric analyses where appropriate. Findings associated with each hypothesis were used to draw conclusions regarding the components of infant bone quality measured by SOS. Finding significant associations between SOS and the other measures of bone health and bone strength would indicate that SOS measures aspects of infant bone health. If it is found that chronic illness and prematurity adversely affect other indicators of bone health and strength, a significant association between SOS and chronic illness and/or prematurity would indicate SOS is influenced by factors affecting bone health and strength. Such findings would support the argument that SOS measures infant bone quality and, therefore, QUS is a valid method for evaluating infant bone quality.

Validating QUS as a method for evaluation of bone health and strength in infants has far reaching implications. Age-specific SOS thresholds could be used to differentiate between infants with normal and abnormal bone strength. These thresholds may be applicable to both living and deceased infants. In the clinical setting, the bone strength of premature infants could be easily and routinely monitored without exposure to ionizing radiation. Bone strength could be regularly evaluated during infant well visits. Therapeutic interventions could be initiated prior to the development of skeletal fractures. Infants presenting with skeletal fracture/s in the emergency setting could be quickly assessed to determine whether abnormal bone strength was a contributing factor. Similarly, the bone strength of infants in the medical examiner setting that present with fractures could be easily assessed. In cases of non-accidental injury, quantitative

measures of infant bone strength could be offered at trials as evidence to dispute infant bone fragility. Conversely, showing that QUS is not a validated method for evaluating infant bone strength is also an important finding. Negative results would indicate that it is necessary to explore other avenues for the evaluation of infant bone strength.

## CHAPTER 2 : LITERATURE REVIEW

### Introduction

This chapter discusses the background research that is necessary for understanding the relationship between SOS and bone quality in infants. Before it can be assessed whether QUS is a valid technique for evaluating infant bone quality, the biological factors that influence SOS values must be established. As infant bone quality is the focus of this research, it is necessary to understand bone formation, development, maintenance, and the factors that affect these processes. It is also important to discuss the material and structural properties of bone that contribute to bone strength and how these properties have been measured. Topics in bone biology are discussed first and include bone structure, bone formation, modeling, remodeling, and the bone cells that are responsible for forming and maintaining bone. These topics are important for understanding growth-related changes in bone size and structure. Bone size and structure is related to bone strength. Secondly, prenatal and postnatal nutritional needs and other factors associated with the prenatal environment that affect skeletal development are discussed. Thirdly, the process by which the body maintains normal serum concentrations of minerals obtained through nutrition is discussed. Maintaining normal serum levels is important for vital bodily functions and can effect skeletal development. Nutritional insufficiencies *in utero* or postnatally compromise bone strength by changing material and structural properties of bone. Metabolic bone disorders occur when normal, mineral serum levels cannot be maintained due to nutritional insufficiencies. Metabolic diseases and other factors (environmental and genetic) that adversely affect the developing skeleton are discussed in the fourth section. Bone biomechanics are discussed in the fifth section. Topics in biomechanics that are discussed include bone material properties, cortical and trabecular bone structural properties, and differences in the properties related to young age. These properties comprise bone quality, defined as a bone's ability to resist fracture, which is also discussed in the fifth section. Finally, the pros and cons of the non-invasive and invasive methods that have been used to assess bone quality are discussed in the sixth and seventh sections, respectively. Understanding which bone properties influence SOS measurements is essential for assessing whether QUS measures bone quality in infants.

## **Bone Biology**

Normal bone is able to sufficiently perform several vital bodily functions. These functions include protection of the internal organs, support for the body, a point of muscle attachment for locomotion, being a cavity for hematopoiesis, and being a mineral source for maintaining mineral homeostasis of the body (Bartl et al. 2009; Burr and Akkus 2013; Marks and Odgren 2002; Rauner et al. 2012; Rodan 1992). There are a large number of factors that can compromise bone's ability to function, starting during formation and continuing throughout growth. Overall health and bone strength suffer when there is a failure in normal bone formation or the ability to maintain mineral homeostasis. Chronic illness can disrupt mineral homeostasis, compromising bone growth and/or strength. Before understanding how these factors negatively influence bone growth and/or strength, normal bone structure and functioning must first be understood. The following section discusses important components of bone, skeletal formation, and growth.

### ***BONE CELLS***

There are four types of bone cells that are responsible for bone formation and maintenance. These are osteoblasts, osteocytes, bone lining cells, and osteoclasts. These cells can be classified into two categories, cells that form bone or have formed bone and cells that resorb bone. Osteoblasts, osteocytes, and bone lining cells are bone formers or previous formers of bone. Osteoclasts resorb bone.

#### ***Osteoblasts and Related Cells***

Osteoblasts begin as undifferentiated mesenchymal progenitor cells. Undifferentiated mesenchymal cells have an irregular form, a single nucleus, minimum cytoplasm, and few organelles (Buckwalter et al. 1995a). These undifferentiated cells reside in the bone canals, endosteum (fibrous tissue lining the inner surface of bone) and periosteum (fibrous tissue lining the outer surface of bone), and marrow (Beresford 1989; Buckwalter 1994; Buckwalter and Cooper 1987; Cooper et al. 1966; Goshima et al. 1991; Haynesworth et al. 1992; Nakahara et al. 1990; Nakahara et al. 1991; Paley et al. 1986; Sevitt 1981) until stimulated to proliferate and differentiate into osteoblasts. Differentiation of mesenchymal cells into osteoblasts occurs over a 2-3 day period and is stimulated by mechanical stress or chemical stimuli such as transcription factors (Bellido et al. 2013; Martin et al. 1998c). Transcription factors of the helix-loop-helix



family are responsible for maintaining the osteoprogenitor population. Transcription factors of the AP-1 family may activate or repress transcription. Runt-related transcription factor 2 (RUNX2, also known as core-binding factor subunit alpha-1, cbfa-1) and transcription factor Sp7/osterix are essential for establishing the osteoblast phenotype (Bellido et al. 2013).

Mature osteoblasts are located on the bone surface. They are cuboidal in shape and have single large nucleus located close to the basal membrane, and an enlarged Golgi apparatus on the apical surface of the nucleus, an extensive endoplasmic reticulum, and multiple mitochondria (Buckwalter et al. 1995a). The osteoid matrix is produced within the cell by the endoplasmic reticulum and is packaged in vesicles for transport out of the cell by the Golgi apparatus. Osteoblasts deposit osteoid matrix at a rate of 1 micrometer per day.

Osteoblasts cells also have cytoplasmic extensions that join with the cytoplasmic extensions of other cells at locations called gap junctions. At the gap junctions, osteoblasts communicate with other osteoblasts, bone lining cells, bone marrow cells and osteocytes embedded within the osteoid matrix and mineralized bone (Bellido et al. 2013).

Osteoblasts secrete non-collagenous proteins along with type 1 collagen. The functions of some of these non-collagenous proteins remain unclear. Some important non-collagenous proteins produced by osteoblasts include bone-specific alkaline phosphatase (B-ALP), receptor activator of Nf-kB ligand RANKL, osteopontin, osteoprotegrin (OPG), osteocalcin, and bone sialoprotein. B-ALP is a potential calcium ion carrier and hydrolyzing inhibitors of mineral deposition; therefore, a marker of bone formation (Burr and Akkus 2013). Osteopontin and RANKL are secreted by immature osteoblasts. Osteopontin promotes adhesion of the cement line and inhibits mineral formation and crystal growth. RANKL regulates osteoclast differentiation and survival. OPG is secreted throughout the life of an osteoblast, even as mesenchymal stem cells, and inhibits osteoclast differentiation. Mature osteoblast cells secrete osteocalcin, calcitonin and bone sialoprotein (Burr and Akkus 2013; Rauner et al. 2012). Osteocalcin enhances calcium binding and controls mineral deposition (Bellido et al. 2013; Burr and Akkus 2013). Calcitonin acts as chemoattractant for bone cells (Martin et al. 1998c). Bone sialoprotein is produced during the early stage of mineralization and is believed to influence the initiation of mineralization, but its function is not yet well understood (Bellido et al. 2013).

Osteoblasts are regulated by hormones and multiple local factors. Osteoblast cells carry receptors for parathyroid hormone (PTH), 1,25-dihydroxyvitamin D<sub>3</sub> (active form of vitamin D), estrogen, glucocorticoids, and leptin. All of these hormones are involved in the regulation of osteoblast differentiation. Some important local factors include bone morphogenic proteins (BMPs- 2, 4, 6, and 7) (Shore et al. 2006; Storm and Kingsley 1999; Wu et al. 2003; Wutzl et al. 2010), growth factors (Canalis 2009), Sonic and Indian hedgehogs (Guan et al. 2009; Maeda et al. 2007), and members of the Wnt family (Bodine and Komm 2006; Rauner et al. 2012).

### **Osteocytes**

Fully differentiated osteoblasts that are embedded within the osteoid matrix or mineralized bone are called osteocytes. Osteocytes are the most numerous cells within the skeletal tissue and are scattered evenly throughout the matrix (Bellido et al. 2013). When an osteoblast becomes an osteocyte, it undergoes a reduction in the amount of cytoplasm present within the cell. An osteocyte cell is ellipsoid in shape with a single nucleus and has numerous, long, branching cytoplasmic processes projecting from the cell body (Buckwalter et al. 1995a; Rauner et al. 2012). A single osteocyte has an average of 50 cytoplasmic processes (Bellido et al. 2013). Each cytoplasmic process ends at a gap junction that connects to the cytoplasmic processes from adjoining osteocytes, osteoblasts, or bone lining cells.

Osteocyte functions include mechanosensation and regulation of bone mineral metabolism through the coordination of osteoblasts and osteoclasts (Bartl et al. 2009; Bellido et al. 2013; Buckwalter et al. 1995a; Paic et al. 2009). Osteocytes are able to function as mechanosensory cells by detecting strain within the skeletal tissue (Paic et al. 2009). Osteocytes form an extensive intercellular communication network through their numerous cytoplasmic processes (Bartl et al. 2009). This intercellular network extends throughout the bone mineral matrix to the bone surfaces and bone marrow, which also reaches the blood vessels (Bellido et al. 2013). When a load is applied to a bone, osteocytes detect changes in the flow of fluid around them and respond by sending signals, electric or chemical, through their cytoplasmic processes into the gap junctions. The reception of these signals in the gap junctions of other osteocytes, osteoblasts, or bone lining cells initiates more signaling and amplifies the signal.

Ultimately, this signaling may result in bone formation or resorption activity through the production secretion of factors. Some of the factors regulate phosphate metabolism, such as

phosphate regulating neutral endopeptidase (PEX), matrix extracellular phosphoglycoprotein (MEPE/OF45), dentin matrix acidic phosphoprotein 1 (DMP-1), and fibroblast growth factor 23 (FGF-23). Some of the factors inhibit bone formation, such as MEPE/OF45, Dickkopf 1 (Dkk-1), and sclerostin. RANKL and M-CSF are factors secreted by osteocytes and are necessary for the proliferation, differentiation, and survival of osteoclasts. Osteocytes produce greater amounts of osteocalcin than osteoblasts. Osteocytes are also able to secrete B-ALP and type 1 collagen, but they secrete lower levels than osteoblasts (Bartl et al. 2009; Bellido et al. 2013).

Through the secretion of these factors and binding of hormones, osteocytes are able to regulate bone metabolism for the purposes of bone repair, maintenance, or mineral homeostasis (Bartl et al. 2009; Bellido et al. 2013). Osteocytes actively participate in mineral homeostasis through the transport of organic and inorganic materials throughout the skeletal tissue via their extensive intercellular network (Bartl et al. 2009). Through binding to their receptors, osteocytes are able to detect levels of circulating hormones such as PTH, estrogen, androgen and glucocorticoids. Binding of estrogens and androgens inhibit osteocyte apoptosis, which in turn prevents bone resorption. Glucocorticoids stimulate bone resorption by stimulating osteocyte apoptosis. Glucocorticoids inhibit osteocytes from producing factors necessary for its survival. Normal PTH expression increases osteoblast survival and over expression of PTH can lead to down regulation of sclerostin by osteocytes (Bellido et al. 2013).

### **Bone Lining Cells**

After the completion of bone matrix synthesis, osteoblasts that do not become embedded within the bone matrix may become bone lining cells. Bone lining cells are flat and elongated with few cytoplasmic organelles (Marks and Odgren 2002). Bone lining cells lie against the inactive bone surfaces and are attached to thin collagenous membranes on the outer and inner surfaces of bone (Bartl et al. 2009). The collagenous membrane on the outer surface of bone is called periosteum. The layer on the inner surface of bone is called the endosteum and separates the inner surface of bone from the bone marrow. Although bodies of bone lining cells reside in the endosteum and periosteum, bone lining cells possess many cytoplasmic processes that penetrate into the bone matrix (Matthews 1980; Recker 1992). At gap junctions, the cytoplasmic processes of bone lining cells contact the cytoplasmic processes of osteocytes within the bone matrix. Through these gap junctions, bone lining cells maintain close communication with osteocytes.

The function of bone lining cells is to form a protective layer over the bone and to act as a surveillance system for bone (Bartl et al. 2009). Through communication with osteocytes within the matrix and in reaction to factors in the bone marrow and blood, bone lining cells can be reactivated as osteoblasts and participate in the activation of osteoclasts for purposes of remodeling (Bartl et al. 2009). In response to PTH, bone lining cells can recover the ability to produce matrix (Bellido et al. 2013). Exposure to PTH may also cue bone lining cells to retract themselves from the bone surface and secrete enzymes that remove the thin layer of osteoid that covers the mineralized bone matrix (Bellido et al. 2013; Recker 1992). Removal of the thin osteoid layer allows osteoclasts access to the bone surface for resorption (Buckwalter et al. 1995a). RANKL secreted from bone lining cells react with the receptor RANK on osteoclasts, which ultimately results in the initiation of remodeling. Bone lining cells also actively participate in the remodeling process. During remodeling, bone lining cells are responsible for removing fragments of collagen left behind by osteoclasts and initiating new bone formation at those sites (Bartl et al. 2009).

### ***Osteoclasts***

Unlike osteoblasts, osteoclast stem from hematopoietic cells. Hematopoietic stem cells differentiate into monocytes within the bone marrow. The monocytes remain in the bone marrow or circulate in the blood until they are recruited to a resorption site (Buckwalter et al. 1995a). Monocytes are recruited to the site of bone resorption by changes in calcium gradients and factors secreted by osteoblasts and osteocytes. Upon reaching the resorption site, the monocytes will become committed mononuclear preosteoclasts, proliferate, and differentiate. Multiple mononuclear osteoclasts will then fuse to become large multinucleated cells. Osteoclasts do not become mature activated cells until they bind to the bone surface. Binding of the osteoclast to the bone surface signals the osteoclast to undergo cytoskeletal and membrane reorganization. Reorganization results in polarization of the osteoclast cell (Bellido et al. 2013). Due to this polarization, the osteoclast cell can be divided into two sections, an apical membrane domain that is held in contact with the bone surface and a basolateral membrane domain that is located away from the bone surface. Vital structures for resorption within the apical domain are the ruffled border and sealing zone. The ruffled border is formed by the fusion of transport vesicles and the apical membrane. The ruffled border is recognized as the central, highly infolded area of the osteoclast plasma membrane which appears brush-like (Marks and Odgren 2002). The edge

of the ruffled border has a ring of membrane that circumscribes it, which is called the sealing zone. The sealing zone adheres tightly to the bone surface through the binding of its receptors to various extracellular matrix proteins. The seal creates a closed space between the osteoclast and the bone matrix where resorption occurs. Within the sealing zone, small structures called podosomes aid in the adhesion of the osteoclast to the bone surface as well as function in the migration of the osteoclast along the bone surface (Bellido et al. 2013; Rauner et al. 2012). On the opposite side of the cell, the basolateral domain contains a functional secretory domain that is connected to the ruffled border via microtubules. The nuclei are also located on this side of the cell. Large numbers of mitochondria and lysosomes are present within the osteoclast cell.

The function of the osteoclast is to remove bone through a process called resorption. Once the sealing zone of an osteoclast has adhered itself to the bone surface, proton pumps within the osteoclast migrate and insert themselves in the apical membrane and a ruffled border forms. Within the cell, protons ( $H^+$ ) and bicarbonate ( $HCO_3^-$ ) are produced from the reaction of carbon dioxide and water catalyzed by the enzyme carbonic anhydrase. The proton pumps transport the protons through the ruffled border into the resorption space (Baron et al. 1985; Bellido et al. 2013; Buckwalter et al. 1995a).  $HCO_3^-$  is pumped out of the cell and into the extracellular space by a  $HCO_3^-/Cl^-$  exchanger located in the basolateral membrane. To prevent intracellular polarization caused by the transport of protons out of the osteoclast,  $Cl^-$ , which was transported into the cell by a bicarbonate  $HCO_3^-/Cl^-$  exchanger is then transported out of the osteoclast through the ruffled border and into the resorption space. HCl is formed in the resorption space, creating an acidic environment which dissolves the bone mineral (Silver et al. 1988). To degrade the organic matrix, osteoclasts secrete lysosomal enzymes such as tartrate-resistant acid phosphatase (TRAP), cathepsin K and matrix metalloproteinase-9 (MMP-9) into the resorption space (Bellido et al. 2013; Rodan 1992; Teitelbaum 2000). After the bone matrix has been dissolved, the degraded bone matrix is internalized by osteoclasts through phagocytosis. The internalized degraded products travel inside vesicles to lysosomes, where they are degraded further, or they are transported to the functional secretory domain on the basolateral surface and discharged into the extracellular environment (Bartl et al. 2009; Bellido et al. 2013). Degraded bone products can also be directly released to the extracellular environment after osteoclasts release from the bone surface. After resorption is complete, the osteoclast may migrate to an

adjacent area to continue resorption or undergo apoptosis. Osteoclasts resorb bone at a rate of tens of micrometers per day (Martin et al. 1998c; Rauner et al. 2012).

Recruitment, differentiation, and activation of osteoclasts are also influenced by numerous hormones (PTH, androgens, estrogens, leptin, and thyroid hormones) as well as factors secreted by osteoblasts and osteocytes. Preosteoclasts proliferation occurs in response to growth factors such as interleukin-3 and macrophage colony-stimulating factor (M-CSF). Exposure to RANKL causes committed mononuclear osteoclasts to differentiate, fuse into large, multinucleated osteoclasts, acquire osteoclast-specific markers, and attach to the bone surface. It also initiates resorption and promotes survival of mature active osteoclasts (Bellido et al. 2013). M-CSF contributes to osteoclast differentiation, survival and migration. Estrogens and androgens inhibit osteoclast recruitment by regulating the production of pro-osteoclastogenic factors by cells of the osteoblastic lineage. Estrogens also induce apoptosis in osteoclasts. Glucocorticoids extend the life of mature osteoclasts which leads to an initial increase in bone resorption. However, glucocorticoids also decrease osteoclastogenesis through their negative effect on the number of osteoblasts, leading to a reduction in remodeling.

### ***BONE STRUCTURE***

At the ultra-structural level, bone is composed of an organic matrix, non-organic components, and water. Approximately 90% of the organic component of bone is type 1 collagen and the remaining 10% is non-collagenous proteins (Burr and Akkus 2013). Collagen provides bone with its toughness, which will be discussed further in the Bone Biomechanics section. Non-collagenous proteins are responsible for the organization of the collagenous matrix, mineralization of bone, and cellular signaling by bone cells (Buckwalter et al. 1995a; Burr and Akkus 2013). The inorganic matrix portion of bone consists of some variant of the mineral calcium phosphate, such as hydroxyapatite. The inorganic matrix contains ~99% of the calcium, 85% of the phosphorus and between 40-60% of the total body sodium and magnesium (Glimcher 1992). The mineral portion of bone provides bone its strength and stiffness, as well as a reservoir for mineral ions, and will be discussed further in the in the sections on **Mineral Homeostasis and Bone Biomechanics**.

### ***Collagen Organization***

Individual collagen molecules are formed from two  $\alpha 1$  chains and 1  $\alpha 2$  chain. These chains assemble into a triple helix to form single collagen molecule called a tropocollagen. Five tropocollagen molecules organize into a pattern that is stacked and staggered by approximately one-fourth their length in a semihexagonal arrangement (Burr and Akkus 2013). The aggregate of 5 tropocollagens is referred to as a collagen microfibril. Due to the stacked and staggered arrangement of tropocollagens within the microfibril, there are empty spaces between the heads of a tropocollagens in one microfibril and the tails of the tropocollagens in the neighboring microfibril (Currey 2002), as well as empty spaces that run longitudinally between the tropocollagens of a single microfibril (Burr and Akkus 2013). The empty spaces between the heads and tails of the tropocollagens of neighboring microfibrils are called holes and the spaces between the tropocollagens within a single microfibril are called pores. These holes and pores are populated by some variant of calcium phosphate, such as a hydroxyapatite crystal, that increase in size during mineralization (Buckwalter et al. 1995a; Burr and Akkus 2013).

The tropocollagens within a single microfibril are held together by intermolecular cross-links. The type of cross-link connecting the collagen molecules can have profound effects on the material properties of collagen tissue and ultimately in the mechanical behavior of the whole bone (Burr and Akkus 2013). There are two types of intermolecular cross-links, enzymatically mediated and non-enzymatically mediated collagen cross-links. The bonds of the enzymatically mediated collagen cross-links are formed through a highly regulated process and mature quickly (Allen and Burr 2014a). They are trivalent and very stable. An increased number of enzymatically mediated collagen cross-links has been related to increased compressive strength and stiffness in bone. Non-enzymatically mediated collagen cross-links form from the condensation of arginine, lysine, and ribose. Non-enzymatically mediated cross-links accumulate with age and create advanced glycation end products (AGEs). AGEs have been linked with reduced collagen fibril diameter, impaired osteoblast differentiation, and decreased resorption by osteoclasts. All of which contribute to bone fragility (Burr and Akkus 2013).

### ***Bone Microstructure***

At the microstructural level, collagen microfibrils aggregate to form collagen fibers. Collagen fibers are organized into a regular or irregular structure. Acting upon this organization,

osteoblasts form either woven or lamellar bone. In woven bone, collagen fibers are irregular in formation and appear randomly oriented (Baron 1999; Martin et al. 1998c; Sommerfeldt and Rubin 2001). Woven bone is synthesized by osteoblasts during times of rapid bone formation, such as growth, or in response to bone or soft-tissue injury, and some pathological conditions (Buckwalter et al. 1995a). Woven bone is more highly mineralized than lamellar bone, but the mineral crystals also appear randomly arranged and leave mineral free spaces within the collagen. Microscopically, woven bone appears porous. Due to its disorganization, woven bone is weaker than lamellar bone and not capable of providing long-term, structural support. In lamellar bone, osteoblasts deposit collagen fibers in densely packed, highly organized parallel sheets (Burr and Akkus 2013). These parallel sheets of collagen fibers are called lamellae. Collagen fibers often interconnect within and between lamellae, which increases the strength of bone (Buckwalter et al. 1995a) (Torzilli et al. 1981). Lamellar bone replaces woven bone that is laid down during growth and fracture healing, increasing bone strength.

Most of the bone found in the body is a form of lamellar bone. Lamellae create circumferential bands of bone, each 3-7  $\mu\text{m}$  thick, that give the appearance of tree rings. Each sheet of lamella is separated from the next sheet by an interlamellar layer about 1  $\mu\text{m}$  thick (Burr and Akkus 2013). The collagen fibers within each sheet of lamella lie at a 90 degree angle to the collagen fibers in the adjacent sheets. A helicoidal arrangement of collagen fibers has also been found within regions of bone. In this arrangement, collagen fibers continuously change direction and the orientation of the collagen fibers rotates through 180 degree cycles, continuously repeating itself (Martin et al. 1998c).

Lamellar bone can be further divided into 4 types based on how the sheets of lamellae are arranged. These types are circumferential, trabecular, concentric, and interstitial. Circumferential lamellae compose the outer (periosteal) and inner (endosteal) surfaces of cortical bone. Lamellae form individual spicules of trabecular bone, which will be discussed shortly. Lamellae arranged around vascular channels within the bone matrix are called concentric lamellae. Concentric lamellae form larger structures within the bone matrix called osteons. Osteons will be discussed further with cortical bone. Lamellae located between osteons are called interstitial lamellae (Buckwalter et al. 1995a; Burr and Akkus 2013).



## ***Bone Macrostructure***

At the macro-structural level, bone is divided into two types, cortical (or compact) and trabecular (or cancellous). With the naked eye, cortical bone appears solid and trabecular bone appears porous. Cortical bone forms the outer, dense bone envelope. Trabecular bone is found within the dense cortical envelope and is exposed to bone marrow. Cortical bone is the primary component of the shafts (diaphyses) of long and short bones comprising the appendicular skeleton and surrounds the trabecular bone of the axial skeletal elements and the flat bones. Trabecular bone is found primarily in the metaphyses (flared ends) and in the bones of the axial skeleton and flat bones. Cortical bone performs support and protection functions, while trabecular bone primarily serves as a structural support for the cortical bone without adding excessive weight.

### **Cortical Bone**

Cortical bone architecture consists of a combination of circumferential, concentric and interstitial lamellae, as well as spaces within the cortical bone for osteocytes and their cytoplasmic processes, blood vessels and resorption cavities. The majority of cortical bone is composed of structures called osteons. A single osteon is cylindrical in shape and composed of concentric lamellae. The concentric lamellae surround a central canal that is called a Haversian canal. Haversian canals are lined with discontinuous layer of osteoprogenitor cells and contain blood vessels, lymphatic vessels, and sometimes nerves (Buckwalter et al. 1995a; Burr and Akkus 2013; Downey and Siegel 2006). Osteocytes are located between the sheets of concentric lamellae in open spaces called lacunae. Small tunnels, called canaliculi, radiate from the lacuna like spokes from a wheel (Buckwalter 1994; Buckwalter and Cooper 1987; Sevitt 1981). Canaliculi connect lacunae within and between lamellae of a single osteon. Osteocyte cytoplasmic processes are housed within the canaliculi. Canaliculi also connect osteocytes to the Haversian canal. In general, osteons are arranged longitudinally within the long axis of the bone. However, the orientation of any individual osteon may be variable because the Haversian canals they surround branch extensively. The vessels within the Haversian canals also anastomose with one another through canals called Volkmann canals. These canals run in a mostly transverse direction and also open to the inner and outer surfaces of the cortical bone where the vessels can join vessels in the marrow cavity and outer surface of bone (Burr and Akkus 2013).

There are two types of osteons, primary and secondary. Osteons formed in a space that had no prior bone matrix are called primary osteons. The osteons that replace primary osteons during remodeling are called secondary osteons or Haversian systems. Primary osteons structurally differ from secondary in several ways. Primary osteons are smaller than a secondary osteons. Primary osteons have no well-defined border separating them from surrounding osteons or bone matrix. Secondary osteons are isolated from the surrounding matrix by a thin layer of organic matrix called the cement line (Buckwalter 1994; Buckwalter and Cooper 1987; Burr and Akkus 2013; Cooper et al. 1966; Currey 1984). Secondary osteons will be discussed in more detail in the **Remodeling** section.

When secondary osteons replace primary osteons or other secondary osteons, fragments of the old osteon may be left behind. These fragments of old lamellae between osteons are called interstitial lamellae (Sevitt 1981). Interstitial lamellae have lacunae and canaliculi with osteocytes and their processes, but have no Haversian canal and therefore have no access to blood vessels. The tissue in interstitial lamellae usually dies (Currey 2002). However, osteocytes may survive within the interstitial lamellae if they are able obtain adequate nutrients from anastomosing network of canaliculi in areas above or below the invading osteon (Ortner and Turner-Walker 2003).

Circumferential lamellae form the periosteal and endosteal walls of bone and encompass all of the osteonal and interstitial lamellae. As with the other types of lamellar bone, osteocytes are found within the sheets of circumferential lamellae. Osteocytes are able to communicate with other osteocytes within their own lamella and adjacent lamella through their cytoplasmic processes that are located in canaliculi. Circumferential lamellae do not have Haversian canals but are able to access nutrients from the few vessels entering the bone and through special membranes on the outer and inner surface of the bone, which will be discussed in the **Skeletal Envelopes** section.

The extensive system of canaliculi, as well as Haversian and Volkmann canals is a vital structure in the performance of communication and mechanosensory functions by bone cells. Via migration through the canal system, communication from outside the cortices is able to make its way through the cortex and to the medullary cavity, and vice versa. Osteocytes fulfill their

mechanosensory function by sensing changes in the flow of fluid and ions through the canals. Changes in fluid flow and ions through the canal network are caused by load generated strains on bone. Osteocytes are able to pass on mechanosensory and other signals to other bone cells through the release of factors into the fluid filled canal system. The canal network also enables bone cells to adequately access nutrients from the circulating blood via the connection to the vascular canals (Haversian and Volkmann) and the vasculature running along the surfaces of the bone. Connection to the vascular canals also permits factors released by bone cells to migrate into the circulating blood or on to other bone cells within the matrix (Burr and Akkus 2013).

### **Trabecular Bone**

Trabecular bone forms a honeycomb network of cylindrical struts of lamellar bone (Ortner 2008). A single strut of bone within this network is called a trabecula and is approximately 1 mm long. Trabeculae can either have a plate-like or rod-like appearance depending on the amount of lamellae present in each trabecula. Due to the large numbers of trabeculae present within bone, the surface area of the trabeculae is greater than the surface area of the cortical bone. In general, lamellae are arranged parallel to the trabecular surface, but replacement of old lamellae can produce structures that appear like half osteons or hemiosteons. One surface of a hemiosteon borders the marrow cavity and the opposite surface is separated from the rest of the lamellae within a trabecula by a cement line. Complete osteons are rarely found within trabeculae. The open spaces between trabeculae are filled with hematopoietic bone marrow. Trabeculae derive their nutrient supply from the marrow require no central vascular channel (Burr and Akkus 2013). Trabeculae join one another at locations called nodes. Within the bone, the trabeculae are oriented along the lines of stress. At joint surfaces, stress is transferred from the cortical bone to the trabeculae and into the nodes. The greater the number of plate-trabeculae and the more closely the trabecular nodes are spaced, the greater the overall stability and strength of the bone they support (Rauner et al. 2012).

### ***Skeletal Envelopes***

The inner and outer surfaces of bone are covered by membranes called endosteum and periosteum, respectively. The periosteum serves as a boundary between the skeletal and muscle tissues by adhering to the external surfaces of bone, except in the regions around or within synovial joints. There is an inner and outer layer of the periosteum. The inner layer is also called the cambium layer. The cambium layer contacts the bone surface and is vascular, cellular, and

innervated (Allen et al. 2004; Buckwalter 1994; Recker 1992). The cambium layer is the source of cells necessary for the growth, development, modeling/remodeling, and fracture repair of the skeleton (Burr and Akkus 2013). The cambium layer contains bone lining cells and mesenchymal stem cells, which can be reactivated into osteoblasts. Mesenchymal stem cells can also differentiate into chondrocytes (cartilage forming cells), which is important for fracture healing. The cytoplasmic processes on bone lining cells within the cambium layer penetrate the bone through canaliculi. At gap junctions, bone lining cells are able to communicate with osteocytes. The cambium layer is much thicker during growth than it is in adults. As adults age it, becomes thinner until it almost completely disappears (Whiteside 1983). There are blood vessels, progenitor cells, and mononuclear cells between the inner and outer layer of periosteum (Allen et al. 2004). The outer layer of the periosteum is more dense and fibrous than the inner layer because it contains more collagen than the inner layer. The outer layer also contains fibroblasts, a neural and vascular network (Chanavaz 1995), and elastin fibers (Taylor 1992). The outer layer continues to the joint capsule and connects adjacent bones. Some tendons and ligaments insert primarily into this layer of the periosteum (Buckwalter and Cooper 1987; Cooper and Misol 1970). During development and skeletal maturity, the fibrous layer increases in density but decreases in thickness (Ellender et al. 1988).

The periosteum performs vital functions in the regulation of bone formation on the periosteal surface of bone. The cells within the periosteum respond to physiological levels of mechanical strain by cell proliferation, blood vessel formation, the release of nitric oxide, and prostaglandin E<sub>2</sub> production. The release of these factors stimulates bone formation through various molecular pathways (Keila et al. 2001; McKenzie and Silva 2011; Robling et al. 2006; Turner and Robling 2004). Also, periosteal cells respond to PTH, insulin-like growth factor (IGF-I), and growth hormone (GH) with bone formation. Estrogens inhibit periosteal bone formation, while androgens promote periosteal bone formation (Gosman et al. 2011).

The endosteum consists of a discontinuous layer of bone lining cells that lines the medullary cavity. The endosteum is not a true membrane because it is discontinuous. The endosteum functions as a regulator for calcium exchange by forming somewhat of a barrier between the extravascular fluid in the marrow cavity and the extracellular fluid within the bone matrix (Burr and Akkus 2013). Although extracellular fluid separates the endosteum from the endocortical

surface, bone lining cells are associated with capillaries near the endocortical bone surface and sinusoids within the marrow cavity. Diffusion is the principal mechanism for exchange between extracellular fluid in the bone marrow and the bone capillaries. Also, the cytoplasmic processes of endosteal bone lining cells penetrate the endocortical bone surface through canaliculi and maintain communication with osteocytes at gap junctions (Bellido et al. 2013). Similar to the endosteum, a discontinuous layer of bone lining cells also covers the trabecular surfaces (Burr and Akkus 2013).

### ***BONE FORMATION***

Skeletal development begins during the 6<sup>th</sup> week of gestation and continues into the postnatal years. Skeletal development occurs through intramembranous and endochondral ossification (Allen and Burr 2014a). Intramembranous ossification occurs in a condensation (aggregation into layers) of mesenchymal stem cells that differentiate directly into osteoblasts (Marks and Odgren 2002). Most cranial bones, all facial bones, the mandible, scapula, pelvis, and the central portion of the clavicle develop by intramembranous ossification (Buckwalter et al. 1995b; Scheuer and Black 2000a). Endochondral ossification occurs on a cartilage template called an anlage that is produced by chondrocytes. Bones that bear weight and participate in joints form by endochondral bone formation (Marks and Odgren 2002). Within the embryo, the first bones to form from endochondral bone formation are the long bones, such as the femur, tibia, fibula, humerus, radius and ulna. After formation of the long bones, short bones, and epiphyseal centers of ossification, endochondral ossification continues in the growth plate and epiphyses until skeletal maturity in the late teens to early adulthood (Buckwalter et al. 1995b). Remaining *in utero* until ~37 weeks gestation has important consequences for postnatal bone health and growth, which will be discussed further in the **Disease and Bone** section.

#### ***Intramembranous Bone Formation/Ossification***

At the start of skeletal development, intramembranous bone formation initiates prior to endochondral bone formation. The first step in intramembranous bone formation is the condensation of mesenchymal stem cells at the site of future bone formation (Arcy 1965; Buckwalter 1994; Buckwalter and Cooper 1987; Recker 1992; Sevitt 1981). A mesenchymal condensation is a membrane that consists of mesenchymal cells, a loose organic matrix synthesized by the mesenchymal cells, blood vessels, and fibroblasts (Buckwalter et al. 1995b).

This structure is also called a bone blastema. A mesenchymal condensation can develop as the result of increased proliferation mesenchymal stem cells or through the aggregation of mesenchymal stem cells drawn to a specific site (Hall and Miyake 1992). As the mesenchyme condenses, cells become more rounded and the intercellular substance decreases (Streeter 1949). Under the influence of the transcription factor RUNX2, mesenchymal stem cells within the blastema differentiate into osteoblasts. The osteoblasts begin to produce woven bone in the form of spicules which then mineralize. This initial production of bone matrix is called the primary ossification center and growth proceeds from this site (Allen and Burr 2014a). Eventually, the initial osteoblasts produce a small island of woven bone. Some osteoblasts become embedded within the matrix and develop into osteocytes. Additional osteoblasts are then recruited to the surface of the island of woven bone. These additional osteoblasts produce either woven or lamellar primary bone matrix. Once the growing island of bone becomes so large that the osteocytes at the center are not able to access an adequate blood supply, the osteocytes at the center undergo apoptosis. Blood vessels from nearby capillary networks penetrate the middle of the ossification center. Osteoblasts deposit matrix between the vessels. The matrix mineralizes and continues to extend and expand as more matrix is added by osteoblasts, leading to the formation of a trabecular network. The intervascular spicules of bone enclose the blood vessels as more mesenchymal cells differentiate into osteoblasts. This initial trabecular network is called the primary spongiosa. The primary trabeculae radiate centrifugally from the center of ossification and increase in length by accretion to their ends (Ogden 1979; Weinmann 1947). Small secondary trabeculae develop at right angles to the primary trabeculae, which develop into the cortical walls and enclose the vascular space that becomes the marrow cavity. As the rate of growth slows, the secondary trabeculae are replaced with a primary osteonal system to form the cortex (Scheuer and Black 2000a). Mesenchyme on the surface of the developing bone condenses and forms the periosteal membrane. As periosteal osteoblasts continuously produce layers of matrix, more osteoblasts become trapped within the matrix and develop into osteocytes within lacunae. The ultimate result is a bone with a cortex, extensive intracortical network of canals, trabeculae, and a marrow cavity. The scapula and clavicle are exceptions and do not form marrow cavities (Allen and Burr 2014a).

### ***Endochondral Bone Formation***

Like intramembranous bone formation, endochondral bone formation begins with mesenchymal condensation. However, under the influence of transcription factor Y-box 9 (SOX-9), the mesenchymal stem cells differentiate into chondroblasts instead of osteoblasts (Allen and Burr 2014a). The chondroblasts produce a hyaline cartilage matrix which consists of type II collagen and chondroitin sulfate (Scheuer and Black 2000a). As the matrix is being produced, some chondroblasts become embedded within the matrix and develop into chondrocytes. Eventually, a hyaline cartilage template that resembles the shape of the future bone is produced. The entire cartilage template is surrounded by a connective tissue layer called the perichondrium, which contains chondroblasts, mesenchymal stem cells and a vascular network. The cartilage template continues to grow in size through the proliferation of chondroblasts within the perichondrium and the deposition of cartilage matrix by these chondroblasts on to the cartilage template. At the center of the cartilage model, there is a linear, interstitial (between the cells) proliferation of columns of chondrocytes. As the cartilage model grows, the oldest chondrocytes near the center of the cartilage model begin to swell (hypertrophy).

Also as chondrocytes hypertrophy, the perichondrium develops osteogenic properties through the influence of transcription factor RUNX2 (Allen and Burr 2014a). In the central region of the cartilage template, the perichondrium thickens and osteoblasts differentiate from the mesenchymal stem cells within the perichondrium (Scheuer and Black 2000a). The osteoblasts are arranged in stacked layer of 4-6 cells that completely surround the cartilage template (Bruder and Caplan 1989). The osteoblasts surround capillaries from the perichondrial arterial network and deposit osteoid matrix on the surface of the cartilage template. The osteoid matrix is lamellar in organization and is quickly mineralized. Initially, the lamellar bone is restricted to the circumference of the cartilage model, forming a constricting cuff or bone collar. Ossification then radiates toward the epiphyses resulting in a sleeve of bone that envelops the entire diaphysis of the cartilage template. Once the bone collar has formed, the perichondrium surrounding the bone collar becomes populated with osteogenic precursor cells and develops into the periosteum. The periosteum is continuous with the perichondrium that covers the cartilaginous epiphyseal surfaces that remain unmineralized (Scheuer and Black 2000a).

Simultaneous to chondrocyte hypertrophy, the cartilage in between the hypertrophied columns of chondrocytes begins calcification. Formation of the bone collar limits the diffusion of nutrients into the cartilage matrix and may be responsible for initiating chondrocytes hypertrophy (Bruder and Caplan 1989). Calcification of the cartilage matrix surrounding the hypertrophied chondrocytes initiates near the center of the cartilage template and radiates outward. After the cartilage calcifies at the center of the template, the hypertrophied chondrocytes embedded in this calcified cartilage matrix undergo apoptosis and blood vessels are recruited to center of the bone collar. Chondrocyte apoptosis may release chemical factors that recruit a blood vessel or vascular bud to the bone collar. The vascular bud penetrates the bone collar through the formation of an irruption canal by osteoclastic resorption (Scheuer and Black 2000a). Although more than one blood vessel may penetrate the bone collar, only one will be dominant and develop into the nutrient artery. Ultimately, the site of penetration of the bone collar by the primary blood vessel becomes the nutrient foramen of the mature bone.

Penetration by the blood vessel into the center of the cartilage template permits hematopoietic and mesenchymal stem cells to enter the cartilage template. This increases the rate of calcification occurring in the remaining uncalcified portion of the cartilage template. The hematopoietic stem cells that enter the template differentiate into osteoclasts. The osteoclasts resorb the central portion of calcified cartilage resulting in the formation of the marrow cavity. As the marrow cavity forms and is populated with cells, bone matrix is continuously added to the periosteal surface of the bone collar. Meanwhile, the mesenchymal stem cells differentiate into osteoblasts and lay down osteoid in the walls of the calcified cartilage between the hypertrophied and dying chondrocytes forming an internal trabecular network of woven bone. Over time, osteoclasts resorb the immature woven bone and the calcified cartilage that remains at the center of the trabeculae, while osteoblasts replace it with a trabecular network of mature lamellar bone. Once ossification has commenced, the site becomes the primary ossification center. Bone matrix ossification occurs centrifugally from the primary ossification center and will eventually involve the middle third of the hyaline cartilage template.

Shortly after the primary ossification center has been established, a growth plate (also called the epiphyseal plate or physis) forms between the cartilaginous epiphyseal ends and the metaphysis of the ossifying diaphyseal shaft (Scheuer and Black 2000a). The growth plate is responsible for



longitudinal growth of bones through the continuous secretion of cartilage matrix by chondrocytes embedded within the matrix. Bones increase in length and not in thickness at the growth plate because upon reaching the metaphysis expansion is restricted, the matrix ossifies and is incorporated into the metaphysis. This will be covered in more detail below. The growth plate is described as having distinct zones with each representing a stage in the life cycle of the chondrocytes it contains (Martin et al. 1998c). These zones are called the resting zone (also reserve or germinal zone), proliferative zone, hypertrophic zone, zone of calcified cartilage, and the zone of ossification.

The zone most distant from the primary ossification center and closest to the epiphysis of the cartilage template is called the resting zone. The resting zone is comprised of hyaline cartilage in which mesenchymal cells are randomly distributed (Scheuer and Black 2000a). Each mesenchymal cell divides (mitosis) to produce a chondroblast and a remaining mesenchymal cell. Like the mesenchymal stem cells, the chondroblasts are randomly distributed. Chondroblasts that become embedded within the hyaline cartilage develop into chondrocytes. Type II collagen is continually produced by chondroblasts near the perichondrium, as well as chondrocytes already embedded within the resting zone matrix. The chondrocytes within the resting zone receive nutrients from epiphyseal blood vessels (Allen and Burr 2014a).

The proliferative zone follows the resting zone. Within the proliferative zone, chondrocytes repeatedly undergo mitosis and proliferate. Proliferation occurs in columns along the longitudinal axis causing the arrangement of chondrocytes to resemble stacked coins. Initially the chondrocyte cells are wedge-shaped and division occurs in the transverse plane. Following mitosis, the wedge-shaped daughter cells lay side-by-side with their narrow edges overlapping. As cells migrate towards the epiphyses, the narrow edges of the wedge-shaped chondrocytes expand and the chondrocytes become rectangular in shape (Scheuer and Black 2000a), forcing the originally oblique intercellular septum to become transverse. This results in chondrocytes that are aligned in columns. The chondrocytes within the proliferative zone continue to produce type II collagen and proteoglycans, but not as much as was produced in the resting zone.

The subsequent zone is the hypertrophic zone and it can be further divided into a prehypertrophic region and a lower hypertrophic region. The prehypertrophic zone is responsible for the majority

of longitudinal bone growth. In the prehypertrophic region, chondrocytes cease proliferation, increase in size, and transition from producing type II collagen to secreting large amounts of type X collagen and alkaline phosphatase (Rauner et al. 2012). The bone collar restricts growth in the radial direction, forcing growth in the longitudinal direction (Martin et al. 1998c). Type X collagen contains fibers that are not present in type II collagen, which increases the stiffness of type X collagen in comparison to type II collagen. The increased stiffness of the surrounding cartilage matrix decreases the diffusion rate of nutrients through the matrix. Without adequate access to nutrients or removal of extracellular waste, chondrocytes in the lower hypertrophic zone stop producing cartilage matrix. The chondrocytes continue to enlarge and enter the early stages of apoptosis by producing molecules that prepare adjacent cartilage for calcification. Release of these molecules is a requirement for the initiation of vascular invasion which occurs in the subsequent zones.

The next zone is called the calcified cartilage zone. As the cartilage matrix around the dead or dying chondrocytes condenses due to the incorporation of type X collagen, it also begins to calcify. After or prior to apoptosis, chondrocytes release vesicles into the condensed, extracellular cartilage matrix. The vesicles contain alkaline phosphatase (ALP), ATPase, and enzymes. ALP is a key contributor to the mineralization of the cartilage matrix by increasing the localized phosphate levels (Anderson and Morris 1993). The ATPase provides energy for the transport of calcium ions into the vesicles against the concentration gradient (Martin et al. 1998c; Scheuer and Black 2000a). Enzymes cleave calcium and phosphate from the surrounding environment, which increases the local mineral concentrations within the vesicles. Increased concentrations initiate calcium-phosphate (calcium hydroxyapatite) crystal growth which grow in size within the vesicle until they rupture the vesicle membrane and break free (Eanes and Hailer 1985). The hydroxyapatite crystals that break free from the vesicles serve as seed crystals. Through a process called epitaxy, the seed crystals act as substrate for new hydroxyapatite crystal proliferation (Neuman and Neuman 1953). Collagen is a favorable environment for epitaxy to occur (Arsenault 1989). The growing hydroxyapatite crystals displace water molecules within the collagen matrix by embedding themselves within the collagen, leading to the calcification of the collagen matrix. As the matrix calcifies through the process of epitaxy, more chondrocytes undergo apoptosis which signals for local vascular invasion metaphyseal vessels (Scheuer and Black 2000a).

The last zone of the growth plate is called the zone of ossification and is located where the growth plate ends and the metaphysis begins. As chondrocytes hypertrophy, they produce matrix metalloproteinase 13, which dissolves some of the surrounding cartilage (Stickens et al. 2004). The transversely oriented calcified cartilage septa are dissolved and the vertically oriented septa, although more narrow, remain mostly intact (Rauner et al. 2012). Once the chondrocytes die, only narrow walls called septa are left between the large and now empty lacunae. Monocyte derived cells called septaclasts resorb the septa at the bottom of each chondrocyte column (Hunziker 1994; Lee et al. 1995; Price et al. 1994). Once the septa are resorbed, blood vessels and cells from the metaphysis are able to gain access to the bottom of the growth plate through the tunnels and open spaces left behind by dead chondrocytes (Martin et al. 1998c). Trabeculae are the vertical walls of calcified cartilage that form the tunnel walls. The invading vasculature brings progenitor cells to the site. Chondroclasts resorb some of the calcified cartilage on the tunnel walls, or surfaces of the trabeculae. Osteoblasts then line the surfaces of the trabeculae and deposit woven bone on their surfaces. The conversion of calcified cartilage to mineralized bone marks the transition from the growth plate to the metaphyseal trabeculae. The trabecular tissue transitioning from calcified cartilage to ossified bone is called primary spongiosa. The trabecular struts of the primary spongiosa contain calcified cartilage within their cores. Eventually, the calcified cartilage within the trabecular core will be entirely replaced with lamellar bone to form the secondary spongiosa. This will be discussed in more detail in the Remodeling Section. As growth progresses, the trabeculae at the center of the metaphysis are eventually entirely resorbed to make room for the medullary cavity and the remaining trabeculae form an arch to transfer loads from the center of the growth plate to the cortices of the diaphysis.

For simplicity, the zones were described as distinct. However, as growth occurs, there is a gradual transition from one zone to the next (Allen and Burr 2014a). Chemical factors are responsible for the transition of cellular processes from one zone to the next. Growth hormone (GH), insulin-like growth factors (IGFs), Indian hedgehog (IHH) protein, bone morphogenic proteins (BMPs), and the Wnt signaling pathway influence chondrocyte proliferation. Fibroblast growth factor (FGF) inhibits chondrocyte proliferation (Allen and Burr 2014a; Nilsson et al. 1994). Under the influence of thyroxine and the Wnt signaling pathway, chondrocytes hypertrophy, while IHH protein and PTH-related protein (PTHrP) inhibit chondrocyte hypertrophy (Allen and Burr 2014a).

At birth, the growth plate is typically flat and disc-like in shape. During growth, the bones become larger and the growth plate must also increase in diameter. The growth plate increases in diameter by cellular division at the circumference. This zone of dividing cells called the zone of Ranvier. Also during growth, the growth plate transitions from a flat surface to being a curved surface with a system of ridges, valleys, and flaps. The purpose of these ridges is to protect the cartilage within the growth plate from shearing forces (Martin et al. 1998c).

Prior to birth, some of the long bones establish secondary centers of ossification within the epiphyses. Ossification of the secondary centers is similar to the processes described for the ossification of the diaphysis. Ossification initiates through vascular invasion by epiphyseal vessels. However, the trabeculae are retained during ossification of secondary centers, while they are resorbed or largely resorbed during the ossification of primary centers (Alini et al. 1996).

Once the growth plate completely ossifies, longitudinal growth ceases and the epiphyseal and metaphyseal vascular systems unite. The growth plate begins to completely ossify when activity within the zone of ossification exceeds chondrocyte repopulation in the resting zone. This process is called epiphyseal union (Rang and ed 1969). The growth plate shrinks in size until it disappears, leaving behind a thin plate of mineralized bone between the epiphysis and the metaphysis, which is called the epiphyseal line (or physeal scar) (Martin et al. 1998c; Scheuer and Black 2000a). Depending on the specific bony element, this occurs in the late teens to the early twenties (Riggs et al. 1999).

### ***Modeling and Remodeling***

While bone formation results in the basic bone shape, the processes of modeling and remodeling are required for maintaining bone shape during growth and for repair and maintenance of the skeletal tissue throughout life. Therefore, bone remodeling does not usually result in changes to bone shape or size. Bone modeling alters the shape of bones through bone apposition and resorption, but both processes do not occur at the same site at the same time. Bone formation (endochondral ossification and intramembranous ossification) differs from bone modeling in that formation produces a bone where none previously existed, while the bone modeling process can only deposit or resorb bone from a preexisting bone surface. Modeling at a site is usually continuous and prolonged (Martin et al. 1998c). Modeling modifies bone structure in ways that

increases bone strength without adding excessive weight to the skeleton. Bone remodeling is episodic and occurs through the coupled processes of bone resorption and deposition at the same site (Allen and Burr 2014a). Bone remodeling has several functions, which are to mobilize calcium from the skeleton for purposes of calcium homeostasis, replace old bone tissue, repair damaged bone tissue, and to adapt the skeleton to better withstand changes in loading patterns. Bone fragility can result when either of these processes is compromised.

### **Modeling**

Although modeling takes place in adults, it occurs predominantly during growth and occurs on the periosteal, endocortical, and trabecular bone surfaces. Approximately 90% of modeling is complete by the end of adolescence (Bartl et al. 2009). The primary functions of bone modeling are to increase bone mass and maintain or alter bone shape. Bone modeling by osteoblasts is called formation modeling and can be divided into two categories, appositional or periosteal intramembranous bone formation. Formation modeling on the periosteal surface is considered intramembranous bone formation because the osteoblasts and precursor cells that deposit osteoid on the periosteal surface are located within the periosteal membrane and are not directly on the bone surface (Martin et al. 1998c). The deposition of osteoid on the trabecular and endocortical bone surfaces is called appositional formation. Bone modeling by osteoclasts is called resorptive modeling. Locally, formation and resorption modeling occur independently of one another, meaning that bone is added at some sites while simultaneously being removed from others (Martin et al. 1998c). However, formation and resorptive modeling are not globally independent, their simultaneous actions on a single bone are coordinated to alter or maintain a bone's overall shape, which plays an important role in fracture resistance.

Although the actions are coordinated, specific bone surfaces are targeted by osteoblasts and osteoclasts during modeling to alter and maintain bone shape. Metaphyseal modeling is necessary during longitudinal growth in order to maintain normal long bone shape. To maintain long bone shape, the area that was formerly the metaphysis must decrease in diameter to become a new section of the diaphysis. As the bone increases in length, resorption removes bone on periosteal surface of the metaphysis while formation adds bone to the endocortical surface of the metaphysis in order to maintain mechanical strength. Epiphyseal modeling includes both increase in diameter and length.

As bones grow in length, the diaphysis must also increase in diameter (radial growth). Formation modeling on the periosteal surface (appositional formation) is the major mechanism for radial growth of the diaphysis (Allen and Burr 2014a). A relatively consistent cortical thickness is maintained throughout growth by simultaneous resorptive modeling on the endosteal surface of the diaphysis which also increases the size of the medullary cavity (Ortner and Turner-Walker 2003). After completion of growth, the diaphysis continues to increase in diameter by appositional growth and endosteal resorption, but at a greatly reduced rate (Keshawarz and Recker 1984; Ruff and Hayes 1982).

Modeling of the diaphysis is sexually dimorphic. Males have larger and thicker bones than females. During puberty, the release of estrogens in females inhibits periosteal formation which results in smaller bones due to decreased formation modeling in females. Androgens, such as testosterone, growth hormone, and IGF-I, which increase formation modeling on the periosteal surface, are greatly increased in pubescent boys resulting in thicker cortices. Other factors such as mechanical loading, PTH, and sclerostin also affect radial growth (Allen and Burr 2014a).

Predominantly during growth and occasionally after maturity, bone shape needs to be altered to adjust the position of the cortex relative to the bone's central axis. The process of altering a bones shape for these purposes is called bone drift. Bone drift occurs by formation modeling on one periosteal and endosteal surface while resorption modeling is simultaneously occurring on opposing periosteal and endosteal surfaces (Enlow 1963).

Local tissue strain is the primary signal for modeling (Allen and Burr 2014a). During growth, stresses and strains on skeletal tissue change due to increases in bone length and due to alterations in the intensity and type of physical activity (Scheuer and Black 2000a). If tissue strain surpasses a given threshold, formation modeling is initiated and new bone matrix is deposited. If strains remain too low for too long, resorptive modeling is initiated. This is also referred to as the mechanostat theory (Frost 2001; Frost 2003b) and will be discussed in further detail in the **Bone Biomechanics** section. Once modeling has been activated, precursor cells, either hematopoietic or mesenchymal, are recruited to the site and differentiate into osteoclasts or osteoblasts, respectively. Bone lining cells can also be activated and differentiate into

osteoblasts. After enough bone tissue has been added or removed from cortical and/or trabecular bone to normalize local strains, modeling ceases.

### **Remodeling**

Primary bone formed through ossification and modeling is short-lived and is replaced with secondary bone through a process called remodeling (Scheuer and Black 2000a). Remodeling consists of the removal of old bone, both primary and secondary, woven and lamellar, and its replacement with new lamellar bone. Remodeling is continuous throughout life, but the remodeling rate decreases after maturity. Remodeling can be described as targeted or stochastic. The function of targeted remodeling is to repair mechanically compromised bone matrix. In targeted remodeling, there is a specific local signaling event that directs osteoclasts to a particular remodeling site. Signals that initiate targeted remodeling are microdamage and/or osteocyte apoptosis. Microdamage disrupts the cytoplasmic network that connects osteocytes. Once this connection is disrupted, the osteocyte is cut off from communication with other cells and begins to undergo apoptosis. As the cell undergoes apoptosis it releases RANKL, a key factor in osteoclast development. Osteocytes near the dying osteocyte/s secrete OPG, an antiapoptotic signal. This pattern of signals guides osteoclast precursor cells to the targeted resorption site. Stochastic remodeling is a random process in which osteoclasts initiate bone resorption without location-specific signaling. Stochastic remodeling is to have a larger role in calcium homeostasis (Allen and Burr 2014a).

Regardless of whether remodeling is targeted or stochastic, the cellular processes are similar (Allen and Burr 2014a). Remodeling consists of the spatial and temporal coupling of bone resorption and formation by osteoclasts and osteoblasts (Recker 1992; Rodan and Martin 1981), meaning that it is a coordinated effort by osteoclasts and osteoblasts to resorb a discrete section of bone and replace it with a packet of bone called a quantum packet or bone structural unit (Frost 2003a; Parfitt 1994; Parfitt 2000; Parfitt 2003). The collection of osteoblasts and osteoclasts for the purposes of remodeling is called a basic multicellular unit (BMU) and is ~1-2 mm long and 0.2-0.4 mm wide. There are ~1 million active BMUs at any given time and ~3-4 million BMUs are activated per year (Bartl et al. 2009). The BMU travels, resorbing and replacing bone as it moves on the bone surface or through the bone matrix. In general, resorption and formation occur at the same time, but at different location within the BMU. The front end or “head” of the BMU contains a capillary bud at its center to supply nutrients to the bone cells and

progenitor cells to replace the bone cells that undergo apoptosis during the remodeling process (Martin et al. 1998c; Ortner 2008). The collection of cells that form the BMU is covered on the bone surface by a canopy called the bone remodeling compartment (BRC). Research suggests that this canopy is composed of bone lining cells (Rauner et al. 2012). A BMU consists of 9-10 osteoclasts and several hundred osteoblasts operating simultaneously (Jaworski et al. 1981; Martin et al. 1998c). The osteoclasts are located at the head of the BMU, along with the capillary bud. This location is called the cutting cone. The osteoblasts are located at the far end of the BMU. This location is called the closing cone.

Although the processes carried out by the BMU are the same, the results of remodeling differ slightly depending on the surface on which remodeling is occurring, intracortical, endosteal, periosteal, or trabecular. In intracortical remodeling, the BMU will form a cylindrical shaped tunnel (Haversian resorption space) approximately 2,000  $\mu\text{m}$  long and 200  $\mu\text{m}$  wide and replace the resorbed bone with a secondary osteon. Remodeling of trabecular, periosteal, or endocortical is mostly on the surface. BMUs move over these surfaces of bone, digging ditches approximately 50  $\mu\text{m}$  deep and replacing the bone with hemiosteons along the way (Allen and Burr 2014a; Hauge et al. 2001; Martin et al. 1998c; Parfitt 1994; Parfitt 2003; Rauner et al. 2012). Overall, trabecular bone has a much higher turnover rate per year, ~25%, than cortical bone, ~2.5-5% per year, because trabecular bone has a much higher surface area to volume ratio than cortical bone and osteoclasts are readily available for resorption within the marrow cavity (Bartl et al. 2009; Done 2012). For this reason, it was hypothesized that medullary cavity diameter would be positively associated with chronic illness, due to the increased resorption on endocortical surfaces. The periosteal surface has the lowest remodeling rate of all the bone surfaces (Allen and Burr 2014a).

The remodeling cycle carried out by BMU as it moves occurs in a predictable sequence of events, which is activation, resorption, reversal, formation, and quiescence (Allen and Burr 2014a; Jaworski et al. 1983; Parfitt 1988). From activation to quiescence, and absent of pathology, the entire remodeling cycle occurs over 4-6 months (Baron 1999). In the activation stage, chemical signals originating from the marrow cavity, periosteum, or vasculature within an existing osteon activate bone lining cells that cover the resting bone surface (Allen and Burr 2014a; Everts et al. 2002; Hauge et al. 2001; Parfitt 1994; Parfitt 2003; Raisz 1999). Bone lining



cells release signals that recruit a vessel from the local blood supply and precursor cells to the remodeling site. The local blood vessel supplies chemical signals that enable precursor cells to differentiate into osteoclasts and osteoblasts (Parfitt 2003). The activation stage can take up to 3 days (Martin et al. 1998).

The second stage is resorption and occurs over 2-3 weeks (Rauner et al. 2012). Once differentiated osteoclasts are present, bone lining cells retract from the bone surface and expose the mineralized matrix to the osteoclasts (Allen and Burr 2014a). The bone lining cells then form the BRC over the BMU and remodeling site. Newly differentiated osteoclasts adhere to the bone surface and secrete acids and enzymes into the resorption space between the osteoclast and bone surface. The scalloped shaped hole in the bone surface created by a single osteoclast is called a Howship's lacuna. Osteoclasts resorb primary bone at  $\sim 40\text{-}50\ \mu\text{m}$  per day (Martin et al. 1998c). The collection of 9-10 osteoclasts resorbing bone at the front the BMU is called the cutting cone. The cutting cone moves more or less parallel to the longitudinal axis of the bone, but it spirals slightly at an angle of curvature of  $\sim 12^\circ$  (Petryl et al. 1996). There is significant variability in the size of remodeling sites on the endocortical and trabecular surfaces. The width of intracortical resorption sites is relative consistent, but the length varies (Allen and Burr 2014a). As resorption proceeds new osteoclasts are recruited to the site to support the osteoclasts in the cutting cone or to replace osteoclasts that die. The cutting cone tunnels through the matrix without regard for previously established osteons. Fragments of the previous osteons are left between the newly forming secondary osteon and other intact osteons, creating interstitial lamellae.

The third stage is reversal. Reversal is a stage of transition between the leading osteoclastic cutting cone and the following osteoblastic region of bone formation. During reversal, mononuclear cells of an unknown lineage, possibly osteomacs (Pettit et al. 2008), or bone lining cells prepare the bone surface for osteoid deposition by removing any resorption remnants left at the bottom of the pit (Everts et al. 2002; Rauner et al. 2012). Osteomacs have been proposed as a candidate because they produce matrix metalloproteinases (MMPs), which are required for matrix degradation, and transforming growth factor- $\beta$  (TGF- $\beta$ ), and ephrin B2, which may promote osteoblast recruitment, differentiation, and/or activation of bone lining cells (Chang et al. 2008; Compagni et al. 2003). If the remnants of collagen fragments on the exposed surface

are not removed, bone formation by osteoblasts does not proceed (Allen and Burr 2014a). The reversal cells may also be responsible for depositing a thin layer of specialized matrix which forms the cement line. The cement line marks the resorption boundary and isolates secondary osteons and hemiosteons from the surrounding matrix (Baron 1999; Everts et al. 2002; Parfitt 2000). The cement line consists of mineral, glycosaminoglycans, osteopontin, and some collagen (Burr and Akkus 2013). The degree of mineralization of the cement line is not known, but it differs from the surrounding matrix.

During the formation stage, osteoblasts line the surface of the resorption space and deposit osteoid at a rate of 1-2  $\mu\text{m}$  per day (Allen and Burr 2014a). In adults, bone formation occurs over ~2-3 months. Throughout the formation stage, osteoblasts are continuously recruited to the site to replace osteoblasts that undergo apoptosis. In the formation of secondary osteons, osteoblasts deposit osteoid in the form of concentric lamellae and the resorption tunnel is not completely filled with osteoid. A Haversian canal is left behind to house the capillaries that are at the head of the migrating BMU. Within the Haversian canal, there is a supply capillary and a return capillary. These vessels connect with vasculature on the periosteal surface or in the medullary canal (Martin et al. 1998c). In the formation of hemiosteons, it is not necessary to leave an open space for blood vessels. Sheets of lamellae are deposited until the resorption space is filled. In the formation of both hemiosteons and secondary osteons, some of the osteoblasts become embedded in the matrix and develop into osteocytes. The collection of osteoblasts laying down lamellar bone is called the closing cone (Polig and Jee 1990).

The fifth stage of secondary osteon formation is called mineralization. Mineralization of bone collagen fibrils occurs in an organized sequence over two phases. After the osteoid matrix is deposited, mineralization initiates with the growth of mineral crystals between the layers of collagen fibrils of the osteoid matrix (Landis 1995). Initiation of mineralization begins after 10-15 days from the time of osteoid deposition by osteoblasts (Bartl et al. 2009). Once mineralization has initiated, approximately 50-75% (depending on the reference consulted) of an osteon's final mineral content is deposited into the newly formed osteoid within hours (Amprino and Engstrom 1952; Bartl et al. 2009; Buckwalter et al. 1995a; Ortner 2008). This is called primary mineralization. The final addition and maturation of hydroxyapatite crystals will occur during secondary mineralization. Completion of secondary mineralization can take between

several months to a year (Allen and Burr 2014a; Sommerfeldt and Rubin 2001). Secondary mineralization is a much slower process than primary mineralization because the mineral ions, cell nutrients, and cell metabolites must pass through the canalicular system to reach the matrix undergoing mineralization. The rate of secondary mineralization decreases further with increasing age (Ortner and Turner-Walker 2003). Differences in mineral content between newly formed and more mature osteons result in osteons with different mechanical properties.

The last stage is called quiescence. Any remaining osteoclasts and most osteoblasts undergo apoptosis. Some osteoblasts develop into quiescent bone lining cells until another cycle of remodeling is initiated (Allen and Burr 2014a; Martin et al. 1998c; Rauner et al. 2012). An osteon in the quiescent stage is fully mature and its surface is covered with bone lining cells. Secondary mineralization continues into the quiescent stage. In adult bone, the degree of overall bone mineralization is dependent on the rate of remodeling (Bartl et al. 2009).

### **Nutrition and other Prenatal Factors Affecting Skeletal Development**

Diet is the second greatest contributor to variation in skeletal development after genetic background (Weaver and Fuchs 2014). Adequate nutrition is important for building a healthy skeleton and is most important during periods of rapid growth. Nutritional deficiencies can adversely affect achievement of peak height and bone mass, as well as increase the risk for age-related bone loss. Protein-calorie malnutrition and mineral deficiencies can cause growth stunting (Weaver and Gallant 2014). Micronutrients, such as minerals and vitamins, play an important role in skeletal health and can only be obtained from the diet. Vitamin D is an exception and will be discussed in more detail below. The skeleton functions as a reservoir for 99% of total body calcium, 85-90% of total body phosphorus, and 50% of total body magnesium (Martin et al. 1998c; Ortner 2008). Calcium, phosphorus, and magnesium are essential for various cellular processes, but only a small portion of these minerals can be stored in the extracellular fluid. The body will sacrifice skeletal health to release these minerals from the bone into the circulatory system to ensure that other more vital organ systems continue to function (Lanham-New et al. 2007). Maintaining a healthy skeleton requires sufficient intake of calcium, phosphorus, and magnesium, as well as other vitamins and macronutrients. Nutritional

insufficiencies can occur as a result of chronic illness or prematurity, putting these infants at greater risk for developing bone fragility.

### ***CALCIUM***

Adequate intake of calcium is extremely important. As much as 500 mg of calcium is mobilized from the skeleton to the extracellular fluid daily (Weaver and Gallant 2014). Dairy products are the primary source of dietary calcium, as well as fortified juices. However, dietary intake of calcium is often below the recommendation, which can create deficiencies that adversely affect bone. Calcium has a structural role within bone. During mineralization and in combination with phosphorus, calcium controls the rigidity and hardness of bones and teeth through the formation of hydroxyapatite crystals. Intestinal absorption and renal reabsorption are major sources of serum calcium. After intestinal absorption, calcium enters the circulation where it is transported to the skeleton or to the kidneys. The skeleton utilizes calcium for mineralization, to line bone surfaces, and also maintains it within the extracellular fluid of the canalicular network (DiMeglio and Imel 2014).

### ***PHOSPHORUS***

Due to the abundance of dietary phosphorus, most individuals consume adequate amounts. Phosphate is a key component of many biochemical compounds and has 3 major roles: structural, regulatory, and metabolic. As a component of hydroxyapatite crystals, phosphorus plays a structural role in bone (Weaver and Gallant 2014).

### ***MAGNESIUM***

On average, magnesium intake is less than the recommendation. Magnesium is the third most abundant mineral in bone and contributes to mineralization, hormone secretion, and energy metabolism. Magnesium seeds hydroxyapatite crystal formation. Due to its smaller ionic radius, magnesium also prevents hydroxyapatite crystals from becoming too large. As hydroxyapatite crystals become larger, they increasingly become more brittle. Magnesium deficiency has been associated with osteopenia and bone fragility (Weaver and Gallant 2014).

### ***OTHER MICRONUTRIENTS***

Other micronutrients, such as zinc, copper, and iron, influence bone quality through their effects on connective tissue synthesis and maturation. Zinc stimulates osteoblastic bone formation, collagen synthesis, and bone resorption. However, excessive zinc consumption limits the size of hydroxyapatite crystals. Iron and copper are cofactors for enzymes involved in collagen synthesis and cross-linking. Iron deficiency increases cortical porosity. Depending on the severity and chronicity, deficiencies in these minerals can have negative effects on bone health, such as osteopenia and increased fracture risk (Shaw 1982; Weaver and Gallant 2014).

Vitamins D, C, K, and A also play important roles in bone health. Vitamin D is an extremely important hormone that can be made endogenously or obtained from dietary sources. Vitamin D increases intestinal absorption of calcium and phosphorus, as well as promotes mineralization. Vitamin D will be discussed further in the Mineral Homeostasis section. Vitamin C is necessary for collagen formation and crosslinking. Also, vitamin C stimulates ALP production, which is important for bone formation. Severe vitamin C deficiency impairs mineralization (Shaw 1955). Vitamin K is a cofactor of vitamin K-dependent gamma carboxylase, which is necessary for the activation of osteocalcin, a factor produced by osteoblasts that is involved in bone formation and mineralization. Osteoblasts and osteoclasts possess vitamin A receptors, suggesting that vitamin A influences bone remodeling. Vitamin A is necessary for epiphyseal cartilage cell function and deficiency will impair growth (Shaw 1955). Excessive intake of vitamin A has also been associated with poor bone mineralization. Both deficiency and excessive intake of vitamin A have been associated with low BMD and fracture risk (Weaver and Gallant 2014).

### ***MACRONUTRIENTS***

Protein and fat are essential macronutrients for bone health. Protein forms an important part of the organic bone matrix and is 5-10% of bone weight. Protein is especially important during growth. Through its positive influence on IGF-I production, high protein intake increases calcium absorption, bone formation and longitudinal bone growth. Fat forms 5-10% of bone weight but an excess of fat intake, resulting in obesity, increases fracture risk in children by adversely affecting peak bone mass during growth (Weaver and Gallant 2014).

## ***OTHER PRENATAL FACTORS AFFECTING SKELETAL DEVELOPMENT***

Intrauterine factors can adversely affect fetal skeletal development (Weaver and Fuchs 2014). Negative stimuli *in utero* can result in slowed growth, reduced bone size, and reduced mineralization of the fetal and infant skeleton. Although there is no way to control for these effects, it is important to be aware of factors that can negatively affect fetal skeletal development and health. Negative effects on trabecular bone microstructure have also been reported as a result of maternal-fetal perturbations (Nuzzo et al. 2003; Salle et al. 2002). Research has shown that maternal obesity, smoking, nutrition at 18 weeks of gestation, and high maternal physical activity negatively affect fetal bone development (Godfrey et al. 2001; Högler et al. 2003). Smoking during pregnancy reduces fetal bone mass by 11% and leads to smaller bone size, possibly by compromising placental function and oxygenation of the fetus (Weaver and Fuchs 2014). The toxic effects of cadmium, which is found in cigarette smoke, negatively affects osteoblastic function and placental transport of calcium (Godfrey et al. 2001). Chronic maternal alcohol abuse inhibits osteoblast differentiation, proliferation, and function, resulting in lower fetal bone mass (Weaver and Fuchs 2014). Maternal inhalant abuse has similar negative effects on fetal skeletal development as maternal alcohol use (Jones and Balster 1998). Gestational diabetes can result from maternal obesity. Neonates born to mothers with gestational diabetes may be born with hypocalcemia due to reduced placental transport of calcium during gestation. The hypocalcemia may continue postnatally, resulting in decreased skeletal mineralization (Weaver and Fuchs 2014).

## **Mineral Homeostasis**

As stated previously, mineral homeostasis is the process by which the body maintains normal serum calcium and phosphorus concentrations. Serum calcium and phosphorus levels are maintained within a limited range, with serum calcium concentrations being more strictly maintained than phosphorus concentrations. Mechanisms for the regulation of calcium homeostasis operate within minutes to correct aberrant serum calcium concentrations, while the mechanisms that maintain phosphorus concentrations are slower and can take hours to days. The total serum calcium concentration is maintained between 8.5-10.5 mg/dL (DiMeglio and Imel 2014). Approximately half of the total serum calcium concentration is ionized ( $\text{Ca}^{2+}$ ) and the remainder is protein bound (Salter 1999a). Normal serum phosphorus concentration is ~3

mg/100 mL in adults and 5 mg/100 mL in children (Salter 1999a). It is important to understand mineral homeostasis and the hormones that regulate it because they can greatly affect bone structure and strength through its influence on bone resorption. An excess of bone resorption caused by various mineral and vitamin deficiencies can weaken the bone. Deficiencies resulting in excessive bone resorption will be discussed further in the section **Disease and Bone**.

Mineral homeostasis can be maintained by keeping dietary intake of calcium and phosphorus above the level of excretion (Ortner 2008). A feedback system maintains this balance through regulation by hormones. PTH, the active metabolite of vitamin D [1,25(OH)<sub>2</sub>D], calcitonin, and PTHrP are the primary regulators of mineral homeostasis (Bartl et al. 2009). Postnatally, PTH and 1,25(OH)<sub>2</sub>D are the most important hormones for mineral homeostasis. These hormones also partially regulate the feedback system through direct effects on bone cells. Calcitonin and PTHrP play a larger role in fetal skeletal development and will be discussed below in the **Fetal and Neonatal Mineral Homeostasis section**.

### ***SERUM CALCIUM HOMEOSTASIS***

Serum calcium concentration is detected by calcium receptors (CaSRs) on C cells of the parathyroid gland. Calcium binding to CaSRs on the parathyroid gland, which occurs during normal and excessive serum calcium concentrations, inhibits PTH secretion (Allgrove 2009). The interaction of calcium with a CaSR activates phospholipase C (PLC) on the C cells, stimulating the release of diacylglycerol (DAG) from phosphatidylinositol-4,5-bisphosphate (PIP<sub>2</sub>), and the production of inositol-1,4,5-triphosphate (IP<sub>3</sub>). IP<sub>3</sub> triggers intracellular release of calcium from the endoplasmic reticulum, which increases the intracellular calcium concentration and suppresses secretion of the stored PTH secretory granules. The binding of calcium to the CaSR also suppresses the expression of PTH genes by activating inhibitory G proteins. Inhibitory G proteins inhibit adenylate cyclase functioning, which then inhibits the production of cAMP by inhibiting the action of adenylate cyclase on ATP. Without cAMP, signaling for the production of PTH is suppressed.

Under conditions of low calcium intake, serum calcium concentrations decrease and calcium fails to bind CaSRs of the parathyroid gland. Without the calcium binding, CaSR signaling decreases, increasing cAMP formation and increasing the production and secretion of PTH. PTH

is released into the circulatory system where it binds to receptors in the kidneys and bone (Rauner et al. 2012). Within the kidneys, PTH increases renal reabsorption of calcium through active pathways and promotes the synthesis of  $1,25(\text{OH})_2\text{D}$  (Allgrove 2009). Through its effect on bone resorption, renal reabsorption, and the production of  $1,25(\text{OH})_2\text{D}$ , PTH increases the overall calcium serum concentration (Buckwalter et al. 1995b).  $1,25(\text{OH})_2\text{D}$  increases the efficiency of calcium absorption within the intestines through active pathways, thereby increasing the serum calcium and phosphorus concentrations (Civitelli et al. 1998; Heaney 1997; Wasserman 1997).

$1,25(\text{OH})_2\text{D}$  is essential for the metabolism of calcium and phosphorus. To maintain calcium homeostasis under conditions of low serum calcium, active transport of calcium is upregulated by  $1,25(\text{OH})_2\text{D}$  to increase the efficiency of intestinal absorption. The metabolically active form of vitamin D ( $1,25(\text{OH})_2\text{D}$ ) is formed within the body from the hydroxylation of inactive forms (Francis and Selby 1997; Hochberg 2003; Holick 2003; Mankin 1974). Pre-vitamin D can be synthesized in the skin or obtained from the diet. The majority of pre-vitamin D is made within the skin (Allgrove 2009) when 7-dehydrocholesterol is exposed to ultraviolet B light (UVB) and heat (DiMeglio and Imel 2014). Pre-vitamin D produced within the skin is referred to as vitamin  $\text{D}_3$ . With adequate sun exposure, supplementation of vitamin  $\text{D}_3$  with dietary sources is not necessary, but this is not always possible. With regard to dietary sources, vitamin D can be obtained from plant (ergocalciferol,  $\text{D}_2$ ) or animal (cholecalciferol,  $\text{D}_3$ ) sources. After production in the skin or absorption from dietary sources, vitamin D (unspecified source) is incorporated into fat-containing particles (micelles). Incorporation of vitamin D into micelles allows it to diffuse across the enterocytes of the intestines and enter the circulation. Approximately 40% of the circulating vitamin D is stored in fatty particles called chylomicrons. The remainder of the vitamin D is bound to vitamin D-binding protein (DBP) and remains within the circulation.

The vitamin D bound to DBP is transported through circulation to the liver. Within the liver and mediated by 25-hydroxylase, vitamin D is hydroxylated once on its side chain carbon-25 to form 25-hydroxyvitamin D [ $25(\text{OH})\text{D}$ ]. Like the preform of vitamin D,  $25(\text{OH})\text{D}$  is transported within the serum by DBP. Generally,  $25(\text{OH})\text{D}$  is a stable metabolite of vitamin D and has a biological half-life of 2-3 weeks in the circulation. However,  $25(\text{OH})\text{D}_2$  (derived from plant sources) has a shorter half-life in the circulation than  $25(\text{OH})\text{D}_3$  (from animal and endogenous sources) because



of its lower affinity for DBP. Upon reaching the kidneys through the circulation, most of the 25(OH)D-DBP complexes are reabsorbed. Cell membrane receptor complexes (cubilin and megalin) bind the 25(OH)D-DBP complexes and endocytosis is initiated. The process is very efficient and little 25(OH)D is excreted in the urine (DiMeglio and Imel 2014). 25(OH)D remains in the circulation until it degrades or is activated by a second hydroxylation stimulated by PTH.

Low serum calcium concentration stimulates PTH secretion, which is transported by the circulation to the kidneys. Within the kidney, PTH stimulates  $1\alpha$ -hydroxylase production by initiating transcription of the *CYP27B1* gene (DiMeglio and Imel 2014). The  $1\alpha$ -hydroxylase adds an OH molecule to the carbon-1 position, creating the active vitamin D metabolite 1,25(OH)<sub>2</sub>D (Holick and Adams 1990; Raisz and Rodan 1990; Russell et al. 1990).

Overproduction of 1,25(OH)<sub>2</sub>D is suppressed through the binding of 1,25(OH)<sub>2</sub>D to vitamin D receptors (VDRs) within the parathyroid glands and vitamin D responsive elements (VDREs) within the *CYP27B1* gene, which suppresses PTH and  $1\alpha$ -hydroxylase production respectively. Binding of 1,25(OH)<sub>2</sub>D also induces 24-hydroxylase expression, which suppresses the actions of 1,25(OH)<sub>2</sub>D and 25(OH)D. Hydroxylation of 1,25(OH)<sub>2</sub>D and 25(OH)D by 24-hydroxylase forms 1,24,25(OH)<sub>3</sub>D and 24,25(OH)<sub>2</sub>D, resulting in their inactivation and degradation (DiMeglio and Imel 2014).

Increased serum calcium concentration is also gained through bone resorption triggered by PTH. (Bellido and Hill Gallant 2014). Bone's response to PTH is surface-specific and has multimodal-metabolic effects which depend on length of exposure (Gosman et al. 2011). Cells of the mesenchymal/osteoblastic lineage possess PTH/PTHrP receptors (PTH1-R) (Bellido and Hill Gallant 2014). Binding of PTH by these cells stimulates RANKL and IL-6 production and downregulates OPG production. The processes stimulated by PTH result in rapid (minutes to hours) loss of calcium adhered to the canalicular and lacunar surfaces that surround osteocytes and their cytoplasmic extensions (DiMeglio and Imel 2014; Jande 1972). RANKL and IL-6 stimulate osteoclast precursor cells to differentiate and become active, as well as promotes osteoclast survival (Dai et al. 2006; Greenfield et al. 1993; Ibbotson et al. 1984; Raisz 1965; Raisz and Rodan 1990). PTH may also stimulate osteoclasts to increase the size and volume of their ruffled border and bone lining cells to retract from the bone surface so osteoclasts may gain

access (Dietrich et al. 1976; Jones and Boyde 1978; Raisz 1965; Raisz and Rodan 1990). Continuous exposure to PTH results in high remodeling rates and bone loss from the overproduction and excessive activity of osteoclasts and osteoblasts (Bellido and Hill Gallant 2014; Locklin et al. 2003; Ortner and Turner-Walker 2003), which ultimately leads to the release of calcium and phosphorus from the skeleton into the circulation (Jüppner and Kronenberg 1999). Although PTH promotes bone resorption through its effects on osteoclasts, intermittent daily exposure to PTH has a net result of bone formation. Intermittent daily exposure to PTH increases the proliferation of osteoblast precursors, inhibits osteoblast apoptosis, and reactivates bone lining cells to become osteoblasts. After the induction of the initial bone resorption process, osteoblasts secrete matrix on bone surfaces for longer periods of time due to the inhibition of osteoblast apoptosis, resulting in a net increase in trabecular and cortical wall thickness (i.e. remodeling) (Burr et al. 2001; Dempster et al. 2001; Jüppner and Kronenberg 1999; Lindsay et al. 2007; Rauner et al. 2012). Intermittent PTH exposure prevents osteoblast apoptosis by inhibiting *SOST* gene expression in osteocytes, which inhibits sclerostin (bone formation inhibitor) production. Downregulation of sclerostin also promotes Wnt signaling, which stimulates osteoblast differentiation. The overall effect of inhibiting sclerostin production is increased bone formation on trabecular, endocortical, and periosteal surfaces. However, continuous exposure to PTH does not prevent sclerostin production and therefore does not promote osteoblast survival (Bellido and Hill Gallant 2014).

The hormone  $1,25(\text{OH})_2\text{D}$  affects skeletal tissue by ensuring that sufficient calcium and phosphate are available within the blood and extracellular fluid for normal bone mineralization and through its direct influence on bone cells (Bellido and Hill Gallant 2014; Raisz and Rodan 1990; Russell et al. 1990).  $1,25(\text{OH})_2\text{D}$  binds to VDRs that are present on the parathyroid gland, chondrocytes, osteoblast progenitor cells, osteoblast precursor cells, and mature osteoblasts (Brook and Brown 2008a). Similar to PTH, binding of  $1,25(\text{OH})_2\text{D}$  promotes bone resorption by stimulating osteocytes to produce RANKL and decrease production of OPG, a hormone that increases osteoclastogenesis (Bartl et al. 2009; Bell 1985; DeLuca and Schnoes 1976; Holick and Adams 1990; Maierhofer et al. 1983; Ortner 2008; Raisz et al. 1980; Raisz and Kream 1983; Raisz and Rodan 1990; Roodman et al. 1985; Russell et al. 1990; Stern 1980). Binding of  $1,25(\text{OH})_2\text{D}$  also promotes mineralization by increasing the production of RUNX2, a transcription factor necessary for osteoblast differentiation, and by inducing osteoblasts to

produce osteopontin and osteocalcin, proteins necessary for mineralization. However, serum concentrations of 1,25(OH)<sub>2</sub>D that are too high can have negative effects on bone. Overexposure of osteoblasts to 1,25(OH)<sub>2</sub>D inhibits osteoblastic bone mineralization (Bellido and Hill Gallant 2014).

Calcitonin is an important regulator of mineral homeostasis, but its role in adults is not as important as in fetal mineral homeostasis. In adults, a deficiency or excess of calcitonin will not result in a calcium disorder. Calcitonin's role in fetal mineral homeostasis will be discussed further in the Fetal Mineral Homeostasis section below. In adults, the binding of serum calcium to the C cells of the thyroid gland results in the secretion of calcitonin by the thyroid gland (DiMeglio and Imel 2014). Calcitonin lowers serum calcium concentration through its inhibitory effects on osteoclasts (Downey and Siegel 2006; Friedman et al. 1968; Friedman and Raisz 1965; Gaillard 1966; Hirsch and Munson 1969; Martin 1990; Martin et al. 1966; Mundy and Roodman 1987). Calcitonin binds receptors on osteoclasts and prevents PTH from binding to them, effectively prohibiting osteoclast differentiation and proliferation (DiMeglio and Imel 2014; Peck and Woods 1988). Calcitonin may also play a role in causing osteoclasts to withdraw from the bone surface and revert back to mononuclear cells. High levels of calcitonin can prevent bone resorption, which results in lowering serum calcium and phosphorus concentrations (Downey and Siegel 2006). If calcitonin induces hypocalcemia, the parathyroid gland will sense the deficiency and secrete PTH, starting the cycle anew.

Maintaining serum calcium concentrations within a narrow normal range is important. An overabundance or lack of calcium in the extracellular fluid can have adverse to lethal effects depending on the severity. Hypercalcemia (> normal serum calcium concentrations) can cause abdominal and bone pain, nausea, vomiting, polyuria (excessive urine production), and kidney or biliary stones. Depression, anxiety, cognitive dysfunction, and possibly coma can also occur when calcium concentrations exceed more than 2 times the normal level (DiMeglio and Imel 2014). Hypocalcemia (< normal serum calcium concentrations) can cause neurological excitation including paresthesias (tingling sensations), hyperactive reflexes, muscular spasms of the hands and feet, laryngospasm, cardiac arrhythmias, or seizures (DiMeglio and Imel 2014).

## ***SERUM PHOSPHORUS HOMEOSTASIS***

Typically, phosphorus dietary intake is more than adequate to meet the required level. The typical diet is higher in phosphorus than calcium and, moreover, intestinal absorption of phosphorus is much more efficient than calcium absorption. Approximately 60-70% of ingested phosphate is absorbed by the intestines (DiMeglio and Imel 2014). However, phosphate absorption is more efficient when it is ingested separately from calcium. Phosphate binds calcium, which interferes with the absorption of both. Serum phosphorus concentration is maintained by a feedback system similar to calcium homeostasis with absorption by the intestines and excretion by the kidneys. Regulation of serum phosphate within the kidneys is the greatest contributor to overall serum phosphate concentration. Active transport of phosphorus in the intestines is regulated by  $1,25(\text{OH})_2\text{D}$ . PTH and FGF-23 regulate phosphorus reabsorption in the kidneys. Unlike calcium, serum phosphorus concentrations are maintained within a wider range and changes more substantially after birth (4.3-9.4 mg/dL in newborns, 4.8-8.1 mg/dL in infants 1-5 months old, and 4.0-6.8 mg/dL in infants 6-24 months) (DiMeglio and Imel 2014). High serum phosphate concentration also impairs calcium absorption, which may result in hypophosphatemia.

Failing to maintain serum phosphorus homeostasis has serious consequences.

Hyperphosphatemia can cause renal failure by the deposition of calcium-phosphate complexes in the vasculature, soft tissues, and nephrons of the kidneys. Hypophosphatemia may result in muscle weakness, cardiac dysfunction, and adverse neurologic symptoms. Chronic hypophosphatemia causes bone pain and osteomalacia. Osteomalacia is an impairment of bone mineralization, resulting in increased bone fragility (Weaver and Gallant 2014).

Hypophosphatemia will be discussed further in the section **Disease and Bone**.

## ***FETAL AND NEONATAL MINERAL HOMEOSTASIS***

During fetal development, The growth rate exceeds 100 cm/yr (Anderson and Shapiro 2010). Approximately 33 g of calcium and 100 g of bone mass are accumulated in utero, with ~80% of the total bone mineral content present at birth (in a normal infant) added during the last three months of gestation (1981; Weaver and Fuchs 2014). At 20 weeks gestation, the calcium accretion rate is ~50 mg/day, but during the last trimester calcium requirements increase to 200-

250 mg/day and by the 35<sup>th</sup> week of gestation the calcium accretion rate increases to 330 mg/day (DiMeglio and Imel 2014). During the last trimester, there is a rapid rate of bone metabolism, cell division, and modeling (Done 2012). This results in increased bone volume, trabecular thickness, rapid matrix mineralization, and increasing hydroxyapatite crystal size (Gosman et al. 2011). Infants born before the last trimester, premature infants, do not experience this rapid rate of bone mineral accretion, which has detrimental effects on postnatal bone health and growth.

Mineral homeostasis differs during fetal development and after birth. During gestation, fetuses receive all calcium, phosphorus, and magnesium from the mother through placental transfer. Transfer of calcium and phosphorus across the placenta is an active process (Kovacs and Rosen 2008) that is stimulated by PTHrP and 1,25(OH)<sub>2</sub>D. PTHrP is produced in the fetal tissues and the placenta (Done 2012) and is essential for the regulation of endochondral bone formation and mineralization (DiMeglio and Imel 2014). High maternal serum calcium concentration is maintained by 1,25(OH)<sub>2</sub>D. The placenta produces some 1,25(OH)<sub>2</sub>D, but most is acquired from maternal sources and stored in the fetal liver in the form of 25(OH)D. During pregnancy, prolactin levels are also elevated, increasing maternal serum calcium levels by upregulating calbindin-D<sub>9K</sub>, TRPV6, and 1 $\alpha$ -hydroxylase. High fetal calcium and 1,25(OH)<sub>2</sub>D concentrations are maintained at the expense of maternal levels and maternal health.

Pregnant women experience a large increase in serum 1,25(OH)<sub>2</sub>D concentration, which results in doubling their calcium absorption efficiency and an increase in maternal bone resorption. The extra calcium is transported to the placenta. Upon entering the placental tissue the calcium binds to protein calbindin-D<sub>9K</sub> and is transported to the basolateral side of the placenta where it is pumped into the fetal circulation by PMCA proteins (DiMeglio and Imel 2014). Similar to mechanisms in extrauterine life, excessive calcium and phosphorus in the fetal serum are excreted in the urine. However, since fetal urine makes up the majority of amniotic fluid, calcium and phosphorus remain present for reuptake. When the fetus swallows the amniotic fluid, the calcium and phosphorus are available for intestinal absorption. Very little calcium is transferred back across the placenta to the maternal circulation (Glorieux et al. 2003).

Research indicates that maternal vitamin D deficiency affects fetal bone development (Javaid and Cooper 2002). However, only extremely severe cases of maternal vitamin D deficiency or

hypocalcemia will detrimentally affect fetal skeletal development (Done 2012). During late gestation, maternal transport of  $1,25(\text{OH})_2\text{D}$  almost completely stops and most, if not all,  $1,25(\text{OH})_2\text{D}$  is produced by the fetus (Kovacs and Kronenberg 1997; Kovacs and Rosen 2008). At this point, fetal serum  $1,25(\text{OH})_2\text{D}$  concentration decreases below the maternal concentration. However, fetal serum  $1,25(\text{OH})_2\text{D}$  is not as important during gestation as it will be after birth because the active transport of calcium across the placenta is regulated by PTHrP and not  $1,25(\text{OH})_2\text{D}$ . The lack of vitamin D receptors in fetal tissues also indicates that  $1,25(\text{OH})_2\text{D}$  is not as important for fetal calcium homeostasis as it is postnatally (DiMeglio and Imel 2014).

Due to the active transport of calcium, phosphorus, and magnesium across the placenta, fetal serum concentrations of these minerals are greater than maternal concentrations. To prevent fetal hypercalcemia, calcitonin is also produced within the placental tissues to decrease calcium transport across the placenta. Fetal calcitonin concentration is greater than maternal concentration, but maternal serum calcitonin concentration is elevated compared to nonpregnant women. Elevated maternal serum calcitonin concentration may place a limit on maternal skeletal resorption (DiMeglio and Imel 2014).

After birth, normal term infants depend on the mineral stores built up during the last trimester and dietary sources of minerals to maintain mineral homeostasis. Lacking the active transport of minerals across the placenta, infants must obtain all minerals through intestinal absorption from dietary sources. Furthermore, all of the  $25(\text{OH})\text{D}$  that was stored in the fetal liver is utilized by the neonate within the first 3-4 weeks (Hess 1930; Holick and Adams 1990; Pettifor and Daniels 1997). Regardless of gestational age, after birth there is a decrease in neonatal serum calcium level. The decrease in serum calcium concentration triggers PTH secretion to maintain mineral homeostasis, ultimately resulting in bone resorption to release calcium and phosphorus into the neonatal circulation (Mayne and Kovar 1991). Approximately 30% of neonatal bone is lost to bone resorption, but this does not result in compromised bone structure or strength because of the skeletal mineral buildup which occurred during the last trimester (Sharp 2007). This is not true for premature infants, in which postnatal bone resorption can be detrimental to bone structure and strength.

Maintaining calcium and phosphorus intake over excretion is very important during infancy because of initial bone resorption after birth and due to the high growth rate during the first year of life, 50 cm/year (Anderson and Shapiro 2010). For normal term infants, breast milk contains adequate amounts of calcium, phosphorus, and vitamin D for the production and mineralization of new bone during the first 6 months of growth. PTHrP produced by the mammary glands stimulates maternal bone resorption during lactation. Sufficient amounts of calcium and phosphorus are mobilized from the maternal skeleton, and along with maternally produced vitamin D are transferred to the breast milk. Prolactin is also elevated during lactation, contributing to increased maternal serum calcium concentrations. Maternal vitamin D status does not affect the amount of calcium and phosphorus that is resorbed from the maternal skeleton and transported to the breast milk, but maternal vitamin D deficiency will negatively affect the concentration of vitamin D transferred to the breast milk (DiMeglio and Imel 2014). After the first 6 months of growth, human milk needs supplementation to meet the energy, iron, and fiber needs of a growing infant (Weaver and Gallant 2014).

Preterm infants have difficulty maintaining mineral homeostasis after birth because they missed or did not complete the rapid rate of bone mineral accretion which would have occurred during the last trimester. As a result, preterm infants are born without sufficient stores of calcium, phosphorus, iron, and copper. Supplementation with a formula fortified with calcium and phosphorus is necessary for preterm infants receiving breast milk. Without supplementation, concentrations of calcium, phosphorus, and vitamin D in breast milk are insufficient for preterm infants (Backstrom et al. 1996; Bishop et al. 1996). The consequences of preterm birth on bone health will be discussed below in the section **Disease and Bone**.

## **Disease and Bone**

Bone structure and function can be affected by numerous factors such as chronic illness (genetic and acquired), nutritional deficiencies, and metabolic and endocrine disorders. In addition, these factors are not mutually exclusive and are often associated. Despite the very large number of diseases and factors that adversely affect the skeleton, bone is limited in its reactions (Salter 1999b). Under abnormal conditions, bone can react by apoptosis, altering bone deposition (osteoid and/or mineral deposition), altering bone resorption, or mechanical failure. Due to the

limited number of bony reactions to abnormal conditions, skeletal manifestation of different chronic illness may be the same or similar. The severity of the skeletal manifestations depends on the duration and severity of the abnormal condition. Understanding the effects of pathological conditions on bone structure is needed to appreciate how these conditions compromise bone health and structure. Compromised bone health and structure can result in compromised bone strength. For the purposes of being aware of which infants in the current study sample may have compromised bone health, and not for diagnostic purposes, the skeletal manifestations of some of the diseases and factors that have the potential to adversely affect bone are described in this chapter.

### ***DISORDERS OF BONE AND MINERAL METABOLISM***

Most metabolic disorders are caused by nutritional imbalances, which may result from over or under consumption of some food component or a defect in intestinal absorption (Ortner 2003c). Bone mineral metabolism is commonly affected by deficiencies in vitamin D, calcium, phosphorus, and vitamin C. For simplicity, these deficiencies will be discussed separately, but overlap is possible and does occur. Skeletal manifestations of these diseases are very similar due to bone's limited response to abnormal conditions. Distinguishing between these diseases based on macroscopic observation may not be possible. For the purposes of the current study, distinguishing between diseases is not important. It is important to evaluate whether there are significant differences in SOS between infants with and without chronic illness, as these infants are at greater risk for compromised bone health and strength.

#### ***Deficiencies of Vitamin D, Calcium, and Phosphorus***

During growth, deficiencies in vitamin D, calcium, and/or phosphorus have the potential to cause the coexistence of 2 types of metabolic bone disease, rickets and osteomalacia. Rickets specifically refers to a defect in mineralization occurring at the growth plate. Osteomalacia is a defect in the mineralization of osteoid deposited on previously formed bone (Mankin 1974; Pettifor 2003). In infants, osteomalacia coexists with rickets, but osteomalacia can also be present without obvious skeletal manifestations of rickets (Imel et al. 2014). Vitamin D, calcium, and phosphorus deficiency also cause increased bone resorption and growth retardation (Ortner 2003c). As deficiencies become more severe, PTH increases in an attempt to increase serum mineral concentrations through bone resorption.



Vitamin D deficiency due to inadequate intake or exposure to sunlight is the most common cause of rickets (Brickley and Ives 2008c; Ortnier 2003c; Pitt 1995). In normal term infants, rickets are rarely seen before the age of 4 months due to the storage of vitamin D in the fetal liver. Rickets is most commonly seen between the ages of 6 months and 2 years. The severity of skeletal manifestations depends on the stage of rickets, which relates to the length of time the infant has been deficient and the severity of the deficiency. Short periods of vitamin D deficiency are not sufficient to produce active rickets. Also, an insufficient, but not deficient, serum vitamin D concentration may be inadequate to produce macroscopically identifiable skeletal manifestations (Imel et al. 2014). However, short periods of deficiency and insufficiency can cause bone loss and decreases in mineralization.

Rachitic bone (bone affected by rickets) is unable to support biomechanical function and when normal loading forces are applied the bone may become deformed and/or fracture. The earliest skeletal manifestations occur in the areas of rapid growth, such as the growth plates (Pettifor 2003). Within the growth plate, the vitamin D deficiency interrupts the mineralization of the chondrocytes within the zone of hypertrophy. Without mineralization, the cells fail to undergo apoptosis and resorption, and the zone increases in size (Imel et al. 2014). Meanwhile, the cartilage proliferation and osteoid deposit continues (Mankin 1974; St-Arnaud and Glorieux 1997). As a consequence, the unmineralized cartilage and osteoid accumulate next to the growth plate and the normally columnar organization of the cartilage becomes disorganized. The unmineralized, disorganized tissue cannot support biomechanical function and daily stresses and strains cause deformation. Mechanical forces applied to rachitic bone will spread the cartilage further apart, giving it a flared and horizontal appearance. Deformation is particularly prominent at the costochondral junctions of ribs, the distal metaphyses of the femur, radius, and ulna, and the proximal humerus (Brickley and Ives 2008c). Osteomalacia also develops as newly deposited osteoid on surfaces of previously formed and mineralized bone remains unmineralized. Cortices become soft as unmineralized osteoid builds up on diaphyseal surfaces (Imel et al. 2014), further decreasing biomechanical stability.

There are two forms of rickets which differ based on the nutritional status of the infant (Brickley and Ives 2008c). The coincidence of malnutrition and vitamin D and/or mineral deficiency results in the porotic (or atrophic) form of rickets. Characteristic features of the porotic form

include generalized osteopenia, thin and brittle cortices, and sparse trabeculae. Stress fractures are common in the porotic form and may result in deformities of the axial skeleton and bending deformities of the extremities. The hypertrophic form, described above, occurs in well nourished, but vitamin D and/or mineral deficient infants. This form is referred to as hypertrophic because the child continues to rapidly produce and deposit osteoid in large amounts. In the hypertrophic form, the large amount of osteoid makes the long bones appear plump with narrow medullary spaces (Brickley and Ives 2008c).

Although these two forms are described separately, there is considerable overlap in the skeletal manifestations of atrophic and hypertrophic rickets (Silverman 1985). The skeletal manifestations of rickets change as severity and the period of deficiency increases. During early stages of rickets, the costochondral junctions of the ribs appear flared and swollen. As the disease increases in severity, the costochondral junctions develop a bead-like appearance, making the chest wall appear lumpy ('rachitic rosary'). Curvature of the ribs may become flattened from bending of the rib cartilage at the costochondral junction. Also due to the bending of the rib at the costochondral junction, the sternum may become bent forward, producing a pigeon breast deformity. In severe cases, pressure from the weight of the arms depresses the rib contour on the lateral aspect the rib cage (Pettifor 2003; Pettifor and Daniels 1997; Scheuer and Black 2000b). Cranial skeletal manifestations include generalized thinning of cranial bones, thin and softened parietal and occipital squama (craniotabes), delayed closure of fontanelles, and subperiosteal deposition on cranial and facial bones (Hess 1930; Mays 2006; Ortner and Mays 1998; Pettifor 2003; Pettifor and Daniels 1997). The inner and outer tables of the cranial vault may be completely remodeled, making the entire cranial vault appear like diploë. Deformation of the curvature of the spine may result in kyphoscoliosis (outward and lateral curvature of the spine) (Hess 1930; Pettifor 2003; Pettifor and Daniels 1997). Height of vertebral bodies may decrease with scalloped appearing endplates. The bones of the pelvis appear smaller more plump than normal. Overall, the pelvis has a flattened appearance because maximum growth of the iliac bones occurs during infancy and deficiency in the growth of the iliac bones leads to an anteroposterior narrowing of the pelvic canal. The sacrum may protrude into the pelvic canal and the acetabula face more forward than normal (Hess 1930; Ortner and Mays 1998).

With regard to the long bones, metaphyses become flared and swollen during the early stages of rickets. The growth plate is porous and the margins are frayed. Both the metaphyses and growth plate display cupping deformities. Diaphyseal bending occurs during more advanced stages of rickets and may be variable between limbs. Porosity may be present on the concave side of the bent limb. In crawling infants, humeral shafts may be bent in the forward and lateral directions with medially depressed humeral heads. After walking has commenced, active rickets results in femoral necks that are bent downward and femoral shafts bent at the distal metaphysis with an anterolateral convexity. Shafts of the tibia and fibula may present with anterior bowing at the distal metaphysis (Hess 1930; Mays 2006; Ortner and Mays 1998; Pettifor 2003; Pettifor and Daniels 1997).

After the development of active rickets, small amounts of vitamin D are sufficient to initiate mineralization, also referred to as healing. However, mineralization can only take place on preexisting surfaces, which may be deformed. Remodeling during growth may eventually correct the deformities, but major deformities will become permanent. For example, vertebrae that developed major deformities, such as kyphoscoliosis, will mineralize and be permanent (Hess 1930; Pettifor 2003; Pettifor and Daniels 1997).

The characteristic distribution of periosteal deposition during healing is dependent on bone type. On the long bones, periosteal deposition of osteoid is thickest at the mid-diaphyseal region, giving the diaphysis a columnar appearance (Schmidt 1929). On the ribs, deposition is limited to the anterior surface and margins. Deposition on the posterior surface of the femur is more prominent than the anterior. On the tibia, deposition occurs on the posterior and medial surfaces (Brickley and Ives 2008c). Prolonged and untreated rickets may permanently stunt growth (Imel et al. 2014).

Rickets diagnosis typically occurs through qualitative assessment of bony morphology on radiographs, followed by testing of serum mineral concentrations. Generally, rachitic bone appears osteopenic on radiographs, giving it a more radiolucent appearance. The costochondral junctions appear bulbous. The margins of cortices and epiphyses lose their distinction. The growth plates of the long bones, especially at the wrists, knees, and ankles, appear widened and brush-like with fringed bony projections. The trabeculae appear coarse. Long bones may exhibit

torsional or bowing deformation (Berry et al. 2002; Hess 1930; Pettifor and Daniels 1997; Reynolds and Karo 1972; Silverman 1985).

Characteristics of healing rickets can also be observed radiologically. In healing rickets, the cranium shows increased periosteal apposition on the ectocranial surface with apparent trabecular spurs. In long bones, new trabecular structure is apparent along the metaphysis. Due to the mineralization of previously formed defects, the disorganized orientation of the trabeculae may be present for some time. Cortical outlines and the margin of the growth plate appear defined while cortices may appear thickened due to the mineralization of periosteal apposition (Berry et al. 2002; Hess 1930; Pettifor and Daniels 1997; Reynolds and Karo 1972; Silverman 1985).

Abnormalities caused by rickets are also evident histologically. Osteoid seams are widened with delayed mineralization. Growth plates appear widened and irregular with delayed apoptosis of hypertrophied chondrocytes (Imel et al. 2014). There is a loss of new cortical bone formation and the number of resorption sites on the cortical bone increases. Cortical porosity is increased with Haversian canals and lacunae that appear larger than normal. Any new bone formation is poorly mineralized with mineralization defects adjacent to cement lines. The number of resorption sites on surfaces of trabecular bone is also increased and appear as bite-like defects and tunneling resorption. In cases of severe rickets, trabecular struts may be perforated. Newly deposited trabecular bone may appear separated from more mature bone. Similar to cortical bone, newly formed trabeculae bone is poorly mineralized with defects adjacent to cement lines. In healing rickets, resorption sites at the metaphyses may increase as remodeling removes cupping deformations (Mankin 1974; Mays et al. 2007; Pitt 1988).

### ***Vitamin C Deficiency***

Ascorbic acid (vitamin C) is essential in collagen fibril formation (Hodges 1980) and deficiency results in decreased or absent bone matrix formation (Brickley and Ives 2006; Ortner et al. 2001; Ortner and Ericksen 1997). Vitamin C deficiency disease is called scurvy. Although scurvy is rare in the modern population, autopsy findings suggest that sub-clinical and clinical vitamin C deficiency may be increasing (Akikusa et al. 2003; Brickley and Ives 2008b; Fain 2005). Incipient scurvy has been identified in children that died from acute infections (Milgram 1990).

Vitamin C deficiency rarely occurs in neonates because vitamin C easily passes to the fetus by active placental transport and to the infant in breast milk. However, maternal vitamin C deficiency decreases the vitamin C concentration in breast milk (Fain 2005). Yet, even if an infant receives no vitamin C following birth, the disease still takes several months to manifest (Ortner 2003c). Infantile scurvy is rarely seen before 4 months of age and is most prevalent in infants 8-10 months of age (Wimberger 1925). Once vitamin C intake is reestablished, scurvy heals relatively quickly. Clinical signs of scurvy begin to improve in 48 hours (Greenfield 1990) and are almost completely resolved within 2 weeks (Pimentel 2003). In children, the histological signs of scurvy may be completely obliterated after three months of treatment (Follis et al. 1950).

Scurvy causes a decrease or cessation of osteoblastic activity while osteoclastic and chondroclastic (cartilage resorption) activity continues, resulting in osteopenia. Meanwhile, subperiosteal hemorrhage causes skeletal lesions. The cellular disruption weakens the developing bones. The skeletal manifestations of scurvy are most severe in infants due to their rapid growth and are most prominent on bones that grow rapidly, such as the costochondral junctions of ribs, the distal metaphyses of the femur, radius, and ulna, as well as the proximal metaphysis of the humerus (Ortner 2003c). With growth, the calcified cartilage accumulates on the metaphyseal side of the growth plate in absence of normal ossification. As a result, the metaphyseal zone becomes unstable and trabeculae fail to form. The region becomes susceptible to transverse fractures (i.e., classic metaphyseal lesions), epiphyseal dislocation and fragmentation of the calcified cartilage (Milgram 1990; Ortner 2003c). In severe cases, the proximal epiphysis of the femur may collapse resulting in a depressed angle of the femoral neck. The costochondral junctions may fracture causing an inward dislocation of the sternum and rib cartilages or may become abnormally large and flared, scorbutic rosary. Bone formation on the periosteal and endocortical surfaces is adversely affected, resulting in decreased cortical thickness (Ortner 2003c).

Periosteal hemorrhages are caused by collagen deficiency within the vascular walls. Most periosteal hemorrhages are observed in the weight-bearing bones (Ortner 2003c). Fractured metaphyses, trauma, or normal biomechanical stresses and strains may initiate subperiosteal hemorrhaging (Follis 1948). The hemorrhaging can strip the periosteum from the entire surrounding shaft. Only very small amounts of vitamin C are required for the subperiosteal

hemorrhage to trigger new bone formation (Bourne 1942). Subperiosteal new bone formation presents as a thin shell of new bone that envelops the old bone or as spicules on the cortical surface (Ortner 2003c). Spicules deposited on the cortical surface are hypertrophic and have a porous, pumice-like appearance. On the scapulae, porosity has been observed on the supraspinous and infraspinous aspects of the cortex (Brickley and Ives 2006; Ortner et al. 2001). In infants with scurvy, hypertrophic and porous lesions have been observed on the frontal and parietal bosses of the skull, orbital roofs, sphenoid, maxilla, and mandible (Brickley and Ives 2006; Fraenkel 1929; Ortner 2003c; Ortner and Ericksen 1997; Ortner et al. 1999; Sloan et al. 1999).

Infantile scurvy must be relatively severe before it is observed on radiographs (Follis et al. 1950). Radiological features of scurvy includes metaphyseal ‘white lines’ (‘white lines of Frankel’), radiolucent lines (‘scurvy lines’ or ‘Trümmerfeld zone’) adjacent to the ‘white lines’, white outlining of the epiphyses (‘Wimberger ring’ or ‘pencilled effect’), corner fractures located at the lateral edges of the metaphyseal ‘white lines’ (‘Pelkan spurs’), micro-fractures of the cancellous bone (‘corner sign’ or ‘corner sign of Park’), and fractures of the cortex below the provisional line of calcification. The preservation of areas of provisional calcification at the ends of the metaphyses produces ‘white lines’ (Chatproedprai and Wananukul 2001; Grewar 1965; McCann 1962; Tamura et al. 2000). Adjacent to the ‘white lines’ bone mineral density is diminished, producing radiolucent lines. The ‘Wimberger ring’ or ‘pencilled effect’ is caused by intensified calcification of a limited area due to the cessation of new bone matrix formation. Generalized osteopenia is also visible on radiographs, along with cortical walls that appear irregular and thin.

### ***Metabolic Bone Disease of Prematurity***

As has been stated previously, failure to reach a certain degree of skeletal maturity by time of birth has detrimental effects on the postnatal bone health and growth. Research has shown that preterm infants have a significantly lower bone mineral content than term infants, even after correcting for size differences (James et al. 1986). Preterm infants are at higher risk for developing metabolic bone disease than term infants, especially infants born prior to 28 weeks gestation (Griscom and Jaramillo 2000). Approximately 55% of infants weighing <1000 g and 23% of infants weighing <1500 g at birth develop metabolic bone disease (Done 2012).

Furthermore, reduced bone mineralization is found almost universally in infants with a birth weight <1500g (Barltrop et al. 1977; Senterre and Salle 1982; Shaw 1976). As a result, it was hypothesized that skeletal maturity at birth is significantly related to body size, bone structure, and BMD.

Increased risk of metabolic bone disease in premature infants occurs for many reasons. The majority of bone mineral accretion occurs during the last 3 months of gestation and at a very high rate (Widdowson et al. 1988; Widdowson and Spray 1951). Premature infants miss the last trimester of gestation causing them to be born without the normal skeletal store of minerals. Due to the normal postnatal drop in serum calcium concentration and increase bone resorption, the already deficient bone mineral content decreases even further. Also, premature infants are born with immature organ systems creating a higher risk for developing malabsorption disorders, as well as diseases of the lungs and heart. Premature infants have greater fluid and calorie requirements than term infants, but may be intolerant to feeding due to incomplete development of the oral reflex and immature digestive systems (Darby and Loughead 1996; Johnson 1991). An immature digestive system are typically deficient in digestive enzymes and are at an increased risk for developing necrotizing enterocolitis (inflammatory disease of the bowel) (King 2008). Preterm infants with malabsorption disorders may require the use of parenteral (intravenous) nutrition (Darby and Loughead 1996), but parenteral nutritional may not meet all nutritional requirements. The maximum amount of soluble calcium and phosphorus in parenteral nutrition approaches but does not match fetal mineral accretion (Specker et al. 2001). Furthermore, the underdeveloped lungs of premature infants often require treatment glucocorticoids and diuretics. Glucocorticoids increase bone resorption, downregulate the differentiation of osteoblast precursors, and increase osteocyte apoptosis. Diuretics, such as furosemide, cause excess excretion of important nutrients and minerals (King 2008). Heparin is another medication that may be prescribed to premature infants. Heparin prevents the formation of blood clots, but has been shown to adversely affect bone formation (Imel et al. 2014).

Lack of mechanical loading is another reason that premature infants have increased risk of developing metabolic bone disease. Premature infants experience less mechanical loading in the extrauterine environment than would have been experienced in the intrauterine environment,

increasing bone loss after birth (Sharp 2007). Furthermore, severely ill infants are likely to be sedated, decreasing mechanical loading and increasing bone resorption (Done 2012).

### ***OTHER ENVIRONMENTAL FACTORS***

External factors such as general malnutrition, diseases of other organ systems, trauma, and infections can also have adverse effects on bone formation and development. For this reason, it was hypothesized that chronic illness would be significantly associated with body size, bone structure, and BMD. Some examples are discussed below.

#### ***Protein/Calorie Malnutrition***

Adequate protein and fat intake are required for proper intestinal absorption of calcium. Severe prolonged malnutrition results in the arrest of all growth. Undernutrition causes a decline in osteoblast function resulting in decreased bone formation (Grinspoon et al. 1995; Orden et al. 2002; Shires et al. 1980). In less severe cases, malnutrition, disordered eating, and/or starvation cause osteopenia. Osteopenia results from increased PTH secretion and bone resorption, in an attempt to increase serum calcium concentration (Brickley and Ives 2008a; Rizzoli and Bonjour 2004).

#### ***Other Systemic Diseases***

Diseases occurring in other organ systems adversely affect bone development and structure by interfering in processes necessary for normal bone metabolism. For example, renal insufficiency is the most common cause of secondary hyperparathyroidism, which results in excessive bone resorption. Hyperparathyroidism disorders are characterized by high serum PTH concentration that is unaffected by serum calcium concentration or by imbalanced PTH concentration in relation to serum calcium concentration (Brickley and Ives 2008a). The skeletal manifestation of secondary hyperparathyroidism are highly variable and include rickets-like changes, growth stunting, generalized bone loss, and an overall reduction of bone quality (Ortner 2003a; Ross 1998).

Inflammatory diseases, liver disease, and chronic kidney disease also adversely affect bone (Imel et al. 2014). Liver disease can cause malabsorption disorders by impairing 25-hydroxylation of vitamin D (Imel et al. 2014). Chronic kidney disease impairs renal clearance of phosphorus and results in abnormally high serum phosphate concentrations



(Hyperphosphatemia). In an attempt to increase phosphorus excretion, calcium excretion increases, resulting abnormally low serum calcium concentration. The low serum calcium concentration interferes with mineralization.

### ***Secondary Osteopenia***

Osteopenia can occur secondary to any illness that causes immobility or a decrease physical activity (Brickley and Ives 2008a). Mobility can be affected by congenital and developmental skeletal abnormalities, such as spina bifida cystica, severe congenital scoliosis, and neuromuscular conditions. Any trauma or pathology which limits mobility or leads to immobilization may cause osteopenia of the affected areas. Immobilization increases calcium excretion, which stimulates PTH secretion and osteoclastic resorption in order to increase serum calcium concentration (Epstein et al. 2003; Jenny Kiratli 2001). Bone loss and decreased osteoblastic activity following immobilization can occur rapidly and may be localized or generalized. Characteristics of secondary osteopenia on radiographs include thin cortices, increased intra-cortical porosity, sparse and/or thin trabeculae. Histologically, there is an overall increase in bone resorption, number of resorption sites, and size of Haversian canals. Size of osteons and bone formation will be limited.

### ***Medication***

Medications necessary for the treatment of other diseases and illness in infants can also adversely affect bone. Medications that affect bone include anticonvulsants, diuretics, glucocorticoids, and heparin (Imel et al. 2014). Anticonvulsants are prescribed to infants with seizure disorders. Anticonvulsants may contribute to bone loss by affecting vitamin D metabolism, but the mechanism by which anticonvulsants increase bone loss is not well understood. The adverse effects of diuretics, glucocorticoids and heparin on bone were described previously in the section **Metabolic Bone Disease of Prematurity**. Infants in the current study sample with histories of long-term use of medications that may have adversely affected bone health were classified as chronically ill due to the possibility of compromised bone health and strength.

## ***GENETIC DISORDERS***

Several genetic disorders interfere with the hydroxylation of vitamin D, renal function, FGF23, or collagen production and produce rachitic skeletal manifestations. Hereditary vitamin-D-

dependent rickets is a rare autosomal disorder resulting from mutations which disrupt the production of metabolically active vitamin D or its metabolism (Malloy and Feldman 2010). There are three forms. Types 1 and IIA are inherited in a recessive pattern. In type 1, there is a mutation in the *CYP27B1* gene, which produces  $1\alpha$ -hydroxylase. Without  $1\alpha$ -hydroxylase,  $25(\text{OH})\text{D}$  cannot be converted to the metabolically active form in the kidneys, resulting in low serum concentrations of  $1,25(\text{OH})_2\text{D}$ . The skeletal manifestations of this condition are usually observed by the age of 2 years. Type II is more severe than type I. In type II, there is a mutation in the *VDR* gene and affected children usually present with severe rickets within months of birth and may have stunted growth (Malloy and Feldman 2010). Serum concentrations of  $1,25(\text{OH})_2\text{D}$  are high in the type II form, but the organ tissues cannot respond to the hormone because the defect in the *VDR* does not permit binding. Type IIB is the third type of vitamin-D-dependent rickets. Similar to the other types it has an early onset, but type IIB is caused by an abnormal expression of the hormone response binding element, preventing vitamin D from binding to *VDRs* (Ortner 2003c). The inheritance pattern of type IIB is not clear due to the isolated number of cases (Chen et al. 2006). Regardless of the type, the skeletal manifestations of vitamin D-dependent rickets are similar to the manifestations of severe rickets caused by nutritional deficiency (Imel et al. 2014).

Hypophosphatasia (HPP) is a rare genetic condition in which a missense mutation in the *ALPL* gene results in decreased or no ALP production (Rathbun 1948). HPP is inherited in either an autosomal dominant or recessive pattern. ALP deficiency results in an abnormal and deficient mineralization of bone matrix. Skeletal manifestations are widely variable and depend on age of onset (Brickley and Ives 2008a). Perinatal and infant forms of HPP tend to be inherited in a recessive pattern and are more severe than dominant forms. Affected neonates are usually stillborn or survive only a few days (Imel et al. 2014). On radiographs, severe cases exhibit characteristic ‘punched out’ defects of the metaphyses (Grech et al. 1985). Infants and neonates with HPP are dwarfed with long bone deformities, poorly mineralized skulls, and skeletal manifestations of active rickets (Ortner 2003c). In perinatal HPP, skeletal manifestations may be apparent in utero or at birth. In infantile forms, moderate to severe skeletal defects usually present before 6 months of age (Imel et al. 2014). Less severe forms of the disease may not become apparent till later childhood (Ortner 2003c).

Chronic hypophosphatemia can be acquired or inherited. The most common cause of chronic hypophosphatemia is X-linked hypophosphatemia (XLH). XLH is a dominant disorder resulting from a mutation that inactivates the *PHEX* gene (Imel et al. 2014). Deficiency in PHEX protein increases the expression and secretion of FGF-23, leading to renal wasting of phosphorus and decreased production of the active metabolite of vitamin D. There are also autosomal dominant and recessive forms of chronic hypophosphatemia. Recessive forms are caused by mutations in the *DMP1* or *ENPP1* genes and the dominant form is caused by a mutation in the *FGF23* gene. Recessive or dominant, these disorders result in excess FGF-23 production. Chronic hypophosphatemia, regardless of the cause, manifests skeletally as rickets. However, the severity of skeletal effects is highly variable (Imel et al. 2014; Ortner 2003c).

A rare autosomal recessive disorder called Hyperphosphatemic familial tumoral calcinosis (TC) causes chronic hyperphosphatemia. TC results from a mutation in the *FGF23* gene which impairs phosphate excretion. Mutations in the *GALNT3* and *FL* genes can also cause TC. In TC, there is an increase in serum calcium and phosphorus concentrations causing soft tissue calcifications and areas of skeletal hyperostosis may also develop (Imel et al. 2014).

Osteopetrosis is a rare inherited disorder which causes increased bone mass and mineralization due to a defect in osteoclast function. Overmineralization of bone causes it to become increasingly brittle, resulting in bone fragility. Osteopetrosis can be inherited in an autosomal recessive, autosomal dominant, or X-linked pattern. Infantile forms of osteopetrosis are recessive. Mutations in genes *CLCN7*, *OSTM1*, *TNFRSF11A*, or *CA2* can cause the disease. Severity of skeletal manifestations varies widely. Some perinatal forms are lethal and individuals with infantile forms rarely survive to adulthood (Brickley and Ives 2008a). The infantile form presents shortly after birth with fractures, cranial deformities, and poor growth (Imel et al. 2014).

Infantile Cortical Hyperostosis (Caffey's Disease) affects the skeleton of infants in the first year of life. The cause is unknown, but may occur occasionally or sporadically in several siblings. In Caffey's disease, areas of massive deposition of layered periosteal woven bone occur on one or several bones. The most frequently involved bones are the mandible and clavicle, followed by the long bone diaphyses and rib shafts. The excess bone is usually resorbed after weeks or months (Ortner 2003c).

Osteogenesis imperfecta (OI) refers to a number of rare genetic diseases that disrupt the amount or structure of type 1 collagen. The prevalence of OI is 1/10,000 persons. There are 12 types of OI and expression of the disease is highly variable regardless of type classification. Most cases are autosomal dominant, but recessive types also occur. Genetic mutations that cause abnormalities in the structure of the collagen protein tend to be more severe than mutations that result in a functionally null allele. A null allele will result in less collagen, but the collagen that is present is functionally normal. Collagen with an abnormal structure cannot fold into its proper shape which impedes functionality and results in a disorganized and weaker bone tissue. Types I-IV are autosomal dominant disorders that considered the classic types of OI. Types I-IV directly affect the type 1 collagen protein. Type I is a mild expression of OI with few or no fractures occurring throughout the individual's lifetime. Type II is lethal. Type III is progressively deforming. Type IV is an intermediate form in terms of severity. Type V is also autosomal dominant and is characterized by bone fragility, hypertrophic callus formation, and interosseous membrane calcification. Type V affects a gene (interferon-induced transmembrane protein-5) that plays an important role in osteoblast maturation and bone formation. Types VI-XII are recessive disorders. In type VI, the mutation of a gene responsible for inhibiting angiogenesis causes a defect in mineralization. In types VII-IX, there are defects in genes encoding 3-hydroxylation proteins, which are necessary for proper folding or posttranscriptional modification of type 1 collagen. Types VII-VIII can be severe to lethal, while type IX is moderate to lethal. Types X-XII involve mutations of chaperone proteins that are necessary for the proper folding of type 1 collagen. Type X is severe to lethal. Type XI is progressively deforming. Type XII is intermediate in its severity and involves a genetic mutation of the *SP7* gene, which regulates bone cell differentiation (Imel et al. 2014).

Other inherited non-skeletal disorders that are known to affect bone density include cystic fibrosis, galactosemia, muscular dystrophy, lipid and glycogen storage diseases, Ehlers-Danlos syndrome, and Marfan syndrome (Imel et al. 2014).

### ***ENDOCRINE DISORDERS***

Abnormalities and dysfunctions of the endocrine system affect bone metabolism by interfering with the production of hormones necessary for normal bone mineral metabolism. The endocrine system consists of several glands that perform bodily functions by secreting hormones into the

circulatory system. Hormones secreted by the pituitary, thyroid, parathyroid, adrenal, and gonadal glands have important effects on bone growth, maturation, and maintenance during infancy. Defects in hormone secretion can be caused by intrinsic abnormalities in the tissue causing overproduction of hormones (hyperplasia), tumors, or congenital absence of glandular tissue (Ortner 2003a).

The pituitary gland produces somatotrophic (growth) hormone which affects skeletal growth and regulates thyroid function. Excess production of growth hormone (hyperpituitarism) causes a rare disorder called pituitary gigantism. Excess growth hormone overstimulates both endochondral and intramembranous bone growth. The thickness, length, and diameters of bones are affected and produce individuals with abnormally large proportions. Hypopituitarism results in a deficiency of growth hormone and causes dwarfism. Both bone length and width are reduced. Overall, the skeleton is gracile, with thin cortices and porotic and sparse trabeculae (Ortner 2003a).

The thyroid gland produces the hormones thyroxine and triiodothyronine (Resnick 1995). Secretion of thyrotropic hormone by the pituitary gland stimulates the thyroid gland to secrete thyroxine. Thyroxine stimulates skeletal maturation in local tissues and the secretion of growth hormone by the pituitary. Congenital absence of the thyroid gland causes severe dwarfing, delay in formation of secondary ossification centers, and epiphyseal plates that never fuse. Hyperthyroidism causes excessive secretion of thyroxine, which results in accelerated skeletal maturation and premature closure of epiphyseal plates (Ortner 2003a).

Adrenal glands secrete adrenocortical glucocorticoid hormone when stimulated by pituitary adrenocorticotrophic hormone (ACTH). Excessive adrenocortical glucocorticoid suppresses collagen production causing severe osteoporosis, Cushing's syndrome. The vertebrae and ribs are the most severely affected, with thin cortices and small, sparse trabeculae. Long bones have sparse trabeculae and endocortical resorption (Ortner 2003a). Compression fractures are common in the vertebrae along with kyphotic deformation of the spine. Multiple fractures may be present in the ribs (Sissons 1956). Cushing's syndrome is rare in infancy, but has been reported (Loridan and Senior 1969).

The gonads produce sex hormones, such as estrogen and testosterone. Sex hormones stimulate endochondral growth and skeletal maturation. Hypogonadism is the deficient production of sex hormones. Hypogonadism delays the appearance of the secondary ossification centers and closure of epiphyseal plates. Intramembranous bone formation is also affected, resulting in thin cortices and an overall gracile skeleton. Due to the delay in closure of epiphyseal plates, the period of endochondral growth is extended, resulting in abnormally long limbs. Excessive amounts of estrogen or testosterone are produced in hypergonadism. Excessive sex hormone stimulates endochondral growth and causes premature closure of epiphyseal plates, resulting in a short and stocky skeleton (Ortner 2003a; Wilkins 1950).

Primary hyperparathyroidism is one of the most common endocrine disorders. Primary hyperparathyroidism is characterized by high serum calcium concentration coupled with normal or high PTH concentrations (Ortner 2003a). The elevated PTH concentration increases osteoclastic activity and bone resorption, resulting in generalized bone loss throughout the skeleton (Greenfield 1990; Mays et al. 2001; Potts 1998). Bone loss in the spine may cause wedging and biconcavity of the vertebral bodies (Jaffe 1972; Milgram 1990). In radiographs, the endplates appear relatively dense in comparison to the generalized osteopenia observed in the rest of the vertebral body (Aufderheide and Rodriguez-Martin 1998; Greenfield 1990). The inner and outer cranial tables may be severely diminished and the diploë may be transformed into poorly mineralized, fine trabeculae (Bilezikian 1999; Greenfield 1990; Potts 1998). Pathological fractures and bone deformities may occur (Ortner 2003a). On radiographs, tunneling absorption may be seen within the cortices of the long bones, as well as cortical thinning, increased trabecular volume, loss of cortical definition, fractures, and tumors appearing as well-defined radiolucencies (Greenfield 1990; Jaffe 1972; Mays et al. 2001; Resnick and Niwayama 1988).

Primary hypoparathyroidism is characterized by serum PTH concentrations that are low or imbalanced. Hypoparathyroidism disorders can be caused by PTH resistance, which is characterized by low serum calcium concentration despite elevated PTH concentration and normal vitamin D status. Low serum PTH concentration impairs bone resorption, decreases renal calcium reabsorption, and decreases the production of the active metabolite of vitamin D (Imel et al. 2014). Skeletal manifestations of hypoparathyroidism include excessive cortical thickening, periosteal hyperostosis, and abnormally enlarged trabecular bone (Ortner 2003a).

## **Basic Bone Biomechanics**

Along with its role in mineral homeostasis, the skeleton also serves as a mechanical support structure that resists deformation during muscle activity and functions as physical protection for the organs and soft tissues. In order to meet these mechanical requirements, bone must be stiff enough for muscles to work against and compliant enough to absorb energy during loading and impacts. When loading exceeds a bone's strength, failure or fracture occurs. The ability to adequately resist fracture by forming a compromise between stiffness and compliance is called bone strength. Bone strength is affected by material composition, cortical structure, and trabecular structure. Disease also influences bone strength by altering bone material composition and structure (Cullinane and Einhorn 2002; Seeman 2008; Wallace 2014). The biological processes that alter bone material and structural properties were discussed in the previous sections. The relationship between bone material and structural properties, and bone strength are discussed below. Bone strength also varies by load type and magnitude, but a detailed discussion of variation in mechanical properties based on load type and magnitude are beyond the scope of this study. Compression, tension, and bending will be briefly mentioned throughout this section to facilitate the discussion of factors which affect bone strength. The purpose of this section is a general discussion of the factors that affect bone's ability to resist fracture.

### ***BONE TISSUE MATERIAL COMPOSITION***

Fracture resistance begins at the material level. The composite nature of bone allows it to be both stiff and compliant when loaded. This balance is achieved through the interaction of collagen and mineral within the composite material. The mineral phase of the composite provides stiffness and strength in compression (forces directed toward the center of the object) (Burstein et al. 1975). As the amount of bone mineral content within the bony material increases, stiffness also increases (Seeman and Delmas 2006). Bone mineral density (BMD) is the quantifiable measure of the proportion of bone mineral content relative to the total mass of the composite material. Therefore, bone stiffness increases as BMD increases. The measure of a material's stiffness is called its elastic modulus or Young's modulus. BMD is closely correlated with elastic modulus. The collagenous phase of bone provides ductility and strength in tension (forces pulling away from the object). The collagenous portion also increases a bone's ability to absorb energy during loading. This characteristic is called a material's toughness (Martin et al. 1998a). Although both

stiffness and toughness are of vital importance to fracture resistance, a bone cannot be both very stiff and very tough. As elastic modulus increases, bone becomes increasingly brittle and toughness decreases (Currey 2006; Wallace 2014). The balance formed between elastic modulus and toughness to adequately resist fracture depends on the bone's function and is affected by the daily loads experienced by that bone. Therefore, there is no ideal stiffness and toughness value for bone. Different bones have different functions and therefore have different mechanical demands and those demands can change (Martin et al. 1998b; Wallace 2014).

The strength of bone tissue is greatly affected by degree of mineralization, or BMD. A study examining the effects of matrix mineralization on breaking stress reported that an 8% increase in bone mineral content increased bone strength 3.7 fold (Vose and Kubala 1959). Due to this relationship, BMD estimates were used in the current study as indicators of bone strength. Degree of mineralization is influenced by disease. Diseases, such as metabolic bone disease, can increase bone turnover or delay mineralization. In both cases, bone mineral content is decreased, adversely affecting bone tissue stiffness and strength (Martin et al. 1998a). As a result, it was hypothesized in the current study that infants with chronic illness had significantly lower BMD than infants without chronic illness.

Collagen fiber orientation also affects bone strength. As previously discussed, collagen fibers in woven bone have a random organization with widely varying degrees of mineralization. As a consequence, woven bone is not as strong and has a lower elastic modulus than lamellar bone. However, the random orientation of collagen fibers allows woven bone to perform equally well at resisting loads in all directions (isotropic). Lamellar bone performs best at resisting tensile and compressive loads in the longitudinal direction and less so in the perpendicular directions (anisotropic) (Martin et al. 1998b; Martin and Ishida 1989). Fiber orientation also varies within bone depending on the specific type of loading experienced within a specific area. Longitudinally oriented fibers promote strength in tension, while the transversely oriented fibers are stronger in compression. A study examining the femur found that regions habitually loaded in tension tend to have a larger number of longitudinally oriented fibers, while areas that are habitually loaded in compression have fewer (Portigliatti Barbos et al. 1984). Collagen cross-link maturity and quantity also influence bone tissue strength through their effect on tissue stability (Martin et al. 1998a; Wallace 2014). The effects of collagen cross-links on tissue stability were



discussed previously in the **Bone Biology** section. Although the relationship between collagen cross-link maturity and quantity, and SOS were not addressed in this study, it is important to be aware of other factors that influence bone strength and should be evaluated in future studies for potential associations with SOS.

## ***STRUCTURE***

Whole bone strength can be increased either by increasing bone mass or changing the structural dimensions of the whole bone (Schmidt-Nielsen 1984). However, there is a limitation to the amount of bone mass that can be added to increase bone strength. Skeletal weight increases with added bone mass, which increases the amount of metabolic energy required for locomotion and maintaining the added mass. The hierarchical structure of bone allows it to achieve a certain degree of strength with less material. The quantity, distribution, and geometry of cortical and cancellous bone contribute to the overall structural strength of bone (Martin et al. 1998a; Wallace 2014). Due to the association of bone shape and structure with bone strength, tibial measurements (tibial length, midshaft diameter, medullary cavity diameter, cortical thickness, and cortical index) were used in the current study as proxies for bone strength. The relationship between cortical and cancellous bone structure and overall bone strength is discussed further below.

### ***Cortical Bone***

Overall bone strength is related to the section modulus ( $Z$ ) and porosity of cortical bone. In long bones, the section modulus is a measure of the distribution of bone mass about the neutral axis (axis of bending). The section modulus is proportional to a bone's bending strength and depends on the fourth power of the radius of the bone. As the diameter of the bone increases, section modulus and bone strength in bending increase. Bone diameter has a greater influence on section modulus than bone mass. As long as the diameter does not change, a 16% decrease in the cortical area will only decrease the section modulus by 2.5%. Yet, in two bones with equal cortical mass, a 30% increase in diameter will increase the section modulus by 70%. Therefore, greater bending strength can be achieved without increasing bone mass by changing the geometry of cortical bone (Martin et al. 1998a; Wallace 2014). In the current study, it was hypothesized that tibial midshaft diameter was negatively associated with chronic illness and prematurity due to the negative effects these factors have on growth. It was also hypothesized that midshaft diameter

was positively associated with BMD, as both BMD and increased midshaft diameter should be correlated with increased strength.

Small changes in overall bone size by the redistribution of bone mass further away from the neutral axis can also compensate for losses in bone material tissue strength. As discussed previously, disease can result in decreased bone mineral content for various reasons. Bone size and shape may adjust in an attempt to maintain structural integrity while using a weaker material (Martin et al. 1998a; Wallace 2014). For example, rickets results in curvature of the bones, producing large bending forces. Rachitic long bones alter their cross-sectional shape to compensate for these large bending forces (Martin et al. 1998a).

Cortical porosity is another important factor influencing bone strength. Cortical bone is very dense (low porosity) relative to cancellous bone. Typically, larger bone size indicates greater bone mass due to the low porosity of cortical bone. However, diseases, such as metabolic bone diseases, can increase the porosity of cortical bone by increasing resorption or bone turnover. Increased cortical porosity decreases bone mass and stiffness, affecting its overall strength, but not necessarily influencing bone size or distribution of the bone mass (Martin et al. 1998a; Wallace 2014).

### ***Trabecular Bone***

The strength of trabecular bone is greatly influenced by both bone mass and its distribution. Trabecular bone is very porous, which makes bone mass an important contributor to the strength of cancellous bone. Bone mass accounts for 85% of the variation in cancellous bone stiffness or strength in compression. The mass of cancellous bone is found by calculating the bone volume fraction or the BMD. Bone volume fraction is calculated by dividing the volume of cancellous bone tissue by the total tissue volume. The BMD of cancellous bone is determined by both the bone volume fraction and the degree of mineralization of the bone volume fraction (Martin et al. 1998a; Wallace 2014). Trabecular bone has a lower bone mineral content, and therefore lower elastic modulus, than cortical bone (Cullinane and Einhorn 2002; Dyson and Whitehouse 1968; Gong et al. 1964; Norrdin et al. 1977), as a result of its higher turnover rate. Small variations in either bone volume fraction or degree of mineralization can greatly affect the strength of cancellous bone (Martin et al. 1998a; Wallace 2014).

Bone tissue distribution of cancellous bone has major impacts on bone strength. The distribution of trabecular bone is described by its architecture and anisotropy. The architecture of cancellous bone explains 70-80% of the variation in compressive strength (Martin et al. 1998a; Wallace 2014). Important measures of trabecular architecture include trabecular spacing, thickness, number, and connectivity (Goldstein 1987; Raux et al. 1975; Townsend et al. 1975). Decreases in trabecular number, thickness, and connectivity and increased spacing between trabeculae adversely affect bone strength. Also, the trabeculae of cancellous bone have a preferred orientation or direction, making it anisotropic. Cancellous bone is strongest when loaded in the direction of primary trabecular orientation (Martin et al. 1998a; Wallace 2014). Although trabecular bone plays an important role in overall bone strength, it was not evaluated in the current study because SOS measurements were taken at the tibial midshaft which consists primarily of cortical bone.

### ***SPECIAL CONSIDERATIONS FOR INFANT BONE***

The bones of infants/children have different mechanical demands than adults. Fetal/infant/child bone needs to be more compliant than adult bone for birth purposes and increased impact strength. The fetal skeleton, especially the skull, has a very low elastic modulus, making it very ductile and resistant to fracture. Increased ductility and resistance to fracture is exceedingly important for squeezing through the birth canal without injury. Due to the greater risk of falling, impact strength is an important characteristic for infants/children. The ductility in infant/child bone is achieved through a lower bone mineral content compared to adult bone (Martin et al. 1998a). A study which compared the mechanical properties of femora from children ranging in age from 2-8 years old to adults ranging in age from 26-48 years old found that children's bone was only 68% as stiff and required 48% more energy to break than the adult bone (Currey and Butler 1975). The decreased stiffness of children's bone makes locomotion less energetically efficient than in adults. However, greater fracture resistance is more important to the survival of infants/children than locomotor efficiency. Also due to the increased ductility of infant/child bones, an impact with enough energy to cause the bone to fail usually does not result in a complete fracture. As the fracture travels, most of the energy is expended before the fracture can make it all the way through the bone, resulting in a greenstick fracture. As infants/children age, elastic modulus increases rapidly due to the age-associated increase in bone mineral content. As

a result, bending strength increases gradually, while impact strength declines rapidly with increasing age in infants/children (Currey 2006). Therefore, BMD was hypothesized to be significantly associated with age in the current study.

### ***BONE QUALITY AND BMD***

Bone quality has not been clearly defined nor has it been quantified due to the numerous factors that contribute to it. Yet, bone quality is often mentioned in the literature as a determinant of bone strength. Bone quality has been described as the “totality of features and characteristics that influence a bone’s ability to resist fractures (Bouxsein 2003).” BMD is the most often used surrogate measure, and sometimes the only measure, of bone strength. BMD is a very important component of bone strength, but it is not the only important factor that contributes to fracture resistance (Boyce and Bloebaum 1993; Marshall et al. 1996). Not all individuals that suffer fragility fractures have BMD measures that are considered osteoporotic (Browne et al. 2010; Schuit et al. 2004). In a study examining the mechanical strength of vertebral cancellous bone, BMD only accounted for ~80% of the variance in bone strength (Banse 2002). The difference in fracture resistance between individuals with similar BMD is found within the remaining unexplained ~20% of variance. The remaining ~20% of unexplained variance is an important component of bone quality. The term bone quality is used in this study to describe all of the factors, including BMD, that affect a bone’s ability to resist fracture. If SOS measures infant bone quality, it was assumed that SOS and BMD would be significantly positively associated due to the important role BMD plays in bone quality.

### **Bone Histology**

Bone histomorphometry is an invasive method for the evaluation of bone health and structure. In bone histomorphometry, thin sections of bone tissue are microscopically examined for cellular and structural characteristics, which provide insight into the biological processes affecting bone function at the cellular level. Histological examination of bone sections is critical for understanding the balance between bone formation and resorption processes and whether these processes are functioning normally. Histological analysis of bone sections can range from simple evaluations of bone structure to more detailed measurement of cell numbers and functions. Histological analysis can include static or dynamic measurements. Dynamic measurements

include rate measurements of bone formation and resorption and are obtained from living individuals. The special labeling required for dynamic measurements is administered to the individual over in a single dose or over period of time and its absorption by the bone tissue depends on rates and magnitude of change in the bone tissue (Allen and Burr 2014b).

Static measurements characterize bone structure or describe the amount of tissue and the type and number of cells present. Static measurements describe the totality of growth, modeling, and remodeling processes that have occurred without reference to rate or time. Bone volume, cortical volume, trabecular volume, osteoid surface, mineralized surface, osteoid seam width, resorption surface, number of resorption sites, porosity, and number of osteoblasts and osteoclasts are all static measurements. Although some of these measurements are referred to as volumes, they are actually measurements of area. Differentiation between woven and lamellar bone is also evaluated in histological analysis and can be used to determine whether bone formation is occurring normally. Most evaluations of lamellar and woven bone are qualitative assessments. Examination of mineralized bone versus unmineralized bone provides information regarding changes in the mineralization process. Analysis of osteoid requires an assessment of the amount of osteoid covering the bone surface and normalizing that amount to the total bone surface under examination. Osteoid width and the total amount of osteoid surface are used to determine if bone formation is occurring normally. If osteoid width is normal, increased osteoid surface is an indication of bone formation. If osteoid width is abnormally large along with increased total osteoid surface, it is an indicator of a defect in mineralization (Allen and Burr 2014b).

In clinical evaluations, the iliac crest is the most common biopsy site for obtaining bone histology samples due to its proximity to the skin surface relative to other bones. In the medical examiner's setting, a rib sample is usually taken for histological analysis. After the bone samples are obtained, they are decalcified for better assessment of cellular and structural detail. However, decalcification prevents the assessment of remodeling. The decalcified samples are embedded in paraffin wax or plastic. Paraffin wax is preferred over plastic because it is less harmful to the proteins within the sample. However, a disadvantage of embedding samples in paraffin wax is that they have a tendency to distort and shrink up to 15%. Plastic embedded samples only shrink 1-2%. Shrinking is a problem for analyses which require measurements. The block of paraffin wax with the embedded sample is then thin sectioned. The thin sections are placed on slides and

stained. Staining is used to differentiate between cells, collagen, and previously mineralized osteoid within the bone tissue section during microscopic analysis (Allen and Burr 2014b).

Osteoclasts and osteoblasts are identified by their morphological characteristics and are important indicators of bone formation and resorption processes. The amount of surface covered by osteoblasts and osteoclasts provides an index of bone formation to bone resorption. Identification of active osteoblasts can provide important information, but can be difficult. Active formation surfaces are identified as osteoid covered surfaces with osteoblasts present. Osteoid surfaces without osteoblasts present are considered inactive formation surfaces. The presence of osteoclasts does not always indicate that active resorption is occurring. Resorption activity is evaluated by measuring the resorption surfaces or resorption depth. Resorption surfaces are easily identified by their characteristic scalloped shape and resorption surfaces with osteoclasts present are considered sites of active resorption. Resorption surfaces without osteoclast present are considered inactive. Osteoclasts may be absent from resorption surfaces for two reasons. The region may be undergoing remodeling and was in the reversal phase or the osteoclasts were simply not present on the sample section used for that particular slide (Allen and Burr 2014b).

Bone abnormalities caused by diseases such as osteoporosis, osteomalacia, defective mineralization and vitamin D deficiency can be observed during histological analysis. In osteoporosis, there is a loss of cancellous and cortical bone mass causing an overall reduction in total bone volume. Cortical bone appears more porous due to the greater number of absorption cavities that are not filled or not completely filled. The trabeculae that are present appear thin and with reduced connectivity. Typically in osteoporosis, bone formation is low with normal or high resorption. Histologically, this appears as low bone volume with reduced osteoid surface and a normal or high number of osteoclasts. However, the presentation of osteoporosis can vary. Formation may appear normal, but with high resorption. This appears as low bone volume despite normal bone formation. The amount of resorption surface may be increased or normal with increased resorption depth. Decreased bone volume can also be caused by low formation and low resorption with greater reduction in formation relative to resorption. Decreased bone volume can be caused by high formation and high resorption, with greater increase in resorption relative to formation. High formation and resorption is identified by the presence of high

resorption surface with osteoclasts present and high osteoid surface with osteoblasts present. The average width of secondary osteons in cortical bone or hemiosteons in trabecular bone may also be reduced in individuals with osteoporosis. Osteomalacia is identifiable in histological evaluation by the presence of abnormally wide osteoid seams. The overall osteoid volume will be larger than normal and may be present with up to a 40% volume in extreme cases. The number of resorption sites and amount of resorption surface in osteomalacic bone appears normal (Jaworski 1983). Defective mineralization is identifiable as increased osteoid volume due to increased overall osteoid surface, but with normal osteoid seam width (Allen and Burr 2014b). Vitamin D deficiency also results in increased overall osteoid surface, but is differentiated from defective mineralization by increased osteoid seam width (Bordier et al. 1968; Jaworski 1972; Meunier et al. 1973). Osteoid volume may represent 20-40% of the total bone volume (Bordier et al. 1968; Melsen and Leif 1978; Meunier et al. 1973; Mosekilde and Melsen 1976). The number of resorption sites and total resorption surface is also moderately increased in bone affected by vitamin D deficiency (Jaworski 1983). Primary hyperparathyroidism elevates bone remodeling and results in increased number and size of osteoclasts and osteoblasts, osteoid surface, and mineralized surface relative to total bone surface. Marrow fibrosis may also be present (Bingham et al. 1969; Jaworski 1983). In trabecular bone, resorption depth is reduced and normal to high bone formation results in increased average width of hemiosteons. Cortical bone affected by primary hyperparathyroidism appears more porous and cortical width is reduced. Secondary parathyroidism also results in high bone turnover with increased numbers of osteoclasts and osteoblasts. However, secondary hyperparathyroidism is differentiated from primary hyperparathyroidism by the formation of woven bone and the presence of a large amount of marrow fibrosis. The bone volume of cancellous tissue may appear increased, but this is due to the increased accumulation of woven bone (Allen and Burr 2014b).

Histological analysis makes several assumptions. It assumes that bone turnover was occurring at a steady state at the time of bone sampling. Another assumption is that the results obtained from the 2D histological evaluation are applicable to the 3D structure. The quality of the slides should also be considered. Slide quality affects the quality of the data obtained from the histological analysis. Folds in the thin section, loss of marrow adjacent to the trabeculae, cracked or incomplete bone specimens, and incomplete or heavy staining can reduce the quality of data obtained from the analysis (Allen and Burr 2014b). A limitation to the use of bone histology in

the evaluation of infant bone quality is that pediatric reference material is not readily available. As such, the normal range of variation in bone formation and turnover has not been clearly defined. Equally as unclear is how the normal range of variation changes with increasing age over the first year of life. Therefore, severe abnormality may be easily identifiable upon histological evaluation of infant bone; mild to moderate deviations from normal may not be as easily detected. Additionally, it is unknown how, or even if, mild to moderate deviations from histological normality compromise bone strength.

### **Imaging Methods for Assessing Bone Quality**

Many different methods have been developed to evaluate bone health, structure, and integrity. Skeletal imaging is a category of technologies used to non-invasively assess skeletal health and structure (Allen and Krohn 2014). Several technologies fall under the umbrella of skeletal imaging, such as radiography, absorptiometry, quantitative computed tomography (QCT), magnetic resonance imaging (MRI), and quantitative ultrasound (QUS). The imaging modality chosen depends on the nature of the information to be obtained, qualitative or quantitative, and the resolution required for obtaining that information. In the clinical setting, it is desirable to use an imaging modality that obtains the necessary information with the least number of consequences. With regard to skeletal imaging, this means the lowest exposure to ionizing radiation. Most imaging modalities use of ionizing radiation and degree of exposure increases in proportion to the level of resolution (Allen and Krohn 2014). Some of the most commonly used imaging technologies along with their advantages and disadvantages are discussed below.

#### ***RADIOGRAPHY (X-RAY)***

Conventional radiography is the most widely used skeletal imaging technique and is usually the first imaging modality of choice for infants due to its lower level of radiation exposure relative to other modalities (Done 2012). Radiography relies on the theory of attenuation. In radiography, X-rays are used to visualize objects inside of the body. X-rays are attenuated (weakened) in proportion to the density of the objects through which it passes. In other words, the amount of X-ray absorbed by the bone is proportional to the density of the bone. The density of the bone attenuates the amount of X-ray that reaches the film or cassette on the opposite side of the anatomy being radiographed. A bone with increased density will appear more opaque on



radiographs than a less dense bone because of the greater degree of attenuation. Radiographs are most commonly used to assess skeletal fractures and evaluate changes in bone morphology (Allen and Krohn 2014).

Changes in skeletal morphology can be assessed both qualitatively and quantitatively using radiographs. In terms of qualitative assessment, bone density is evaluated by making subjective decisions about the degree of opacity versus transparency of bone on radiographs. Cortical wall thickness is also qualitatively assessed based on radiologists' experience of normal cortical width. Traditionally, rickets and osteomalacia diagnoses are based on qualitative assessments of radiographs. However, there are several disadvantages to the qualitative assessment of bone morphology on radiographs. Due to the subjective nature of qualitative assessment, there is a large degree of intra- and inter-observer variability in radiographic assessment of rachitic changes and demineralization. In a study evaluating the radiographic findings of children with vitamin D deficiency, intra-observer variability accounted for 55% of the variation in demineralization scores and inter-rater agreement was only 65% for rachitic changes and 70% for demineralization (Perez-Rossello et al. 2012). Another study found that inter-rater agreement was lowest (0%) for radiographs taken of mildly osteopenic children in comparison to radiographs taken from children with normal bone mineralization (71%) and severely osteopenic children (25%) (Mulugeta et al. 2011). This is suggestive of another problem with qualitative assessment of bone mineralization and integrity on radiographs. A significant amount of bone loss must occur before it can be detected on radiographs. The amount of bone loss that must occur before it can be detected on radiographs varies depending on the source, but reports range between 20-40% (Allen and Krohn 2014; Lachman 1955; Mazess and Cameron 1972; Mimouni and Littner 2004). Due to its frequent use in the assessment of bone quality and bone morphology, qualitative radiographic assessment of the radius/ulna and tibia/fibula were conducted in the current study. It was hypothesized that greater qualitative radiographic score, an indication of possible demineralization or abnormal mineralization, would be negatively associated with BMD. Due to the negative effects of chronic illness and prematurity on BMD, it was hypothesized that qualitative radiographic score would be positively associated with chronic illness and prematurity. Additionally, it was hypothesized that, if SOS measured infant bone quality, SOS would be negatively related to qualitative radiographic score.

Cortical width and BMD can be quantitatively assessed from radiographs. Radiogrammetry is a technique for measuring periosteal and endosteal diameters to obtain widths of cortical walls. Measurements can be made directly on radiographs using calipers or from digital radiographs with the help of special computer software. BMD can be quantitatively evaluated on radiographs using a technique called radiographic absorptiometry (RA) (previously called photodensitometry). RA requires the placement of a reference standard of known density, usually an aluminum wedge or hydroxyapatite phantom, within the field of view of the radiograph (Mack and Vogt 1971; Vose 1969; Yates et al. 1995). The use of the reference standard accounts for variations in voltage setting, exposure time, and processing. The radiographs undergo computer analysis to obtain grayscale values from the pixels representing the reference standard. These grayscale values are used to calculate the BMD of the region of interest. Studies have shown that BMD values obtained by RA are as precise and accurate as BMD values obtained by DXA (Cosman et al. 1991; Kleerekoper et al. 1994; Swezey et al. 1996; Takada et al. 1997; Yates et al. 1995). An advantage of RA is that it enables the quantification of BMD using equipment that is already widely available and obtaining the radiographs is relatively quick. Due to the readily available radiography equipment within the medical examiner setting, BMD was estimated using the RA method. However, RA has several disadvantages. RA requires radiation exposure, which is typically 600  $\mu\text{Sv}$  (Allen and Krohn 2014). Furthermore, the type of BMD calculated is areal BMD, not volumetric. Areal BMD does not account for size differences, meaning that the areal BMD of a larger child or infant may artificially appear to be greater due to the larger overall bone size, while in actuality a smaller child may have greater bone density. Due to this limitation, it was hypothesized that BMD estimates would be significantly positively associated with body size and tibial size. Another disadvantage of the use of radiographs is their low resolution, which inhibits measurements specific to trabeculae and may result in underestimates of BMD. Underestimation results from averaging the total bone mineral content over the entire measurement area, which includes the medullary cavity, to calculate BMD. Due to this issue, it was hypothesized that BMD would be negatively related to medullary cavity diameter and positively related to cortical thickness and cortical index.

## ***ABSORPTIOMETRY***

Absorptiometry techniques also rely on the theory of attenuation, but certain absorptiometry techniques, such as dual-energy X-ray absorptiometry (DXA), have the capability of differentiating between bone, fat, and soft tissue. Techniques have advanced from the use of photons in the 1960s to X-rays beginning in the 1980s (Allen and Krohn 2014). DXA is the most widely used modality for measuring areal BMD in children and infants (Adams and Shaw 2004; Kalkwarf et al. 2013). DXA emits an X-ray beam that alternates between 2 different energies. As the beam passes through the bodily tissues, the interaction of the X-ray with chemical compounds within the body differentially attenuates the 2 energies of the X-ray (Laskey 1996; Lukaski 1993; Sartoris and Resnick 1989). Differential attenuation of the two energies allows for the discrimination between soft tissue and bone (Ward et al. 2007). Water and organic compounds attenuate the intensity of an X-ray beam less than bone. An external detector/s on the opposite side of the body determines the value of attenuated energy that reaches it and a computer interface provides an image of the scanned areas. Attenuation values of the bone are calculated for each pixel of the image by subtracting soft tissue values from the combined soft tissue and bone value. The attenuation values of the bone are converted into areal BMD ( $\text{g}/\text{cm}^2$ ) by comparing the attenuation values with values obtained from a reference standard. Bone area is calculated by summing the pixel areas within the bone edges. BMC (g) is obtained by multiplying bone area by BMD (Mimouni and Littner 2004; Ward et al. 2007).

Currently, DXA is considered the gold standard for measuring bone mass (Allen and Krohn 2014). Numerous studies have shown that DXA is a valid technique for assessing fracture risk and diagnosing osteoporosis in adults (Black et al. 1992; Cummings et al. 1993; Gärdsell et al. 1993; Hui et al. 1989; Melton et al. 1993; Nguyen et al. 1993; Ross et al. 1991). The most commonly assessed regions for measuring bone mass using DXA are the whole body, lumbar spine, proximal femur, forearm, or a hand (Mimouni and Littner 2004). DXA has become the gold standard for measuring BMD in adults because it has several advantages. The whole body and specific regions can be scanned rapidly, ranging from 2-15 minutes (Chan 1992) and the exposure to ionizing radiation is low ( $\sim 1\text{-}4 \mu\text{Sv}$ ) relative to traditional radiography (Allen and Krohn 2014; Lewis et al. 1994). DXA also has high precision and accuracy of measurement of bone mineral content (Lukaski 1993).

Although DXA is used to measure bone mass in infants/children, there are many disadvantages to its use for infants/children. Although the radiation dose from DXA scans is low (Lewis et al. 1994), there is an ethical debate on the use of any amount of ionizing radiation on infants/children without medical necessity (Mimouni and Littner 2004). Even though normative pediatric data for DXA measured areal BMD is available in the literature and included in most DXA software packages, manufacturers of DXA systems caution against using data taken from the literature for comparison purposes. It is recommended that users obtain institutional and device specific normative data (Laskey 1996). For any given bone, different devices produce substantial variations in BMD values and standardization of the data is difficult (Benmalek and Sabatier 1998; Specker and Schoenau 2005). Furthermore, there are significant differences in the published normative pediatric data. Due to the difference in reference data used, there have been inconsistencies in the diagnosis of osteopenia in children with chronic disease (Leonard et al. 1999). Also, there are holes in the normative pediatric data that is available. Data on whole body BMC and areal BMD of children younger than 3 years of age is lacking, especially in the newer generation fan-beam scanners (Kalkwarf et al. 2013).

Another drawback for the use of the DXA on infants/children is the 2-dimensional (2D) nature of the data that is obtained. The 2-dimensional nature of DXA BMD measurements cannot account for differences in bone size, which is major limitation because of growth (Ward et al. 2007). Even if volumetric BMD is identical in 2 children, a larger child will have a greater areal BMD than a smaller child. In a study conducted on small and large piglets, DXA consistently underestimated BMC in small piglets by range of 17-40% (Brunton et al. 1993). A study of sick and healthy children reported similar findings. DXA underestimated BMD in children, regardless of age, sex, or health status, in comparison to volumetric BMD obtained with QCT (Wren et al. 2005). The normative reference data that is available are based on infants/children that are average size for their age. This reference data can be misleading when being used to assess normality of areal BMD in infants/children that are large or small for their age (Gafni and Baron 2004; Schoenau et al. 2004). To decrease error, normative reference data should be specific for age, sex, ethnicity, body size, and pubertal status. An attempt to correct for this problem has been made by estimating volumetric BMD from DXA scans, but the calculation of the volumetric measurements use inferences of bone geometry based on a database of 3-dimensional (3D) QCT datasets. However, the use of these methods is controversial because it may not reflect true

volumetric BMD (Gafni and Baron 2004). A third limitation is DXA scans cannot differentiate between cortical and trabecular bone. Areal BMD obtained from DXA includes both cortical and trabecular bone (Specker and Schoenau 2005). Due to its 2D nature and to the inability to differentiate between cortical and trabecular bone, DXA scans cannot be used to assess bone architecture or geometry (Allen and Krohn 2014).

Another disadvantage of DXA is due to the equipment itself. The equipment is not portable, which is problematic for ill infants/children that cannot be easily transported to the scanner. Also, a skilled technician is required to conduct the scan and properly analyze the data. Correct positioning within the scanner by the technician has significant effects on the quality of the scan and the resulting data (Allen and Krohn 2014). Movement artifacts are another limiting factor of the quality of DXA scans. It is also necessary for the infant/child to remain motionless during scanning to prevent movement artifacts, which artificially inflate areal BMD values (Koo et al. 1995b). Although scanning times are relatively low, but it may not be possible for an infant/child to remain still for even a short length of time without restraint or sedation (Chan 1992).

### ***QUANTITATIVE COMPUTED TOMOGRAPHY (QCT)***

Computed tomography (CT) is a technique that uses subtle differences in X-ray attenuation to produce a series of 2D images that represent transverse slices of the scanned object. The thickness of each transverse slice is known and used to generate volumetric data. Finally, the transverse slices are reconstructed to produce 3D images of anatomical structures within the body. The 3D data can be used to assess bone geometry (Allen and Krohn 2014). The use of the digital information to obtain quantitative information is called quantitative computed tomography (QCT) (Gilsanz 1998).

CT has many advantages over DXA for measuring bone geometry and BMD in infants/children. Due to its 3D capabilities, QCT bone measurements are independent of size. Another advantage of CT is its higher resolution than radiography and DXA, enabling differentiation between cancellous and cortical bone. CT bone measurements can be obtained from any skeletal site and the addition a bone mineral reference standard to the scan for calibration purposes enables volumetric BMD to be estimated. Measurements obtained by QCT include cancellous bone density, cortical bone density, bone volume, bone size, and geometry measurements (Gilsanz

1998). The coefficients of variation for QCT bone measurements in children range from 0.6 and 2% (Gilsanz et al. 1997; Kovanlikaya et al. 1996). There are limitations to CT measurements obtainable from clinical scanners. Partial volume averaging, also called partial volume effects, is a limitation for the quantification of trabecular parameters using CT. Each image is made up of a large amount of pixels. Each pixel represents an attenuation value or Hounsfield unit (HU). A single trabecula is small in comparison to a pixel. Therefore, each pixel may contain more than just bone and osteoid. A single pixel can include osteoid, bone trabecula, and bone marrow, but the attenuation value representing the pixel is the average attenuation of all densities captured within the pixel (Genant et al. 1996). This is a particular problem at the interface between endocortical bone and bone marrow, and between the bone marrow and trabecular bone. Higher resolution CT scanners use a smaller pixel sizes and can minimize partial volume averaging but not eliminate it. However, increasing the resolution also increases radiation exposure. Clinical CT scanners do not have the resolution to identify individual trabecula and cannot produce data on trabecular architecture.

Peripheral QCT (pQCT) scanners are relatively new and have a higher resolution than clinical CT scanners, which enables the assessment of trabecular architecture (Allen and Krohn 2014). Geometric properties of bone, such as polar moment of inertia and section modulus, can be obtained from pQCT data and are good indicators of bone strength (Augat et al. 1996; Turner and Burr 1993; van der Meulen et al. 2001). Other advantages of pQCT over clinical CT scanners are that pQCT scanners are much smaller than clinical CT scanners, less expensive, and use less ionizing radiation (<1.5-4  $\mu\text{Sv}$ ) (Ward et al. 2007).

Exposure to ionizing radiation is the largest disadvantage of using CT scanners to assess bone status in infants/children. Radiation exposure depends on the duration of the scan and increases with resolution, number of slices, and the specific CT scanner (Allen and Krohn 2014).

Radiation exposure can range from 1.5  $\mu\text{Sv}$  to 90  $\mu\text{Sv}$  (Gilsanz 1998). Like DXA, movement artifacts adversely affect the quality of the scan. It may not be possible for infants/children to remain still during scanning. pQCT also has disadvantages, some of which are similar to CT. Although pQCT scans reduce radiation exposure, it still exposes the infant/child to ionizing radiation. Another disadvantage of pQCT scanners is the restriction to measurements of the appendicular skeleton. Partial volume effects are still a limitation of pQCT scanners for the

measurement of cortical BMD in infant with cortical thickness of less than 2 mm (Binkley and Specker 2000; Schönau 1998). Scan times are relatively long, 2-3 minutes per slice, and the infant/child must remain motionless. Technical expertise is required for proper operation of pQCT scanners and postprocessing protocols have significant effects on analysis integrity. Moreover, pQCT scanners are still relatively expensive, although less than clinical scanners, and require costly maintenance (Allen and Krohn 2014). Also, pediatric reference data remains limited for both clinical CT and pQCT scanners (Ward et al. 2007).

### ***MAGNETIC RESONANCE IMAGING (MRI)***

Magnetic resonance imaging is a technique based on the resonance and relaxation of protons, which generate a magnetic signal in lipids and water within the body. Different tissues have varying amounts of water and lipids, which allows the imaging and differentiation of various anatomical structures (Ward et al. 2007). Bone is an exception and has no or few free protons, which MRI interprets as a void space (Allen and Krohn 2014). Bone appears black on MRI images, while the marrow appears white as it is composed of a large degree of lipids (Ward et al. 2007). Like QCT, the scans are obtained in slices. The voids produce a negative image of the cortical bone and trabecular network in 2D on each slice. The slices are reconstructed to obtain 3D volumes (Allen and Krohn 2014). Greater resolution is required to evaluate trabecular bone. Clinical MRI scanners typically do not have the resolution necessary to clearly delineate individual trabecula, but structural parameters can be determined using postimage processing techniques. Quantification of bone parameters using MRI correlate well with ash weight and bone parameters obtained from QCT scans (Hong et al. 2000). High resolution MRI (hrMRI) and micro-MRI ( $\mu$ MRI) can achieve the resolutions necessary to evaluate individual trabecula, but hrMRI and  $\mu$ MRI are currently used for research and their applicability to clinical practice has not been assessed (Allen and Krohn 2014; Ward et al. 2007).

There are several advantages to MRI. The major advantage of MRI is that it does not require the use of ionizing radiation. Also, measures taken by MRI are independent of size, which is especially important for measurements obtained from infants/children. MRI can distinguish between cortical and trabecular bone and measures of bone morphometry can be obtained and used to calculate bone strength. There are several disadvantages to using MRI. MRI devices are extremely expensive and require trained technicians to operate the device. MRI has long

scanning times (20-30) and the process is very noisy. Long scanning times and loud noise is especially problematic for infants/children that may not be able to remain still and have a higher likelihood of being frightened by the loud noise. Furthermore, parents cannot remain in the room during scanning, which may contribute to the distress of the infant/child (Allen and Krohn 2014; Ward et al. 2007).

### ***QUANTITATIVE ULTRASOUND (QUS)***

Quantitative Ultrasound (QUS) is a non-invasive technique for assessing the physical properties of bone. QUS measures speed of sound (SOS, m/s) of an ultrasound wave and the broadband attenuation (BUA, dB/MHz) of the signal strength as it travels along the bone. Ultrasound waves are inaudible and range in frequency from the upper end of the audible range and into the Megahertz range (Mimouni and Littner 2004). BUA will not be discussed further because it is not being measured in this study. QUS measurements are restricted to areas of the skeleton with limited amounts of overlying soft tissue because ultrasound waves are almost completely attenuated by air, restricting QUS measurements to the appendicular skeleton (Allen and Krohn 2014).

SOS is a measure of the speed and distance ultrasound waves travel from the transmission source, through the bone, and to the detector (Allen and Krohn 2014). SOS is also referred to as the velocity of sound and apparent velocity of ultrasound. There are 2 methods for measuring SOS using QUS, the transverse transmission technique and the axial transmission technique. These techniques differ based on transducer placement. The transducers are placed on opposite sides of the measured bone site in the transverse transmission technique. A transducer on one side of the bone transmits the signal while the transducer on the opposite side of the bone receives the signal after it has traveled through the bone. In the axial transmission method, the transducers are aligned along the long axis of the bone. The signals obtained by the receivers are the combination of all waves propagating axially along the long axis of the bone. A single probe contains all of the transducers and with a set distance between them. The known distance and propagation times are used to calculate SOS (Laugier 2011).

SOS is influenced by the material and physical properties of the bone (Specker and Schoenau 2005). Bone mineral density and elastic modulus are positively correlated with SOS (Mimouni



and Littner 2004). In a study of 20 human calcaneal samples, SOS explained 71.6% of the variation in elastic modulus (Hodgskinson et al. 1997). Several other studies have reported a strong relationship between SOS taken at the tibia and elastic modulus and BMD (Abendschein and Hyatt 1970; Ashman et al. 1987; Ashman and Rho 1988; Lee et al. 1997; Yoon and Katz 1976a; Yoon and Katz 1976b). Structural properties also influence SOS. Research has also shown that bone SOS is influenced by cortical thickness, porosity, and anisotropy (Bossy et al. 2004b; Foldes et al. 1995; Greenfield et al. 1981; Guglielmi et al. 2009; Kann et al. 1993; Kaufman and Einhorn 1993; Kohles et al. 1994; Lee et al. 1997; Mimouni and Littner 2004; Njeh et al. 1997; Prevrhal et al. 2001; Raum et al. 2005; Specker and Schoenau 2005; Tansug et al. 2011). Due to the findings of these previous studies, it was hypothesized that SOS would also be significantly related to BMD, cortical thickness, and by extension cortical index in the current study.

SOS is influenced by many of the same material and structural properties that determine bone strength. Studies have shown that QUS can be used as a tool to assess bone strength (Foldes et al. 1995; Kang and Speller 1998; Njeh et al. 1999; Pearce et al. 2000; Prins et al. 1997). In a cadaveric study, heel SOS measurements were strongly correlated with femur strength. Tibial SOS was only weakly correlated with femur strength (Bouxsein et al. 1999), but a study conducted on cadaveric tibia specimens found that tibial SOS was highly correlated with ultimate and yield strength of cortical specimens taken from the tibia (Lee et al. 1997). Similar findings have been reported for SOS measurements of the phalanges in comparison to radial strength (Njeh et al. 2000). Currently, QUS is only used for the assessment of osteoporosis in adults. Specifically, heel QUS measures taken using the transverse transmission technique have been proven to predict hip fractures and other osteoporotic fractures comparably to DXA (Hartl et al. 2002; Laugier 2011). Yet, several clinical studies have shown that the axial technique is capable of discriminating healthy from osteoporotic individuals using other bone sites (Barkmann et al. 2000; Hans et al. 1999; Njeh et al. 2001; Talmant et al. 2009; Weiss et al. 2000). Prospective studies found that SOS measurements are capable of predicting fracture risk independently of BMD (Bauer et al. 1997; Hans et al. 1997). Research also shows that SOS measurements are capable of discriminating between adults patients with osteoporotic fractures and age-matched controls (Gluer et al. 1996; Gregg et al. 1997; Njeh et al. 1997).

SOS may be a better candidate parameter than BMD for the evaluation of osteoporosis because it is influenced by both bone mass and structure (Drozdowska and Pluskiewicz 2001; Kaufman and Einhorn 1993; Miller 2000; Njeh et al. 2000; Njeh et al. 2001; Töyräs et al. 1999; Wear 2000; Wuster et al. 1992). Several studies have suggested that SOS is directly related to bone quality (McDevitt et al. 2005; Pereda et al. 2003; Ritschl et al. 2005; Rubinacci et al. 2003) because it is influenced by structural properties as well as BMD (Chen et al. 2004). In patients with Paget's disease, SOS measurements were able to discriminate between affected and unaffected limbs within the same individual, even though there was no difference in estimated vBMD between the limbs (Pande et al. 2000). This indicates that SOS measures something besides BMD that affects bone strength and it also indicates that there are aspects of bone fragility not captured by BMD.

The clinical use of QUS in infants/children has yet to be established because of the lack of adequate normative reference data (Specker and Schoenau 2005). The majority of research on bone SOS and infants focuses on newborn term and preterm infants during the immediate neonatal period or the preterm infant at term corrected age (Ahmad et al. 2010; Altuncu et al. 2007; Chen et al. 2012; Gursoy et al. 2008; Koo et al. 2008; Littner et al. 2004a; Littner et al. 2003; Littner et al. 2005; McDevitt et al. 2005; Nemet et al. 2001; Pereda et al. 2003; Rigo and De Curtis 2006; Rubinacci et al. 2003; Tomlinson et al. 2006; Wright et al. 1987; Yiallourides et al. 2004). Longitudinal studies are limited by small sample sizes, restricted to preterm or very low birth weight infants, or their measurement intervals are inconsistent (Gonnelli et al. 2004; Litmanovitz et al. 2003; Litmanovitz et al. 2004; McDevitt et al. 2007; Mercy et al. 2007; Rack et al. 2012; Ritschl et al. 2005; Tansug et al. 2011; Tomlinson et al. 2006; Zadik et al. 2003).

QUS performed as well as DXA in identifying low BMD in children with fragility fractures (Fielding et al. 2003). Also, QUS performed better at predicting fractures in isolated infant bones in vitro than BMC (Wright et al. 1987). There are several advantages of using QUS over other skeletal imaging modalities to assess bone strength in infants/children. Scan time is quick and the device is portable and much less expensive than other skeletal imaging modalities. Moreover, QUS does not use ionizing radiation nor does it require technical expertise to operate the device (Allen and Krohn 2014).

Based on the above mentioned research, QUS appears to be a promising tool for evaluating infant bone quality. However, there are gaps in the literature that have prevented QUS from being identified as a diagnostic tool. More research is necessary to clarify exactly what aspects of bone quality are being measured by SOS. It is also unclear how changes in bone quality influence SOS readings or how sensitive SOS readings are to changes in bone quality. Additionally, the normal range of variation in SOS readings, that is specific to age in months throughout the first year of life, remains unknown. The current research uses what is known about bone biology and bone biomechanics to fill these gaps in the literature for the purposes of determining whether QUS can be used as a diagnostic tool for the evaluation of infant bone quality.

### **Summary**

Bone's ability to resist fracture depends on its structural and material biomechanical properties. These properties are affected by biological and environmental factors beginning *in utero*. Biological factors that affect bone include genetics and any congenital disease that interferes with development and growth. There are a large number of environmental factors that can affect bone beginning with the prenatal environment. Any maternal nutritional deficiencies or toxins introduced into the maternal body can have adverse effects on the skeletal development *in utero*. After birth, nutritional deficiencies, regardless of etiology, can adversely affect skeletal growth and development. Adverse effects on growth and development affects bone material and/or structural properties, affecting bone quality and possibly resulting in bone fragility. Aspects of bone quality can be assessed through invasive (bone histology) and non-invasive (imaging) methods. QUS is a promising non-invasive technique for the evaluation of infant bone quality that does not expose the infant to ionizing radiation. However, gaps in the literature have prevented QUS from definitively being identified as a diagnostic tool for infants. This study uses what is known about the adverse effects of chronic illness and prematurity on infant bone growth and strength to assess what SOS is measuring and, therefore, whether QUS is a valid diagnostic tool for the assessment of infant bone quality.

## CHAPTER 3 : MATERIALS AND METHODS

In both the medical examiner and clinical setting, the assessment of bone fragility may be pivotal to the diagnosis or exclusion of non-accidental injury as the cause of trauma. However, there is no non-invasive quantitative method for evaluating infant bone quality that does not require the use of ionizing radiation, with one exception. Magnetic-resonance imaging (MRI) with powerful magnets is capable of measuring aspects of bone quality in infants, but scan times are relatively long (20-30 minutes) and may require sedation (Ward et al. 2007). QUS may be a feasible alternative for measuring bone quality in infants, as it does not use ionizing radiation and scan times are relative short (2-3 minutes). The purpose of this research was to assess QUS as a possible method for evaluating bone quality in infants. In order to address this issue, the study sample was drawn from infants receiving autopsies in the medical examiner and hospital settings. A combination of qualitative and quantitative data was collected from the study sample as indicators of the infant's bone health. The following data were collected from each infant: areal bone mineral density values (aBMD), bone cross-sectional measurements taken in the medio-lateral plane, qualitative evaluations of bone mineralization from radiographs, histological evaluation of bone normality/abnormality, as well as demographic and developmental information, individual and family medical histories, and details regarding the circumstances surrounding death. See **Figure A- 1** of the Appendix for a complete list of variables collected for each infant. SOS readings obtained from each infant in the study sample were compared with these bone health indicators to assess the validity of QUS as a technology for the evaluation of infant bone quality. This chapter describes the variables collected, study sample, data collection methods, statistical analyses, and limitations of the materials and methods utilized in this research.

### Infant Injury Database

The Infant Injury Database (IID) contains an extensive amount of de-identified information gathered from medical records, family medical history, investigator reports (medical examiner, law enforcement, and child protective services), and autopsy findings associated with infants that received examinations at Harris County Institute of Forensic Sciences (HCIFS). The variables recorded in the IID pertain to each infant's demographic information, as well as information on

health, development, and circumstances surrounding the death. The IID was developed as a tool for understanding infant death. All data pertaining to the current study sample, including bone measurements, were recorded in the IID by the researcher. A brief description of the data recorded in the IID follows. See **Figure A- 1** of the Appendix for a more detailed explanation of each variable recorded in the IID.

The IID contains demographic information, such as sex, race, date of birth, and date and time of death. These variables were obtained from investigator reports and medical records. Date of birth and death were then used to calculate chronological age in months. Data associated with the circumstances surrounding the death were also obtained from investigator reports. These variables include the location the infant was found (bed, crib, floor, etc.), the relationship of the person that found the infant to the infant (mother, father, mother's boyfriend, etc.), and where the infant died (hospital or residence). Other variables include whether the infant was sleeping alone or co-sleeping. If the infant was co-sleeping, the relationship of each individual in the bed was recorded (mother, father, siblings, etc.) along with their approximate weights. If the infant died at the hospital, method of transportation to the hospital (EMS or private vehicle) was documented. If emergency medical services (EMS) were contacted, the time EMS arrived on scene was recorded along with the time of arrival to the hospital. Cardiopulmonary resuscitation related variables were also documented in the IID and include whether the infant received CPR, who performed the CPR (bystander, medical personnel, or both), and the type of CPR performed (anterior, two-thumb, or both). For cases in which the infant survived for greater than 1 day in the hospital, the date/time of arrival to the hospital and date/time of death were used to calculate the length of the hospital delayed death.

Information for variables pertaining to infants' health at birth were obtained from birth records and recorded in the IID. These variables include whether the mother obtained prenatal care, estimated gestational age (EGA), and birthweight. EGA was used to determine whether an infant was born prematurely. Any infant born less than 37 weeks gestation was categorized as premature or preterm, while infants born at 37 weeks gestation or later were categorized as full term or term infants. EGA was also used to calculate term-corrected age by subtracting the number of weeks born prior to term, 40 weeks gestation, from chronological age in weeks. This value was then converted back to age in months. Birth records were also reviewed for reports of

congenital anomalies and maternal tobacco, alcohol, prescription and illicit drug use during pregnancy. In the IID, this information was recorded as medical history.

Information for variables associated with infants' health and development was obtained through review of medical records and investigator reports. Reports of congenital anomalies or chronic illness were recorded under medical history. There is no commonly used definition for chronic illness in the clinical literature, but a definition for chronic illness was developed for use in the current study based on definitions used by other studies and recommendations made in the literature (Mokkink et al. 2008; Perrin et al. 1993; Stein et al. 1993; van der Lee et al. 2007). Chronic illness was defined as any disease or condition that was diagnosed during or prior to autopsy which likely had a negative effect on the growth and development of the infant, or required pharmacological treatment that has known side effects impacting the growth and development of the child (Mokkink et al. 2008). An exclusionary criteria based on duration of illness was not used for two reasons. First, the most commonly used duration for a chronic illness is three months, but this duration is not based on systematic research or on conceptual grounds (Stein et al. 1993). Secondly, the duration of time required before illness begins to adversely effects the skeleton is unknown and likely depends on the scale at which the bone is being examined. The current study examined bone at more than a single scale. Current and past medications, as well as any genetic disorders were documented in the IID. Level of gross motor development (non-ambulatory, crawling, cruising, or walking) and indications of developmental delays were also recorded variables.

Autopsy reports also provided information for variables associated with infant health and traumatic injury. Recorded variables obtained from the autopsy report include cause of death (COD), manner of death (MOD), pathological findings, and traumatic injuries. With regard to pathology, each organ with pathological findings was documented individually and specific findings noted. If traumatic injuries were present, specific locations of external and internal traumatic injuries were recorded. Variables associated with skeletal injuries included specific skeletal element (rib, femur, occipital bone, etc.), location on the bone (proximal, distal, distal 1/3 shaft, etc.), side (right or left), number of element (rib 1, rib 2, rib 3, etc.), type of fracture (buckle, transverse, oblique, etc.), and degree of healing assessed macroscopically (no healing, soft callus, hard callus, etc.). Variables such as height (cm) and weight (kg) at the time of death

were also obtained from autopsy reports and were used to calculate growth percentiles for each infant, such as length for age, weight for age, and weight for length. Growth percentiles were calculated based on growth standards specific to sex published by the World Health Organization (WHO) in 2006 (WHO Multicentre Growth Reference Study Group 2006). The Center for Disease Control and Prevention (CDC) recommends using the WHO growth standards for individual's under the age of 2 years. These growth standards are used by pediatricians to determine how an infant, for their age and sex, compares in size to other infants of similar age.

### **Study Sample**

The study sample consisted of infants ranging in age from 30 weeks gestation (actual or corrected) to 1 year postnatal at the time of death. All infants included in this study received autopsies at the Harris County Institute of Forensic Sciences (HCIFS) or Texas Children's Hospital (TCH) in Houston, Texas. During the autopsy, the pathologists recorded all injuries and pathological findings as well as growth measurements. The cases autopsied by HCIFS also received full rib examinations. Full rib examinations consisted of removing the periosteum and all soft tissue from the pleural surface of the ribs and examining each rib from sternal to vertebral end for fractures. When non-accidental injury was suspected, a forensic anthropologist performed a pediatric skeletal examination as described by Love and Sanchez (2009) to identify skeletal injury. For infants receiving autopsies at TCH, the pathologist submitted a form for each infant describing the autopsy findings and all relevant medical and family history information (**Figure A-2** and **Figure A-3** of the Appendix). This information was recorded in the IID.

This research employed a prospective research design. All infants within the specified age range, regardless of medical history or circumstances surrounding death, autopsied at HCIFS over a 9 month period were included in the study. The prospective and all inclusive research design increased the probability that infants included in this study formed a representative study sample of the medical examiner and chronically ill infant population.

## Methods

### *OBTAINING AREAL BMD ESTIMATES FROM DIGITAL RADIOGRAPHS*

Radiographic absorptiometry was used to calculate areal BMD estimates from pixel gray-scale values obtained from digital radiographs of the forearm and leg. All radiographs were taken with an Aribex Nomad Pro handheld cordless x-ray system (Aribex, Inc., Orem, UT) on 10" x 12" x-ray cassettes. All radiographs were taken at 60 kVp for 0.75 seconds at 2.5mA. Exposure time was selected based on the apparent contrast between bone and soft tissue, as well as the amount of apparent saturation of the density spheres where were to calculate the bone mineral density estimates. The x-ray unit was placed in a custom built stand to maintain a consistent 895 mm distance between the x-ray cassette and the x-ray unit and to ensure that the x-ray was perpendicular to the plane of the table (**Figure 3-1**). A plumb-bob was also used to ensure that the center of the x-ray unit's collimator cone was aligned with the midshaft region of the forearm and leg. A lead apron was draped over the open side of the stand to protect the user from radiation backscatter while the x-ray unit was in use. For each decedent, the left arm and leg were radiographed in anatomic position (**Figure 3-2-Figure 3-3**). Masking tape was used to secure the limb to the x-ray cassette in anatomic position. When therapeutic equipment obstructed radiographs of the left limbs, radiographs of the right limbs were taken. Spherical phantom rods (CIRS, Norfolk, VA) of known hydroxyapatite density ( $250 \text{ mg/cm}^3$  and  $500 \text{ mg/cm}^3$ ) were placed to the right and left of the limb, near the mid-shaft of the tibia/fibula and radius/ulna, in each radiograph (**Figure 3-2-Figure 3-3**). The spherical phantom rods allowed for calibration of the radiograph when the basic image intensity values (gray-scale values) from the radiographic images were converted to units ( $\text{g/cm}^2$ ) of hydroxyapatite. While the density phantoms were placed near the midshaft of the tibia/fibula and radius/ulna, care was taken to ensure that there was not tissue overlying the spheres in the radiographs. X-ray cassettes were processed using a VertX (iCRco, Goleta, CA) computed radiography unit and Clarity PACS software (iCRco, Goleta, CA). After processing, all radiographs were exported in DICOM format and sent to a biomechanical engineer at Medical Metrics Inc. and a pediatric radiologist at TCH.





**Figure 3-1. Setup for obtaining radiographs.**

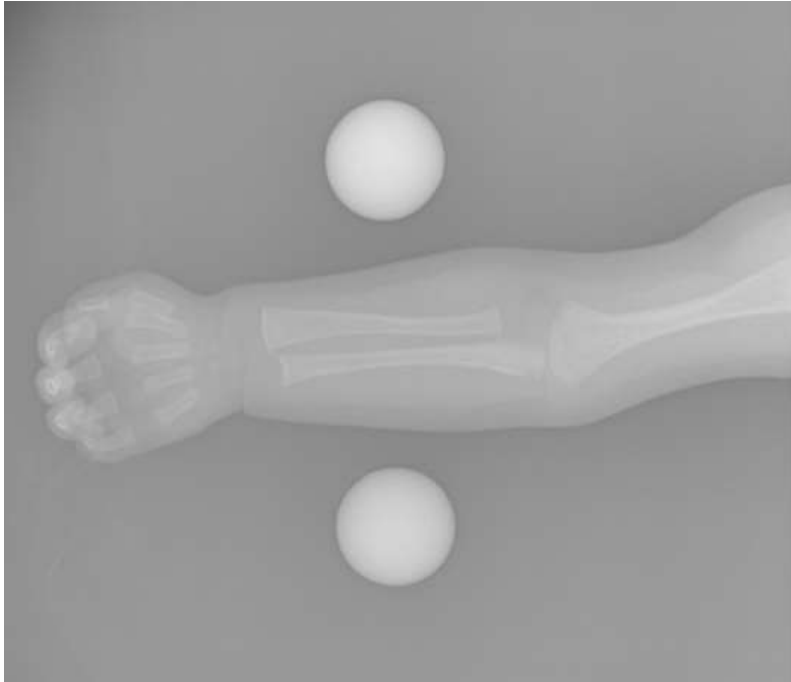


**Figure 3-2. Radiograph of right forearm in anatomic position with spherical density phantoms alongside.**

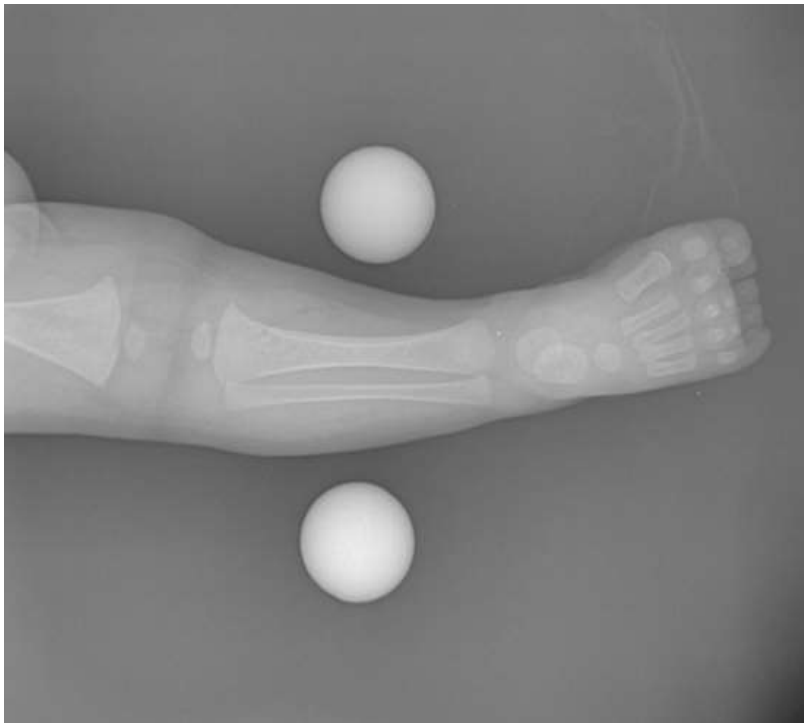


**Figure 3-3. Radiograph of left leg with spherical density phantoms alongside.**

A custom computer program was developed by a biomechanical engineer at Medical Metrics Inc. (Houston, TX) to convert basic image intensity values (gray-scale values) of the radiographic images to units ( $\text{g}/\text{cm}^2$ ) of hydroxyapatite. The basic image intensity values were obtained from the pixels which comprised the radiographic image. The program functioned by first prompting the user to identify the approximate center of the phantom sphere within the radiographic image. Then the program automatically identified the perimeter of the sphere. In order for the program to correctly identify the perimeter of the sphere, the density phantom must be located in a relatively homogeneous area without any overlying tissue. The program then identified the image intensity values from the periphery of the density phantom (background intensity values). The background intensity values were subtracted from the intensity values obtained within the radiographic image of the density phantom. The program then calculated a linear regression between the known bone mineral content at each location within the phantom and the background-subtracted image intensity values of the density phantom. The program performed this calculation by calculating the length of the path of the x-ray beam through the sphere at each location, and determining the volume as the x-ray path length times the pixel size squared. The known density of the sphere, times the volume that the x-ray beam passed through, gave the bone mineral content.

Pilot experiments revealed that the radiographs tended to saturate toward the center of the radiographic image of the sphere. Thus, a regression formula was developed using only the outer third of the density phantom with the hydroxyapatite content of  $250 \text{ mg}/\text{cm}^3$ . Despite only using the outer third, hundreds of data points were still available to obtain the regression equation, and the correlation coefficients were consistently  $> 0.95$  within the same radiograph. Reliability of the custom program was estimated by the biomechanical engineer. BMD measurements were repeated for 21 of the radiographs. The average difference between measurements was  $-0.0054 \text{ g}/\text{cm}^2$ .

After the regression equation for converting image intensity values into hydroxyapatite content was established, the center of the target diaphysis (radius or tibia) was identified. The program prompted the user to identify the most proximal and distal points of the long bone diaphysis to be measured. After these points were identified, the program placed a 10 mm x 10 mm box at the midshaft of the bone. The box edges were placed parallel to the periosteal surfaces of the bone. If

necessary, the box was adjusted by the user. The program used the box to differentiate between the image intensity values associated with the image of the diaphysis and those associated with the surrounding soft tissue. The background image intensity values obtained from the surrounding soft tissue were subtracted from the image intensity values obtained from the image of the diaphysis. An example of the image intensity values plotted by their associated pixel spatial coordinates is provided in **Figure 3-4**. After subtracting image intensity values associated with the surrounding soft tissue, the program used the previously determined regression equation from the density phantom to calculate the total bone mineral content of the 10 mm section of the bone, as well as the areal bone density ( $\text{g}/\text{cm}^2$ ). The program failed to obtain a BMD value when the spherical phantom was not in a relatively homogeneous area of the image (e.g. due to overlying soft-tissue or artifacts in the imaging). The program also failed if there was not at least a few millimeters of bone to either side of the diaphyseal region being measured. This procedure was carried out by the biomechanical engineer for each radiograph. The data were output in excel file format, assembled into one master excel file, and sent to the researcher to enter into the IID.

### ***QUALITATIVE RADIOGRAPHIC EVALUATION***

All radiographic images were also sent in DICOM format to a pediatric radiologist for qualitative evaluation of bone mineralization. The pediatric radiologist qualitatively assessed bone mineralization by scoring each radiograph for rachitic changes and degree of demineralization. Rachitic changes were scored as present or absent and characteristics associated with rachitic changes, such as metaphyseal widening, irregular and/or fraying margins, and metaphyseal cupping, were recorded. Mineralization was scored on a scale of 0-2, with 0 indicating normal mineralization, 1 indicating indeterminate, and 2 indicating abnormal mineralization. An indeterminate score was given to bones which appeared somewhat demineralized, but not abnormal. Characteristics associated with demineralization, such as cortical and trabecular thickness and lucency were also recorded. The form used by the pediatric radiologist to record scores and observations for each infant is provided in **Figure A-4** of the Appendix. All scores and observations were entered in the IID.

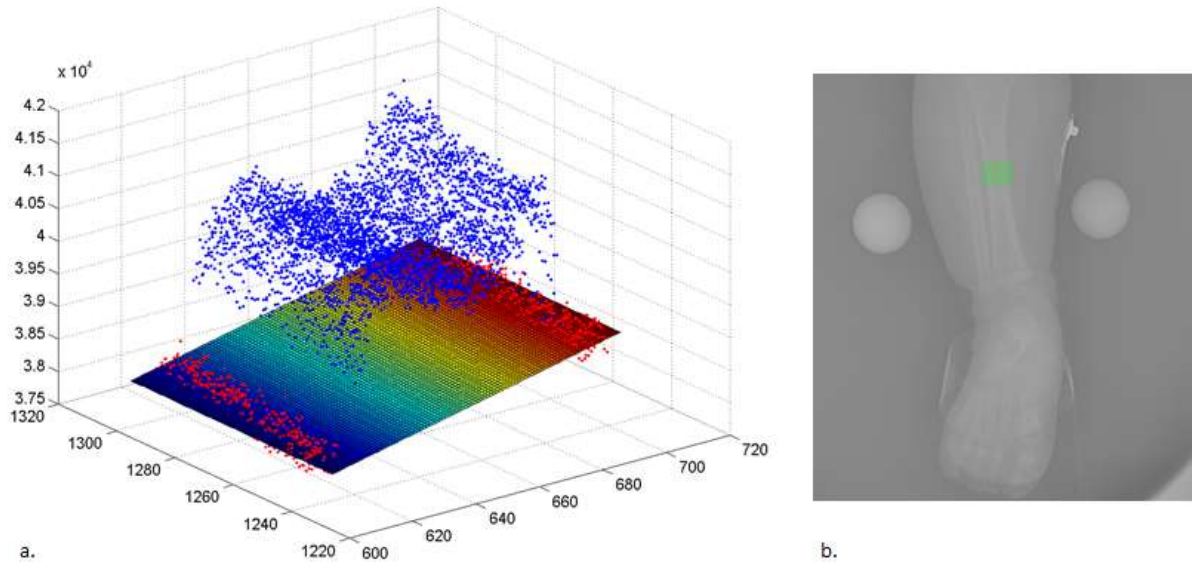


**Figure 3-4. a. Plot of image intensity values by spatial coordinates of the pixels in the image. Note that the plot of image intensity values has two peaks. Each peak corresponds to image intensity values obtained from the medial and lateral cortical walls. The valley between the two peaks represents image intensity values obtained from the medullary cavity. b. Radiograph of leg with green highlighted area representing the location where image intensity values were obtained for the plot (a).**

### ***TIBIAL MEASUREMENTS***

Digital radiographs of the tibia were used to obtain midshaft cross-sectional measurements. Using the software program ImageJ (Rasband 1997-2014), diaphyseal diameter, cortical thickness, and medullary diameter at the midshaft of the tibia were measured in mm. For each radiograph, the measurement scale was calibrated prior to obtaining any measurements. Calibration was carried out using the known diameter (25 mm) of the spherical density phantom. A line was drawn across the center of the image of the density phantom and a plot profile of the image intensity values associated with the line was generated by the program. The plot profile was used to identify the edges of the density phantom in a systematic manner by using the half-maximum intensity values to define the edge locations (**Figure 3-5**). Half-maximum intensity values are the halfway point between the lowest image intensity value and the highest image intensity value for each slope of the line. The midshaft of the tibia was identified by drawing a line from the most proximal to the most distal points on the tibial diaphysis. The center of the line is automatically indicated by the program. After the midshaft was identified, a line

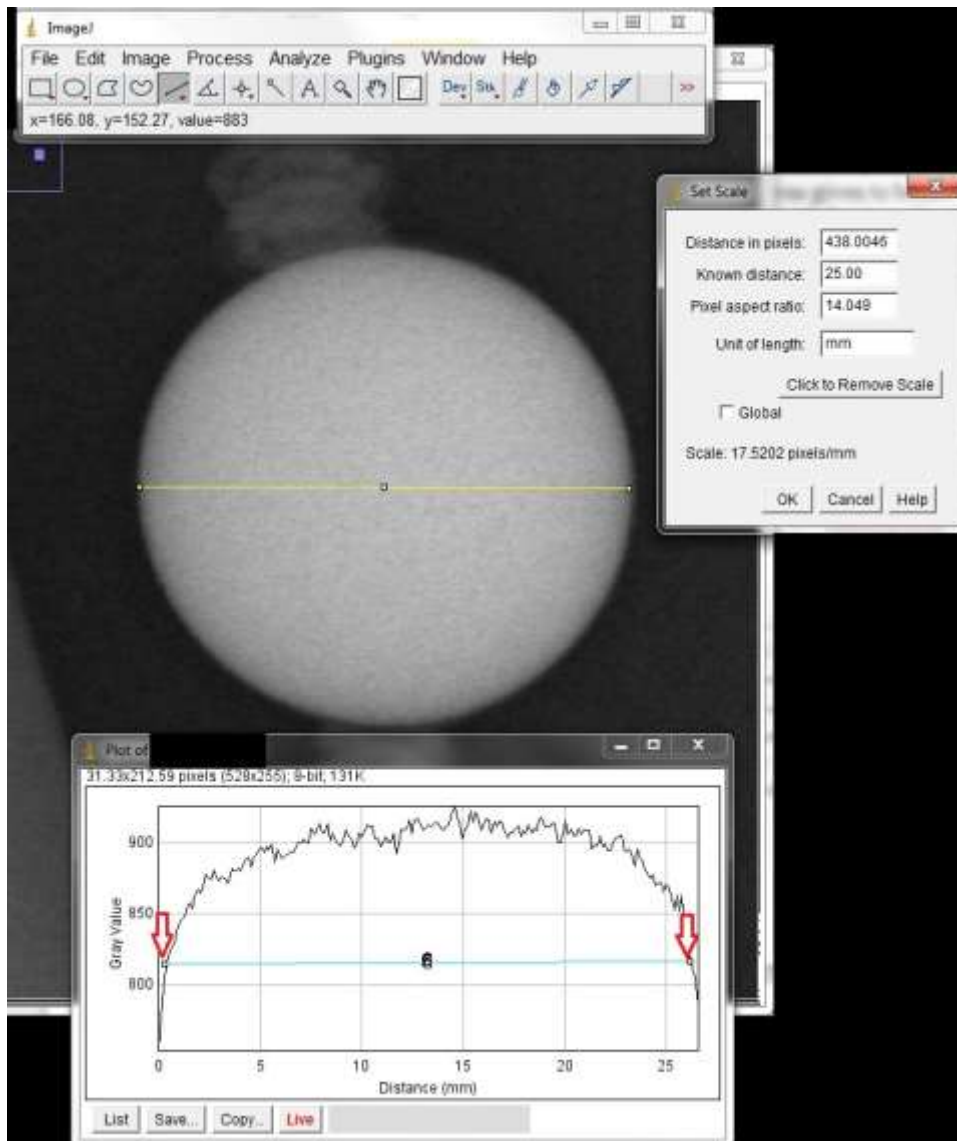


Figure 3-5. Setting the scale in ImageJ. Plot profile of the image intensity values is shown at the bottom of the figure. Red arrows on the plot profile indicate half-maximum intensity points along plot profile line.

perpendicular to the long axis was drawn across the midshaft and a plot profile of the image intensity values across the midshaft was generated by the program. The plot profile of the line across the midshaft had two peaks. Each peak corresponded to the image intensity values across one of the cortical walls. Similar to locating the edges of the density phantom, the edges of the periosteal and endocortical surfaces of the cortical walls were identified using a plot profile. The length of the line on the radiographs was adjusted until the endpoints were at locations associated with the half-maximum intensity values along the plot profile line. In the plot profile, the half-maximum intensity values along the outer slopes of the peaks defined the edges of the periosteal surface. The length of the line associated with the half-maximum intensity values defined the diameter of the tibial midshaft. The half-maximum intensity points on the inner slopes of the peaks defined the edges of the endocortical surface (**Figure 3-6**). The length of the line associated with the half-maximum intensity values on the inner slopes of the peaks on the plot profile line defined the medullary cavity diameter. All measurements were taken in mm. Medullary cavity diameter was subtracted from midshaft diameter to obtain the cortical thickness measurement. The ratio of cortical thickness to diaphyseal diameter was then used to calculate cortical index.

#### ***QUANTITATIVE ULTRASOUND EVALUATION (SOS MEASUREMENT)***

Bone SOS readings were measured with the Sunlight MiniOmni Bone Sonometer (BeamMed Ltd, Petah Tikva, Israel). The MiniOmni™ Ultrasound Bone Sonometer uses the axial transmission technique to measure SOS along long bones, such as the radius, metatarsal, tibia, or the phalanx (Mimouni and Littner 2004). The ultrasound probe emits an array of ultrasound waves with a center frequency of 1.25 MHz, from a pair of transmitting transducers at one end of the probe. The signal travels through the soft tissue until it encounters bone. Some of the ultrasound waves encounter the bone at a critical angle and are refracted such that the waves propagate along the long axis of the bone. These waves then exit the bone at the same critical angle at which they entered the bone. A pair of receiving transducers at the opposite end of the probe detects these waves once they exit the bone. The first signal to be detected by the receiving transducers is used to calculate SOS. The ultrasonic pulses are only transmitted and received by the transducers when there is good acoustic contact between the probe surface and the patient's skin, which is accomplished using ultrasound transmission gel (Aquasonic 100 Ultrasound Transmission Gel, Parker Laboratories Inc., Fairfield, NJ).

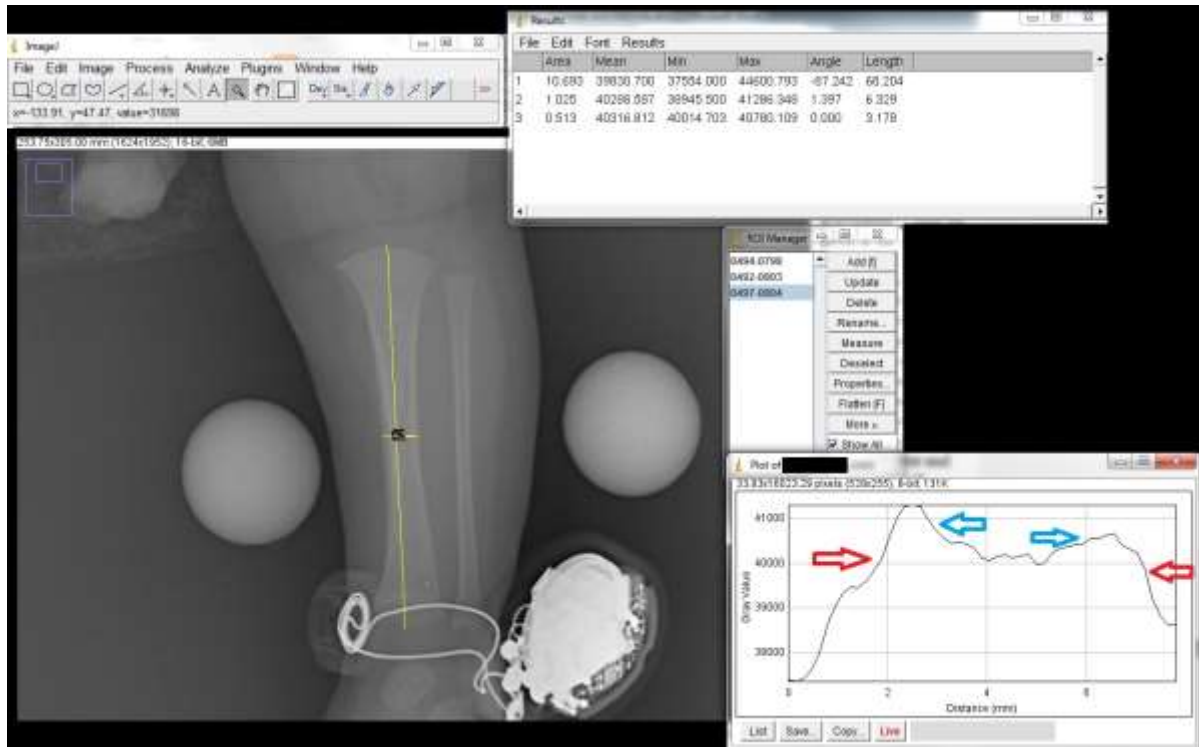


Figure 3-6. Obtaining cross-sectional measurements of the tibia in ImageJ. Measurement results of the tibial length, midshaft diameter and medullary cavity diameter are shown in the upper right hand corner of the figure. Plot profile of the image intensity values across the entire midshaft is shown in the lower right hand corner of the figure. Note that the plot profile line has two peaks. Red arrows point to the portion of the plot profile line (outer slopes) generated from image intensity values associated with the periosteal surface of the tibial midshaft. Blue arrows point to the portion of the plot profile line (inner slopes) generated from image intensity values associated with the endocortical surface of the tibial midshaft.



The speed of the signal is calculated by dividing the known distance between the transmitting and receiving transducers within the probe and the signal's time of travel from the transmitting transducer through the bone to the receiving transducer (Barkmann et al. 2000; Njeh et al. 1999). The SOS measurement result is obtained after performing at least three statistically consistent measurement cycles. Each measurement cycle lasts ~20 seconds. If the coefficient of variation between the first three cycles exceeds 1.2%, a fourth and possibly fifth cycle must be conducted. If three statistically consistent measurements cannot be found after five measurement cycles, the entire measurement is aborted (Mimouni and Littner 2004). Differences in soft tissue thickness are accounted for through proprietary algorithms that subtract the duration of time it takes the signal to travel through soft tissue (BeamMed 2010). By accounting for the effects of soft tissue thickness on SOS, SOS measurements can be compared between infants with differing tissue thickness. Reference standards for preterm and term neonates have been developed for this device, but the sample size is small and will not be used in this study (Littner et al. 2003).

Prior to use on each infant, the ultrasound probe was calibrated with a perspex phantom provided by the device manufacturer. After calibration, SOS readings were taken on the antero-medial region of the left leg at the midshaft. If therapeutic equipment obstructed access to the left leg, readings were taken on the right side. Three consecutive SOS readings were taken and recorded for each infant to assess intra-observer error. Although proprietary algorithms reportedly account for differences in soft tissue thickness, the circumference (mm) of the measured leg was still taken to test whether tissue thickness significantly affected SOS readings. The circumference was measured near the mid-point of the leg using a vinyl measuring tape. Vinyl measuring tape was used because it is flexible and is resistant to stretching. SOS readings and circumference of the leg were recorded in the IID. An average of the three SOS readings was calculated for each infant to be used for statistical analyses.

### ***QUALITATIVE BONE HISTOLOGY EVALUATION***

During the autopsy, samples of the costochondral junction of the left fourth rib and the mid-point of the left iliac crest were obtained for histological evaluation of bone health (**Figure 3-7**). A Stryker autopsy saw was used to excise all bone samples. When the left fourth rib could not be obtained, another rib was substituted. Rib number and side and iliac crest side were recorded. Samples were put in labeled specimen containers with EDF<sup>TM</sup> fixer/decalcification solution

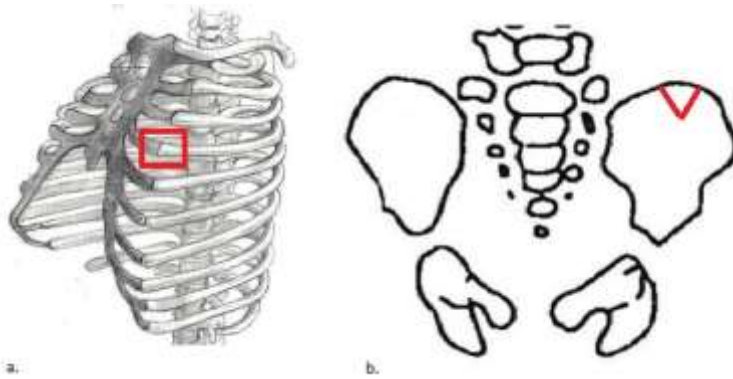


**Figure 3-7: a. Costochondral junction of left 4<sup>th</sup> rib (area marked in red) or other available rib taken for qualitative histological evaluation. b. Bone sample excised from mid-point of iliac crest (area marked in red) for qualitative histological evaluation.**

(StatLab, McKinney, TX) for at least 24 hours. A histology technician thin sectioned and stained each tissue slice with Hematoxylin and Eosin and Masson's Trichrome using traditional histological methods. The stained specimen slides were then delivered to a bone pathologist for qualitative histological evaluation. Using a self-developed protocol that was developed specifically for this study, the bone pathologist evaluated the bone and cartilage of each rib and iliac crest section for the following characteristics: current vasculature, current mineralization, current volume, current formation, and current resorption. Each variable was scored as 0 (normal), 1 (indeterminate), or 2 (abnormal). Native collagen architecture and native mineralization was also scored to evaluate the infant's ability to produce normal bone. After evaluating all previously mentioned variables, the bone pathologist classified each bone sample as histologically normal or abnormal overall. The form used by the bone pathologist to record scores and observations for each infant is provided in **Figure A-5** of the Appendix. The histology evaluation scores and observations for each decedent were recorded in the IID.

### ***METHODS LIMITATIONS***

The methods used to conduct this research introduce several limitations. While x-ray equipment is more readily available than CT and DXA devices, digital x-ray is a lower resolution technology relative to these other technologies for estimating BMD. X-ray attenuation values, or image intensity values, are averages of the x-ray attenuation occurring within each pixel. The x-ray attenuation values assigned to each pixel are a combination of the attenuation produced by both the cortical and trabecular bone and the overlying soft tissue, decreasing the precision of the

BMD estimates. Also, calculation of BMD estimates from radiographic images is sensitive to inhomogeneities within the image, which can be introduced by damaged x-ray cassettes or problems with the computed radiography processing unit. Another limitation to the use of digital radiographs to obtain BMD is that the estimates are areal ( $\text{g}/\text{cm}^2$ ), not volumetric ( $\text{g}/\text{cm}^3$ ). Areal estimates are sensitive to size differences. This is problematic for BMD comparisons made among infants due to their rapid growth rates.

Poorly developed standards for the assessment of infant bone also results in research weaknesses. No infant standards have been developed for calculating BMD estimates from image intensity values. For this reason, the biomechanical engineer developed his own protocol for converting image intensity values to BMD estimates. It could not be known at the outset of this research that the density phantom with the lowest density ( $250 \text{ mg}/\text{cm}^3$ ) was slightly too dense for comparison with infant bone. However, this limitation was overcome by using the outer third of the density phantom's radius to calculate the BMD estimates. Furthermore, there is no published normative BMD data for infants that are specific to the tibia, which prevents the validation of our BMD estimates with other published data. Ahmad and colleagues (Ahmad et al. 2010) published BMD data for the infant tibia, but these data were obtained from newborn infants within a few days of birth or preterm infants up to 3 months of age. In addition, standards have not been developed for the qualitative evaluation of mineralization on radiographs. Specifically for this study, a pediatric radiologist developed a standardized scoring system to consistently evaluate the degree of mineralization of each radiograph. The low resolution of radiographs was also a weakness for qualitative radiographic evaluation. It is reported that up to 30% of bone mineral must be lost before it is detectable on radiographs (Done 2012). Neither have standards been developed for the histological evaluation of infant bone normality/abnormality. Specifically for this study, a bone pathologist developed a scoring system for the evaluation of infant bone based on characteristics commonly evaluated for the assessment of bone health in the field of bone histology.

### ***STATISTICAL METHODS***

Tibial measurements (tibial length, midshaft diameter, medullary cavity diameter, cortical thickness, and cortical index), BMD, and SOS were evaluated for significant influences from demographic characteristics (race, sex, and age), proxies for overall health (prematurity and

chronic illness), body size (weight, weight for age percentile, height, length for age percentile, weight for length percentile, and leg circumference), and skeletal maturity at birth (EGA and birthweight). In addition, the relationships between tibial measurements and, BMD and SOS were investigated. Understanding how these variables were related to BMD and SOS provided insight into the factors measured by SOS and added clarification to the relationship between SOS and BMD.

Detailed analyses were carried out to assess what SOS measured in term of bone quality and bone health. As such, a large number of statistical tests were conducted, which can be problematic. Conducting a large number of statistical tests increases the likelihood of a Type 1 error, false rejection of the null hypothesis. A Bonferroni correction, an adjustment of the p-value, can be applied to reduce the likelihood of a Type 1 error. A Bonferroni correction was not used in the current study for several reasons. The statistical power of the current study was reduced due to small sample size, which reduces the likelihood of a Type I error. Other reasons a Bonferroni correction was not utilized in the current study pertain to associated problems with the method. Bonferroni corrections reduce statistical power by increasing the likelihood of a Type II error, falsely accepting the null (Cabin and Mitchell 2000; Moran 2003; Nakagawa 2004). As the number of planned tests increases, the significance value decreases, making this test overly conservative. Due to the increasingly small p-value, the probability of finding a significant result declines as the number of statistical tests increases (Moran 2003). Moran (2003) refers to this paradox as the hyper-Red Queen phenomenon. Secondly, statistical significance does mean the differences are biologically significant. Finally, there is no consensus among statisticians regarding how and when the Bonferroni correction should be applied (Cabin and Mitchell 2000).

The data were analyzed using various univariate statistics. Descriptive statistics were used to describe the overall distributions and trends in the categorical and quantitative data. Ranges for minimum-maximum values of histologically normal and abnormal infants were reported for SOS, BMD (radius and tibia), tibial length, and tibial measurements (tibial length, midshaft diaphyseal diameter, cortical thickness, medullary cavity diameter, and cortical index). Normality testing (Shapiro-Wilks test) was carried out on the following pieces of data: SOS, BMD (radius and tibia), tibial length, and cross-sectional measurements of the midshaft. Prior to

their use as independent variables in statistical analyses that did not include age as a covariate, the following variables were centered on the mean: weight, height, leg circumference, EGA, birthweight, tibial length, midshaft diameter, cortical thickness, and medullary cavity diameter. Data were centered on the mean to provide more meaningful interpretation of the intercept calculated by regression analyses. All statistical analyses were carried out in version 22.0 of the software program IBM SPSS statistics or R.

Wilcoxon signed-rank tests were performed to test for significant differences in the qualitative histological scores between the iliac crest and rib samples. Scores for each variable examined for the costochondral rib and iliac crest sections were paired by infant to assess intra-infant differences in histological qualitative evaluations of bone health.

Non-parametric tests were performed to determine whether qualitative radiographic evaluations scores were significantly associated with sex, race, or age. The Mann-Whitney *U* test was used to test for sex differences and Kruskal-Wallis tests were used to test for differences based on race and age. Qualitative radiographic evaluation scores were also evaluated for significant differences based on chronic illness and prematurity using Mann-Whitney *U* tests.

Most of the statistical tests performed on the data were ANOVAs and regression analyses. An assumption of ANOVA is that variances are equal between groups. An assumption of linear regression is that regression residuals are normally distributed. Levene's test was used to evaluate the homogeneity of variances between groups for ANOVAs. Probability-probability (P-P) plots were examined for all regression analyses to evaluate deviations of the regression residuals from normality. Deviations from normality were noted, but no attempt was made to correct for these violations due to the small size of the study sample.

One-way ANOVAs were used to determine whether there were significant differences in size and growth based on chronic illness, prematurity, or the presence of traumatic injury. The dependent variables tested include weight, height, weight for age percentile, length for age percentile, and weight for length percentile. Additionally, chi-square tests were used to evaluate whether there were significant associations between chronic illness and prematurity, traumatic injury and chronic illness, or traumatic injury and prematurity.

Tibial length and midshaft cross-sectional measurements were evaluated for significant effects of race, sex, chronic illness, prematurity, and age. One-way ANOVAs were used to analyze these relationships. For sex, chronic illness, and prematurity, direction of statistically significant differences between groups was evaluated by examining the group means. Post analyses of statistically significant differences based on race were evaluated using Least Significant Difference (*LSD*) tests when variances between groups were equal or Tamhane's T2 tests when variances were not equal between groups. Analyses of significant differences between racial groups were repeated with chronically ill infants excluded to determine if this had any effect on results. Relationships between the tibial measurements and age were analyzed using ANOVA and simple linear regression. Separate analyses with premature and chronically ill infants excluded were conducted for comparison of results with analyses conducted on the pooled data. In addition, multiple regression analyses predicting the tibial measurements using age as a covariate and prematurity and chronic illness as predictors in individual models were conducted. Two-way ANOVAs were conducted to determine there was a significant interaction between sex and age in models predicting the tibial measurements. These analyses were also conducted with chronically ill infants excluded to determine whether it had any effect on results.

Effects of growth and skeletal maturity at birth on the tibial measurements were evaluated using ANOVA and simple linear regression. The independent variables used to evaluate the relationship between growth and the tibial measurements include height, length for age percentile, weight, weight for age percentile, and weight for length percentile. These data were reanalyzed with chronically ill infants excluded to evaluate whether this had any significant effect on results. Similar analyses were conducted using EGA and birthweight as independent variables to evaluate how skeletal maturity at birth effected the tibial measurements. These data were also reanalyzed with chronically ill infants excluded from analyses.

The BMD data underwent multiple analyses. Nonparametric related-samples sign test was used to compare the radial and tibial BMD estimates obtained from the same infant. Radial BMD data was excluded from further analyses to prevent decreasing the overall sample size as a result of their inclusion. One-way ANOVAs were used to determine if the presence of traumatic injury, chronic illness, or prematurity had any effect on BMD of the tibia. A two-way ANOVA was performed to evaluate whether there was a significant interaction effect of chronic illness and

prematurity on BMD. Significant effects of sex and race on BMD were evaluated with one-way ANOVAs. Analyses assessing significant effects of sex and race on BMD were repeated with chronically ill infants excluded to evaluate whether results were affected. The relationship between BMD and chronological age, variables associated with body size and growth, variables associated with skeletal maturity at birth, and tibial measurements were evaluated using ANOVA and simple linear regression. Regression analyses were also conducted with the chronically ill infants excluded to evaluate the effects on results.

ANOVA and linear regression analyses were used to evaluate the effects of size, growth, skeletal maturity at time of birth on BMD. To evaluate the effect of skeletal maturity reached by time of birth on BMD at time of death, birthweight and EGA were used to predict BMD. To evaluate the effect of size and growth on BMD, BMD was predicted by height, weight, leg circumference, and growth percentiles. To evaluate the relationship between BMD and changes in tibial size and structure, tibial length, tibial midshaft diameter, cortical thickness, medullary cavity diameter, and cortical index were used to predict BMD. All analyses were repeated with chronically ill infants excluded from analyses to evaluate how their exclusion affected results.

The reliability of the QUS device used to conduct this research was evaluated by estimating Cronbach's alpha from the three consecutive SOS readings obtained from each infant. Cronbach's alpha is an intra-class correlation coefficient, which measures internal consistency among the three SOS readings. A high Cronbach's alpha indicates a high degree of internal consistency or high reliability.

The SOS data underwent thorough evaluation for significant effects of overall health, demographic characteristics, size, growth, skeletal maturity at birth. One-way ANOVAs were used to evaluate the relationship between SOS and chronic illness, prematurity, and traumatic injury. One-way ANOVAs were also used to determine whether sex or race had significant effects on SOS. These analyses were repeated with premature infants excluded from analyses to assess whether their exclusion affected results.

Prior to assessing the relationship between age and SOS, the SOS data was tested for significant differences in age-specific means based on age grouping method (chronological age vs. term-corrected age). A paired *t*-test was used to conduct the analysis. The Shapiro-Wilk test was used

to assess whether differences between pairs were normally distributed. A one-way ANOVA was used to test for significant differences between group mean SOS based on chronological age in months. The analysis was repeated with premature infants excluded to assess whether there were significant effects on results. *LSD* tests were used for post hoc analyses to determine which ages had significant different group means for SOS. To gain further clarity regarding the relationship between SOS and age, simple linear regression analysis was conducted using chronological age in months to predict SOS. Regression analyses predicting SOS from age were also conducted on the term born and premature infants separately to determine how the relationship between SOS and age may have been differentially affected by skeletal maturity at birth.

The effects of growth, body size, skeletal maturity at birth, and tibial size and structure on SOS were assessed using ANOVA and simple linear regression. Size and growth effects on SOS were evaluated by using height, weight, leg circumference, and growth percentiles to predict SOS. To evaluate the effect of skeletal maturity at birth on SOS, birthweight and EGA were used to predict SOS. It is reported in the literature that cortical thickness has a significant effect on SOS. To evaluate this relationship and any other relationship between SOS and the size and structure of the tibia, tibial length, cortical thickness, medullary cavity diameter, and cortical index were used to predict SOS. To assess the relationship between SOS and the tibial measurements without the effects of size differences resulting from age differences, partial correlations and regression models predicting SOS from the tibial measurements while using age as a covariate were also tested. All analyses were repeated with chronically and premature infants excluded to assess the effect their exclusion had on the results. Chronically ill and premature infants were not excluded simultaneously to prevent the reduction of statistical power as a result of small sample size.

Multiple regression analyses were conducted to determine which combination of variables best predicted SOS. Several models were constructed using the following variables as possible predictors: age, birth weight, EGA, height, height percentile for age, weight, weight percentile for age, cortical thickness, medullary cavity diameter, tibial midshaft diameter, and cortical index. Weight and EGA were not entered into the same model due to multicollinearity. Also due to multicollinearity, height and height percentile, weight and weight percentile, birthweight and EGA, tibial midshaft diameter and cortical index, cortical thickness and tibial midshaft diameter,



or cortical index and cortical thickness were not entered into the same model. Stepwise variable selection was conducted. A variable was entered into the model if the significance level of its F value was  $<.05$  and was removed from the model if the significance level was  $>.10$ . After exclusion of premature and chronically ill infants from the analysis, the model that best predicted SOS was retested using stepwise variable selection to assess how the exclusion of these infants changed the model.

Comparisons between methods of bone assessment (BMD, SOS, and qualitative radiographic evaluation) were conducted using ANOVA and simple linear regression. The relationship between radiographic mineralization scores from qualitative radiographic evaluations and BMD was evaluated to assess whether low BMD estimates were associated with increased qualitative radiographic evaluation scores. To evaluate the relationship between SOS and mineralization, qualitative radiographic evaluation scores and BMD estimates were used to predict SOS in separate analyses.

## **Summary**

The purpose of this research was to assess QUS as a possible method for evaluating bone quality in infants by comparing SOS measurements to proxies of infant health, bone strength, and bone health. Comparison of SOS to influential factors of infant bone health and strength provided insight into what SOS measures and helped determine whether SOS is a valid measure of infants bone quality. The study sample consisted of 78 infants ranging in age from 30 weeks gestation (actual or corrected) to 1 year postnatal at the time of death. All infants included in this study were autopsied at HCIFS or TCH in Houston, Texas. Three SOS readings were obtained from each infant. Digital radiographs of the arm and leg, and samples from the iliac crest and costochondral junction of rib, were obtained from each infant. Digital radiographs were used to calculate BMD estimates of the midshaft radius and tibia, and to obtain cross-sectional measurements of the tibial midshaft. Qualitative radiographic evaluations of bone mineralization were conducted on radiographs of the forearm and leg of each infant. Qualitative histological evaluations of infant bone health were conducted on the iliac crest and costochondral rib sections. Each infant's medical history, growth and development, and autopsy findings was

obtained and converted into variables used for statistical analyses. Statistical analyses were conducted using IBM SPSS Statistics version 22.0, or R.

## CHAPTER 4 : RESULTS

### Introduction

Various univariate statistical analyses were performed with the goal of answering the following questions. Is QUS a valid technique for evaluating infant bone quality? Can SOS be used to differentiate between infants with normal and abnormal bone? If so, what is the age-specific range of SOS readings for infants with normal bone? Five major hypotheses were constructed to answer these questions. Hypothesis 1: Growth-related changes in tibial structure and body size are significantly associated with each other, and both are significantly associated with age-related changes in BMD and SOS. Hypothesis 2: The presence of traumatic injury is not associated with indicators of overall health, body size, or bone health. Hypothesis 3: Chronic illness is negatively associated with growth and bone health. Hypothesis 4: Skeletal maturity at birth is positively associated with body size, bone size, and bone health. Hypothesis 5: The methods used to assess infant bone quality are significantly associated. This chapter is organized into 6 sections. Descriptive statistic of the study sample and the data collected are presented in the first section. The following five sections report analyses that pertain to the five major hypotheses laid out above. Interpretations of results as supporting or refuting hypotheses are stated throughout each section.

There is a small degree of missingness in the dataset. BMD data could not be calculated for the radius of 30 infants and the tibia of 8 of the infants. For one infant, qualitative radiographic evaluation and calculation of a BMD estimate could not be obtained for the radius due to x-ray cassette malfunction, which resulted in the loss of a radius/ulna radiograph. For the remaining infants with missing BMD data, the custom computer program was unable to calculate BMD due to several possibilities. The BMD may have been too low to differentiate between the tissue and bone attenuation in the radiographic image. The cortices may have been too thin ( $< 2$  mm), causing the inability to differentiate between attenuation values produced by tissue and bone. Inhomogeneities in the radiographic image may have also resulted in the inability to calculate BMD. SOS data could not be obtained from one infant. This missing data was either due to a SOS value that was below the lowest SOS reading allowed by manufacturer settings or size

incompatibility between the probe (too large) and the infant's leg. This infant also lacked BMD data, resulting in its exclusion from all comparative analyses.

## **Descriptive Analyses**

### ***STUDY SAMPLE***

The total sample comprised 78 decedents; 75 were autopsied at HCIFS and 3 were autopsied at TCH. Study sample demographics are provided in **Table 4-1** to **Table 4-2** and **Figure 4-1** to **Figure 4-3**. The median chronological age of the total sample was 3.0 months with an inter-quartile range of 2-6 months (**Figure 4-1**). The median term-corrected age of the total sample was also 3.0 months with an interquartile range of 1-6 months (**Figure 4-1**). The sex distribution of the sample was fairly equal with females comprising a slightly larger proportion (53%) of the study sample than males (**Figure 4-1**). Black infants contributed to the greatest proportion (46%) of the study sample, followed by Hispanic (35%), White (17%), and Asian (3%) (**Figure 4-2**). Considering sex distribution by race, there were a greater number of black male infants than black females and a greater number of white female infants than white male infants (**Figure 4-3**). The number of male and female Hispanic infants was fairly equal. Two Asian female infants and no Asian male infants were also included in the study sample.

Most of the infants in the study sample appeared relatively healthy at the time of their death. Only 13 of the 78 infants had medical histories significant for chronic illness. A list of disease and disorders affecting the chronically ill infants in the study sample is provided in **Table 4-3**. Seven of the 13 chronically ill infants were also premature at time of birth. Eight of the 13 infants lived with chronic illness for at least 3 months. Three of the infants identified as chronically ill were 1 month of age or less at the time of death.

Estimated gestational age was known for 74 of the 78 infants in the study sample (**Figure 4-4**). Of these 74 infants, 17 were premature at time of birth. Of the 17 premature infants, 7 were also chronically ill (**Table 4-3**).

**Table 4-1. The demographic breakdown of the study sample by race, sex, median chronological age, and term-corrected chronological age.**

		Chronological Age (months)		Term-corrected Age <sup>a</sup> (months)	
		<i>n</i>	<i>Mdn</i>	<i>n</i>	<i>Mdn</i>
Black	Female	14	3.0	13	2.0
	Male	22	5.0	21	5.0
Hispanic	Female	15	3.0	15	3.0
	Male	12	2.5	11	2.0
White	Female	9	4.0	8	3.5
	Male	4	5.0	4	5.0
Asian	Female	2	4.5	2	3.0
	Male	0		0	
Total		78	3.0	74 <sup>b</sup>	3.0

a. Term-corrected age was calculated by subtracting the number of weeks born prior to term (40 weeks gestation) from chronological age in weeks and converting back to months.

b. Term-corrected age could not be calculated for 4 infants due to unknown estimated gestational age.

**Table 4-2. Age (months) frequencies by chronological age and term-corrected age.**

Age (months)	Chronological Age			Term-Corrected Age <sup>a</sup>		
	Frequency	%	Cumulative %	Frequency	%	Cumulative %
>1	4	5.1	5.1	15	20.3	20.3
1	11	14.1	19.2	7	9.5	29.7
2	15	19.2	38.5	13	17.6	47.3
3	12	15.4	53.8	6	8.1	55.4
4	6	7.7	61.5	8	10.8	66.2
5	10	12.8	74.4	4	5.4	71.6
6	4	5.1	79.5	8	10.8	82.4
7	3	3.8	83.3	1	1.4	83.8
8	2	2.6	85.9	2	2.7	86.5
9	4	5.1	91.0	2	2.7	89.2
10	3	3.8	94.9	3	4.1	93.2
11	4	5.1	100.0	3	4.1	97.3
12	0	0		2	2.7	100.0
Total	78	100		74 <sup>b</sup>	100	

a. Term-corrected age was calculated by subtracting the number of weeks born prior to term (40 weeks gestation) from chronological age in weeks and converting back to months.

b. Term-corrected age could not be calculated for 4 infants due to unknown estimated gestational age.

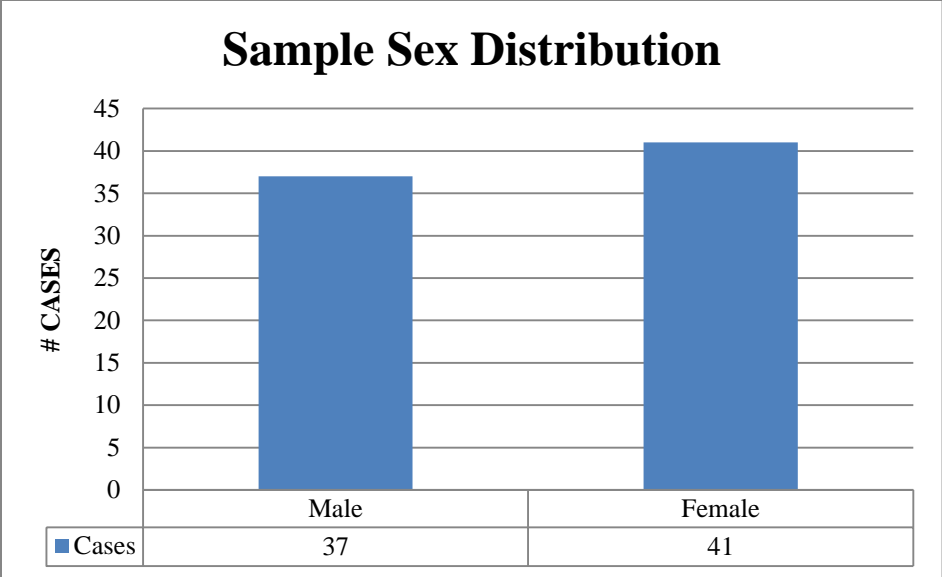


Figure 4-1. Sex distribution of the study sample.

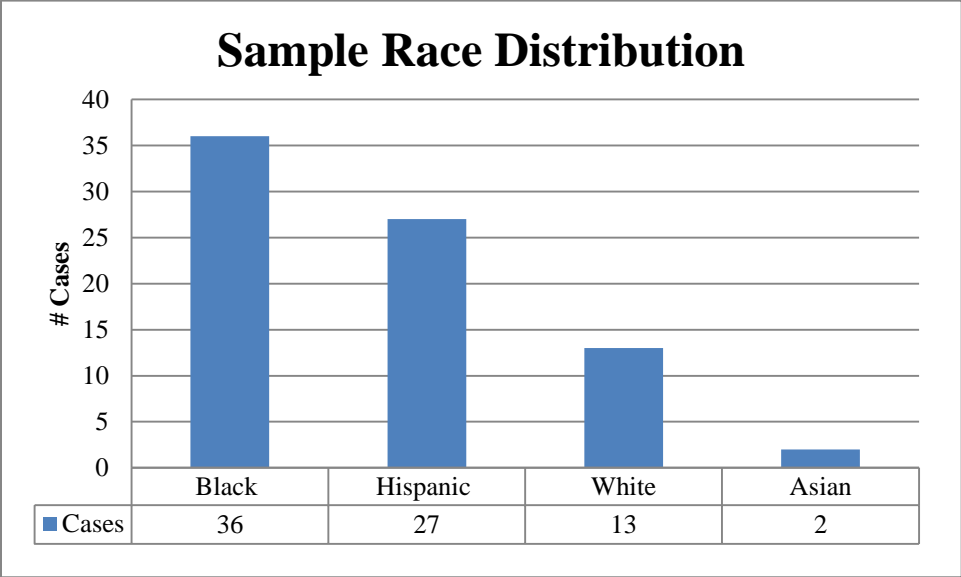


Figure 4-2. Race distribution of the study sample.

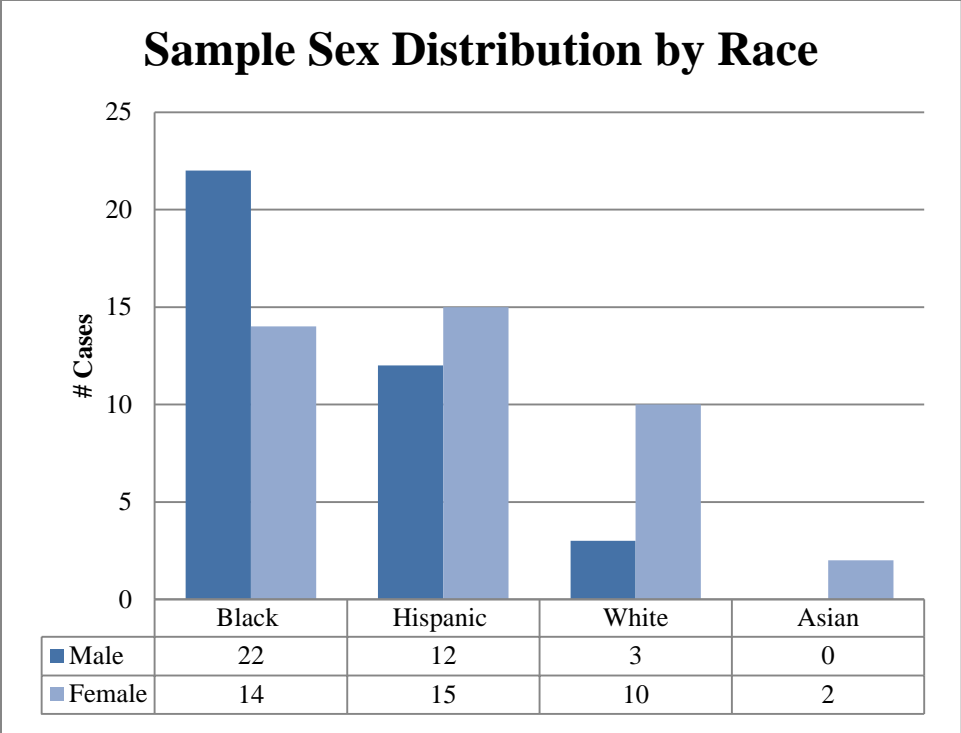
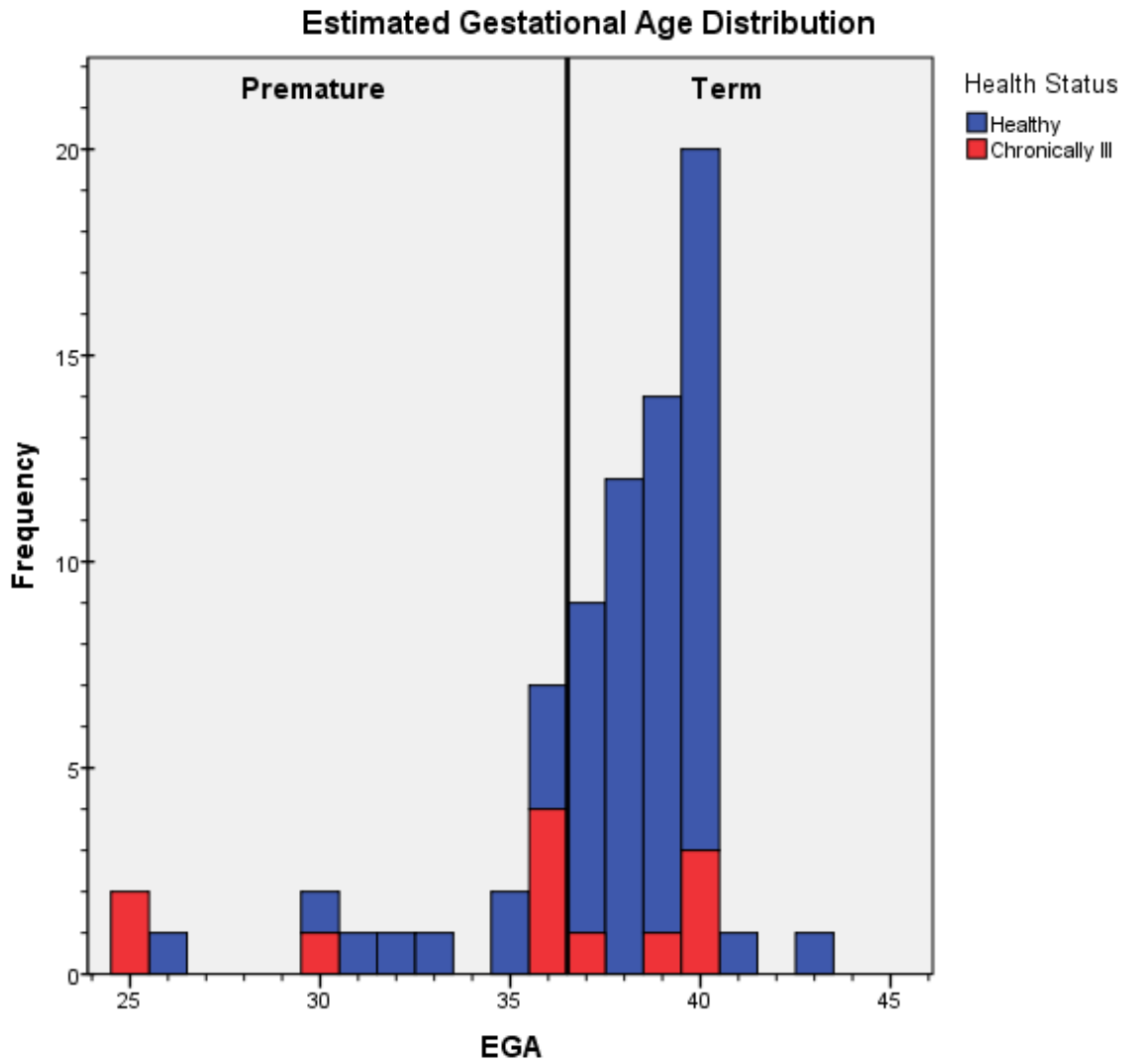


Figure 4-3. Sex distribution of the study sample by race.

**Table 4-3. Description of infants with chronic illness.**

Case ID	EGA <sup>a</sup>	Age <sup>b</sup>	Description of Chronic Illness
225	36	0	Patent ductus arteriosus with persistent fetal circulation; thickened pulmonary vasculature, right ventricular hypertrophy and dilatation
218	36	1	Trisomy 21, congenital heart disease, neonatal hemochromatosis, total parenteral nutrition
222	36	1	Campomelic dysplasia due to Sox9 gene mutation- cleft palate, clinodactyly, clubbed feet, bowing of long bones, 46 XY, biologically female
213	37	2	Mitochondrial myopathy
152	40	2	Cardiomegaly with widely patent foramen ovale
215	40	3	Subtotal occlusion of coronary arteries involved with fibromuscular dysplasia
178	25	4	Extreme prematurity, patent ductus arteriosus with surgical repair, cardiomegaly, atrial and right ventricular dilation
172	25	5	Extreme prematurity, cardiomegaly with atrial septal defect and right ventricular hypertrophy, chronic neonatal lung disease with pulmonary arterial hyperplasia
212	Unk. <sup>c</sup>	5	Seizure disorder since 1 month of age treated with anticonvulsants
205	40	6	Multiple congenital anomalies: abnormal facial features, underdeveloped left lung, abnormal liver lobes, heart abnormalities (biventricular hypertrophy along with dilation, right atria and right ventricle dilatation, right ventricle extends into the apex, patent ductus arteriosus)
174	36	6	Seizure disorder since 3 weeks of age treated with anticonvulsants, descending spinal tract degeneration
191	30	8	Prader-Willi syndrome, endocrinopathy treated with human growth hormone
181	39	9	Collagen 4A1 disorder, cerebral palsy, seizure disorder (3-4 seizures per day) since birth, treated with anticonvulsants
<p>a. EGA=Estimated gestational age  b. Chronological age in months  c. Unk. = Unknown</p>			





**Figure 4-4. Distribution of study sample by estimated gestational age (EGA). One case with unknown EGA is excluded from the plot.**

Forty-two percent of the infants in the study sample fell below the 25th percentile in length for age at the time of death (**Figure 4-5**). In weight for age, 47% fell below the 25<sup>th</sup> percentile for their sex at the time of death (**Figure 4-6**). In weight for length, 36% fell below the 25<sup>th</sup> percentile for their sex at the time of death (**Figure 4-7**). This indicated that a large proportion of the infants in the study sample were small in size for their sex and age at the time of their deaths. However, this is not an indication of growth status since the length and weight of each infant was measured at a single point in time and not tracked over a period of time.

The manner of death for the majority of infants ( $n = 33$ , 42%) in this study sample was a natural disease process (chronic or acute) and recorded as Natural (**Table 4-4**). Deaths caused by Sudden Unexplained Infant Death (SUID) were classified as Natural. In 32% ( $n = 29$ ) of infants, the manner of death could not be determined. Undetermined manners of death included cases of co-sleeping, in which no natural disease was found to be a contributing factor and accidental asphyxiation could not be ruled out. Manner of death was classified as Accident for 9% ( $n = 7$ ) of infants. Twelve percent ( $n = 9$ ) of infant deaths were classified as Homicide (defined as death attributable to the actions of another individual).

Cause of death for each infant in the study sample was categorized as Asphyxia/Drowning, Co-sleeping, Infectious, Other, SUID, Trauma, or Undetermined based on the finalized classification made by the pediatric pathologist (TCH cases) or the medical examiner (HCIFS cases). The Cause of death for most of the infants in the study sample ( $n = 17$ , 22%) was categorized as Co-sleeping, a subcategory of Undetermined (**Table 4-5**). For 20% ( $n = 16$ ) of the study sample deaths, the cause of death was categorized as SUID. The cause of death for 18% ( $n = 14$ ) of the study sample was categorized as Other. All causes of death categorized as Other, except for one, were associated with a Natural manner of death. The manner of death for the exception was Homicide with a non-traumatic cause of death. The cause of death was Undetermined for 14% ( $n = 11$ ) of the study sample, not including the co-sleeping cases. Nine percent ( $n = 7$ ) of the infants died due to accidental asphyxia/drowning. Trauma was the cause of death for 12% ( $n = 9$ ) of the infants in this study. All traumatic causes of death were associated with homicides, except one. This traumatic case was classified as an Accident and involved a motor vehicle accident. Five percent ( $n = 4$ ) of causes of death were categorized as Infectious.

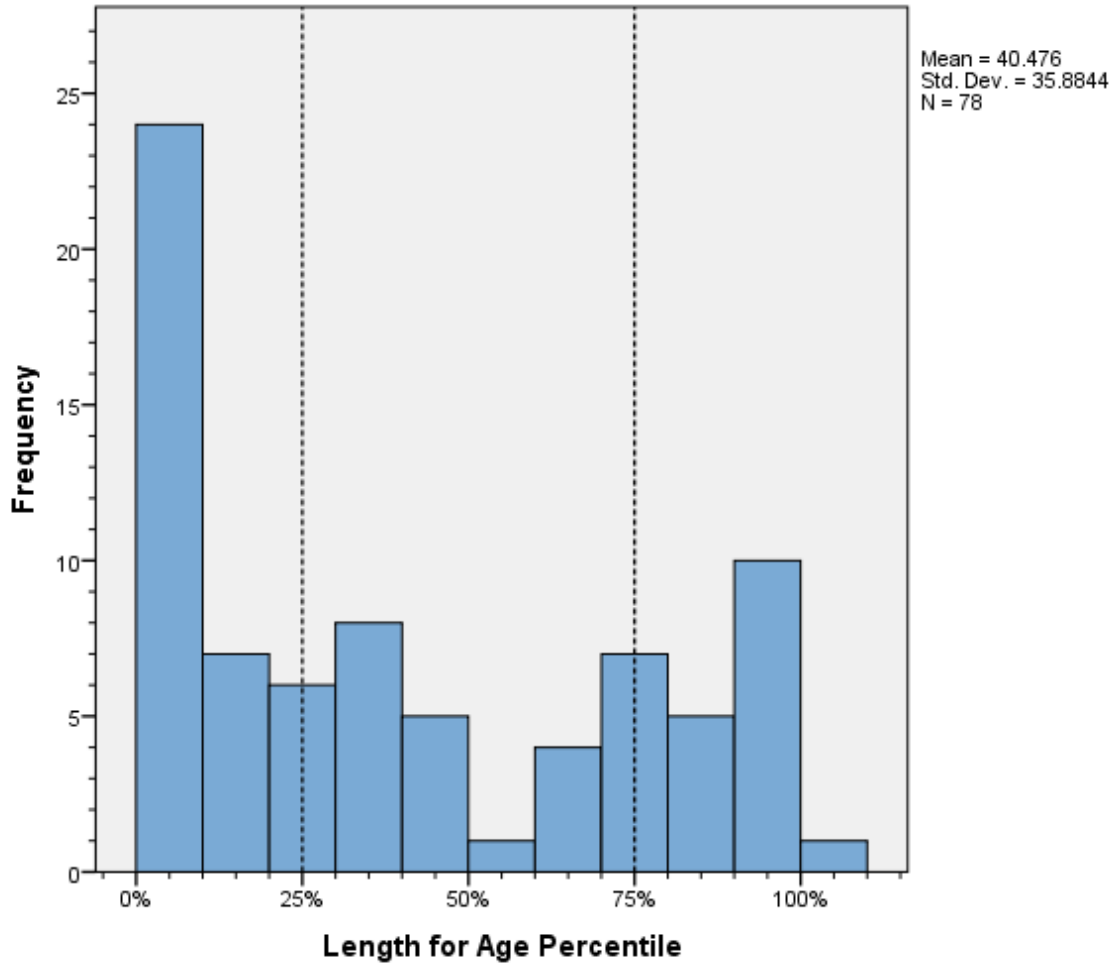


Figure 4-5. Distribution of study sample by length for age percentile.

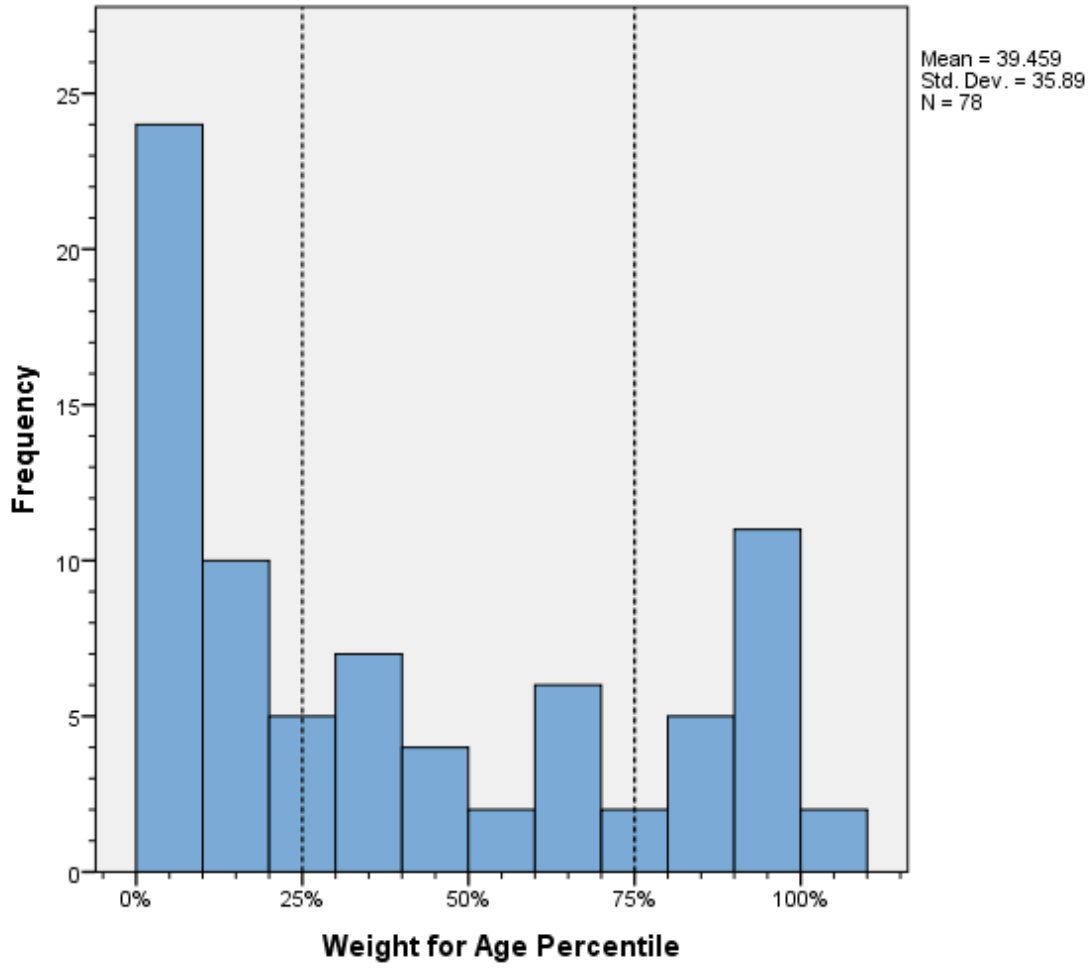


Figure 4-6. Distribution of study sample by weight for age percentile.

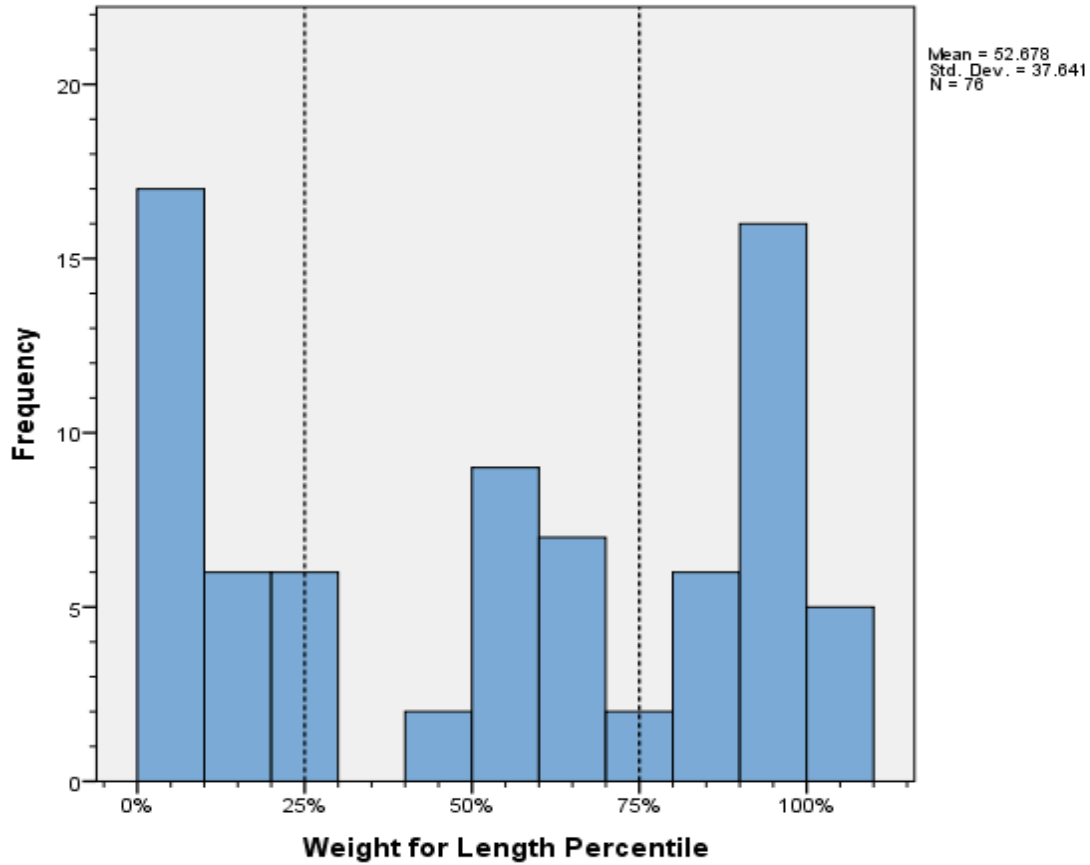


Figure 4-7. Distribution of study sample by weight for length percentile. Weight for length could not be calculated for two cases and were excluded from the above plot.

Table 4-4. Frequency of study sample cases by Manner of Death classification.

Manner of Death	<i>n</i>	%
Natural	33	42
Undetermined	29	37
Homicide	9	12
Accident	7	9
<b>Total</b>	<b>78</b>	<b>100</b>

**Table 4-5. Frequency of study sample cases by Cause of Death category.**

<b>Cause of Death</b>	<b><i>n</i></b>	<b>%</b>
Co-sleeping	17	22
SUID	16	20
Other	14	18
Undetermined	11	14
Trauma	9	12
Asphyxia/Drowning	7	9
Infectious	4	5
<b>Total</b>	<b>78</b>	<b>100</b>

Most infants in the study sample (83%,  $n = 65$ ) showed no evidence of traumatic injury (**Table 4-6**). Injuries resulting from therapeutic intervention, such as cardiopulmonary resuscitation, were not considered traumatic. Twelve percent ( $n = 9$ ) of the sample had fatal injuries caused by blunt force trauma. In 5% ( $n = 4$ ) of the study sample evidence of healing injuries was found, but the cause of the injury, traumatic vs. non-traumatic, could not be determined.

### ***QUALITATIVE HISTOLOGY EVALUATION***

Costochondral rib and iliac crest sections were obtained from all infants in the study sample ( $N = 78$ ). A bone pathologist performed qualitative histology evaluations on H&E stained thin sections produced from each tissue sample. Results of the qualitative histological evaluation conducted on the thin sections of the costochondral rib and iliac crest sections are provided in **Table A- 9** and **Table A- 10** of the Appendix, respectively. Five infants were classified as histologically abnormal. Statistical analyses were performed on these data, but these analyses were excluded for several reasons. The evaluation method used to classify the bone samples as histologically normal/abnormal was developed specifically for this study, had not been validated, and the reproducibility of the method is uncertain. The evaluations of the rib and iliac crest as indicators of tibial bone health may be problematic due to differing mechanical environments (Eleazer 2013). Additionally, there appeared to be no relationship between the bone quality indicators and the classification of histological normality/abnormality, which did not justify the separation of the histologically abnormal infants from the histologically normal infants. Therefore, the data from the infants classified as histologically abnormal were pooled with remaining data in all subsequent analyses.

**Table 4-6. Frequency of study sample cases by presence/absence of traumatic injury.**

<b>Traumatic Injury</b>	<b><i>n</i></b>	<b>%</b>
No Trauma	65	83
Trauma-Blunt Force	9	12
Undetermined	4	5
<b>Total</b>	<b>78</b>	<b>100</b>

### ***QUALITATIVE RADIOGRAPHIC EVALUATION***

Radiographs of the radius/ulna and the tibia/fibula were obtained from all infants in the study sample ( $N = 78$ ); but, one radius/ulna radiograph (Case ID # 171) was lost due to x-ray cassette malfunction. Intra-infant radiographic evaluation scores of the radius/ulna and tibia/fibula radiographs did not differ from each other. Based on qualitative radiographic evaluation, bone mineralization appeared normal in 83% (radius/ulna,  $n = 64$ ; tibia/fibula,  $n = 65$ ) of the study sample. Thirteen percent (radius/ulna and tibia/fibula,  $n = 13$ ) of the study sample showed indeterminate or slight demineralization and 4% (radius/ulna and tibia/fibula,  $n = 4$ ) demonstrated abnormal mineralization on radiographs. Rachitic changes were not observed in any of the radiographs. A table of the descriptive statistics pertaining to the qualitative radiographic evaluation results can be found in **Table A- 4** of the Appendix. A Kruskal-Wallis test indicated no significant relationship between radiographic score and chronological age (months) ( $K = 4.17, p = .965$ ). Descriptions of the infants classified as having abnormal mineralization on radiographs and associated data are provided in **Table A- 5** of the Appendix.

### ***TIBIAL MEASUREMENTS***

The Shapiro-Wilk test ( $W$ ) was used to the normality of the data distributions for the cross-sectional measurements of the tibial midshaft. Analyses indicated that tibial length ( $W = 0.983, p = .393$ ), tibial midshaft diameter ( $W = 0.972, p = .089$ ), medullary cavity diameter ( $W = 0.982, p = .355$ ), and cortical index ( $W = 0.987, p = .603$ ) were normally distributed. Cortical thickness was not normally distributed ( $W = 0.961, p = .019$ ). Mean tibial length was 83.58 mm with a standard deviation of 15.62 mm. Mean tibial midshaft diameter was 7.20 mm with a standard deviation of 0.16 mm. Mean medullary cavity diameter was 3.38 mm with a standard deviation of 0.11 mm. Mean cortical index was .53 with a standard deviation of .01. Median cortical thickness was 3.75 mm with an inter-quartile range between 3.09-4.43 mm. A table of the

descriptive statistics pertaining to the tibial measurements can be found in **Table A- 6** of the Appendix.

### ***Age-Related Changes in Tibial Structure***

Before age-related changes in the tibial structure could be related growth-related changes in body size, it was necessary to evaluate the age-related changes in the tibial measurements. ANOVA and simple linear regression analyses were performed to evaluate the relationship between chronological age and the tibial measurements. There was a significant linear relationship between age and tibial length ( $R^2_{Adj.} = .74$ ,  $F(1, 75) = 218.83$ ,  $p < .001$ ). The regression coefficient for age indicated that tibial length increased by 4.40 mm for every 1 month increase in age ( $b = 4.40$ , 95% CI [3.81, 5.00]). The model summary is presented in Model 1 of **Table 4-7** and is illustrated by the black fitted line in **Figure 4-8**. An  $F$  test of the  $R^2$  change was conducted to determine if a cubic model was a significantly better fit than a quadratic model for the relationship between age and midshaft diameter. Analysis indicated a cubic model explained significantly more of the variance in midshaft diameter than a quadratic model ( $F(1, 73) = 8.17$ ,  $p = .006$ ). The curvilinear cubic relationship between age and tibial midshaft diameter was significant ( $R^2_{Adj.} = .51$ ,  $F(3, 73) = 27.57$ ,  $p < .001$ ). The regression coefficients for age ( $b = 1.33$ , 95% CI [0.61, 2.05]), age<sup>2</sup> ( $b = -0.21$ , 95% CI [-0.36, -0.07]), and age<sup>3</sup> ( $b = 0.01$ , 95% CI [0.004, 0.02]) indicated that tibial midshaft diameter initially increased with after birth, the rate of increase gradually decreased at greater age values and then the velocity increases again at the greatest age values. The model summary is presented in Model 2 of **Table 4-7** and is illustrated by the black fitted line in **Figure 4-9**. An  $F$  test of the  $R^2$  change indicated that a cubic model was a significantly better fit than a quadratic model for the relationship between age and medullary cavity diameter ( $F(1, 73) = 5.57$ ,  $p = .021$ ). Medullary cavity diameter had a significant curvilinear cubic relationship with age ( $R^2_{Adj.} = .56$ ,  $F(3, 73) = 32.57$ ,  $p < .001$ ). The regression coefficients for age ( $b = 0.97$ , 95% CI [0.51, 1.42]), age<sup>2</sup> ( $b = -0.13$ , 95% CI [-0.22, -0.04]), and age<sup>3</sup> ( $b = 0.01$ , 95% CI [0.001, 0.01]) indicated that medullary cavity diameter gradually increased after birth, the rate of increase gradually decreased at greater age values and then the rate gradually increased again at the greatest age values. The pattern was similar to that of tibial midshaft diameter and age, but less exaggerated. The model summary is presented in Model 3 of **Table 4-7** and is illustrated by the black fitted line in **Figure 4-10**. Cortical thickness had a



**Table 4-7. Models summaries for regression analyses predicting tibial measurements from age. Tibial length is the dependent variable in model 1. Tibial midshaft diameter is the dependent variable in Model 2. Medullary cavity diameter is the dependent variable in Model 3. Cortical thickness is the dependent variable in Model 4. Cortical Index is the dependent variable of Model 5.**

Model	Unstandardized Coefficients		<i>t</i>	<i>p</i>	<i>F</i>	<i>df</i>	<i>p</i>	Adj. <i>R</i> <sup>2</sup>
	<i>b</i>	<i>SE</i>						
<b>1</b>					218.83	1,75	< .001	.74
	(Constant)	63.28	1.64	38.49	< .001			
	Age	4.40	0.30	14.79	< .001			
<b>2</b>					27.57	3,73	<.001	.51
	(Constant)	4.57	0.50	9.10	< .001			
	Age	1.33	0.36	3.68	<.001			
	Age <sup>2</sup>	-0.21	0.07	-2.89	.005			
	Age <sup>3</sup>	0.01	0.004	2.86	.006			
<b>3</b>					32.57	3,73	<.001	.56
	(Constant)	1.34	0.32	4.20	< .001			
	Age	0.97	0.23	4.22	< .001			
	Age <sup>2</sup>	-0.13	0.05	-2.80	.007			
	Age <sup>3</sup>	0.006	0.003	2.36	.021			
<b>4</b>					10.50	1,75	.002	.11
	(Constant)	3.34	0.18	18.74	< .001			
	Age	0.11	0.03	3.24	.002			
<b>5</b>					13.08	2,74	< .001	.24
	(Constant)	0.65	0.03	25.24	< .001			
	Age	-0.05	0.01	-4.42	< .001			
	Age <sup>2</sup>	0.003	0.001	3.61	.001			

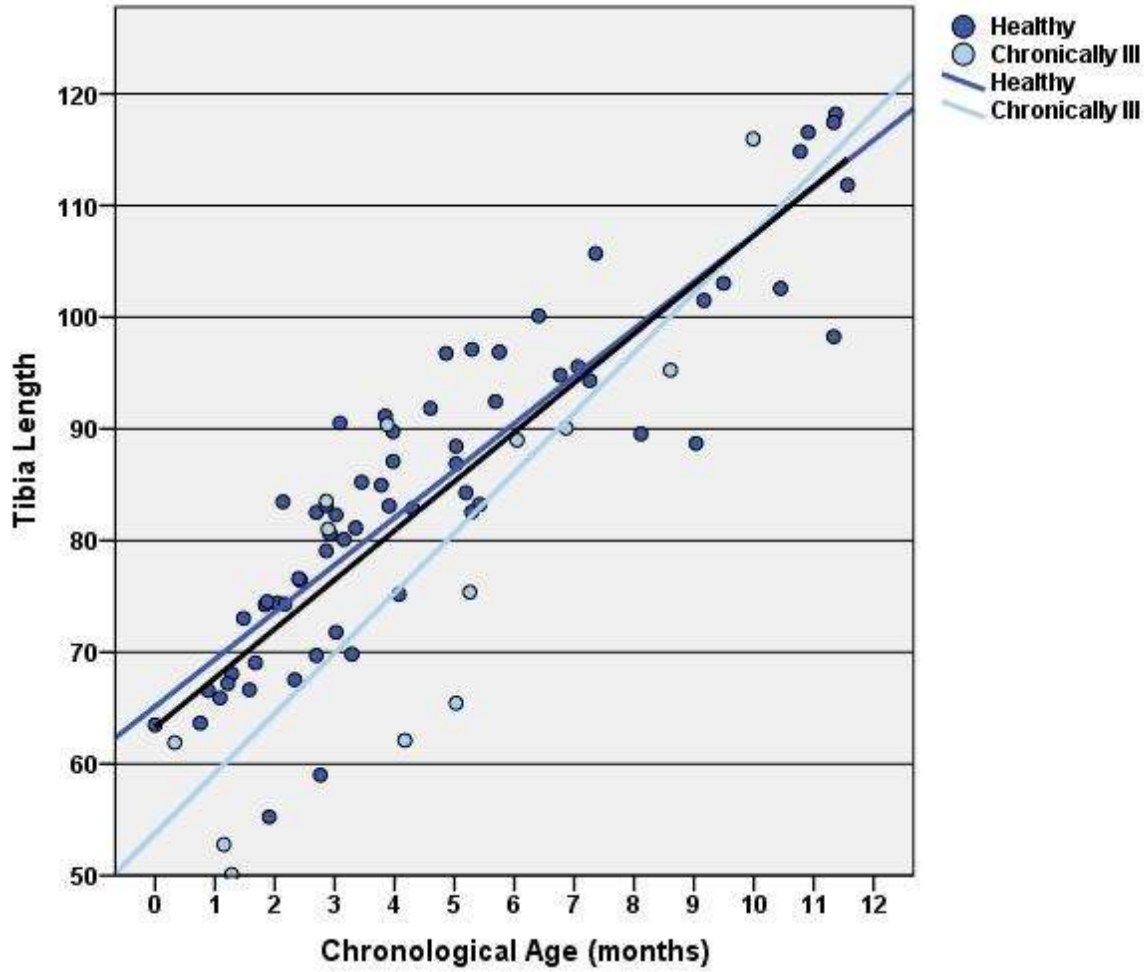


Figure 4-8. Scatter plot of tibial length by chronological age in months. Black regression line is fitted to total sample. Dark blue regression line is fitted to data from infants without chronic illness. Light blue regression line is fitted to data from infants with chronic illness.

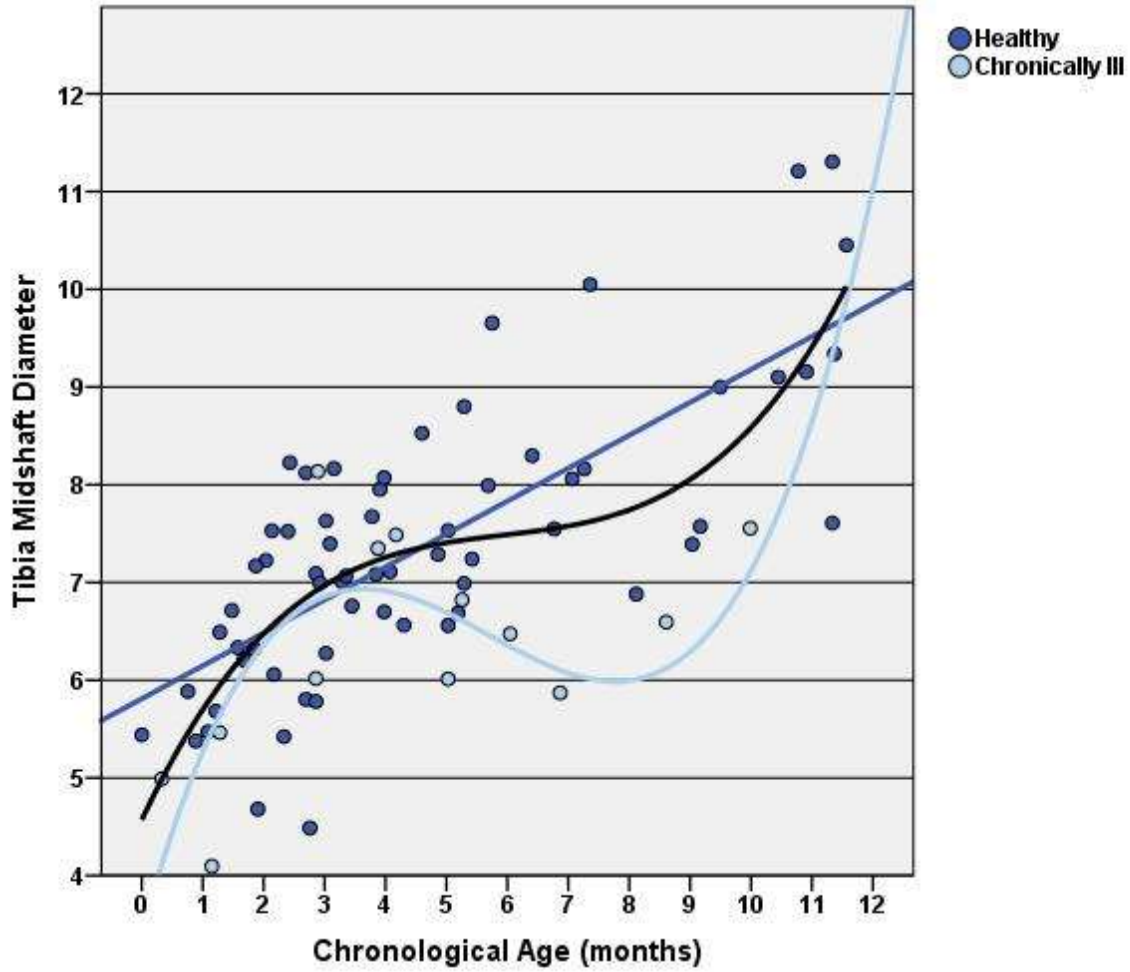


Figure 4-9. Scatter plot of tibial midshaft diameter by chronological age in months. Black regression line is fitted to total sample. Dark blue regression line is fitted to data from infants without chronic illness. Light blue regression line is fitted to data from infants with chronic illness.

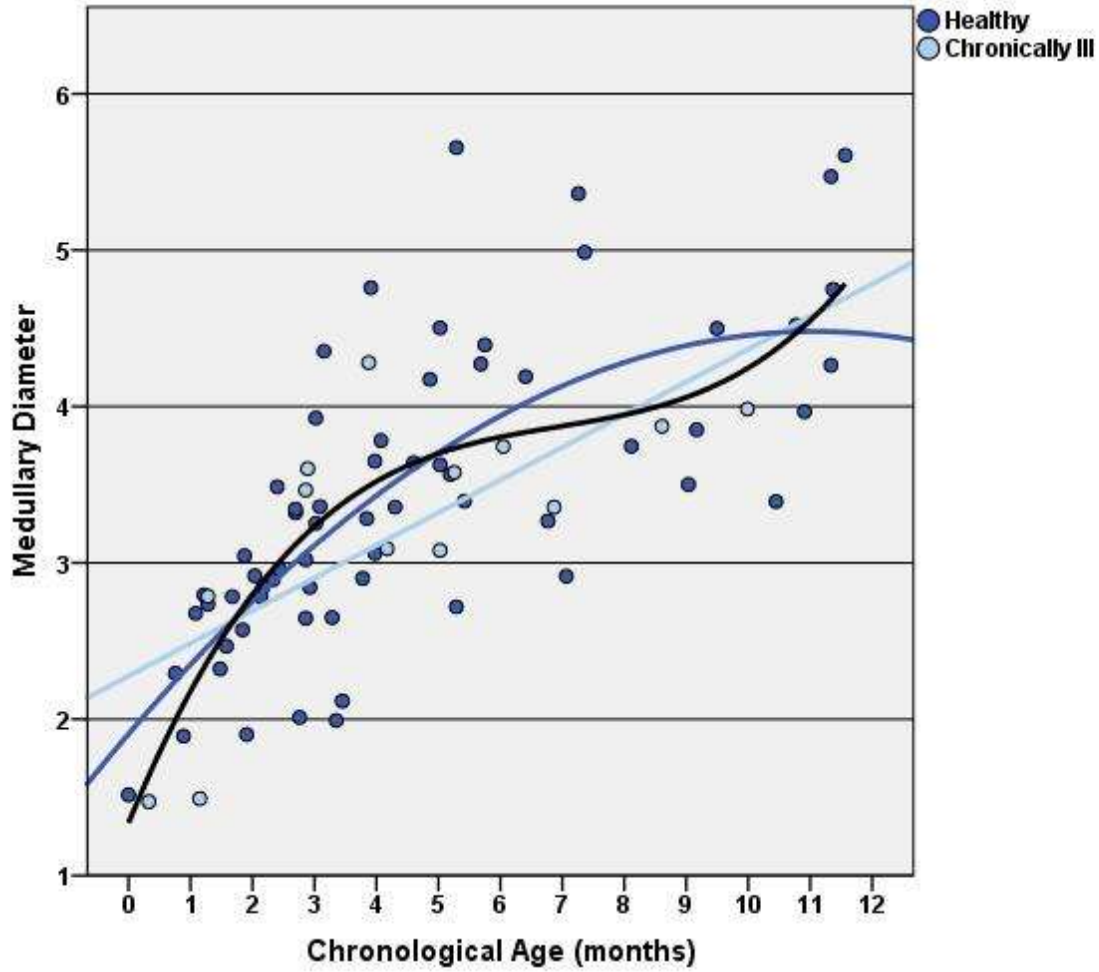


Figure 4-10. Scatter plot of medullary cavity diameter by chronological age in months. Black regression line is fitted to total sample. Dark blue regression line is fitted to data from infants without chronic illness. Light blue regression line is fitted to data from infants with chronic illness.

significant linear relationship with age ( $R^2_{Adj.} = .11$ ,  $F(1, 75) = 10.50$ ,  $p = .002$ ). The regression coefficient for age indicated that for every 1 month increase in age there was a 0.11 mm increase in cortical thickness ( $b = 0.11$ , 95% CI [0.04, 0.17]). The model summary is presented in Model 4 of **Table 4-7** and is illustrated by the black fitted line in **Figure 4-11**. An  $F$  test of the  $R^2$  change indicated that a quadratic model was a significantly better fit than a linear model for the relationship between age and cortical index ( $F(1, 74) = 13.0$ ,  $p = .001$ ). There was a significant relationship between cortical index and age ( $R^2_{Adj.} = .24$ ,  $F(2, 74) = 13.08$ ,  $p < .001$ ). The regression coefficients for age ( $b = -0.05$ , 95% CI [-0.07, -0.03]) and age<sup>2</sup> ( $b = 0.003$ , 95% CI [0.001, 0.005]) indicated that cortical index initially decreased after birth, but at greater age values cortical index increased with increasing age. The model summary is presented in Model 5 of **Table 4-7** and is illustrated in **Figure 4-12**.

### **Chronically Ill Infants Excluded**

Analyses evaluating the relationship between age and the tibial measurements were repeated with chronically ill infants excluded from analyses to assess whether this substantially affected results. After removing the chronically ill infants from analyses, chronological age continued to be a significant predictor tibial length ( $R^2_{Adj.} = .79$ ,  $F(1, 62) = 239.35$ ,  $p < .001$ ). The regression coefficient for age indicated that tibial length increased by 4.23 mm for every 1 month increase in age ( $b = 4.23$ , 95% CI [3.68, 4.77]). An  $F$  test of the  $R^2$  change indicated that a linear model and not a cubic model was the best fit for the relationship between age and midshaft diameter after excluding chronically ill infants from the analysis. Age remained a significant predictor of midshaft diameter ( $R^2_{Adj.} = .55$ ,  $F(1, 62) = 76.56$ ,  $p < .001$ ) and the regression coefficient indicated an increase in midshaft diameter with age ( $b = 0.34$ , 95% CI [0.26, 0.41]). The relationship between age and cortical thickness remained significant ( $R^2_{Adj.} = .17$ ,  $F(1, 62) = 13.48$ ,  $p = .001$ ). The regression coefficient indicated that cortical thickness significantly increased with age ( $b = 0.12$ , 95% CI [0.06, 0.19]). An  $F$  test of the  $R^2$  change indicated that a quadratic model and not a cubic model was the best fit for the relationship between age and medullary cavity diameter with chronically ill infants excluded from the analysis ( $F(1, 61) = 5.63$ ,  $p = .021$ ). The relationship between age and medullary cavity diameter was significant ( $R^2_{Adj.} = .52$ ,  $F(2, 61) = 35.17$ ,  $p < .001$ ). The regression coefficients for age ( $b = 0.47$ , 95% CI [0.25, 0.68]) and age<sup>2</sup> ( $b = -0.02$ , 95% CI [-0.04, -0.003]) indicated that a significant increase in

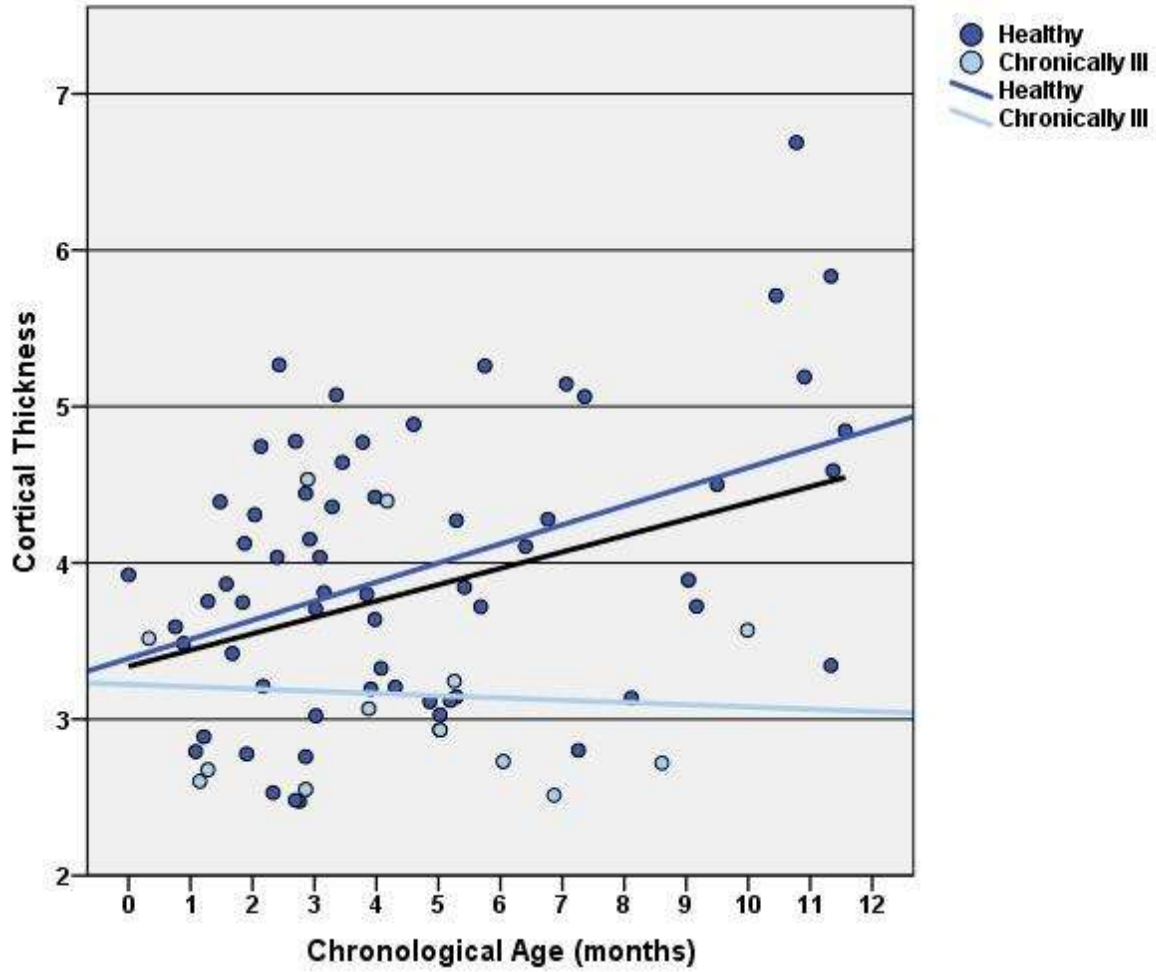


Figure 4-11. Scatter plot of cortical thickness by chronological age in months. Black regression line is fitted to total sample. Dark blue regression line is fitted to data from infants without chronic illness. Light blue regression line is fitted to data from infants with chronic illness.

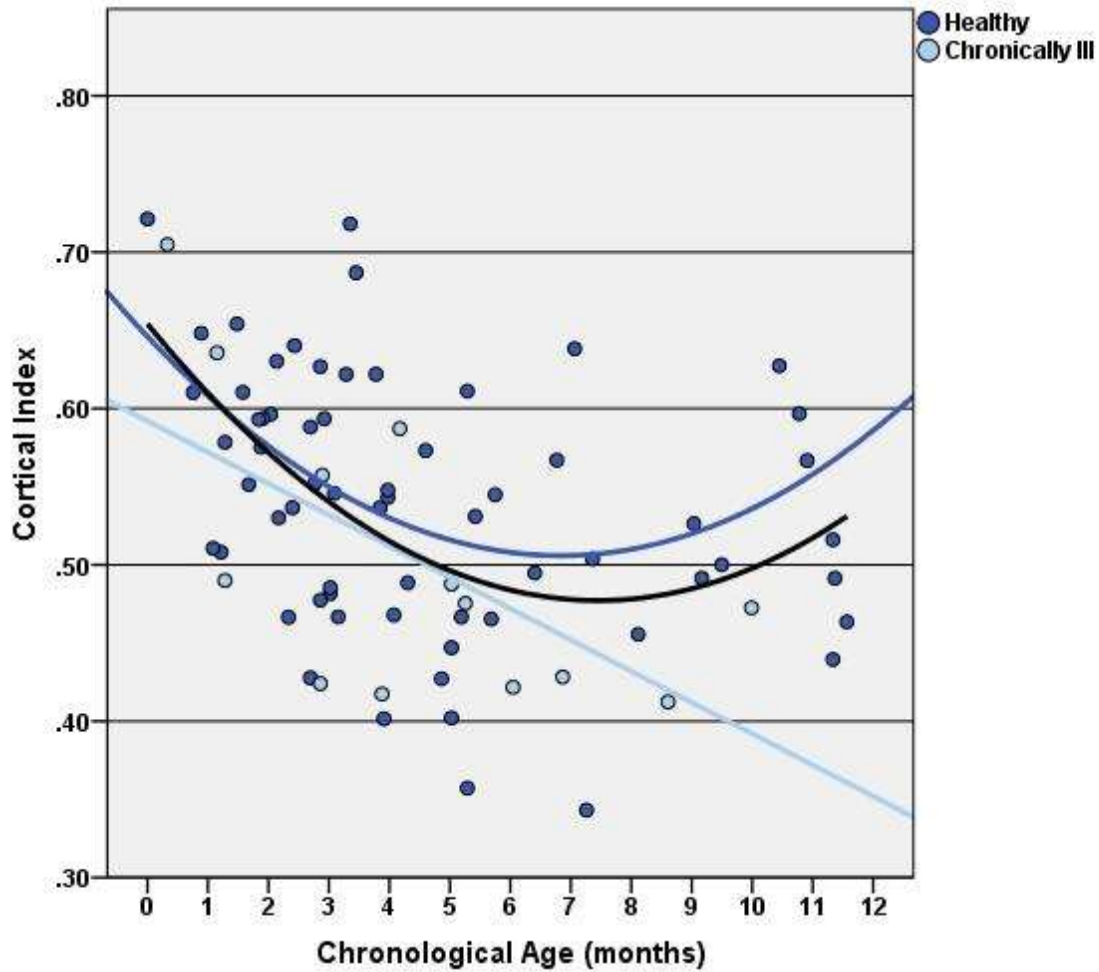


Figure 4-12. Scatter plot of cortical index by chronological age in months. Black regression line is fitted to total sample. Dark blue regression line is fitted to data from infants without chronic illness. Light blue regression line is fitted to data from infants with chronic illness.

medullary cavity diameter after birth, but the rate of increase decreased at greater age ranges. An  $F$  test of the  $R^2$  change indicated that a quadratic model remained the best fit for the relationship between age and cortical index after excluding chronically ill infants from the analysis ( $F(1, 61) = 7.65, p = .008$ ). The relationship between cortical index and age remained significant ( $R^2_{Adj.} = .18, F(2, 61) = 7.73, p = .001$ ). The regression coefficients for age ( $b = -0.04, 95\% \text{ CI } [-0.07, -0.02]$ ) and  $\text{age}^2$  ( $b = 0.003, 95\% \text{ CI } [0.001, 0.005]$ ) indicated an initial decrease in cortical index after birth with increasing age which gradually changed to an increase in cortical index at greater age values. The dark blue regression lines in **Figure 4-8** to **Figure 4-12** illustrate the regression of the cross-sectional variables against age for infants without chronic illness. Model summaries for regression analyses excluding chronically ill infants and predicting the tibial measurements from age are provided in **Table 4-8**.

### **Term Infants**

Due to the significant relationship between prematurity and SOS, regression analyses predicting the tibial measurements from age were repeated with premature infants excluded from analyses. An  $F$  test of the  $R^2$  change indicated that a cubic model was a significantly better fit than a linear or quadratic model for the relationship between age and tibial length among term born infants ( $F(1, 53) = 4.08, p = .048$ ). The relationship between age and tibial length remained significant ( $R^2_{Adj.} = .84, F(3, 53) = 96.54, p < .001$ ). Among term born infants, the regression coefficients for age ( $b = 10.79, 95\% \text{ CI } [5.93, 15.65]$ ),  $\text{age}^2$  ( $b = -1.17, 95\% \text{ CI } [-2.15, -0.19]$ ), and  $\text{age}^3$  ( $b = 0.06, 95\% \text{ CI } [0.42\text{E-}3, 0.11]$ ) indicated that tibial length increased with age, the rate of increase declines at greater age values, and increases again at even greater age values. The model summary is provided in Model 1 **Table 4-9** and is illustrated by the dark blue regression line in **Figure 4-13**. An  $F$  test of the  $R^2$  change indicated that a cubic model was a significantly better fit than a linear or quadratic model for the relationship between age and midshaft diameter ( $F(1, 53) = 6.70, p = .012$ ). The relationship between tibial midshaft diameter and age remained significant ( $R^2_{Adj.} = .53, F(3, 53) = 21.77, p < .001$ ). The regression coefficients for age ( $b = 1.29, 95\% \text{ CI } [0.55, 2.03]$ ),  $\text{age}^2$  ( $b = -0.20, 95\% \text{ CI } [-0.35, -0.05]$ ), and  $\text{age}^3$  ( $b = 0.01, 95\% \text{ CI } [0.002, 0.02]$ ) indicated that tibial midshaft diameter increased with age after birth, the rate of increase decreased for a period of time, and then increased again at greater age values. The model summary is provided in Model 2 **Table 4-9** and is illustrated by the dark blue regression line in **Figure 4-14**. An  $F$  test of the  $R^2$  change indicated that a cubic model was a significantly better fit



than a linear or quadratic model for the relationship between age and medullary cavity diameter after excluding premature infants from the analysis ( $F(1, 53) = 6.67, p = .013$ ). The relationship between medullary cavity diameter and age was significant ( $R^2_{Adj} = .57, F(3, 53) = 25.55, p < .001$ ). The regression coefficients for age ( $b = 1.06, 95\% \text{ CI } [0.56, 1.56]$ ),  $\text{age}^2$  ( $b = -0.15, 95\% \text{ CI } [-0.25, -0.05]$ ), and  $\text{age}^3$  ( $b = 0.007, 95\% \text{ CI } [0.002, 0.01]$ ) indicated that medullary cavity diameter increased with age after birth, the rate of increase decreased for a period of time, and then increased again at greater age values. The model summary is provided in Model 3 of **Table 4-9** and is illustrated by the dark blue regression line in **Figure 4-15**. An  $F$  test of the  $R^2$  change indicated that a linear model was the best fit for the relationship between age and cortical thickness. Cortical thickness had significant relationship with age ( $R^2_{Adj} = .09, F(1, 55) = 6.45, p = .014$ ). The regression coefficient for age indicated that as age increased by 1 month cortical thickness increased by 0.08 mm ( $b = 0.08, 95\% \text{ CI } [0.02, 0.15]$ ). The model summary is provided in Model 4 of **Table 4-9** and is illustrated by the dark blue regression line in **Figure 4-16**. An  $F$  test of the  $R^2$  change indicated that a quadratic model was a significantly better fit than a linear or cubic model for the relationship between age and medullary cavity diameter after excluding premature infants from the analysis ( $F(1, 54) = 1.42, p = .004$ ). The relationship between cortical index and age was significant ( $R^2_{Adj} = .23, F(2, 54) = 9.51, p < .001$ ). The regression coefficients for age ( $b = -0.04, 95\% \text{ CI } [-0.07, -0.02]$ ) and  $\text{age}^2$  ( $b = 0.003, 95\% \text{ CI } [0.001, 0.005]$ ) indicate that cortical index initially declines with increasing age, but changes direction and begins to increase at greater age values. The model summary is provided in Model 5 of **Table 4-9** and is illustrated by the dark blue regression line in **Figure 4-17**.

### ***Sex\*Age Interaction***

Significant sex differences in BMD have been reported in the literature that were attributed to greater bone size in male infants. Due to the possibility of finding significant sex differences in SOS or BMD in the current study, analyses were carried out to evaluate sex differences in bone size. Two-way ANOVAs were conducted on models predicting the tibial measurements using age, sex, and the interaction variable age\*sex. Levene's tests indicated equal variances in tibial length ( $F = 1.56, p = .095$ ), midshaft diameter ( $F = 1.67, p = .065$ ), cortical thickness ( $F = 1.59, p = .084$ ), and cortical index ( $F = 1.72, p = .055$ ) between groups. The variance in medullary cavity diameter was not equal across groups ( $F = 1.91, p = .027$ ). Age was a significant predictor

**Table 4-8. Results of regression analyses of cross-sectional measurements and age, with chronically ill infants excluded. Tibial length is the dependent variable in model 1. Tibial midshaft diameter is the dependent variable in model 2. Medullary cavity diameter is the dependent variable in model 3. Cortical thickness is the dependent variable in Model 4. Cortical Index is the dependent variable of Model 5.**

Model	Unstandardized Coefficients		<i>t</i>	<i>p</i>	<i>F</i>	<i>df</i>	<i>p</i>	Adj. <i>R</i> <sup>2</sup>
	<i>b</i>	<i>SE</i>						
1					239.35	1,62	< .001	.79
	(Constant)	65.14	1.52	42.79	< .001			
	Age	4.23	0.27	15.47	< .001			
2					76.56	1,62	<.001	.55
	(Constant)	5.81	0.22	27.08	< .001			
	Age	0.34	0.04	8.75	< .001			
3					35.17	2,61	<.001	.52
	(Constant)	1.91	0.26	7.24	< .001			
	Age	0.47	0.11	4.27	< .001			
	Age <sup>2</sup>	-0.02	0.009	-2.37	.021			
4					13.48	1,62	.001	.17
	(Constant)	3.39	0.19	18.29	< .001			
	Age	0.12	0.03	3.67	.001			
5					7.73	2,61	.001	.18
	(Constant)	0.65	0.03	21.73	< .001			
	Age	-0.04	0.01	-3.37	.001			
	Age <sup>2</sup>	0.003	0.001	2.77	.008			

**Table 4-9. Results of regression analyses of cross-sectional measurements and age, with premature infants excluded. Tibial length is the dependent variable in Model 1. Tibial midshaft diameter is the dependent variable in Model 2. Medullary cavity diameter is the dependent variable in Model 3. Cortical thickness is the dependent variable in Model 4. Cortical Index is the dependent variable of Model 5.**

Model	Unstandardized Coefficients		<i>t</i>	<i>p</i>	<i>F</i>	<i>df</i>	<i>P</i>	Adj. <i>R</i> <sup>2</sup>
	<i>b</i>	<i>SE</i>						
1					96.54	3,53	< .001	.84
	(Constant)	57.78	3.42	16.89	< .001			
	Age	10.79	2.42	4.46	< .001			
	Age <sup>2</sup>	-1.17	0.49	-2.39	.021			
	Age <sup>3</sup>	0.06	0.03	2.02	.048			
2					21.77	3,53	<.001	.53
	(Constant)	4.90	0.52	9.41	< .001			
	Age	1.29	0.37	3.49	.001			
	Age <sup>2</sup>	-0.20	0.07	-2.71	.009			
	Age <sup>3</sup>	0.01	0.004	2.59	.012			
3					25.55	3,53	<.001	.57
	(Constant)	1.35	0.35	3.83	< .001			
	Age	1.06	0.25	4.25	< .001			
	Age <sup>2</sup>	-0.15	0.05	-3.00	.004			
	Age <sup>3</sup>	0.007	0.003	2.58	.013			
4					6.45	1,55	.014	.09
	(Constant)	3.58	0.18	19.46	< .001			
	Age	0.08	0.03	2.54	.014			
5					9.51	2,54	< .001	.23
	(Constant)	0.65	0.03	22.31	< .001			
	Age	-0.04	0.01	-3.68	.001			
	Age <sup>2</sup>	0.003	0.001	3.00	.004			

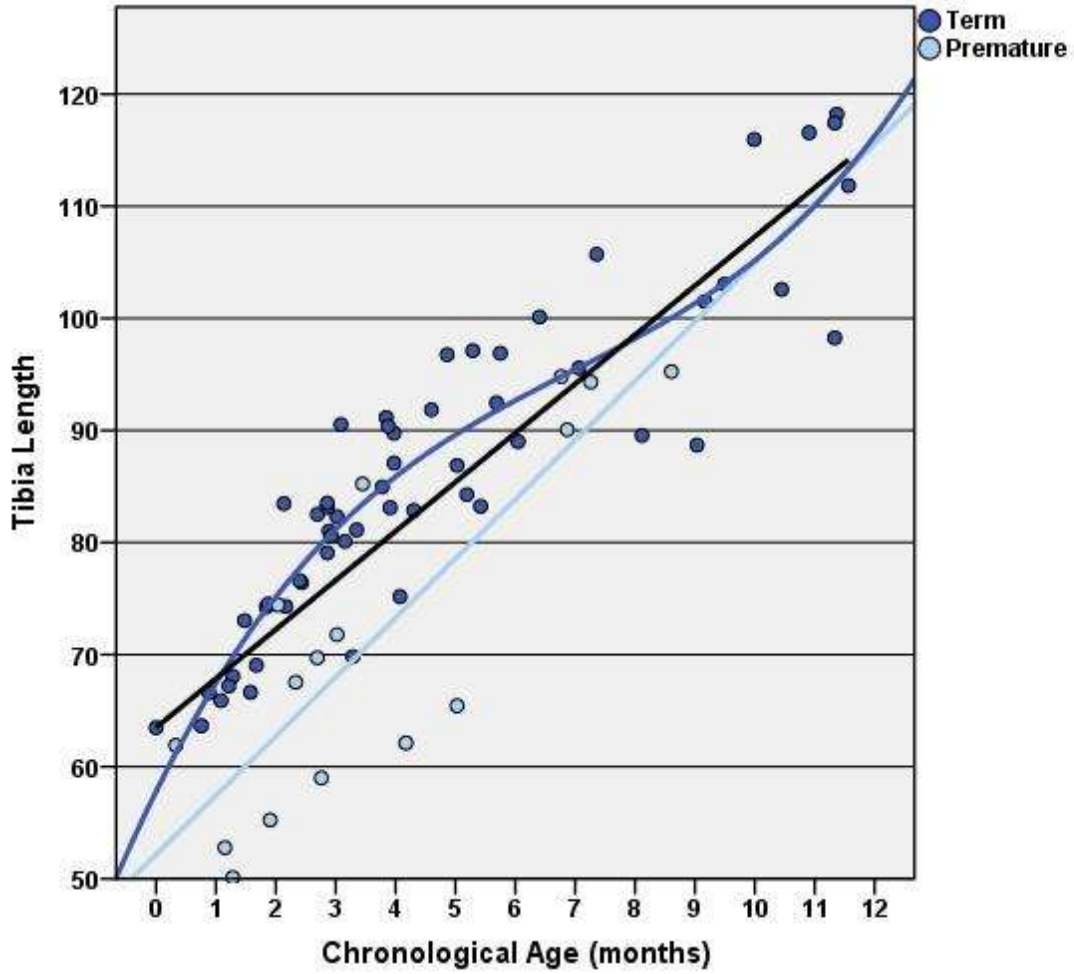


Figure 4-13. Scatter plot of tibial length by chronological age in months. Black regression line is fitted to total sample. Dark blue regression line is fitted to data from term infants. Light blue regression line is fitted to data from premature infants.

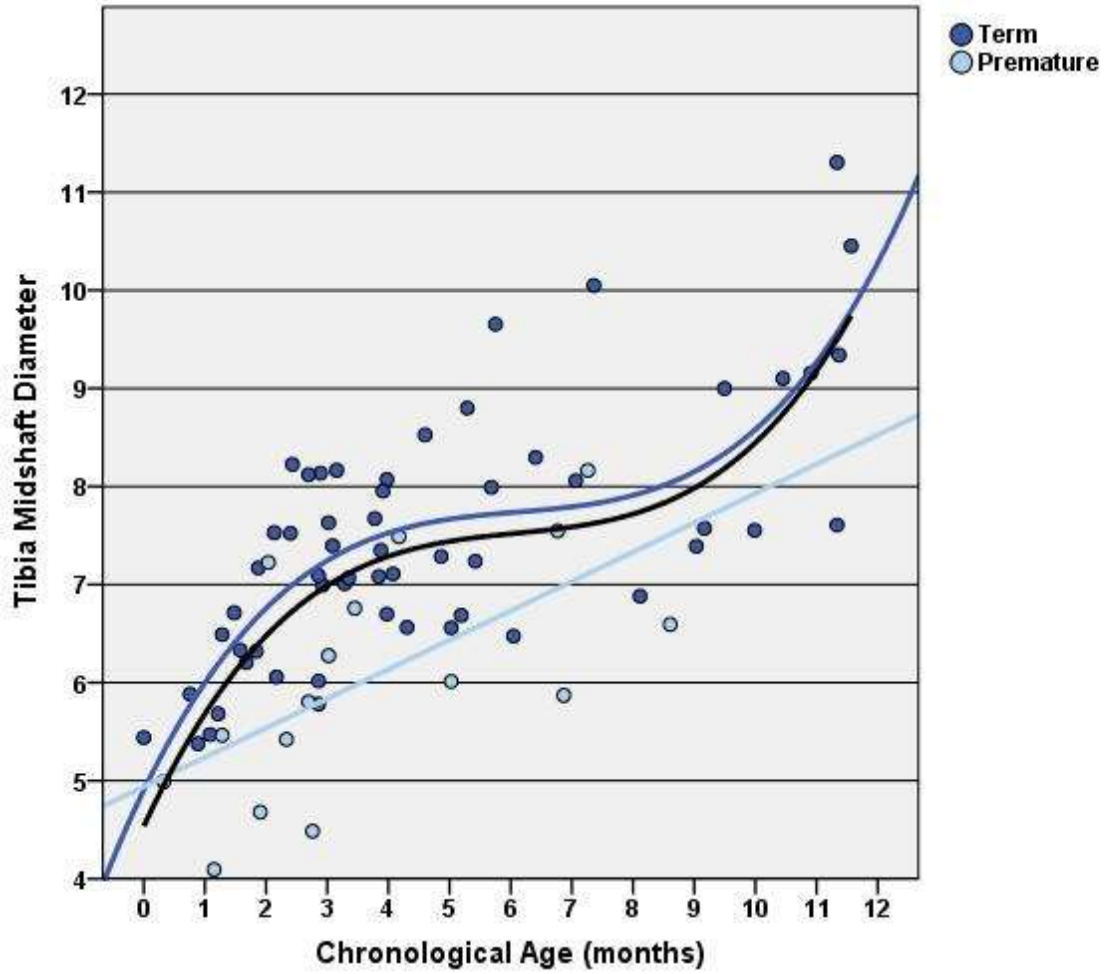


Figure 4-14. Scatter plot of tibial midshaft diameter by chronological age in months. Black regression line is fitted to total sample. Dark blue regression line is fitted to data from term infants. Light blue regression line is fitted to data from premature infants.

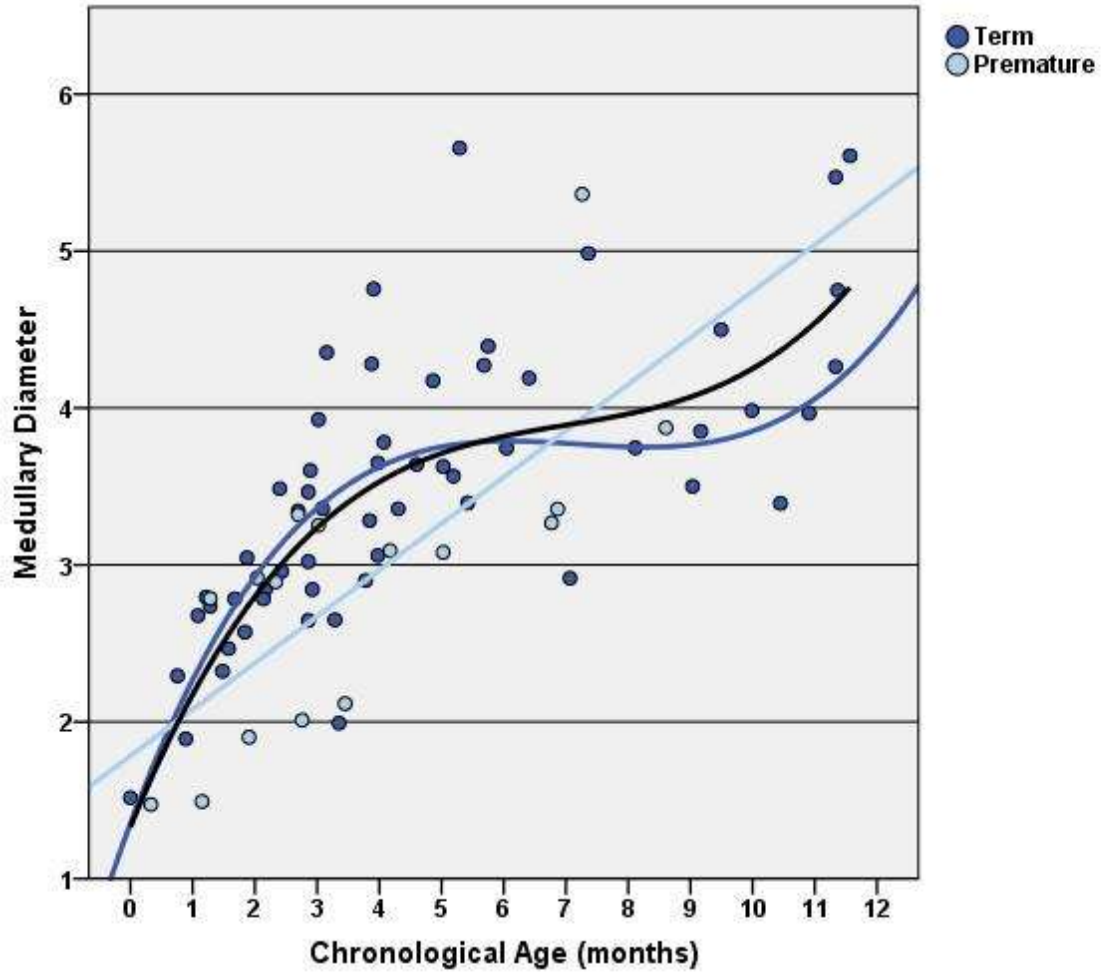


Figure 4-15. Scatter plot of medullary cavity diameter by chronological age in months. Black regression line is fitted to total sample. Dark blue regression line is fitted to data from term infants. Light blue regression line is fitted to data from premature infants.

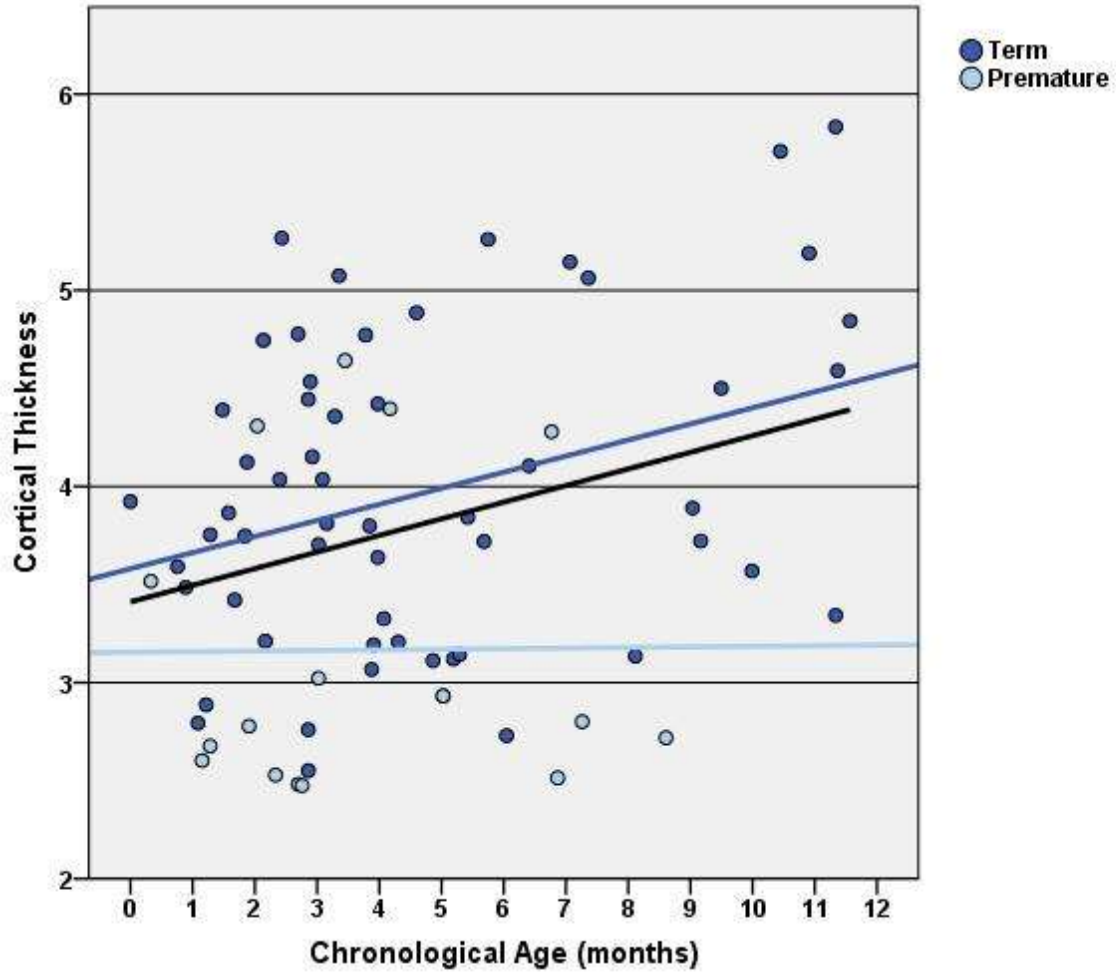


Figure 4-16. Scatter plot of cortical thickness by chronological age in months. Black regression line is fitted to total sample. Dark blue regression line is fitted to data from term infants. Light blue regression line is fitted to data from premature infants.

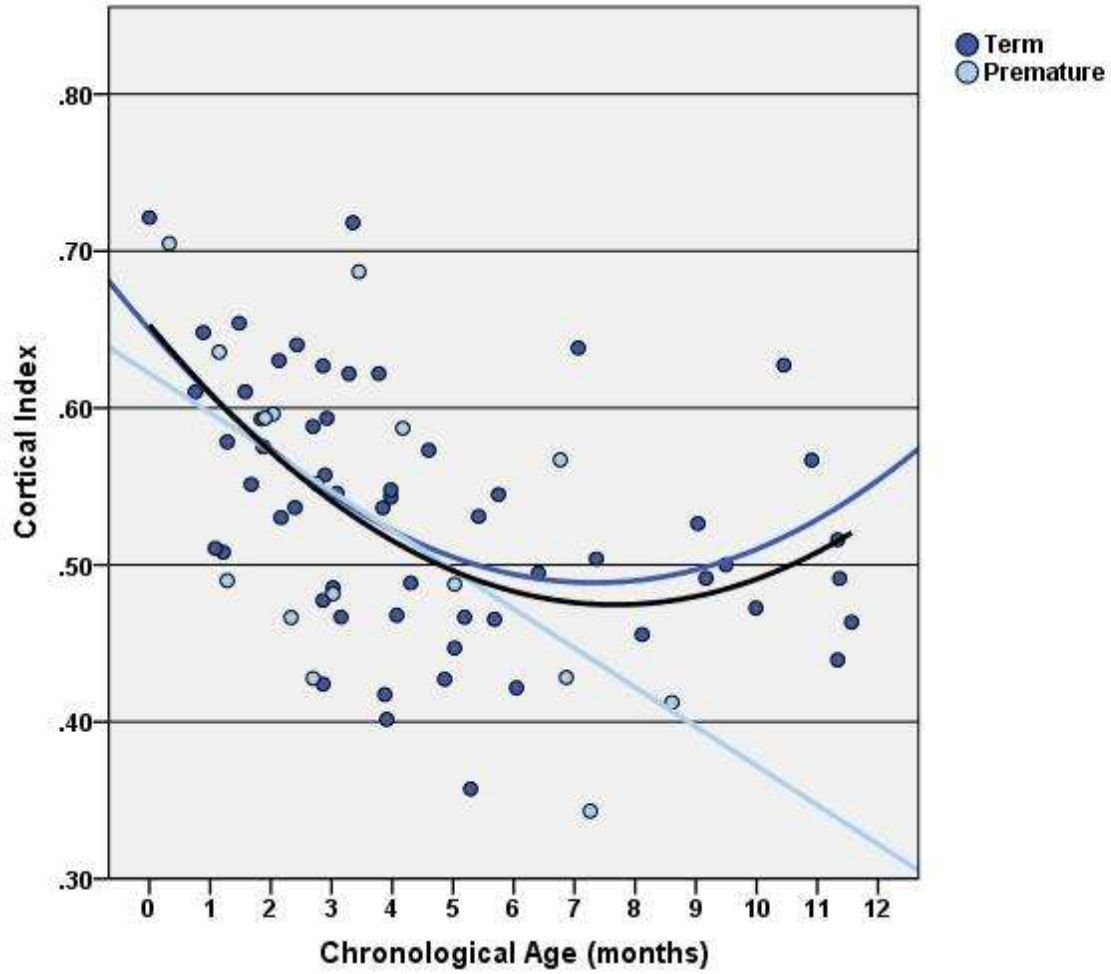


Figure 4-17. Scatter plot of cortical index by chronological age in months. Black regression line is fitted to total sample. Dark blue regression line is fitted to data from term infants. Light blue regression line is fitted to data from premature infants.



in the model predicting tibial length ( $F(11, 54) = 19.82, p < .001$ ), but sex ( $F(1, 54) = 3.77, p = .058$ ) and sex\*age ( $F(10, 54) = 0.94, p = .504$ ) were not significant. Although tibial length was not significantly different between the sexes, a plot of tibial length by age with the data separated by sex suggests that tibial length tended to be greater in males than females **Figure 4-18**. Age was a significant predictor in the model predicting midshaft diameter ( $F(11, 54) = 9.92, p < .001$ ), but sex ( $F(1, 54) = 3.20, p = .079$ ) and sex\*age ( $F(10, 54) = 1.18, p = .323$ ) were not significant. Although midshaft diameter was not significantly different between the sexes, a plot of midshaft diameter by age with the data separated by sex suggests that midshaft diameter tended to be greater in males than females **Figure 4-19**. Age was a significant predictor in the model predicting medullary cavity diameter ( $F(11, 54) = 10.52, p < .001$ ), but sex ( $F(1, 54) = 0.007, p = .934$ ) and sex\*age ( $F(10, 54) = 1.81, p = .081$ ) were not significant. Although medullary cavity diameter was not significantly different between the sexes, a plot of medullary cavity diameter by age with the data separated by sex suggests that medullary cavity diameter tended to be greater in males between 3-8 months of age than females (**Figure 4-20**). Age ( $F(11, 54) = 3.47, p = .001$ ) and sex ( $F(1, 54) = 4.97, p = .030$ ) were significant predictors in the model predicting cortical thickness, but sex\*age ( $F(10, 54) = 1.40, p = .207$ ) was not significant. Males had significantly greater cortical thickness than females after accounting for size differences due to age. The model summary is provided in **Table 4-10**. A plot of cortical thickness by age with the data separated by males and females is provided in **Figure 4-21**. Age ( $F(11, 54) = 3.67, p = .001$ ) was a significant predictor in a model predicting cortical index, but sex ( $F(1, 54) = 3.45, p = .069$ ) and age\*sex ( $F(11, 54) = 1.69, p = .108$ ) were not significant. A plot of cortical index by age with the data separated by sex is provided in **Figure 4-22**. Although there was no significant difference in cortical index between the sexes, the plot suggests that males tended to have greater cortical indices than females after the first 6 months of life.

### **Chronically Ill Infants Excluded**

Analyses were repeated with chronically ill infants excluded to evaluate whether their inclusion substantially affected results calculated from the pooled data. Two-way ANOVAs were conducted on models predicting tibial measurements using age, sex, and the interaction variable age\*sex. Levene's tests indicated that variances in tibial length ( $F = 1.22, p = .287$ ), midshaft diameter ( $F = 1.80, p = .052$ ), medullary cavity diameter ( $F = 1.81, p = .050$ ), cortical thickness

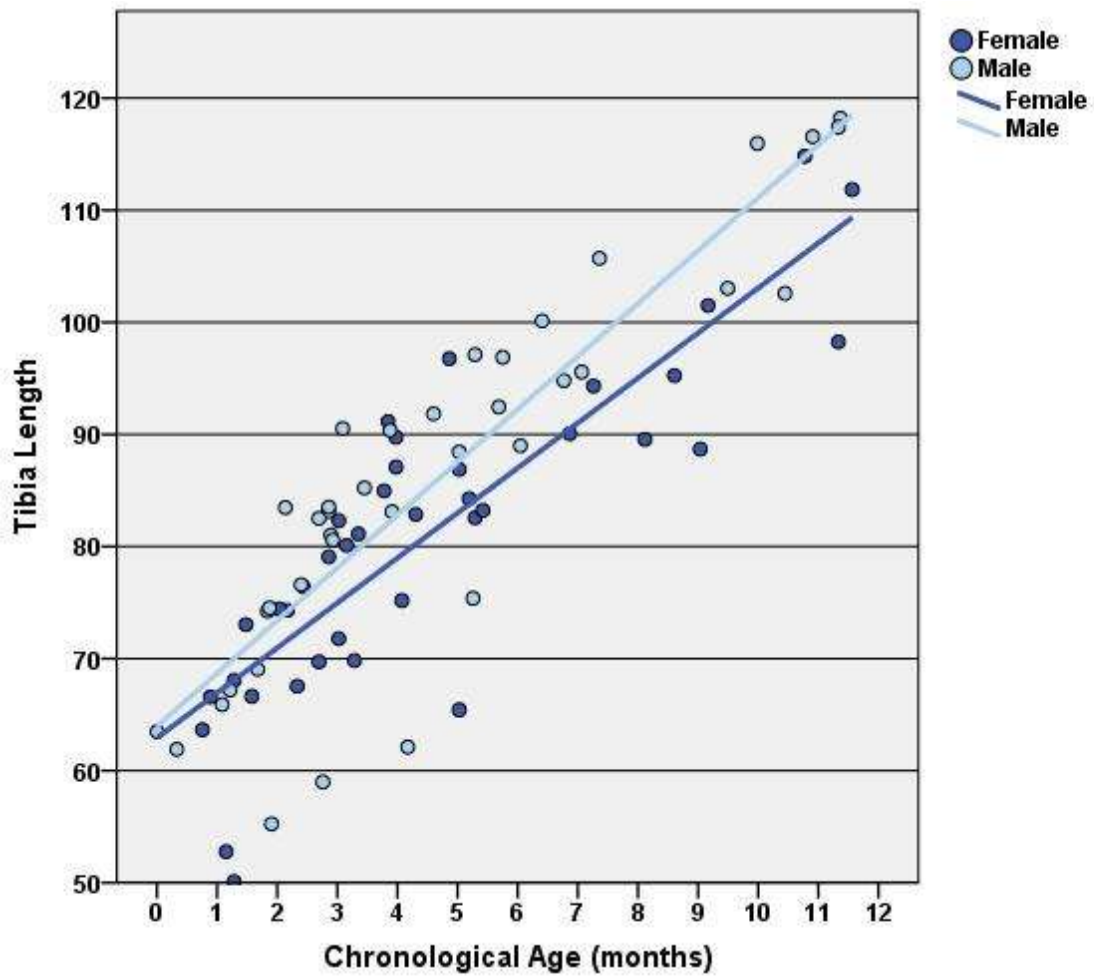


Figure 4-18. Plot of tibial length by age and sex.

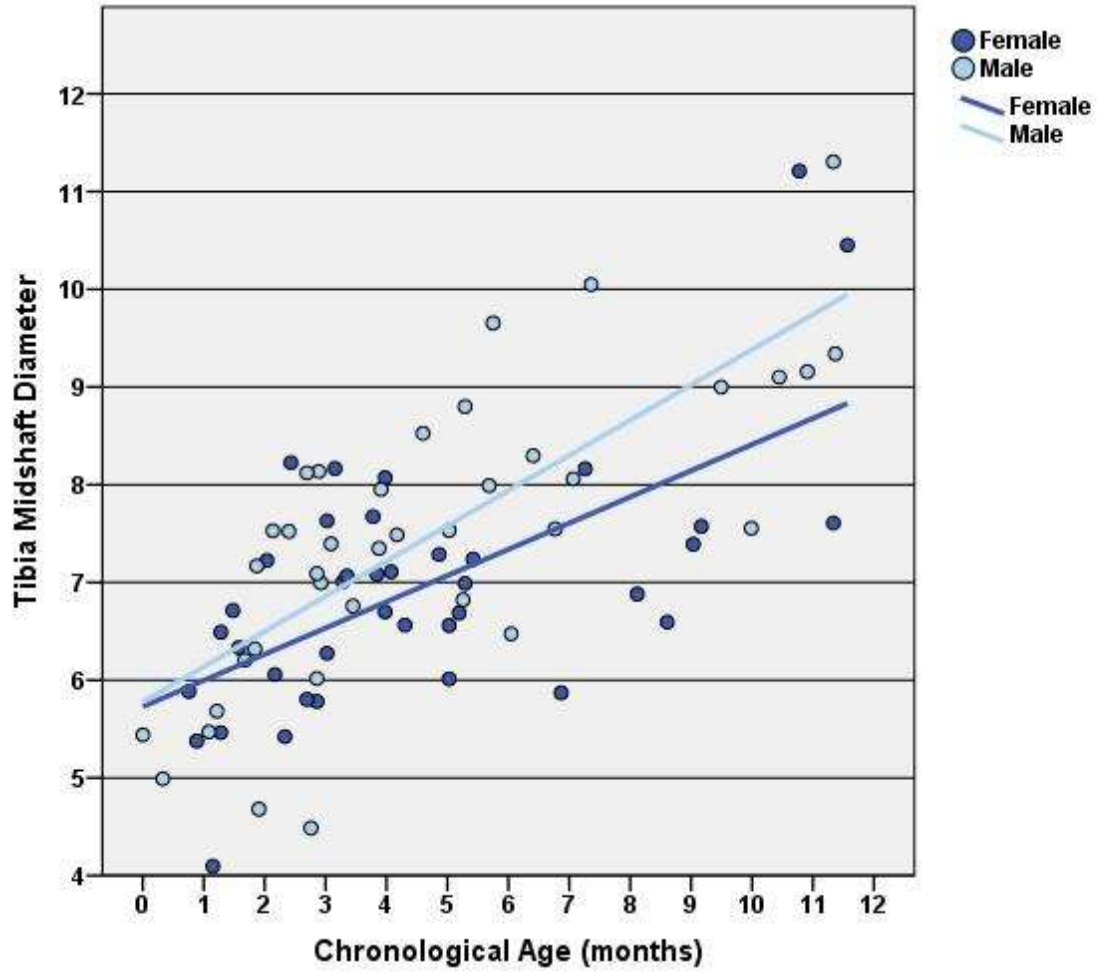


Figure 4-19. Plot of tibial midshaft diameter by age and sex.

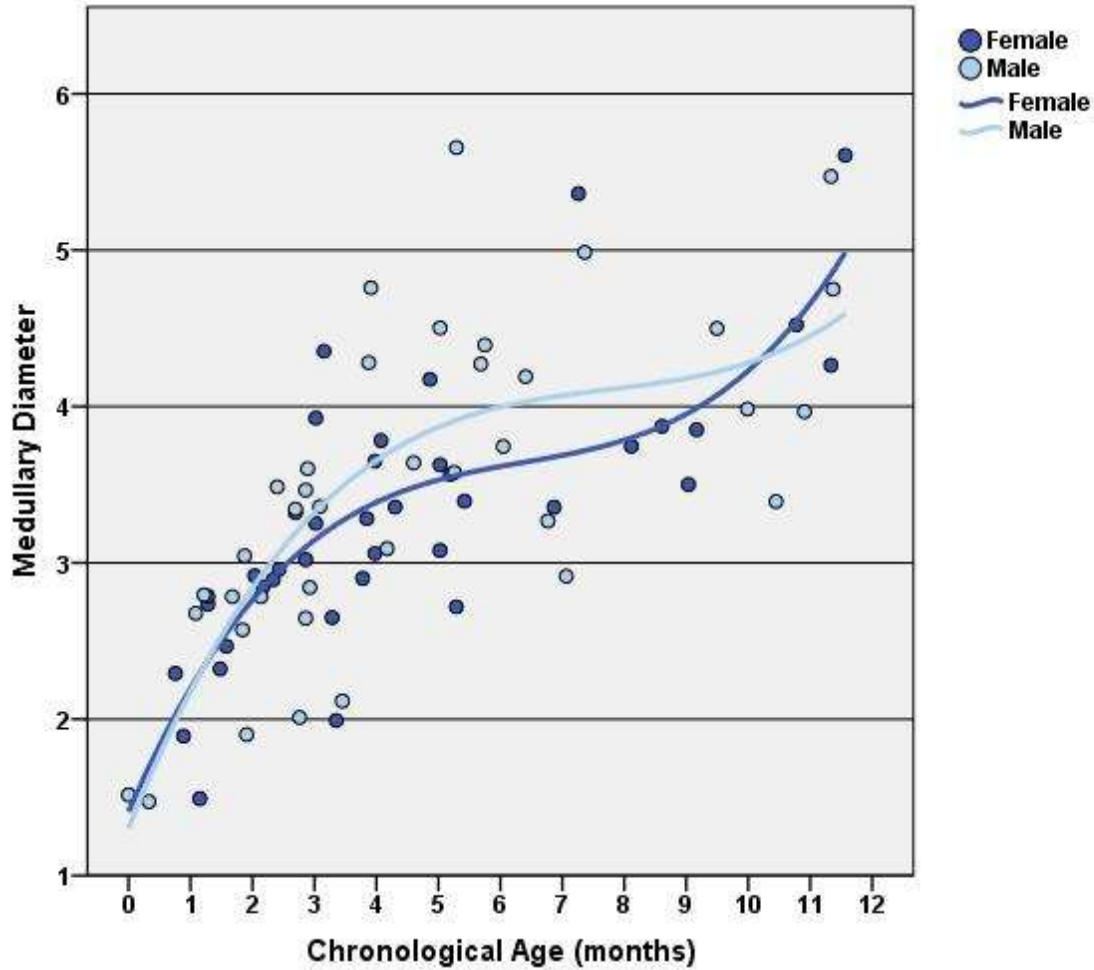


Figure 4-20. Plot of medullary cavity diameter by age and sex.

Table 4-10. Model summary for two-way ANOVA predicting cortical thickness using sex, age, and sex\*age.

Tests of Between-Subjects Effects					
Dependent Variable: Cortical Thickness					
Source	Type III Sum of Squares	<i>df</i>	Mean Square	<i>F</i>	<i>p</i>
Corrected Model	31.90 <sup>a</sup>	22	1.45	2.49	.003
Intercept	816.54	1	816.54	1401.16	< .001
Sex	2.90	1	2.90	4.97	.030
Age	22.24	11	2.02	3.47	.001
Sex * Age	8.14	10	0.81	1.40	.207
Error	31.47	54	0.58		
Total	1187.03	77			
Corrected Total	63.37	76			

a. R Squared = 0.50 (Adjusted R Squared = 0.30)

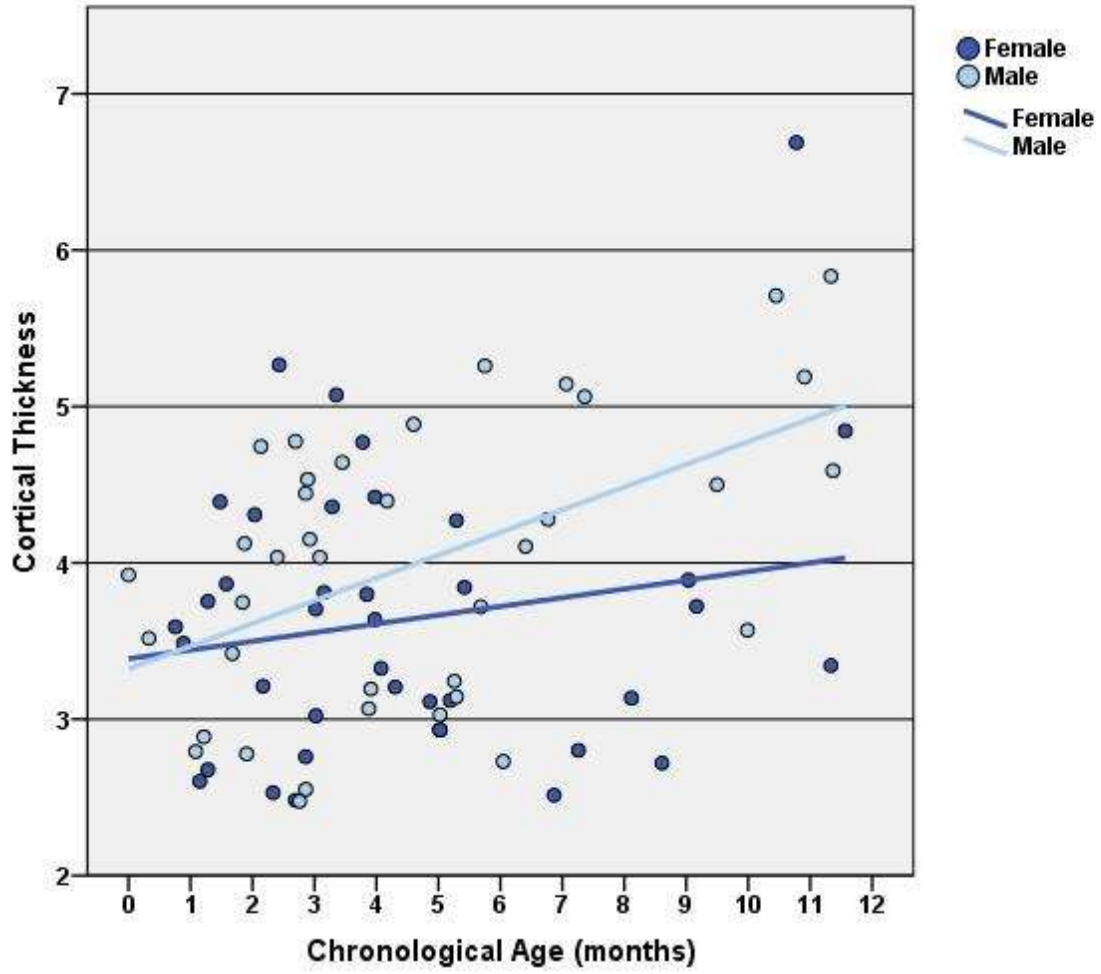


Figure 4-21. Plot of cortical thickness by age and sex.

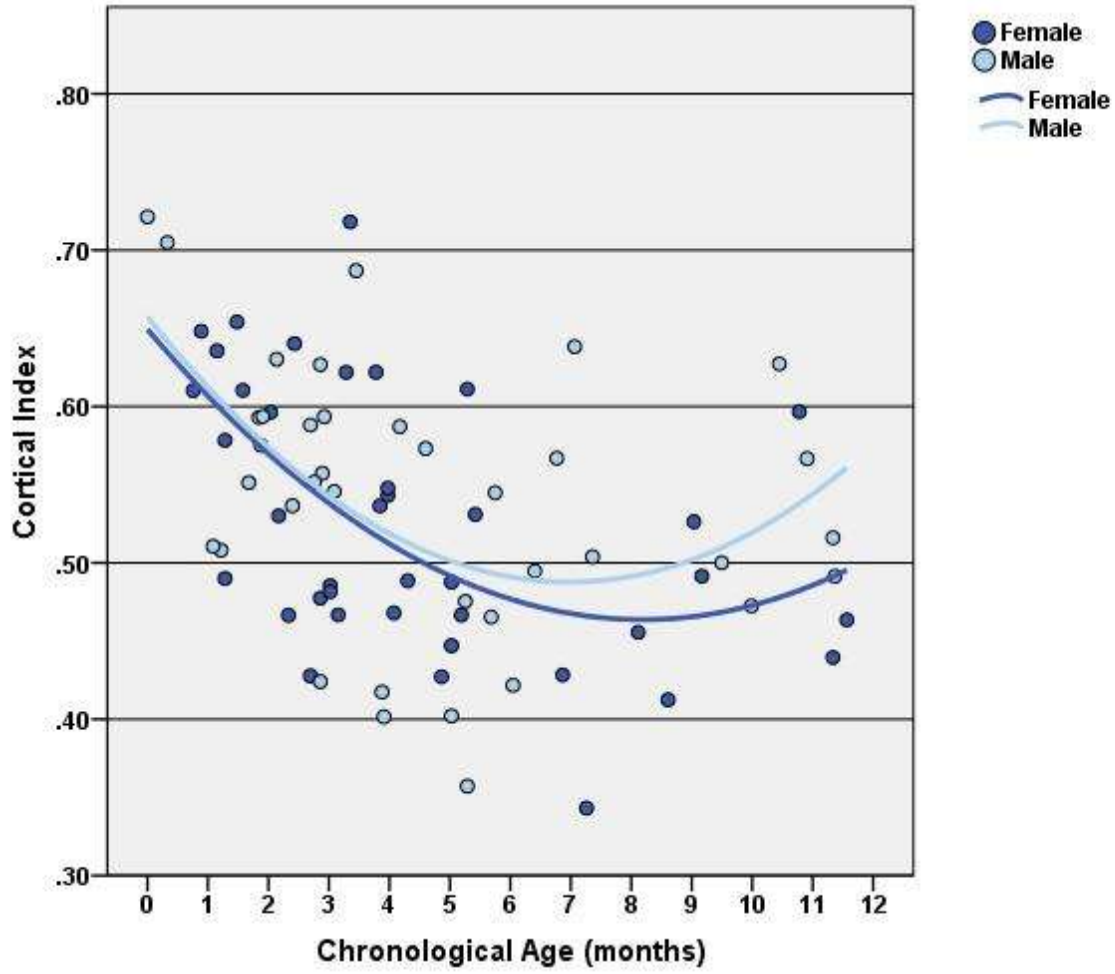


Figure 4-22. Plot of cortical index by age and sex.

( $F = 1.54, p = .115$ ), and cortical index ( $F = 1.71, p = .070$ ) were equal across groups. Age ( $F(11, 42) = 12.75, p < .001$ ) and sex ( $F(1, 42) = 4.14, p = .048$ ) were significant predictors in the model predicting tibial length, but sex\*age ( $F(9, 42) = 0.73, p = .676$ ) was not significant. This finding differed from the results calculated from the pooled data. Males had significantly greater tibial lengths after accounting for age differences. A plot of tibial length by age with the data separated by sex and excluding chronically ill infants is provided in **Figure 4-23**. Age was a significant variable in the model predicting midshaft diameter ( $F(11, 42) = 8.61, p < .001$ ), but sex ( $F(1, 42) = 2.48, p = .123$ ) and sex\*age ( $F(9, 42) = 1.65, p = .131$ ) were not significant. Age ( $F(11, 42) = 8.71, p < .001$ ) was a significant predictor in a model predicting medullary cavity diameter, but sex ( $F(1, 42) = 0.03, p = .862$ ) and age\*sex ( $F(9, 42) = 1.86, p = .086$ ) were not significant. Age ( $F(11, 42) = 2.66, p = .011$ ) was a significant predictor in the model predicting cortical thickness, but sex ( $F(1, 42) = 4.06, p = .050$ ) and sex\*age ( $F(9, 42) = 1.73, p = .113$ ) were not significant. This finding differed from results calculated from the pooled data. Age ( $F(11, 42) = 2.83, p = .007$ ) was a significant predictor in a model predicting cortical index, but sex ( $F(1, 42) = 2.85, p = .099$ ) and age\*sex ( $F(9, 42) = 1.73, p = .113$ ) were not significant.

### ***Race***

Studies have reported significant racial differences in BMD and SOS among infants that may be attributed to significant racial differences in bone size. Due to the possibility of finding significant racial differences in BMD or SOS in the current study, tests were carried out to evaluate racial differences in the tibial measurements. ANOVAs and simple linear regression were used to determine if there were any significant racial differences in the tibial measurements. Variances in tibial length ( $F = 1.10, p = .355$ ), midshaft diameter ( $F = 0.78, p = .512$ ), medullary cavity diameter ( $F = 0.08, p = .973$ ), and cortical index ( $F = 0.32, p = .808$ ) were equal across racial groups. There were significant differences in cortical thickness variance between the racial groups ( $F = 3.68, p = .016$ ). ANOVAs indicated no significant differences in tibial length ( $F(3, 73) = 1.95, p = .130$ ), midshaft diameter ( $F(3, 73) = 2.53, p = .063$ ), medullary cavity diameter ( $F(3, 73) = 0.96, p = .419$ ), or cortical index ( $F(3, 73) = 0.90, p = .447$ ) based on race. There were significant racial differences in cortical thickness ( $F(3, 73) = 2.75, p = .049$ ). Post hoc analyses using Tamhane's T2 test indicated that Asian infants had significantly lower cortical thickness than black, white, and Hispanic infants ( $p < .001$ ). Although analyses for cortical

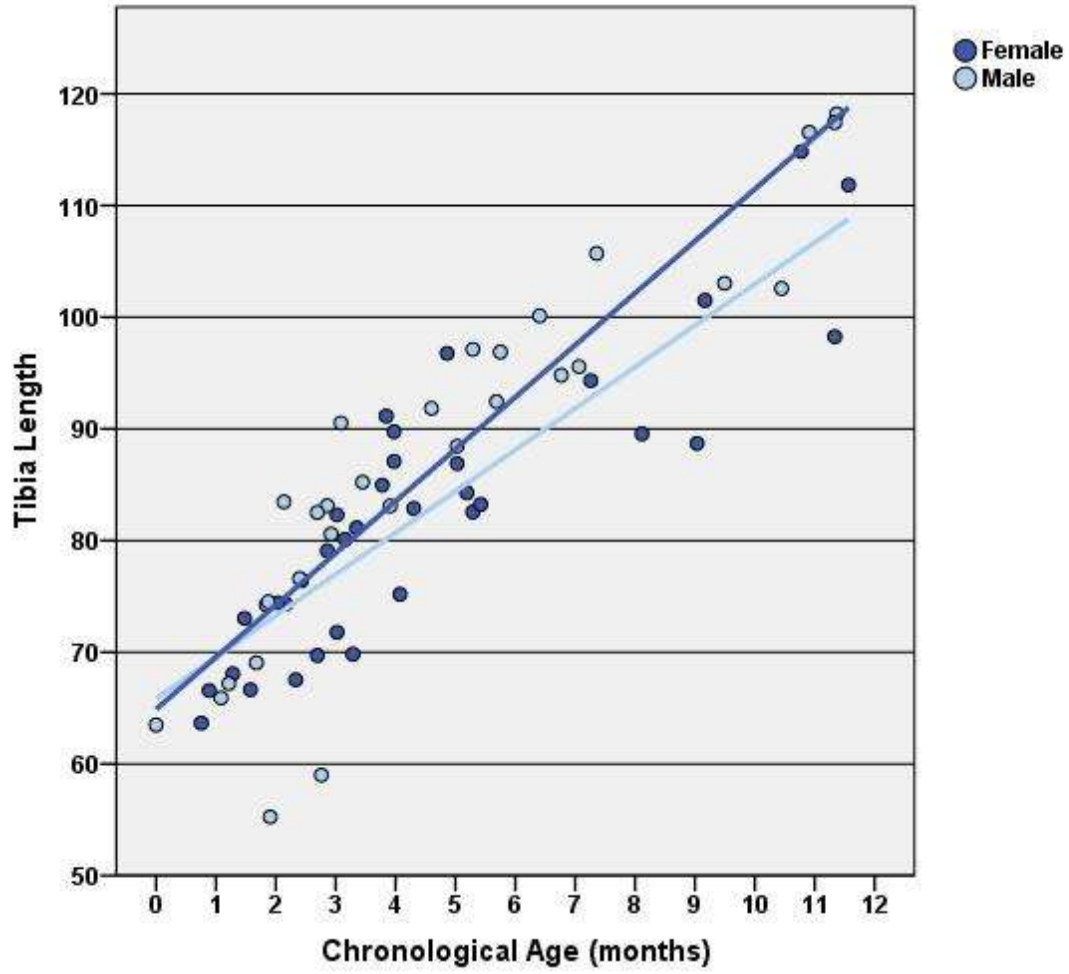


Figure 4-23. Plot of tibial length by age and sex with chronically ill infants excluded.



thickness indicated significant differences between Asian infants and other groups, these results should not be given much weight due to the small number of infants in the Asian group ( $n = 2$ ).

### **Chronically Ill Infants Excluded**

Analyses were repeated with chronically ill infants excluded to evaluate whether their inclusion substantially affected results calculated from the pooled data. Variances in tibial length ( $F = 0.57, p = .569$ ), midshaft diameter ( $F = 0.80, p = .455$ ), medullary cavity diameter ( $F = 0.25, p = .780$ ), cortical thickness ( $F = 2.08, p = .134$ ), and cortical index ( $F = 0.12, p = .885$ ) were equal between the racial groups. The association between race and midshaft diameter was significant after chronically ill infants were removed from the analysis ( $F(2, 61) = 3.42, p = .039$ ). LSD tests indicated that black infants had significantly greater midshaft diameters than white infants ( $p = .013$ ) **Table 4-11**. Racial differences in tibial length ( $F(2, 61) = 3.09, p = .053$ ), cortical thickness ( $F(2, 61) = 2.64, p = .079$ ), medullary cavity diameter ( $F(2, 61) = 1.85, p = .167$ ), and cortical index ( $F(2, 61) = 0.83, p = .439$ ) remained insignificant.

Due to the significant racial differences in midshaft diameter, one-way ANOVAs were conducted to determine if there was a significant relationship between race and age, race and sex, or sex and age that may explain the difference. Asian infants were excluded from analyses because the group consisted only of females. Levene's test indicated equal variances in age ( $F = 0.30, p = .741$ ), sex ( $F = 1.03, p = .315$ ), and race ( $F = 1.54, p = .224$ ) between groups. There was no significant difference in age based on race ( $F(2, 62) = 0.43, p = .653$ ) or sex ( $F(1, 63) = 0.07, p = .791$ ). A significant association was found between race and sex ( $F(2, 62) = 3.74, p = .029$ ). LSD post hoc analyses indicated black infants were significantly more likely to be male than white ( $p = .025$ ) and Hispanic infants ( $p = .035$ ) after excluding chronically ill infants from analyses (**Table 4-12**). Significantly greater midshaft diameter among black infants may be attributable to the greater number of black male infants than white or Hispanic males infants.

### **Term Infants**

To determine if inclusion of the premature infants affected the results, the data were reanalyzed with the premature infants excluded. Of note, exclusion of the premature infants removed the Asian infants from the analyses because both were premature. Levene's test indicated that variances in tibial length ( $F = 1.16, p = .321$ ), midshaft diameter ( $F = 0.96, p = .388$ ), medullary

**Table 4-11. LSD post hoc comparisons between racial groups with tibial midshaft diameter as the dependent variable and chronically ill infants excluded from analyses.**

Multiple Comparisons						
(I) Race	(J) Race	Mean Difference (I-J)	SE	p	95% Confidence Interval	
					Lower Bound	Upper Bound
Black	Hispanic	0.52	0.38	.186	-0.25	1.28
	White	1.19*	0.46	.013	0.26	2.11
Hispanic	Black	-0.52	0.38	.186	-1.28	0.25
	White	0.67	0.49	.177	-0.31	1.66
White	Black	-1.19*	0.46	.013	-2.11	-0.26
	Hispanic	-0.67	0.49	.177	-1.66	0.31

\*. The mean difference is significant at the .05 level.

**Table 4-12. LSD post hoc comparisons between racial groups with sex as the dependent variable (Males = 1) and chronically ill infants excluded from analyses.**

Multiple Comparisons						
(I) Race	(J) Race	Mean Difference (I-J)	SE	p	95% Confidence Interval	
					Lower Bound	Upper Bound
Black	Hispanic	0.29*	0.14	.035	0.02	0.56
	White	0.38*	0.16	.025	0.05	0.70
Hispanic	Black	-0.29*	0.14	.035	-0.56	-0.02
	White	0.08	0.17	.635	-0.27	0.43
White	Black	-0.38*	0.16	.025	-0.70	-0.05
	Hispanic	-0.08	0.17	.635	-0.43	0.27

\*. The mean difference is significant at the .05 level.

diameter ( $F = 0.74, p = .483$ ), cortical thickness ( $F = 2.97, p = .060$ ), and cortical index ( $F = 0.21, p = .815$ ) were equal across racial groups. After excluding premature infants from analyses, there were no significant racial differences in tibial length ( $F(2, 54) = 1.22, p = .303$ ), midshaft diameter ( $F(2, 54) = 2.66, p = .079$ ), medullary cavity diameter ( $F(2, 54) = 0.95, p = .392$ ), cortical thickness ( $F(2, 54) = 2.37, p = .103$ ), or cortical index ( $F(2, 54) = 0.38, p = .684$ ).

## ***QUANTITATIVE ULTRASOUND***

### ***Reliability***

Reliability analyses were conducted on the SOS readings by estimating an intra-class correlation coefficient, Cronbach's alpha, from the three consecutive SOS readings obtained from each infant. Cronbach's alpha was statistically significant and indicated excellent reliability ( $\alpha = .983, p < .001$ ). To determine if there were significant differences in intra-infant SOS readings, a repeated-measures ANOVA was performed. Results indicated there was no significant difference between the three intra-infant SOS measurements ( $F(2, 75) = 0.57, p = .567$ ). Lastly, a coefficient of variation (CV) was calculated for the intra-infant SOS readings. On average the three SOS measurements taken on each infant varied by approximately 1.2% (CV = .012) with a range of 0-6%.

### ***SOS***

Three consecutive SOS measurements were taken from the tibial midshaft of each infant, with the exception of two cases. Only two SOS measurements could be obtained from one infant (Case ID # 180) due to operator error and no SOS readings could be obtained from another case (Case ID # 185). It is possible that QUS could not detect the ultrasound signal reflected from this infant's tibia either due to a low SOS reading or inappropriate probe size. The manufacture sets the lowest SOS signal detected by the QUS device and is not adjustable. The CM probe may have been too large relative to the size of the infant's leg to maintain good contact between the probe and the skin of the leg. The CS probe, a smaller probe designed to measure SOS of the proximal phalanx, was not available at the time the measurement was obtained.

Average SOS measures were calculated from the consecutive SOS measurements obtained from the 77 infants ( $M = 3010.75$  m/s,  $SD = 213.12$ ) (Table A- 6 of the Appendix). A Shapiro-Wilk test was used to evaluate data distribution normality. The average SOS data were normal

distributed ( $W = 0.995, p = .992$ ). A frequency distribution of SOS with the SOS values from premature infants represented in light blue is provided in **Figure 4-24**. To test for significant differences in age-specific SOS means based on type of age grouping method (chronological age in months versus term-corrected age in months), a paired  $t$ -test was conducted. A Shapiro-Wilk test indicated that the differences between pairs were normally distributed ( $W = 0.871, p = .079$ ). There was no significant differences between age-specific SOS means based on type of age grouping method ( $t = -0.21, p = .839$ ). It is recognized that chronological age may not correspond with skeletal development. However, there is no way to correct for this difference. Since there is no way to correct for this difference and was no significant difference in age-specific SOS means between term-corrected and chronological age, chronological age was used in all remaining analyses which included age as a variable.

### **Sex and Race**

ANOVAs were used to test for sex and race dependent differences in SOS data. Levene's tests indicated that variances in SOS were equal between the sexes ( $F = 1.74, p = .192$ ) and racial groups ( $F = 0.05, p = .987$ ) There were no statistically significant differences in SOS based on sex ( $F(1, 75) = 0.56, p = .457$ ) or race ( $F(3, 73) = 0.63, p = .596$ ).

### *Term Infants*

Premature infants are reported to have significantly lower SOS values than term born infants. Analyses were repeated with premature infants excluded to determine whether results calculated using only term born infants different from data calculated using the pooled sample. ANOVAs were performed which predicted SOS by sex and race. The effects of sex ( $F(1, 55) = 0.45, p = .505$ ) and race ( $F(2, 54) = 0.97, p = .387$ ) on SOS remained insignificant.

### ***BMD***

BMD estimates for the radial midshaft and tibial midshaft were obtained for 48 infants and 70 infants, respectively. The custom program could not calculate BMD estimates for 21 radiographs of the radius/ulna and 8 radiographs of the tibia/fibula. There are several possible explanations for the inability to calculate BMD estimates. The program may not have been able to differentiate between the attenuation associated with soft tissue and bone due to inhomogeneities in the radiographic image, low BMD, or thin cortices ( $< 2$  mm). The distribution of the BMD

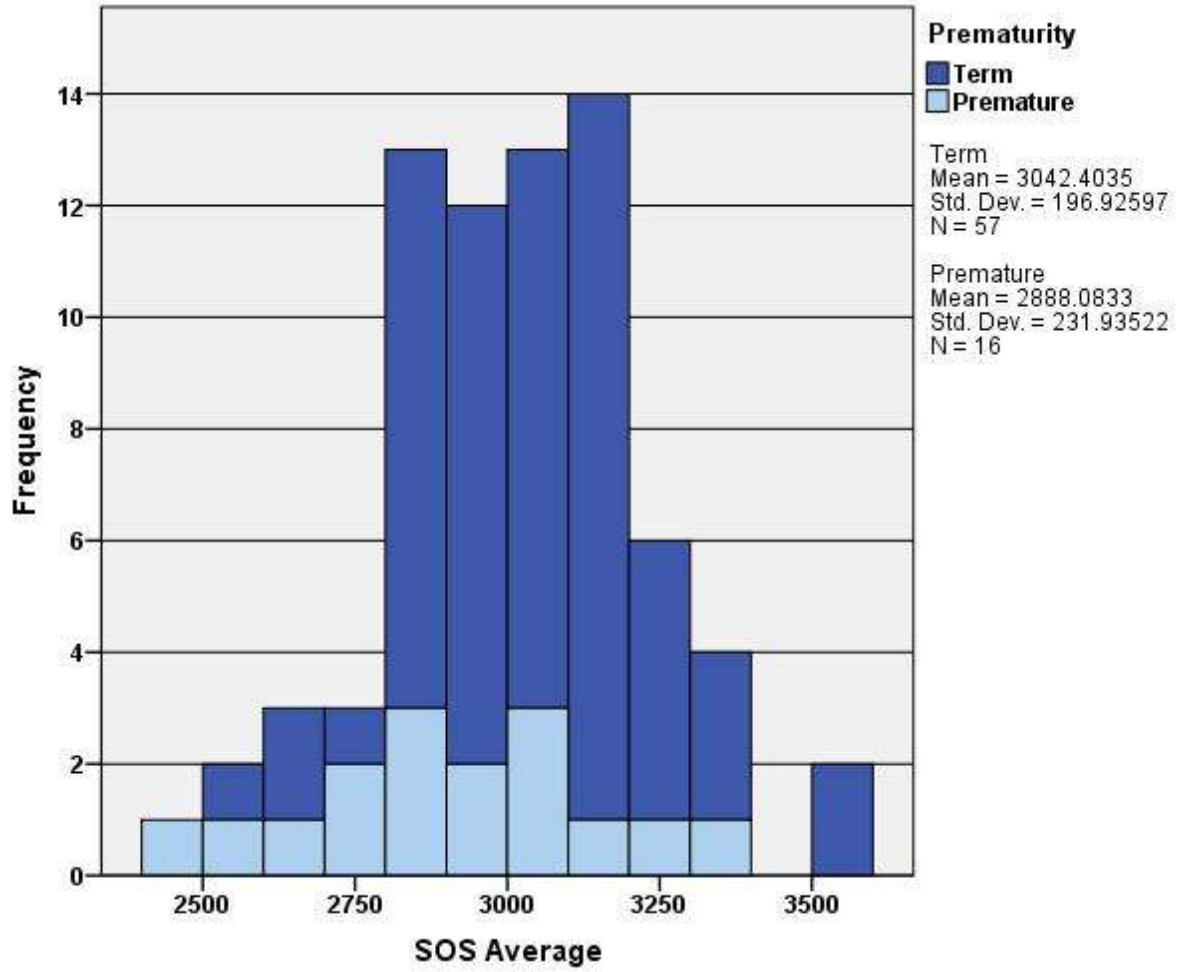


Figure 4-24. Distribution of average SOS readings. Dark blue represents SOS data from term born infants and light blue represents data from premature infants.

data was evaluated for normality using the Shapiro-Wilk test. The radial ( $W = 0.805, p < .001$ ) and tibial ( $W = 0.959, p = .022$ ) BMD data were not normally distributed. Descriptive statistics of the radial and tibial BMD estimates for the entire study sample are given in **Table A- 6** of the Appendix. The median and inter-quartile range for radial BMD estimates were  $0.40 \text{ g/cm}^2$  and  $0.30\text{-}0.58 \text{ g/cm}^2$ , respectively. The median and inter-quartile range for the tibial BMD estimates of the entire study sample were  $0.86 \text{ g/cm}^2$  and  $0.62\text{-}1.15 \text{ g/cm}^2$ , respectively.

A nonparametric paired-sample sign test was used to compare the radial and tibial BMD estimates obtained from the same infant. BMD estimates of both the radius and tibia were obtained for 46 infants. Results indicate that intra-infant radial BMD estimates were significantly lower than tibial BMD estimates ( $Z = 1.0, p < .001$ ). All BMD measurement of the radius were excluded from further statistical analyses in order to prevent decreasing the overall sample size as a result of their inclusion.

### ***Sex and Race***

Significant differences in BMD estimates based on sex and race were evaluated using one-way ANOVA. Levene's test indicated unequal variances in BMD between the sexes ( $F = 5.14, p = .027$ ). Males had significantly lower BMD than the females in the study sample ( $F(1, 68) = 4.72, p = .033$ ). Variances in BMD were equal between groups based on race ( $F = 1.08, p = .365$ ). There were significant differences in BMD estimates based on race ( $F(3, 66) = 2.88, p = .042$ ). *LSD* post hoc analyses indicated that white infants had significantly greater BMD estimates than Hispanic infants. Asian infants had significantly lower BMD estimates than White infants, but these results should be disregarded due to the small number of Asian infants in the group ( $n = 2$ ). Results of post hoc analyses are provided in **Table 4-13**.

Analyses were conducted to determine if the sex difference in BMD was related to an association between sex and age, prematurity, chronic illness, or size. Chi-square tests indicated no significant associations between sex and prematurity ( $X^2(1, n = 74) = 1.58, p = .209$ ) or chronic illness ( $X^2(1, n = 78) = 1.03, p = .311$ ). A one-way ANOVA was used to test for a significant relationship between sex and age, height, weight, and birthweight. Levene's tests indicated that variances in age ( $F = 0.36, p = .552$ ), weight ( $F = 1.40, p = .241$ ), height ( $F = 1.29, p = .259$ ),

**Table 4-13. LSD post hoc comparisons between racial groups with BMD as the dependent variable.**

Multiple Comparisons						
(I) Race	(J) Race	Mean Difference (I-J)	SE	p	95% Confidence Interval	
					Lower Bound	Upper Bound
Black	Hispanic	0.08	0.08	.355	-0.09	0.25
	White	-0.18	0.11	.093	-0.39	0.03
	Asian	0.40	0.23	.085	-0.06	0.85
Hispanic	Black	-0.08	0.08	.355	-0.25	0.09
	White	-0.26*	0.11	.023	-0.48	-0.04
	Asian	0.32	0.23	.170	-0.14	0.78
White	Black	0.18	0.11	.093	-0.03	0.39
	Hispanic	0.26*	0.11	.023	0.04	0.48
	Asian	0.58*	0.24	.018	0.10	1.05
Asian	Black	-0.40	0.23	.085	-0.85	0.06
	Hispanic	-0.32	0.23	.170	-0.78	0.14
	Asian	-0.58*	0.24	.018	-1.05	-0.10

\*. The mean difference is significant at the .05 level.

and birthweight ( $F = 0.18, p = .677$ ) were equal between the sexes. There were no significant sex differences for age ( $F(1, 76) = 0.12, p = .728$ ), weight ( $F(1, 76) = 1.71, p = .196$ ), height ( $F(1, 76) = 1.48, p = .227$ ), and birthweight ( $F(1, 69) = 0.55, p = .463$ ). These results indicated that there were no significant sex differences in age, health, or body size to account for the significant sex differences in BMD.

### **Chronically Ill Infants Excluded**

After removing the chronically ill infants from the analysis, variances in BMD were equal between groups based on sex ( $F = 2.51, p = .119$ ) and race ( $F = 0.70, p = .500$ ). Males continued to have significantly lower BMD than females ( $F(1, 56) = 4.12, p = .047$ ). Racial differences in BMD ceased to be significant after exclusion of chronically ill infants from the analysis ( $F(2, 55) = 2.07, p = .136$ ).

## **Association between Growth-Related Changes in Size and Age-Related Changes in SOS and BMD**

### ***HYPOTHESIS 1A: AGE-RELATED CHANGES IN TIBIAL STRUCTURE ARE ASSOCIATED WITH GROWTH-RELATED CHANGES IN BODY SIZE.***

Age-related changes in tibial structure were hypothesized to be significantly positively associated with variables related to body size and growth percentiles. ANOVA and regression analyses were performed to evaluate the relationship between tibial measurements and variables related to growth and size. Age was a covariate in the model predicting tibial length. Age, age<sup>2</sup>, and age<sup>3</sup> were used as covariates in models predicting midshaft diameter and medullary cavity diameter. Age and age<sup>2</sup> were used as covariates models predicting cortical thickness and cortical index. Models using height to predict tibial length ( $R^2_{Adj} = .90, F(2, 74) = 326.40, p < .001$ ), midshaft diameter ( $R^2_{Adj} = .64, F(4, 72) = 35.23, p < .001$ ), medullary cavity diameter ( $R^2_{Adj} = .61, F(4, 72) = 30.41, p < .001$ ), and cortical thickness ( $R^2_{Adj} = .23, F(3, 73) = 8.47, p < .001$ ) were significant. Regression coefficients for height were significant ( $p < .05$ ) and indicated that, while holding age constant, tibial length ( $b = 1.26, 95\% \text{ CI } [1.03, 1.50]$ ), midshaft diameter ( $b = 0.11, 95\% \text{ CI } [0.07, 0.15]$ ), cortical thickness ( $b = 0.06, 95\% \text{ CI } [0.02, 0.10]$ ), and medullary cavity diameter ( $b = 0.05, 95\% \text{ CI } [0.02, 0.07]$ ) increased as height increased. After accounting for age, height was not a significant predictor of cortical index ( $p = .564$ ).



Models using length for age percentile to predict tibial length ( $R^2_{Adj.} = .10$ ,  $F(1, 74) = 8.94$ ,  $p = .004$ ), midshaft diameter ( $R^2_{Adj.} = .12$ ,  $F(1, 74) = 10.77$ ,  $p = .002$ ), and cortical thickness ( $R^2_{Adj.} = .12$ ,  $F(1, 74) = 10.75$ ,  $p = .002$ ) were significant. The regression coefficient for length for age percentile indicated that tibial length increased by 0.15 mm with every 1 percentile increase in length for age percentile ( $b = 0.15$ , 95% CI [0.05, 0.25]). Regression coefficients for length for age percentile indicated that tibial midshaft diameter ( $b = 0.01$ , 95% CI [0.006, 0.02]) increased by 0.01 mm and cortical thickness ( $b = 0.01$ , 95% CI [0.004, 0.02]) increased by 0.01 mm with every 1 percentile point increase in length for age percentile. No significant relationship was found between length for age percentile and medullary cavity diameter ( $F(1, 74) = 2.82$ ,  $p = .097$ ) or cortical index ( $F(1, 74) = 1.20$ ,  $p = .277$ ).

ANOVA and linear regression analyses were used to predict the tibial measurements from weight while using age as a covariate. Weight was a significant predictor ( $p < .05$ ) in models predicting tibial length ( $R^2_{Adj.} = .82$ ,  $F(2, 74) = 169.76$ ,  $p < .001$ ), midshaft diameter ( $R^2_{Adj.} = .63$ ,  $F(4, 72) = 33.07$ ,  $p < .001$ ), medullary cavity diameter ( $R^2_{Adj.} = .61$ ,  $F(4, 72) = 30.44$ ,  $p < .001$ ), and cortical thickness ( $R^2_{Adj.} = .21$ ,  $F(3, 73) = 7.78$ ,  $p < .001$ ). Regression coefficients for weight indicated that tibial length ( $b = 2.84$ , 95% CI [1.83, 3.84]), cortical thickness ( $b = 0.18$ , 95% CI [0.06, 0.31]), midshaft diameter ( $b = 0.32$ , 95% CI [0.19, 0.45]), cortical thickness ( $b = 0.18$ , 95% CI [0.10, 0.27]), and medullary cavity diameter ( $b = 0.15$ , 95% CI [0.06, 0.24]) increased as weight increased. Weight was not a significant predictor of cortical index after accounting for age ( $p = .708$ ).

ANOVA and linear regression analyses were used to predict the tibial measurements using weight for age percentile. Models using weight for age percentile to predict tibial length ( $R^2_{Adj.} = .14$ ,  $F(1, 74) = 13.39$ ,  $p < .001$ ), midshaft diameter ( $R^2_{Adj.} = .16$ ,  $F(1, 74) = 15.47$ ,  $p < .001$ ), medullary cavity diameter ( $R^2_{Adj.} = .10$ ,  $F(1, 74) = 9.44$ ,  $p = .003$ ), and cortical thickness ( $R^2_{Adj.} = .08$ ,  $F(1, 74) = 7.25$ ,  $p = .009$ ) were significant. The regression coefficients for weight for age percentile indicated that tibial length ( $b = 0.17$ , 95% CI [0.08, 0.27]), midshaft diameter ( $b = 0.02$ , 95% CI [0.01, 0.03]), medullary cavity diameter ( $b = 0.01$ , 95% CI [0.003, 0.02]), and cortical thickness ( $b = 0.008$ , 95% CI [0.002, 0.01]) increased as weight for age percentile increased. There was no significant relationship between weight for age percentile and cortical index ( $F(1, 74) = 0.06$ ,  $p = .808$ ).

ANOVA and linear regression analyses were used to predict the tibial measurements using weight for length percentile. There was no significant relationship between weight for length percentile and tibial length ( $F(1, 72) = 1.04, p = .311$ ), midshaft diameter ( $F(1,72) = 3.71, p = .058$ ), medullary cavity diameter ( $F(1,72) = 3.19, p = .078$ ), cortical thickness ( $F(1,72) = 1.16, p = .286$ ), or cortical index ( $F(1, 72) = 0.58, p = .448$ ).

With the exception of weight for length percentile and cortical index, results indicated that the tibial measurements were positively associated with body size, even after accounting for size differences due to age. These findings support the hypothesis that age-related changes in tibial structure are positively associated with growth related increases in body size.

### ***HYPOTHESIS 1B: BMD AND SOS ARE SIGNFICANTLY RELATED TO AGE.***

#### ***BMD and Age***

ANOVA and simple linear regression were used to evaluate the relationship between age and BMD. Age in months was used in analyses instead of age in weeks due to the low number of infants, 1 in some cases, in each age category when age was subdivided by weeks. There was a significant linear relationship between chronological age (months) and BMD ( $R^2_{Adj.} = .04, F(1, 68) = 4.19, p = .044$ ). An  $F$  test of the  $R^2$  change indicated that adding a quadratic term did not significantly improve the fit of the model. The regression coefficient for age indicated that BMD significantly decreased by  $0.03 \text{ g/cm}^2$  for every 1 month increase in age ( $b = -0.03, 95\% \text{ CI } [-0.05, -0.001]$ ). There was no significant relationship between term-corrected age (months) and BMD ( $F(1, 68) = 2.13, p = .150$ ). The significant association between BMD and chronological age supported the hypothesis.

#### **Chronically Ill Infants Excluded**

Due to the significant negative relationship between chronic illness and BMD, analyses were repeated with the chronically ill infants excluded. The relationship between chronological age and BMD remained significant ( $R^2_{Adj.} = .05, F(1, 56) = 4.11, p = .047$ ). The regression coefficient for chronological age indicated that BMD at the tibial midshaft decreased as postnatal age increased ( $b = -0.03, 95\% \text{ CI } [-0.06, -0.003E-1]$ ). A box and whisker plot of BMD by age and excluding chronically ill infants is presented in **Figure 4-25**. Due to the significant sex differences in BMD, the distribution of BMD by chronological age with the sexes differentiated is presented in **Figure 4-26**.

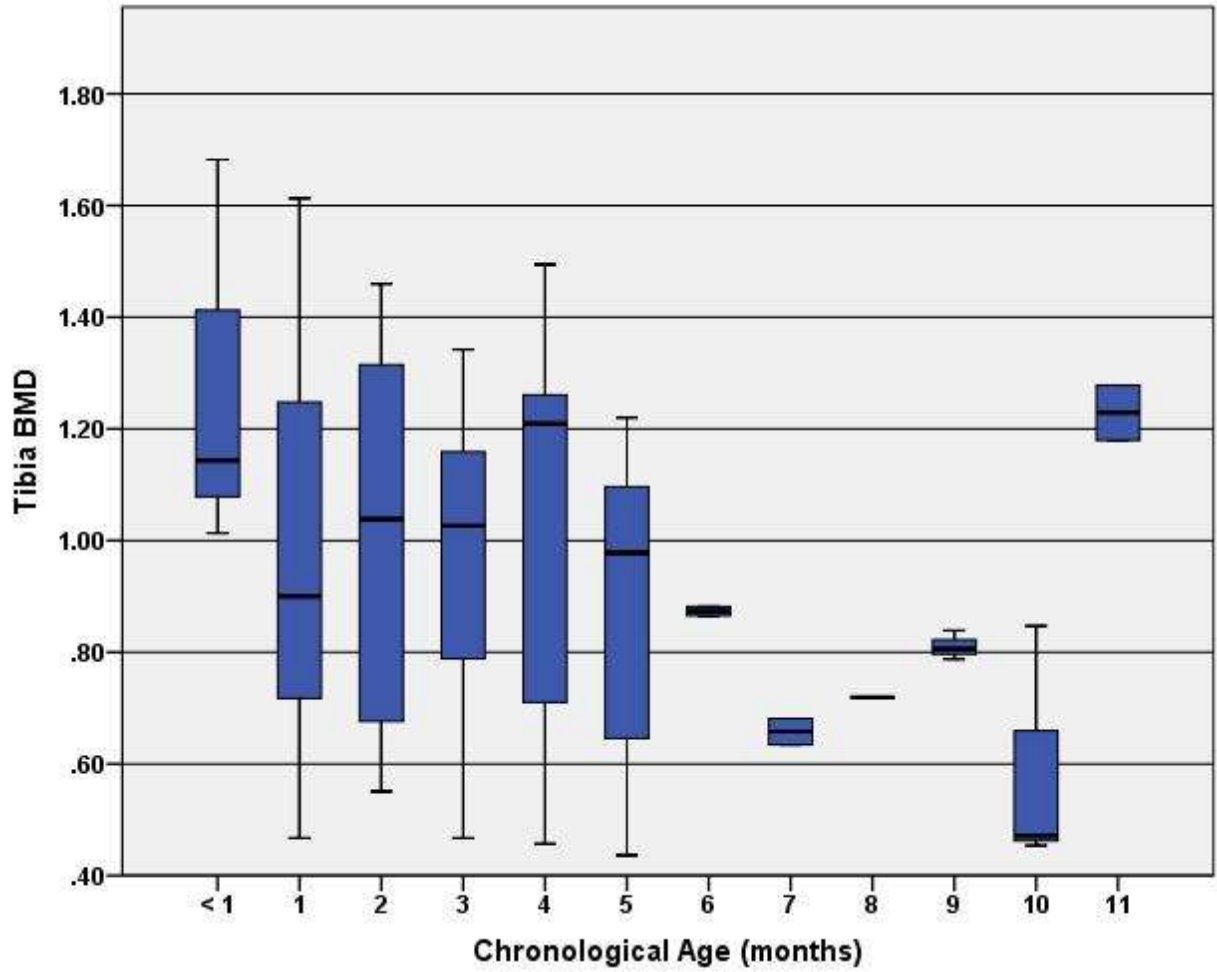


Figure 4-25. Box and whisker plot of BMD by chronological age in months with chronically ill infants excluded.

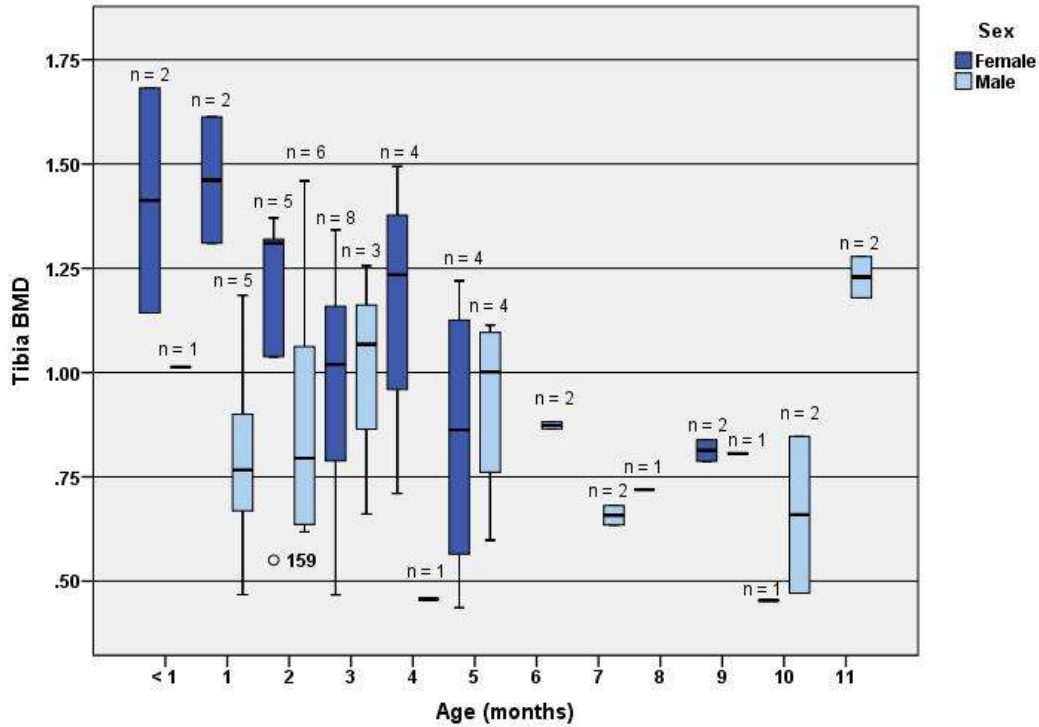


Figure 4-26. Box and whisker plot of BMD distributed by chronological age in months and sex, chronically ill infants excluded. Dark blue boxes represent data from female infants and are located to the left of gridlines representing age and light blue boxes represent data from male infants and are located to the right of gridlines representing age. The dark blue circle is a female outlier (Case ID # 159).

### *SOS and Age*

$F$  tests of the  $R^2$  change indicated that a cubic model was a significantly better fit than a quadratic or linear model for the relationship between age and SOS ( $F(1, 73) = 11.09, p = .001$ ). The regression coefficients for age ( $b = -233.72, p < .001$ ), age<sup>2</sup> ( $b = 48.02, p < .001$ ), and age<sup>3</sup> ( $b = -2.41, p = .001$ ) indicated that for every unit increase in age SOS decreased on average by ~234 m/s. The positive parameter estimate for age<sup>2</sup> indicated a positive quadratic trend in the data as age increased. Larger age values were associated with greater SOS readings. The negative parameter estimate of age<sup>3</sup> indicated a second curvature in the data. While the quadratic trend at smaller values of age was positive, the quadratic trend at larger age values was negative. The model predicting SOS using age explained ~36% of the variance in SOS ( $R^2_{Adj} = .36, F(3, 73) = 14.88, p < .001$ ) (Model 1, **Table 4-14**). A box and whisker plot of the SOS values by age in months for the pooled data is provided in **Figure 4-27**. A regression plot of the curvilinear (cubic) relationship between age and SOS is presented in **Figure 4-28**. The plot suggested that after birth SOS decreased with increasing age until ~3 months of age. After ~3 months of age, SOS gradually increased with increasing age. These results support the hypothesis that SOS has a significant relationship with age.

To evaluate which age ranges had significantly different mean SOS values, a one-way ANOVA was conducted on the SOS data using age in months as a grouping variable. Significant differences in group mean SOS were indicated ( $F(11, 65) = 3.99, p < .001$ ). Levene's test indicated equal variances between groups ( $F = 1.26, p = .270$ ). Results of post hoc tests using *LSD* are provided in **Table 4-15**. Post hoc analyses indicated that mean SOS for infants less than one month of age was significantly greater than the mean for infants 2 and 4 months of age ( $p < .05$ ). Mean SOS for infants 1 month of age was significantly lower than infants 8-11 months of age ( $p < .05$ ). Mean SOS for infants 2 months of age were significantly lower than infants less than 1 month of age and for infants 7-11 months of age ( $p < .05$ ). Mean SOS values for infants 3, 4, and 5 months of age were significantly lower than for infants 8-11 months of age ( $p < .05$ ). Mean SOS for infants 4 months of age was also significantly lower than for infants less than 1 month of age ( $p < .05$ ). For exact  $p$ -values see **Table 4-15**. Mean SOS for infants 6 months of age was significantly lower than for infants 10 months of age ( $p = .016$ ). In general, these analyses

**Table 4-14. Results of regression analyses with SOS as the dependent variable. Model 1 predicts mean SOS using the age variables. Model 2 predicts mean SOS from the age variables with premature infants excluded from the analysis.**

Model	Unstandardized Coefficients		<i>t</i>	<i>p</i>	<i>F</i>	<i>df</i>	<i>p</i>	Adj. <i>R</i> <sup>2</sup>
	<i>b</i>	<i>SE</i>						
1					14.88	3,73	<.001	.35
	(Constant)	3222.64	87.26	36.93	<.001			
	Age	-233.72	62.72	-3.73	<.001			
	Age <sup>2</sup>	48.02	12.70	3.78	<.001			
	Age <sup>3</sup>	-2.41	0.72	-3.33	.001			
2					10.20	3,49	<.001	.33
	(Constant)	3197.63	96.50	33.14	<.001			
	Age	-196.18	68.29	-2.87	.006			
	Age <sup>2</sup>	42.77	13.78	3.10	.003			
	Age <sup>3</sup>	-2.23	0.78	-2.85	.006			

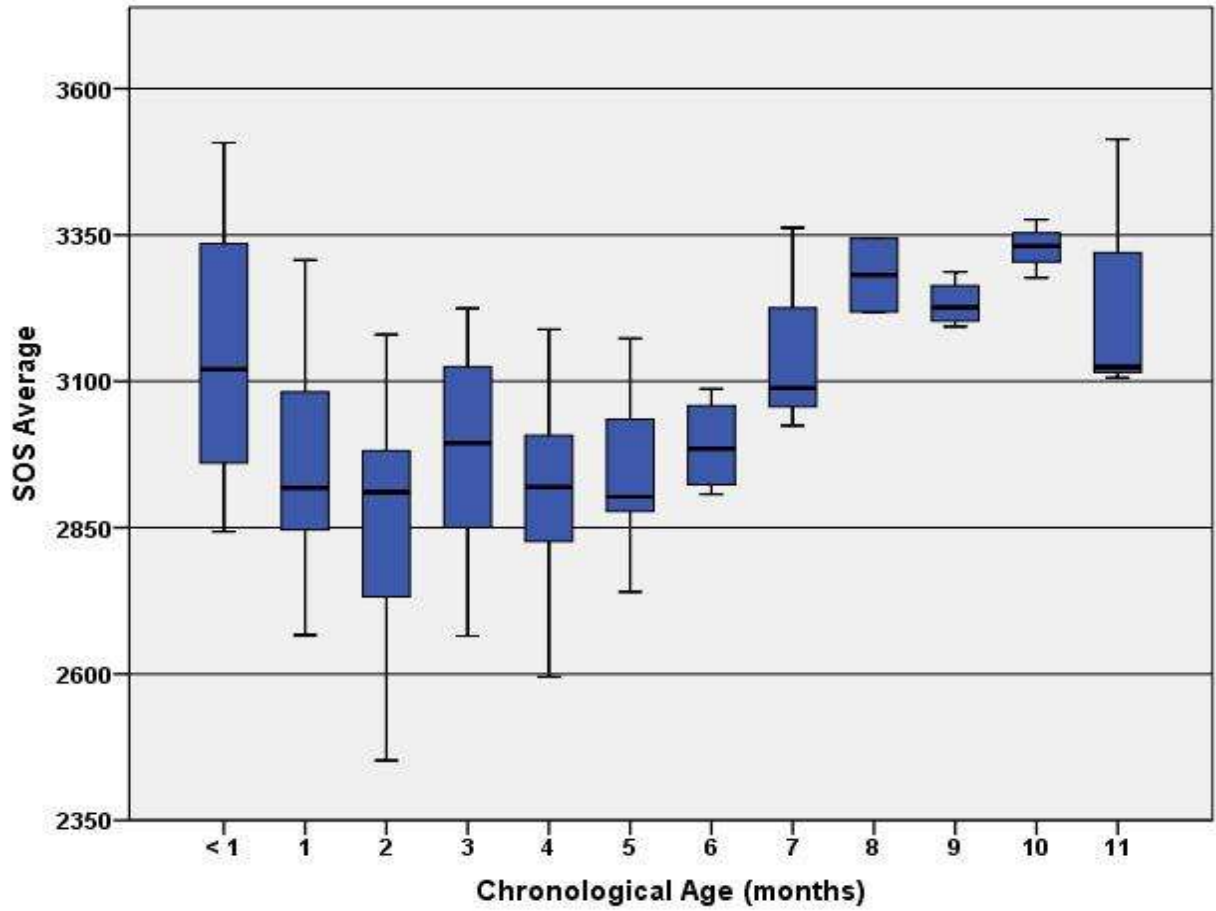


Figure 4-27. Box and whisker plot of SOS by chronological age in months.

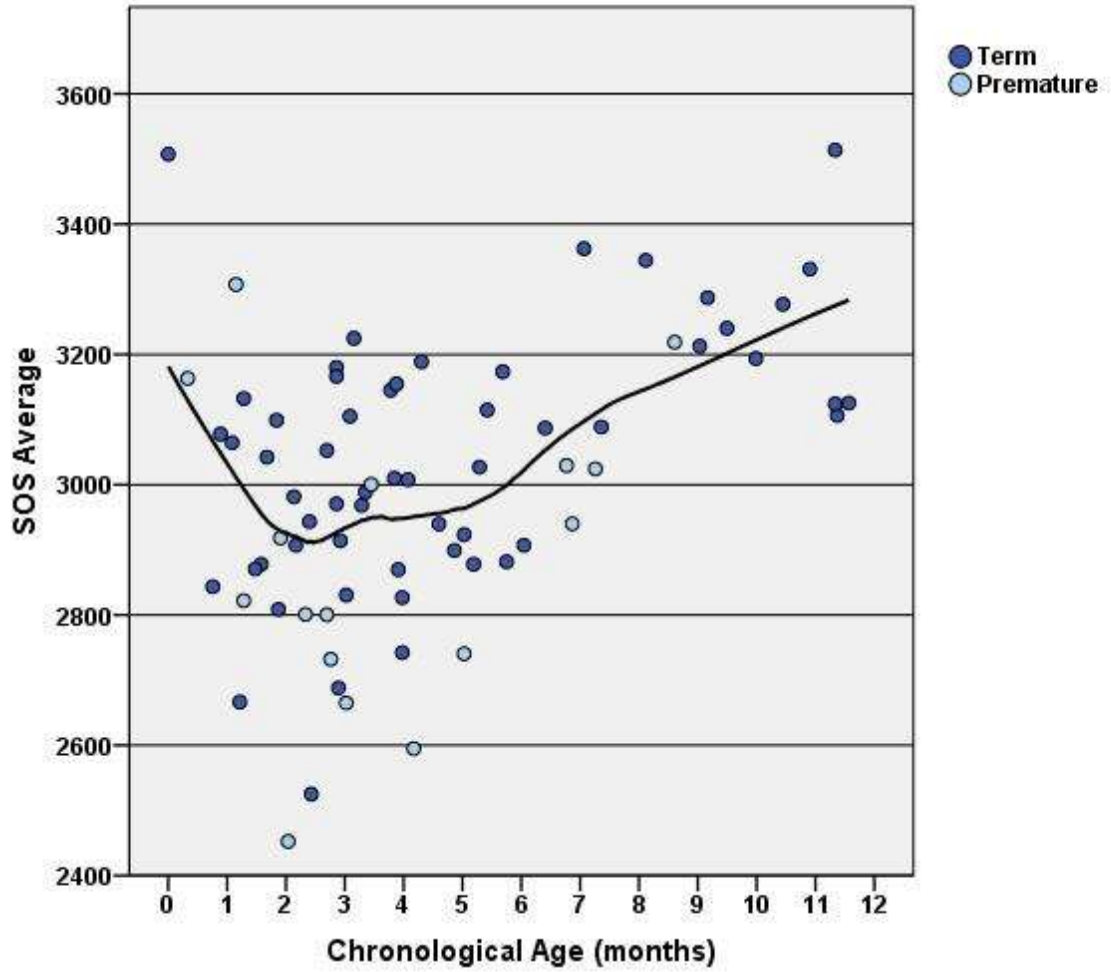


Figure 4-28. Plot of SOS readings against age in months with a Lowess-smoothed regression line. Dark blue circles represent SOS readings from term born infants. Light blue circles represent SOS readings from premature infants.



**Table 4-15. LSD post hoc comparisons of SOS group means by age in months.**

Multiple Comparisons						
(I) Age (months)	(J) Age (months)	Mean Difference (I-J)	SE	p	95% Confidence Interval	
					Lower Bound	Upper Bound
< 1	1	183.46	104.12	.083	-24.47	391.39
	2	282.63*	101.10	.007	80.73	484.54
	3	172.56	102.95	.099	-33.05	378.16
	4	238.47*	115.10	.042	8.59	468.35
	5	200.22	105.49	.062	-10.47	410.90
	6	157.08	126.09	.217	-94.74	408.90
	7	-10.53	136.19	.939	-282.52	261.47
	8	-133.58	154.43	.390	-442.00	174.83
	9	-85.42	126.09	.501	-337.24	166.40
	10	-180.19	136.19	.190	-452.19	91.80
	11	-69.42	126.09	.584	-321.24	182.40
1	< 1	-183.46	104.12	.083	-391.39	24.47
	2	99.17	71.85	.172	-44.32	242.66
	3	-10.91	74.43	.884	-159.56	137.75
	4	55.01	90.50	.545	-125.73	235.75
	5	16.75	77.91	.830	-138.85	172.36
	6	-26.38	104.12	.801	-234.31	181.55
	7	-193.99	116.15	.100	-425.95	37.97
	8	-317.05*	137.07	.024	-590.80	-43.29
	9	-268.88*	104.12	.012	-476.81	-60.95
	10	-363.66*	116.15	.003	-595.62	-131.70
	11	-252.88*	104.12	.018	-460.81	-44.95
2	< 1	-282.63*	101.10	.007	-484.54	-80.73
	1	-99.17	71.85	.172	-242.66	44.32
	3	-110.08	70.15	.121	-250.17	30.02
	4	-44.16	87.01	.614	-217.93	129.61
	5	-82.41	73.83	.268	-229.86	65.04
	6	-125.55	101.10	.219	-327.45	76.36
	7	-293.16*	113.45	.012	-519.73	-66.59
	8	-416.21*	134.80	.003	-685.42	-147.01
	9	-368.05*	101.10	.001	-569.95	-166.14
	10	-462.83*	113.45	.000	-689.40	-236.25
	11	-352.05*	101.10	.001	-553.95	-150.14
3	< 1	-172.56	102.95	.099	-378.16	33.05
	1	10.91	74.43	.884	-137.75	159.56
	2	110.08	70.15	.121	-30.02	250.17
	4	65.92	89.16	.462	-112.15	243.98
	5	27.66	76.35	.718	-124.82	180.15
	6	-15.47	102.95	.881	-221.08	190.14
	7	-183.08	115.10	.117	-412.96	46.80
	8	-306.19*	136.19	.028	-578.13	-34.14
	9	-257.97*	102.95	.015	-463.58	-52.36
	10	-352.75*	115.10	.003	-582.63	-122.87
	11	-241.97*	102.95	.022	-447.58	-36.36

Table 4-15. Continued.

Multiple Comparisons						
(I) Age (months)	(J) Age (months)	Mean Difference (I-J)	SE	<i>p</i>	95% Confidence Interval	
					Lower Bound	Upper Bound
4	< 1	-238.47*	115.10	.042	-468.35	-8.59
	1	-55.01	90.50	.545	-235.75	125.73
	2	44.16	87.01	.614	-129.61	217.93
	3	-65.92	89.16	.462	-243.98	112.15
	5	-38.26	92.08	.679	-222.16	145.65
	6	-81.39	115.10	.482	-311.27	148.49
	7	-249.00	126.09	.053	-500.82	2.82
	8	-372.06*	145.60	.013	-662.83	-81.28
	9	-323.89*	115.10	.006	-553.77	-94.01
	10	-418.67*	126.09	.001	-670.49	-166.85
	11	-307.89*	115.10	.009	-537.77	-78.01
5	< 1	-200.22	105.49	.062	-410.90	10.47
	1	-16.75	77.91	.830	-172.36	138.85
	2	82.41	73.83	.268	-65.04	229.86
	3	-27.66	76.35	.718	-180.15	124.82
	4	38.26	92.08	.679	-145.65	222.16
	6	-43.13	105.49	.684	-253.82	167.55
	7	-210.74	117.38	.077	-445.18	23.69
	8	-333.80*	138.12	.018	-609.65	-57.95
	9	-285.63*	105.49	.009	-496.32	-74.95
	10	-380.41*	117.38	.002	-614.84	-145.98
	11	-269.63*	105.49	.013	-480.32	-58.95
6	< 1	-157.08	126.09	.217	-408.90	94.74
	1	26.38	104.12	.801	-181.55	234.31
	2	125.55	101.10	.219	-76.36	327.45
	3	15.47	102.95	.881	-190.14	221.08
	4	81.39	115.10	.482	-148.49	311.27
	5	43.13	105.49	.684	-167.55	253.82
	7	-167.61	136.19	.223	-439.61	104.38
	8	-290.67	154.43	.064	-599.08	17.75
	9	-242.50	126.09	.059	-494.32	9.32
	10	-337.28*	136.19	.016	-609.27	-65.28
	11	-226.50	126.09	.077	-478.32	25.32
7	< 1	10.53	136.19	.939	-261.47	282.52
	1	193.99	116.15	.100	-37.97	425.95
	2	293.16*	113.45	.012	66.59	519.73
	3	183.08	115.10	.117	-46.80	412.96
	4	249.00	126.09	.053	-2.82	500.82
	5	210.74	117.38	.077	-23.69	445.18
	6	167.61	136.19	.223	-104.38	439.61
	8	-123.06	162.78	.452	-448.15	202.04
	9	-74.89	136.19	.584	-346.88	197.11
	10	-169.67	145.60	.248	-460.44	121.11
	11	-58.89	136.19	.667	-330.88	213.11

Table 4-15. Continued

Multiple Comparisons						
(I) Age (months)	(J) Age (months)	Mean Difference (I-J)	SE	p	95% Confidence Interval	
					Lower Bound	Upper Bound
8	< 1	133.58	154.43	.390	-174.83	442.00
	1	317.05*	137.07	.024	43.29	590.80
	2	416.21*	134.80	.003	147.01	685.42
	3	306.14*	136.19	.028	34.14	578.13
	4	372.06*	145.60	.013	81.28	662.83
	5	333.80*	138.12	.018	57.95	609.65
	6	290.67	154.43	.064	-17.75	599.08
	7	123.06	162.78	.452	-202.04	448.15
	9	48.17	154.43	.756	-260.25	356.58
	10	-46.61	162.78	.776	-371.71	278.49
	11	64.17	154.43	.679	-244.25	372.58
9	< 1	85.42	126.09	.501	-166.40	337.24
	1	268.88*	104.12	.012	60.95	476.81
	2	368.05*	101.10	.001	166.14	569.95
	3	257.97*	102.95	.015	52.36	463.58
	4	323.89*	115.10	.006	94.01	553.77
	5	285.63*	105.49	.009	74.95	496.32
	6	242.50	126.09	.059	-9.32	494.32
	7	74.89	136.19	.584	-197.11	346.88
	8	-48.17	154.43	.756	-356.58	260.25
	10	-94.78	136.19	.489	-366.77	177.22
	11	16.00	126.09	.899	-235.82	267.82
10	< 1	180.19	136.19	.190	-91.80	452.19
	1	363.66*	116.15	.003	131.70	595.62
	2	462.83*	113.45	.000	236.25	689.40
	3	352.75*	115.10	.003	122.87	582.63
	4	418.67*	126.09	.001	166.85	670.49
	5	380.41*	117.38	.002	145.98	614.84
	6	337.28*	136.19	.016	65.28	609.27
	7	169.67	145.60	.248	-121.11	460.44
	8	46.61	162.78	.776	-278.49	371.71
	9	94.78	136.19	.489	-177.22	366.77
	11	110.78	136.19	.419	-161.22	382.77
11	< 1	69.42	126.09	.584	-182.40	321.24
	1	252.88*	104.12	.018	44.95	460.81
	2	352.05*	101.10	.001	150.14	553.95
	3	241.97*	102.95	.022	36.36	447.58
	4	307.89*	115.10	.009	78.01	537.77
	5	269.63*	105.49	.013	58.95	480.32
	6	226.50	126.09	.077	-25.32	478.32
	7	58.89	136.19	.667	-213.11	330.88
	8	-64.17	154.43	.679	-372.58	244.25
	9	-16.00	126.09	.899	-267.82	235.82
	10	-110.78	136.19	.419	-382.77	161.22

\* The mean difference is significant at the 0.05 level.

indicated that mean SOS decreased significantly after the first month of life and did not begin to increase again until after the 5<sup>th</sup> month of life.

### **Term Infants**

Analyses were repeated using data from the term born infants to assess whether there were substantial differences between results calculated from the pooled data and those calculated using only the term infants. To determine if inclusion of the premature infants had a significant effect on age-specific mean SOS, age-specific SOS means from the pooled sample were compared with age-specific SOS means from the term born infants. A Shapiro-Wilk test indicated that the differences between pairs were normally distributed ( $W = 0.865, p = .056$ ). A paired t-test indicated a significant difference in age-specific SOS means based on the pooled data ( $M = 3009.63, SD = 213.46$ ) and data from the term born infants ( $M = 3042.40, SD = 196.93$ ) ( $t = -2.41, p = .035$ ). A box and whisker plot of the SOS data from the term born infants is provided in **Figure 4-29**.

An  $F$  test of the  $R^2$  change indicated that a cubic model was still the best fit for the relationship between age and SOS among term born infants ( $F(1, 53) = 8.14, p = .006$ ). The regression model predicting SOS from the age variables remained significant ( $R^2_{Adj} = .33, F(3, 53) = 10.20, p < .001$ ). Regression coefficients indicated that SOS initially decreased as age increased, but the relationship changed with increasing age as indicated by the significantly positive coefficient for age<sup>2</sup>. Larger age values were associated with greater SOS readings. The significant negative coefficient of age<sup>3</sup> indicated a second curvature in the regression line. The rate of increase in SOS begins to decrease at the largest age values. The model summary is presented in Model 2 of **Table 4-14**.

The one-way ANOVA and post hoc analyses were repeated using SOS data from term born infants to compare the results with those of the pooled data, which were reported above. An 8 month old infant was also removed from the analysis because it was the only infant in that age group. Differences between age groups continued to be significant after exclusion of premature infants ( $F(10, 45) = 2.54, p = .016$ ). Levene's test indicated equal variances between groups ( $F = 1.30, p = .262$ ). *LSD* post hoc tests indicated 1-2 month old infants had significantly lower mean SOS than infants aged 7 and 9-11 months ( $p < .05$ ). Infants ranging in age from 3-4 months had

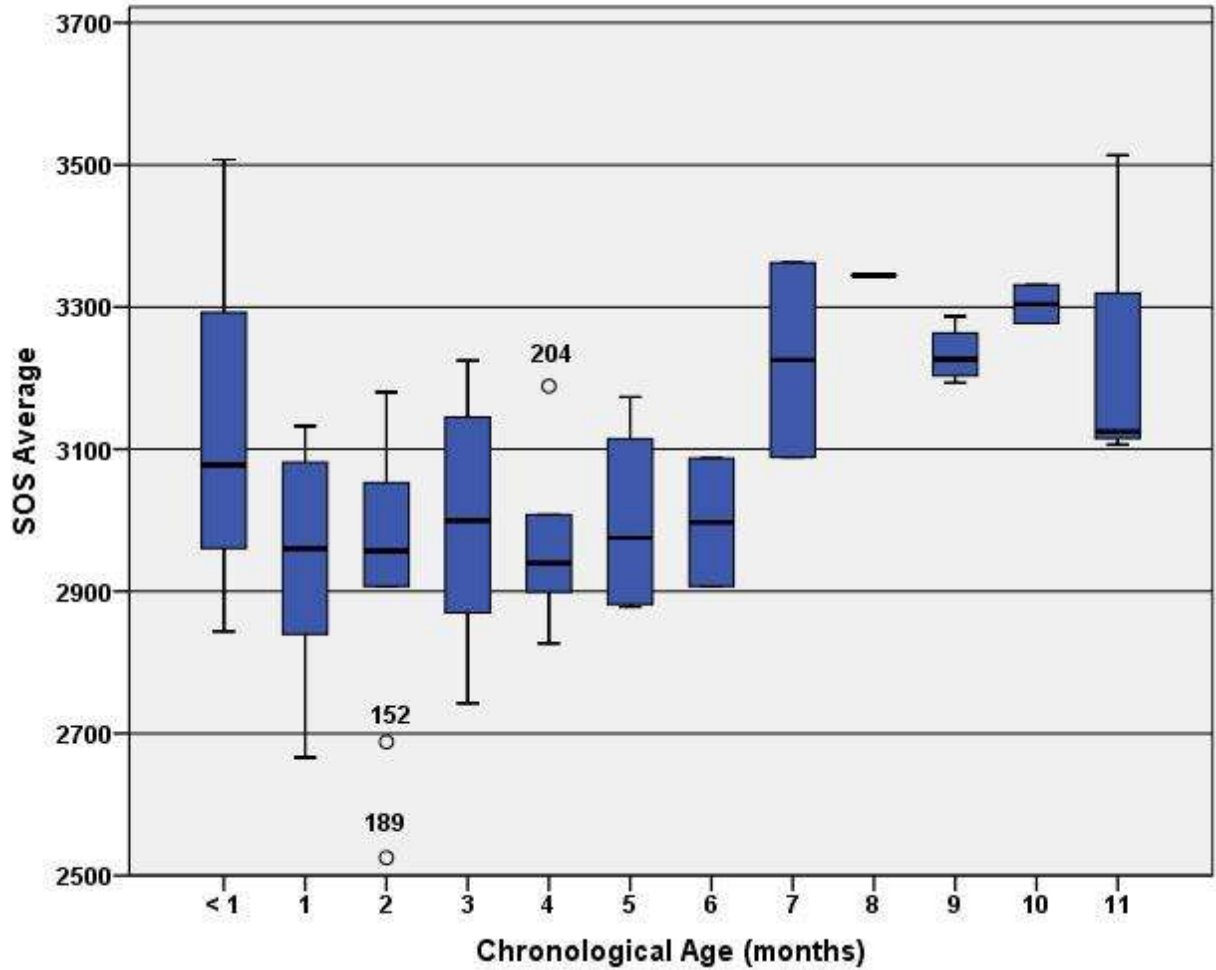


Figure 4-29. Box and whisker plot of SOS by chronological age in months with premature infants excluded. The circles represent outliers. Case ID # 204 is a trauma case. Case ID # 152 was a chronically ill infant. There was nothing remarkable in the case history of Case ID # 189.

significantly lower mean SOS than infants aged 9-11 months ( $p < .05$ ). Infants that were 5 months of age had significantly lower mean SOS than infants 9-10 months of age ( $p < .05$ ). Although the differences were insignificant, it should be noted that infants less than 1 month of age tended to have greater mean SOS than older infants until 7 months of age. These findings were similar to the post hoc analyses that included the premature infants. All post hoc comparisons are provided in **Table 4-16**.

### **Premature Infants**

To demonstrate the effect of prematurity on the regression estimates, separate Lowess-smoothed regression lines predicting average SOS from age were fitted to the term and premature data (**Figure 4-30**). Comparison of the plots in **Figure 4-28** and **Figure 4-30** suggests that the SOS data from the premature infants pulled down the curve fitted to the total sample. **Figure 4-30** demonstrates that the postnatal decrease in SOS was much more severe in premature infants than term infants and the subsequent gradual increase in SOS occurred later in premature infants than term infants. In addition, the shapes of the curves differed. The cubic model was the best fit for the regression line associated with the term infants. An  $F$  test of the  $R^2$  change indicated that a quadratic model was a better fit than a cubic or linear model for the regression line fitted to the data associated with the premature infants ( $F(1, 13) = 12.13, p = .004$ ). However, the shape difference may be related to the fewer number of premature infants in the older age categories relative to the term infants. Regression models for the term and premature infants are presented in Model 2, **Table 4-14** and **Table 4-17**, respectively. Results indicated that SOS was significantly related to age among both term and premature infants, but the pattern of age-related changes in SOS differed between term and premature infants. These findings also gave further support to hypothesis 4c, which stated that SOS was significantly related to skeletal maturity at birth.

### ***HYPOTHESIS 1C: BMD AND SOS ARE SIGNIFICANTLY RELATED TO BODY SIZE AND GROWTH PERCENTILES.***

#### ***BMD***

BMD was hypothesized to be positively related to body and growth percentiles because the measurement did not account for size differences. BMD was regressed against mean centered weight and weight for age percentile. There was no significant relationship between BMD and mean centered weight ( $F(1, 68) = 1.54, p = .220$ ), weight for age percentile ( $F(1, 67) = 0.01, p =$

**Table 4-16. LSD post hoc comparisons of SOS group means by age in months with premature infants excluded.**

Multiple Comparisons						
(I) Age (months)	(J) Age (months)	Mean Difference (I-J)	SE	<i>p</i>	95% Confidence Interval	
					Lower Bound	Upper Bound
< 1	1	197.57	116.30	.096	-36.68	431.82
	2	209.94	113.09	.070	-17.83	437.71
	3	138.88	113.09	.226	-88.89	366.65
	4	170.44	125.46	.181	-82.24	423.13
	5	143.11	121.48	.245	-101.55	387.78
	6	145.78	156.82	.358	-170.08	461.64
	7	-82.72	156.82	.600	-398.58	233.14
	9	-90.56	131.21	.494	-354.82	173.71
	10	-161.22	156.82	.309	-477.08	154.64
	11	-74.56	131.21	.573	-338.82	189.71
	1	< 1	-197.57	116.30	.096	-431.82
2		12.37	81.49	.880	-151.75	176.50
3		-58.69	81.49	.475	-222.82	105.43
4		-27.13	97.94	.783	-224.38	170.13
5		-54.46	92.78	.560	-241.32	132.41
6		-51.79	135.81	.705	-325.33	221.75
7		-280.29*	135.81	.045	-553.83	-6.75
9		-288.13*	105.20	.009	-500.01	-76.24
10		-358.79*	135.81	.011	-632.33	-85.25
11		-272.13*	105.20	.013	-484.01	-60.24
2		< 1	-209.94	113.09	.070	-437.71
	1	-12.37	81.49	.880	-176.50	151.75
	3	-71.07	76.83	.360	-225.81	83.67
	4	-39.50	94.09	.677	-229.02	150.02
	5	-66.83	88.71	.455	-245.51	111.84
	6	-64.17	133.07	.632	-332.18	203.85
	7	-292.67*	133.07	.033	-560.68	-24.65
	9	-300.50*	101.63	.005	-505.20	-95.80
	10	-371.17*	133.07	.008	-639.18	-103.15
	11	-284.50*	101.63	.008	-489.20	-79.80
	3	< 1	-138.88	113.09	.226	-366.65
1		58.69	81.49	.475	-105.43	222.82
2		71.07	76.83	.360	-83.67	225.81
4		31.57	94.09	.739	-157.95	221.08
5		4.23	88.71	.962	-174.44	182.91
6		6.90	133.07	.959	-261.12	274.92
7		-221.60	133.07	.103	-489.62	46.42
9		-229.43*	101.63	.029	-434.13	-24.73
10		-300.10*	133.07	.029	-568.12	-32.08
11		-213.43*	101.63	.041	-418.13	-8.73

Table 4-16. Continued.

Multiple Comparisons						
(I) Age (months)	(J) Age (months)	Mean Difference (I-J)	SE	<i>p</i>	95% Confidence Interval	
					Lower Bound	Upper Bound
4	< 1	-170.44	125.46	.181	-423.13	82.24
	1	27.13	97.94	.783	-170.13	224.38
	2	39.50	94.09	.677	-150.02	229.02
	3	-31.57	94.09	.739	-221.08	157.95
	5	-27.33	104.03	.794	-236.85	182.18
	6	-24.67	143.73	.865	-314.16	264.82
	7	-253.17	143.73	.085	-542.66	36.32
	9	-261.00*	115.24	.028	-493.11	-28.89
	10	-331.67*	143.73	.026	-621.16	-42.18
	11	-245.00*	115.24	.039	-477.11	-12.89
5	< 1	-143.11	121.48	.245	-387.78	101.55
	1	54.46	92.78	.560	-132.41	241.32
	2	66.83	88.71	.455	-111.84	245.51
	3	-4.23	88.71	.962	-182.91	174.44
	4	27.33	104.03	.794	-182.18	236.85
	6	2.67	140.27	.985	-279.85	285.18
	7	-225.83	140.27	.114	-508.35	56.68
	9	-233.67*	110.89	.041	-457.01	-10.32
	10	-304.33*	140.27	.035	-586.85	-21.82
	11	-217.67	110.89	.056	-441.01	5.68
6	< 1	-145.78	156.82	.358	-461.64	170.08
	1	51.79	135.81	.705	-221.75	325.33
	2	64.17	133.07	.632	-203.85	332.18
	3	-6.90	133.07	.959	-274.92	261.12
	4	24.67	143.73	.865	-264.82	314.16
	5	-2.67	140.27	.985	-285.18	279.85
	7	-228.50	171.79	.190	-574.51	117.51
	9	-236.33	148.78	.119	-535.98	63.32
	10	-307.00	171.79	.081	-653.01	39.01
	11	-220.33	148.78	.146	-519.98	79.32
7	< 1	82.72	156.82	.600	-233.14	398.58
	1	280.29*	135.81	.045	6.75	553.83
	2	292.67*	133.07	.033	24.65	560.68
	3	221.60	133.07	.103	-46.42	489.62
	4	253.17	143.73	.085	-36.32	542.66
	5	225.83	140.27	.114	-56.68	508.35
	6	228.50	171.79	.190	-117.51	574.51
	9	-7.83	148.78	.958	-307.48	291.82
	10	-78.50	171.79	.650	-424.51	267.51
	11	8.17	148.78	.956	-291.48	307.82



Table 4-16. Continued.

Multiple Comparisons						
(I) Age (months)	(J) Age (months)	Mean Difference (I-J)	SE	<i>p</i>	95% Confidence Interval	
					Lower Bound	Upper Bound
9	< 1	90.56	131.21	.494	-173.71	354.82
	1	288.13*	105.20	.009	76.24	500.01
	2	300.50*	101.63	.005	95.80	505.20
	3	229.43*	101.63	.029	24.73	434.13
	4	261.00*	115.24	.028	28.89	493.11
	5	233.67*	110.89	.041	10.32	457.01
	6	236.33	148.78	.119	-63.32	535.98
	7	7.83	148.78	.958	-291.82	307.48
	10	-70.67	148.78	.637	-370.32	228.98
	11	16.00	121.48	.896	-228.66	260.66
10	< 1	161.22	156.82	.309	-154.64	477.08
	1	358.79*	135.81	.011	85.25	632.33
	2	371.17*	133.07	.008	103.15	639.18
	3	300.10*	133.07	.029	32.08	568.12
	4	331.67*	143.73	.026	42.18	621.16
	5	304.33*	140.27	.035	21.82	586.85
	6	307.00	171.79	.081	-39.01	653.01
	7	78.50	171.79	.650	-267.51	424.51
	9	70.67	148.78	.637	-228.98	370.32
	11	86.67	148.78	.563	-212.98	386.32
11	< 1	74.56	131.21	.573	-189.71	338.82
	1	272.13*	105.20	.013	60.24	484.01
	2	284.50*	101.63	.008	79.80	489.20
	3	213.43*	101.63	.041	8.73	418.13
	4	245.00*	115.24	.039	12.89	477.11
	5	217.67	110.89	.056	-5.68	441.01
	6	220.33	148.78	.146	-79.32	519.98
	7	-8.17	148.78	.956	-307.82	291.48
	9	-16.00	121.48	.896	-260.66	228.66
	10	-86.67	148.78	.563	-386.32	212.98

\*. The mean difference is significant at the .05 level.

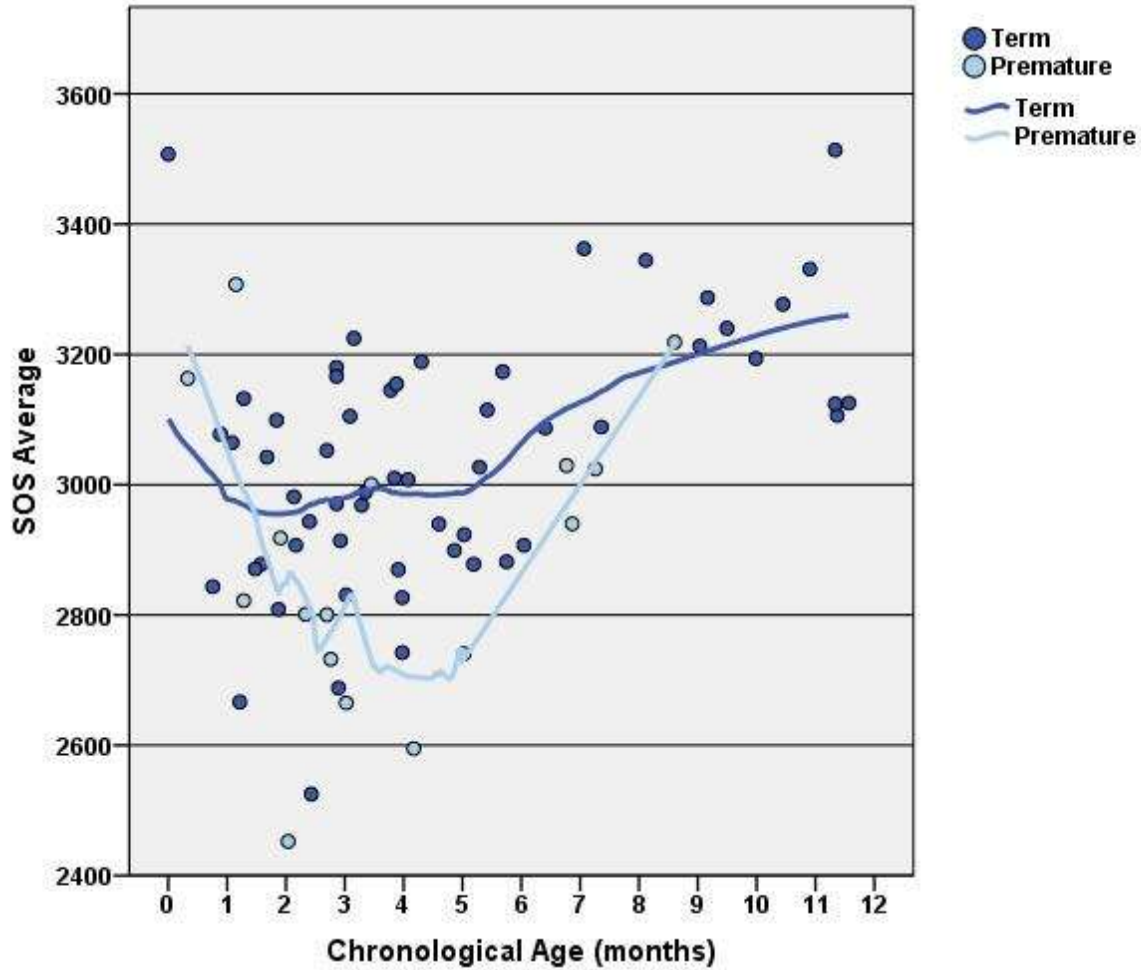


Figure 4-30. Plot of SOS readings against age in months with a separate Lowess-smoothed regression lines for premature and term infants. Dark blue circles with dark blue dashed Lowess-smoothed regression line represent SOS data from term born infants. Light blue circles with light blue dashed Lowess-smoothed regression line represent SOS data from premature infants.

Table 4-17. Model summary for regression analysis of premature infant data with SOS as the dependent variable and using age as the predictor variable.

Model	Unstandardized Coefficients		<i>t</i>	<i>p</i>	<i>F</i>	<i>df</i>	<i>p</i>	Adj. <i>R</i> <sup>2</sup>
	<i>b</i>	<i>SE</i>						
					6.56	2,13	.011	.43
(Constant)	3225.53	141.96	22.72	<.001				
Age	-248.01	78.62	-3.15	.008				
Age <sup>2</sup>	29.87	8.58	3.48	.004				

.925), or weight for length percentile ( $F(1, 65) = 1.77, p = .189$ ). BMD was regressed against mean centered leg circumference. There was no significant relationship between BMD and leg circumference ( $F(1, 68) = 1.84, p = .180$ ). BMD was regressed against mean centered height and length for age percentile. There was no significant relationship between BMD and mean centered height ( $F(1, 68) = 0.89, p = .359$ ) or length for age percentile ( $F(1, 67) = 0.63, p = .432$ ). These results did not support the hypothesis of a positive relationship between BMD and body size.

### **Chronically Ill Infants Excluded**

Analyses were repeated with chronically ill infants excluded to evaluate if the presence of chronically ill infants in the analyses affected the previously reported results. There was still no significant relationship between BMD and mean centered weight ( $F(1, 56) = 1.98, p = .165$ ), weight for age percentile ( $F(1, 55) = 0.004E-1, p = .985$ ), weight for length percentile ( $F(1, 54) = 0.50, p = .484$ ), mean centered leg circumference ( $F(1, 56) = 2.64, p = .110$ ), mean centered height ( $F(1, 56) = 1.99, p = .164$ ), or length for age percentile ( $F(1, 55) = 0.12, p = .732$ ), which did not support the hypothesis.

### **SOS**

SOS was hypothesized to be positively associated with body size. To determine if body size was a significant predictor of SOS after accounting for age-related differences in body size, models predicting SOS using age, age<sup>2</sup>, and age<sup>3</sup> as covariates and the variables related to body size as independent variables. Age was not used as a covariate in models using growth percentiles as predictor variables of SOS. Models predicting SOS using the age variables as covariates and weight ( $R^2_{Adj.} = .40, F(4, 72) = 13.74, p < .001$ ), leg circumference ( $R^2_{Adj.} = .39, F(4, 72) = 12.89, p < .001$ ), height ( $R^2_{Adj.} = .44, F(4, 72) = 15.79, p < .001$ ) were significant. Models predicting SOS using weight for age percentile ( $R^2_{Adj.} = .11, F(1, 74) = 10.32, p = .002$ ) and length for age percentile ( $R^2_{Adj.} = .07, F(1, 74) = 6.71, p = .012$ ) were significant. Model summaries for models with significant body size variables are presented in **Table 4-18**. The regression coefficient for weight was significant ( $p = .011$ ) and indicated that, while holding age constant, SOS increased by 33 m/s for every 1kg increase in weight ( $b = 32.93, 95\% \text{ CI } [7.73, 58.13]$ ). The regression coefficient for leg circumference was significant ( $p = .034$ ) and indicated that, while holding age constant, SOS increased by 2 m/s for every 1 mm increase in leg circumference ( $b = 2.29, 95\% \text{ CI } [0.18, 4.40]$ ). The regression coefficient for weight for age percentile was significant ( $p =$

**Table 4-18. Model summaries of regression analyses with SOS as the dependent variable.**

Model	Unstandardized Coefficients		<i>t</i>	<i>p</i>	<i>F</i>	<i>df</i>	<i>p</i>	Adj. <i>R</i> <sup>2</sup>
	<i>b</i>	<i>SE</i>						
<b>1</b>					13.74	4,72	<.001	.40
	(Constant)	3126.87	91.69	34.10	<.001			
	Age	-273.22	62.25	-4.39	<.001			
	Age <sup>2</sup>	51.51	12.30	4.19	<.001			
	Age <sup>3</sup>	-2.56	0.70	-3.67	<.001			
	Weight	32.93	12.64	2.61	.011			
<b>2</b>					10.32	1,74	.002	.11
	(Constant)	2926.19	34.72	84.27	<.001			
	Weight for Age Percentile	2.10	0.66	3.21	.002			
<b>3</b>					15.79	4,72	<.001	.44
	(Constant)	2565.81	207.23	12.38	<.001			
	Age	-279.59	60.01	-4.66	<.001			
	Age <sup>2</sup>	50.87	11.88	4.28	<.001			
	Age <sup>3</sup>	-2.52	0.68	-3.74	<.001			
	Height	13.19	3.83	3.45	.001			
<b>4</b>					6.71	1,74	.012	.07
	(Constant)	2937.36	36.48	80.52	<.001			
	Length for Age Percentile	1.73	0.67	2.59	.012			
<b>5</b>					12.89	4,72	<.001	.39
	(Constant)	2984.08	139.38	21.41	<.001			
	Age	-270.57	63.53	-4.26	<.001			
	Age <sup>2</sup>	51.86	12.52	4.14	<.001			
	Age <sup>3</sup>	-2.57	0.71	-3.62	.001			
	Leg Circ. <sup>a</sup>	2.29	1.06	2.16	.034			

a. Leg Circ.= Leg Circumference

.002) and indicated that for every 1 percentile point increase in weight for age percentile SOS increased by 2 m/s ( $b = 2.10$ , 95% CI [0.80, 3.41]). The regression coefficient for height was significant ( $p = .001$ ) and indicated that, while holding age constant, SOS increased by ~13 m/s with every 1 cm increase in height ( $b = 13.19$ , 95% CI [5.56, 20.82]). The regression coefficient for length for age percentile was significant ( $p = .012$ ) and indicated that SOS increased by ~2 m/s for every 1 percentile point increase in length for age percentile ( $b = 1.73$ , 95% CI [0.40, 3.06]). Weight for length percentile was not a significant predictor of SOS ( $F(1, 72) = 0.06$ ,  $p = .816$ ). These results support the hypothesis that SOS is significantly positively related body size, even after accounting for body size differences due to age.

### **Chronically Ill Infants Excluded**

After chronically ill infants were removed from analyses, models predicting SOS from weight for age percentile ( $R^2_{Adj.} = .10$ ,  $F(1, 61) = 7.60$ ,  $p = .008$ ) and length for age percentile ( $R^2_{Adj.} = .06$ ,  $F(1, 61) = 5.18$ ,  $p = .026$ ) remained significant. The regression coefficient for weight for age percentile indicated that SOS increased by 2 m/s with every 1 percentile point increase in weight for age percentile ( $b = 2.02$ , 95% CI [0.55, 3.49]). The regression coefficient for length for age percentile indicated that SOS increased by ~2 m/s with every 1 percentile point increase in length for age percentile ( $b = 1.68$ , 95% CI [0.20, 3.16]). The model predicting SOS from height and using the age variables as covariates was significant ( $R^2_{Adj.} = .43$ ,  $F(4, 59) = 12.95$ ,  $p < .001$ ). Height was a significant predictor in the model ( $p = .011$ ) and the regression coefficient indicated that, while holding age constant, SOS increased by ~12 m/s with every 1 cm increase in height ( $b = 12.58$ , 95% CI [2.95, 22.21]). Weight ( $p = .077$ ) and leg circumference ( $p = .127$ ) were no longer a significant predictors of SOS after chronically ill infants were excluded from analyses. Weight for length percentile remained an insignificant predictor of SOS after chronically ill infants were excluded from the analysis ( $p = .767$ ). Model summaries for models with statistically significant body size predictor variables are presented in **Table 4-19**. Although weight was no longer a significant predictor of SOS after chronically ill infants were excluded from analyses, these results continued to support the hypothesis that SOS was significantly positively associated with body size.

**Table 4-19. Model summaries for regression analyses with SOS as the dependent variable and chronically ill infants excluded from analyses.**

Model	Unstandardized Coefficients		<i>t</i>	<i>p</i>	<i>F</i>	<i>df</i>	<i>p</i>	Adj. <i>R</i> <sup>2</sup>
	<i>b</i>	<i>SE</i>						
1					7.60	1,61	.008	.10
	(Constant)	2936.42	39.21	74.89	<.001			
	Weight for age Percentile	2.02	0.73	2.76	.008			
2					12.95	4,59	<.001	.43
	(Constant)	2553.12	261.61	9.76	<.001			
	Age	-257.23	68.43	-3.76	<.001			
	Age <sup>2</sup>	49.05	13.35	3.67	.001			
	Age <sup>3</sup>	-2.49	0.75	-3.32	.002			
	Height	12.58	4.81	2.62	.011			
3					5.18	1,61	.026	.06
	(Constant)	2943.51	41.96	70.16	<.001			
	Length for age Percentile	1.68	0.74	2.28	.026			

### **Term Infants**

Analyses were repeated with premature infants excluded from analyses to evaluate whether the significant association between SOS and body size was being driven by the premature infants in the study sample. Among term born infants, weight while accounting for age ( $p = .556$ ), height while accounting for age ( $p = .276$ ), leg circumference ( $p = .579$ ), weight for age percentile ( $p = .354$ ), weight for length percentile ( $p = .932$ ), and length for age percentile ( $p = .521$ ) were not significant predictors of SOS. These findings indicated that SOS was significantly positively associated with body size among premature infants, but not among term born infants, partially supporting the hypothesis. These findings also gave further support to hypothesis 4c, which stated that SOS was significantly related to skeletal maturity at birth.

### ***HYPOTHESIS 1D: BMD AND SOS ARE SIGNIFICANTLY RELATED TO TIBIAL STRUCTURE.***

#### ***BMD***

BMD was hypothesized to have a significant positive relationship with cortical thickness and cortical index, and a significant negative relationship with medullary cavity diameter. The tibial measurements were regressed on BMD to evaluate the relationship between BMD and tibial structure. There was no significant relationship between BMD and mean centered tibial length

( $F(1, 68) = 0.92, p = .341$ ), mean centered midshaft diameter ( $F(1, 68) = 0.41, p = .525$ ), mean centered medullary cavity diameter ( $F(1, 68) = 2.32, p = .133$ ), or mean centered cortical thickness ( $F(1, 68) = 0.23, p = .634$ ). There was a significant relationship between BMD and cortical index ( $R^2_{Adj.} = .05, F(1, 68) = 4.22, p = .044$ ). The regression coefficient for cortical index indicated that BMD increased as cortical index increased ( $b = 0.97, 95\% \text{ CI } [0.03, 1.91]$ ). The model summary is presented in **Table 4-20**. The significant relationship between BMD and cortical index provided partial support for the hypothesis that BMD was positively associated with tibial structure.

### **Chronically Ill Infants Excluded**

Chronically ill infants were excluded from analyses to evaluate whether inclusion of the chronically ill infants in the above analyses affected results. The relationships between BMD and mean centered tibial length ( $F(1, 56) = 2.37, p = .129$ ), centered midshaft diameter ( $F(1, 56) = 1.89, p = .175$ ), mean centered medullary cavity diameter ( $F(1, 56) = 2.19, p = .144$ ), and mean centered cortical thickness ( $F(1, 56) = 0.40, p = .532$ ) remained insignificant. Cortical index was no longer a significant predictor of BMD after chronically ill infants were excluded from the analysis ( $F(1, 56) = 1.48, p = .229$ ). These findings suggested that BMD was significantly positively associated with cortical index among chronically ill infants, but not among the infants without chronic illness. Although these findings did not support the hypothesis that BMD is significantly associated with tibial structure, these findings did lend support to hypothesis 3c. Hypothesis 3c stated that chronic illness was significantly related to measures of infant bone health.

### **SOS**

SOS was hypothesized to have a significant negative relationship with medullary cavity diameter and a significant positive relationship with cortical thickness and cortical index. ANOVA and regression analyses were conducted the SOS data using age as a covariate and the tibial measurements as predictor variables. Tibial length ( $p = .495$ ), midshaft diameter ( $p = .205$ ), and cortical thickness ( $p = .884$ ) were insignificant predictors of SOS after accounting for age. After accounting for age, medullary cavity diameter had a significant negative relationship with SOS ( $R^2_{Adj.} = .23, F(2, 74) = 12.61, p < .001$ ). The regression coefficient for medullary cavity diameter indicated that SOS decreased by 70 m/s with every 1 mm increase in medullary cavity

**Table 4-20. Model summary of regression analysis predicting BMD using cortical index.**

Model	Unstandardized Coefficients		<i>t</i>	<i>p</i>	<i>F</i>	<i>df</i>	<i>p</i>	Adj. <i>R</i> <sup>2</sup>
	<i>b</i>	<i>SE</i>						
					4.22	1,68	.044	.05
(Constant)	0.37	0.26	1.46	.148				
Cortical Index	0.97	0.47	2.05	.044				

diameter ( $b = -70.00$ , 95% CI [-133.80, -6.19]). After accounting for age, cortical index had a significant positive relationship with SOS ( $R^2_{Adj.} = .23$ ,  $F(2, 74) = 12.18$ ,  $p < .001$ ). The regression coefficient for cortical index indicated that with every .01 increase in cortical index SOS increased by ~6 m/s ( $b = 553.04$ , 95% CI [9.41, 1096.67]). Model summaries of statistically models predicting SOS using age as a covariate and statistically significant tibial measurements as predictor variables are presented in **Table 4-21**. These results supported the hypothesis that SOS was significantly related to tibial structure.

### **Chronically Ill Infants Excluded**

Chronically ill infants were excluded from analyses to determine whether inclusion of chronically ill infants in previous analyses resulted in the significant findings. After controlling for age and removing the chronically ill infants removed from analyses, tibial length ( $p = .839$ ), midshaft diameter ( $p = .252$ ), and cortical thickness ( $p = .803$ ) remained insignificant predictors of SOS. Medullary cavity diameter ( $p = .056$ ) and cortical index ( $p = .097$ ) became insignificant predictors of SOS after removing chronically ill infants from the analyses, which did not support the hypothesis that SOS was significantly associated with tibial structure among infants without chronic illness. Although these findings did not support the hypothesis, these results did support hypothesis 3c which stated that chronic illness was significantly associated with measures of infant bone health such as SOS.

### **Term Infants**

Analyses were repeated with only the term infants included in analyses to evaluate whether the inclusion of the premature infants substantially altered results. After controlling for age and removing the premature infants from the analyses, tibial length ( $p = .110$ ) and cortical thickness ( $p = .395$ ) remained insignificant predictors of SOS. Midshaft diameter became a significant



**Table 4-21. Model summaries of regression analyses with SOS as the dependent variable, age as a covariate, and tibial measurements as independent variables.**

Model	Unstandardized Coefficients		<i>t</i>	<i>p</i>	<i>F</i>	<i>df</i>	<i>p</i>	Adj. <i>R</i> <sup>2</sup>
	<i>b</i>	<i>SE</i>						
1					12.61	2,74	< .001	.23
	(Constant)	3031.37	85.88	35.30	<.001			
	Age	46.66	9.81	4.76	<.001			
	Medullary Cavity Diameter	-70.00	32.02	-2.19	.032			
2					12.18	2,74	< .001	.23
	(Constant)	2543.75	162.57	15.65	<.001			
	Age	37.19	7.54	4.93	<.001			
	Cortical Index	553.04	272.83	2.03	.046			

predictor of SOS ( $R^2_{Adj} = .29$ ,  $F(2, 54) = 12.54$ ,  $p < .001$ ). The regression coefficient for midshaft diameter indicated that, while holding age constant, SOS decreased by ~64 m/s with every 1 mm increase in midshaft diameter ( $b = -63.90$ , 95% CI [-112.95, -14.84]). A model predicting SOS using age and medullary cavity diameter was significant ( $R^2_{Adj} = .29$ ,  $F(2, 54) = 12.43$ ,  $p < .001$ ). The regression coefficient for medullary cavity diameter indicated that SOS decreased by ~88 m/s with every 1 mm increase in medullary cavity diameter while holding age constant ( $b = -88.41$ , 95% CI [-157.12, -19.70]). Cortical index was an insignificant predictors of SOS among term infants after removing premature infants from the analysis ( $p = .187$ ). The model summaries for statistically significant models are presented in **Table 4-22**. Although cortical thickness and cortical index were not significantly predictors of SOS after accounting for age, midshaft diameter and medullary cavity diameter were significant predictors of SOS among term infants. These findings support the hypothesis that SOS is significantly associated with tibial structure.

### **Multiple Regression Analyses**

Multiple regression analyses were conducted to assess which combination of variables best predicted SOS. The following variables were entered into the regression models as possible predictors: age, birthweight or EGA, height or length for age percentile, weight or weight for age percentile, cortical index, cortical thickness, medullary cavity diameter, and midshaft diameter. Stepwise variable selection was conducted. A variable was entered into the model if the

**Table 4-22. Model summaries for regression analyses with SOS as the dependent variable and premature infants excluded from analyses.**

Model	Unstandardized Coefficients		<i>t</i>	<i>p</i>	<i>F</i>	<i>df</i>	<i>p</i>	Adj. <i>R</i> <sup>2</sup>
	<i>b</i>	<i>SE</i>						
1					12.54	2,54	<.001	.29
	(Constant)	3295.31	155.65	21.17	<.001			
	Age	47.43	9.72	4.88	<.001			
	Midshaft Diameter	-63.90	27.47	-2.61	.012			
2					12.43	2,54	<.001	.29
	(Constant)	3129.58	96.61	32.40	<.001			
	Age	46.95	9.65	4.87	<.001			
	Medullary Cavity Diameter	-88.41	34.27	-2.58	.013			

significance level of its *F* value was < .05 and was removed from the model if the significance level was > .10. Although multiple models were produced, only the model accounting for the greatest amount of variance in SOS is presented here. The model accounting for the greatest amount of variance in SOS included age ( $b = 45.77$ , 95% CI [22.39, 69.16]), birthweight ( $b = 92.97$ , 95% CI [29.58, 156.35]), height ( $b = 11.47$ , 95% CI [1.41, 21.53]), cortical index ( $b = 4106.72$ , 95% CI [1623.99, 6589.46]), midshaft diameter ( $b = -328.75$ , 95% CI [-493.34, -164.16]), and medullary cavity diameter ( $b = 486.615$ , 95% CI [138.41, 834.80]). The parameter estimates in the model indicate that as age increased by 1 month SOS increased by ~46 m/s, holding all other variables in the model constant. Holding all other variables in the model constant, a 1 kg increase in birthweight was associated with an increase in SOS by ~93 m/s and a 1 cm increase in height was associated with an increase in SOS by ~11 m/s. An increase in cortical index of .01 was associated with an increase in SOS by ~41 m/s. A 1 mm increase in midshaft diameter was associated with a ~ 329 m/s decrease in SOS and 1 mm increase in medullary cavity diameter was associated with a ~487 m/s increase in SOS, also holding all other variables in the model constant. This model accounted for ~53% of the variance in SOS ( $R^2_{Adj.} = .53$ ,  $F(6, 63) = 13.89$ ,  $p < .001$ ). The model summary is provided in **Table 4-23**. These findings supported hypotheses 1b, 1c, 1d, and 4c. For the pooled sample, SOS was significantly related to age, body size, skeletal maturity at birth, and tibial structure.

**Table 4-23. Summary of multiple regression results with SOS as the dependent variable.**

Model	Unstandardized Coefficients		<i>t</i>	<i>p</i>	<i>F</i>	<i>df</i>	<i>p</i>	Adj. <i>R</i> <sup>2</sup>
	<i>b</i>	<i>SE</i>						
					13.89	6,63	<.001	.53
(Constant)	370.56	668.56	0.55	.581				
Age	45.77	11.70	3.91	.000				
Birthweight (kg)	92.97	31.72	2.93	.005				
Height	11.47	5.03	2.28	.026				
Cortical Index	4106.72	1242.40	3.31	.002				
Midshaft Diameter	-328.75	82.36	-3.99	.000				
Medullary Cavity Diameter	486.61	174.24	2.79	.007				

### **Chronically Ill Infants Excluded**

To assess the effect of chronic illness on the regression model predicting SOS, the multiple regression analysis was repeated with the chronic illness infants excluded from the analysis. The following variables were entered into the regression models as possible predictors: age, birthweight or EGA, height or length for age percentile, weight or weight for age percentile, cortical index, cortical thickness, medullary cavity diameter, and midshaft diameter. Stepwise variable selection was conducted. A variable was entered into the model if the significance level of its *F* value was < .05 and was removed from the model if the significance level was > .10. Age, birthweight, and medullary cavity diameter were selected by stepwise variable selection as the significant predictors of SOS. The model summary is presented in **Table 4-24**. After excluding chronically ill infants, continued to support the hypotheses that SOS was significantly related to age, skeletal maturity at birth, and tibial structure.

### **Term Infants**

Multiple regression analyses were repeated with premature infants excluded to assess whether the regression model constructed from the term infant data substantially differed from the model constructed from the pooled sample data. The following variables were entered into the regression models as possible predictors: age, birthweight or EGA, height or length for age percentile, weight or weight for age percentile, cortical index, cortical thickness, medullary cavity diameter, and midshaft diameter. Stepwise variable selection was conducted. A variable was entered into the model if the significance level of its *F* value was < .05 and was removed

**Table 4-24. Summary of multiple regression results with SOS as the dependent variable and chronically ill infants excluded from the analysis.**

Model	Unstandardized Coefficients		<i>t</i>	<i>p</i>	<i>F</i>	<i>df</i>	<i>p</i>	Adj. <i>R</i> <sup>2</sup>
	<i>b</i>	<i>SE</i>						
					13.63	3,56	<.001	.39
(Constant)	2737.35	125.82	21.76	<.001				
Age	52.91	9.71	5.45	<.001				
Birthweight (kg)	120.56	35.56	3.39	.001				
Medullary Cavity Diameter	-92.46	9.71	-2.89	.006				

from the model if the significance level was  $> .10$ . Age and medullary cavity diameter were chosen by stepwise variable selection as the significant predictors of SOS. The summary of the model is presented in **Table 4-25**. For term infants, results supported the hypotheses that SOS was significantly related to age and tibial structure.

### **Association between Traumatic Injury, Health, and Bone Health**

#### ***HYPOTHESIS 2: THE PRESENCE OF TRAUMATIC INJURY IS NOT ASSOCIATED WITH INDICATORS OF OVERALL HEALTH, BODY SIZE, OR BONE HEALTH.***

Chi-Square and ANOVA tests were performed to determine whether there was a significant association between traumatic injury and the indicators of overall health, such as chronic illness and prematurity. Descriptions of chronic illnesses associated with each infant were previously provided in **Table 4-3**. Descriptions of infants with traumatic injury and associated data are provided in **Table A- 3** of the Appendix. A Fisher’s exact test was used to test for significant associations between traumatic injury and prematurity, as well as traumatic injury and chronic illness, since there were no cases of premature infants with traumatic injury or chronically ill infants with traumatic injury. There was no significant association between the presence of traumatic injury and prematurity ( $p = .185$ ) or traumatic injury and chronic illness ( $p = .342$ ), supporting the hypothesis that the presence of traumatic injury was not associated with overall health.

One way ANOVAs were conducted to evaluate whether there were significant differences in body size or growth percentiles between infants with and without traumatic injury. Variances in

**Table 4-25. Summary of multiple regression results with SOS as the dependent variable and premature infants excluded from the analysis.**

Model	Unstandardized Coefficients		<i>t</i>	<i>p</i>	<i>F</i>	<i>df</i>	<i>p</i>	Adj. <i>R</i> <sup>2</sup>
	<i>b</i>	<i>SE</i>						
					11.46	5,51	<.001	.28
(Constant)	3133.25	96.80	32.37	<.001				
Age	45.63	9.77	4.67	<.001				
Medullary Cavity Diameter	-87.17	34.69	-2.51	.005				

height ( $F = 1.55, p = .217$ ), weight ( $F = 0.53, p = .470$ ), length for age percentile ( $F = 1.03, p = .313$ ), weight for age percentile ( $F = 0.43, p = .513$ ), and weight for length percentile ( $F = 0.07, p = .790$ ) were equal across groups based on the presence/absence of traumatic injury. There was a significant difference in height between infants with and without traumatic injury, but it should be noted that the  $p$  value was only on the borderline of significance significant ( $F(1, 76) = 4.13, p = .046$ ). There were no significant associations between traumatic injury and length for age percentile ( $F(1, 75) = 1.48, p = .228$ ), weight ( $F(1, 76) = 2.72, p = .103$ ), weight for age percentile ( $F(1, 75) = 0.61, p = .436$ ), and weight for length percentile ( $F(1, 73) = 0.12, p = .731$ ) between infants with and without traumatic injury, which supported the hypothesis that there was no association between body size and traumatic injury.

One-way ANOVAs were conducted to evaluate whether there were significant differences in the bone health indicators based on the presence on traumatic injury. Radiographic evaluation score was not significantly associated with traumatic injury ( $U = 289.5, p = .612$ ). Variances in BMD between groups was equal ( $F = 1.10, p = .298$ ). No significant difference in BMD was found between infants with and without traumatic injury ( $F(1, 68) = 0.09, p = .770$ ). There were no statistically significant differences in SOS based on the presence of traumatic injury ( $F(1, 75) = 2.82, p = .097$ ). These findings supported the hypothesis that traumatic injury was not associated with indicators of bone health.

## Association between Chronic Illness, Growth, and Bone Health

### ***HYPOTHESIS 3A: CHRONIC ILLNESS IS NEGATIVELY ASSOCIATED WITH VARIABLES RELATED TO BODY SIZE.***

One-way ANOVAs were conducted to evaluate the relationship between chronic illness and body size/growth. Levene's test of homogeneity of variances indicated the variances in weight ( $F = 0.08, p = .783$ ), height ( $F = 0.94, p = .335$ ), weight for age percentile ( $F = 1.23, p = .272$ ), length for age percentile ( $F = 0.63, p = .429$ ), and weight for length percentile ( $F = 0.05, p = .824$ ) were equal across infants with and without chronic illness. There were no significant differences in weight ( $F(1, 76) = 0.86, p = .357$ ), height ( $F(1, 76) = 2.17, p = .145$ ), weight for age percentile ( $F(1, 75) = 0.36, p = .549$ ), length for age percentile ( $F(1, 75) = 2.61, p = .111$ ), and weight for length percentile ( $F(1, 73) = 0.71, p = .403$ ) based on chronic illness. Analyses indicated no significant relationship between chronic illness and body size.

### ***HYPOTHESIS 3B: CHRONIC ILLNESS IS NEGATIVELY ASSOCIATED WITH TIBIAL GROWTH.***

To determine if chronic illness significantly influenced growth of the tibia, models predicting the tibial measurements were conducted with age as a covariate and chronic illness as a predictor variable. Descriptive statistics of the tibial measurements are presented in **Table A- 6** of the Appendix. Analyses of the relationships between the tibial measurements and age are presented in more detail later in this chapter. Chronic illness had a significant effect on tibial length ( $R^2_{Adj.} = .76, F(2, 74) = 121.74, p < .001$ ), midshaft diameter ( $R^2_{Adj.} = .53, F(2, 74) = 43.78, p < .001$ ), and cortical thickness ( $R^2_{Adj.} = .21, F(2, 74) = 10.86, p < .001$ ) after accounting for age differences. The regression coefficients for chronic illness indicated that tibial length decreased by 6.17 mm ( $b = -6.17, 95\% \text{ CI } [-10.81, -1.54]$ ), midshaft diameter decreased by 0.95 mm ( $b = -0.95, 95\% \text{ CI } [-1.54, -0.36]$ ), and cortical thickness decreased by 0.78 mm ( $b = -0.78, 95\% \text{ CI } [-1.28, -0.29]$ ) in infants with chronic illness after holding age constant. These results support the hypothesis that chronic illness is negatively related to tibial length, midshaft diameter, and cortical thickness. Model summaries are presented in **Table 4-26**. Regression plots of the tibial measurements by age with a regression line representing data from the chronically ill infants in light blue and a dark blue regression line representing data from all other infants are presented in **Figure 4-8** to **Figure 4-12**. The black regression line reflects regression analysis of the pooled

data. After accounting for age, chronic illness was not a significant predictor of medullary cavity diameter ( $p = .409$ ) or cortical index ( $p = .106$ ). These findings did not support the hypotheses that cortical index was negatively associated with cortical index and positively associated with medullary cavity diameter. However, examination of **Figure 4-12** indicates that chronically ill infants tended to have a lower cortical index than infants without chronic illness. Overall, these results supported the hypothesis that chronic illness had a negatively relationship tibial growth.

***HYPOTHESIS 3C: CHRONIC ILLNESS IS SIGNIFICANTLY RELATED TO MEASURES OF INFANT BONE HEALTH.***

A non-parametric Mann-Whitney  $U$  test was performed to determine whether radiographic evaluation scores were significantly associated with chronic illness. Data associated with chronically ill infants are presented in **Table A- 7**. Radiographic evaluation score was significantly associated with chronic illness ( $U = 613.5, p < .001$ ). Infants with chronic illness had significantly greater radiographic evaluation scores (0 = normal, 1 = indeterminate, 2 = abnormally mineralized) than infants without chronic illness, supporting the hypothesis that qualitative radiographic evaluation scores are positively associated with chronic illness.

BMD was hypothesized to have a negative relationship with chronic illness. Prior to analysis, a Chi-square test was performed to assess whether there was a significant association between chronic illness and prematurity in the study sample. The chi-square test indicated a significant association between prematurity and chronic illness,  $X^2(1, n = 69) = 10.07, p = .002$ . Due to the significant association, a two-way ANOVA was performed to evaluate the relationship between BMD as the independent variable and chronic illness, prematurity, and the interaction of prematurity and chronic illness as dependent variables. Levene's test indicated equal variances between groups ( $F = 2.73, p = .051$ ). The model predicting BMD from chronic illness, prematurity, and prematurity\*chronic illness was significant ( $R^2_{Adj.} = .12, F(3, 62) = 3.99, p = .012$ ). Chronic illness ( $F(1, 62) = 7.81, p = .007$ ) was a significant predictor in the model, but prematurity\*chronic illness ( $p = .862$ ) and prematurity ( $p = .681$ ) were not significant predictors in the model. Chronically ill infants had significantly lower BMD estimates than infants without chronic illness. When premature infants were excluded from the analysis, the ANOVA model predicting BMD from chronic illness remained significant ( $F(1, 52) = 5.09, p = .028$ ). These

**Table 4-26. Model summaries of regression analyses with age as a covariate and chronic illness as the predictor variable. Tibial length is the dependent variable in model 1. Tibial midshaft diameter is the dependent variable in model 2. Cortical thickness is the dependent variable in Model 3.**

Model	Unstandardized Coefficients		<i>t</i>	<i>p</i>	<i>F</i>	<i>df</i>	<i>p</i>	Adj. <i>R</i> <sup>2</sup>
	<i>b</i>	<i>SE</i>						
1					121.74	2,74	< .001	.76
	(Constant)	64.38	1.64	39.37	< .001			
	Age	4.39	0.29	15.33	< .001			
	Chronic Illness	-6.17	2.33	-2.65	.010			
2					43.78	2,74	< .001	.53
	(Constant)	5.90	0.21	28.45	< .001			
	Age	0.32	0.04	8.72	< .001			
	Chronic Illness	-0.95	0.30	-3.23	.002			
3					10.86	2,74	< .001	.21
	(Constant)	3.48	0.17	19.98	< .001			
	Age	0.10	0.03	3.37	.001			
	Chronic Illness	-0.78	0.25	-3.16	.002			

findings supported the hypothesis that chronic illness is negatively related to BMD. The frequency distribution of BMD with data from chronically ill infants indicated is presented in **Figure 4-31**.

SOS was hypothesized to have negative relationships with chronic illness. An ANOVA was used to evaluate SOS readings for significant differences based on chronic illness or prematurity. Levene’s test indicated variances in SOS were equal between infants with and without chronic illness ( $F = 0.42, p = .521$ ). There were no statistically significant differences in SOS between infants with and without chronic illness ( $F(1, 75) = 0.73, p = .394$ ), which did not support the hypothesis.

### **Association between Skeletal Maturity at Birth, Body Size, Tibial Structure, and Bone Health**

#### ***HYPOTHESIS 4A: SKELETAL MATURITY AT BIRTH IS SIGNIFICANTLY RELATED TO BODY SIZE.***

One-way ANOVAs and regression analyses were conducted to evaluate the relationship between skeletal maturity at birth and body size. It was hypothesized that EGA and birthweight would be



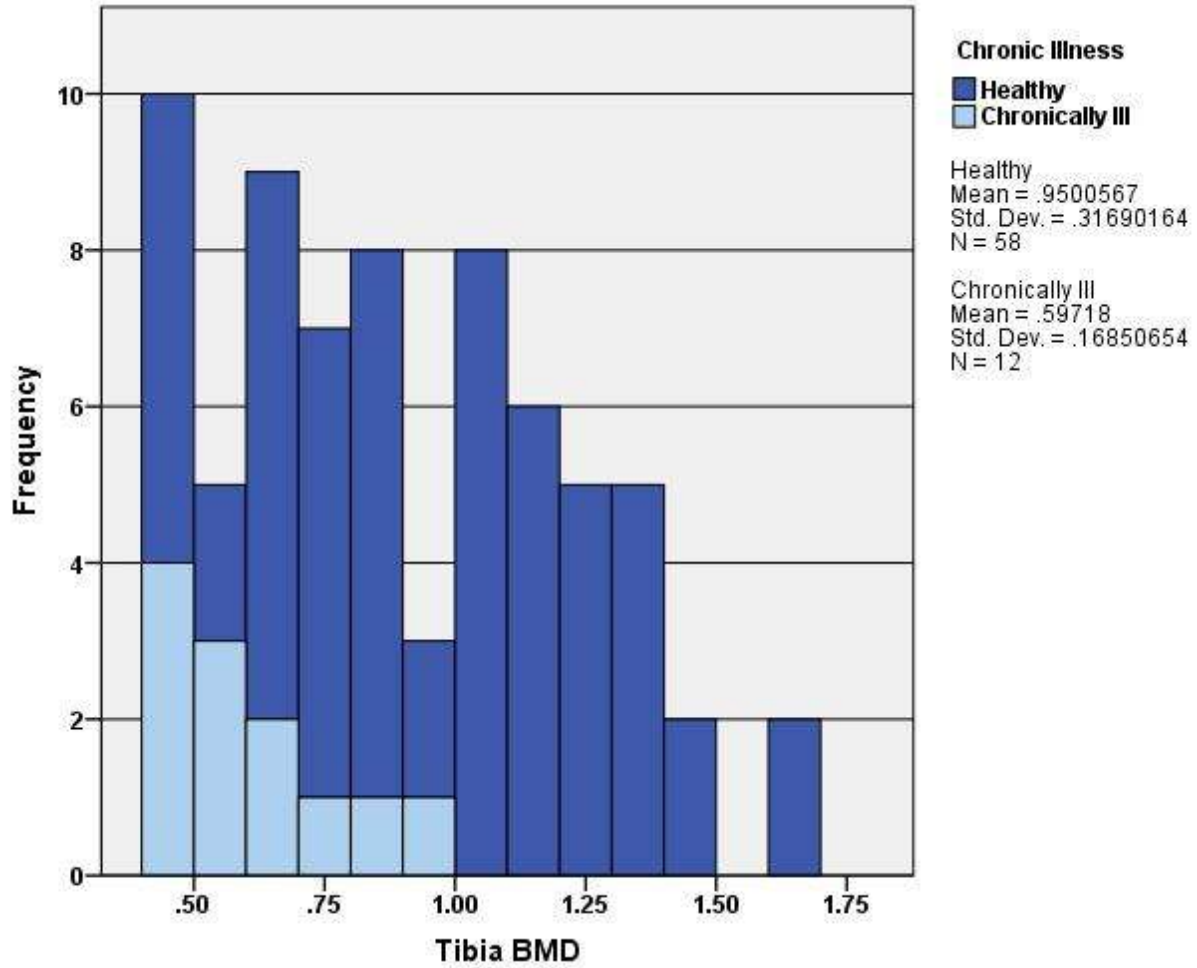


Figure 4-31. Distribution of BMD data differentiating between infants with and without chronic illness. Dark blue represents BMD data from infants without chronic illness and light blue represents data from chronically ill infants.

positively associated with body size, while prematurity would be negatively associated with body size. Mean centered EGA was used to predict weight, height, weight for age percentile, length for age percentile, and weight for length percentile. Age was added as a covariate in models predicting height and weight. Models predicting height ( $R^2_{Adj.} = .78$ ,  $F(2, 71) = 129.38$ ,  $p < .001$ ), length for age percentile ( $R^2_{Adj.} = .19$ ,  $F(1, 71) = 18.00$ ,  $p < .001$ ), weight ( $R^2_{Adj.} = .60$ ,  $F(2, 71) = 56.78$ ,  $p < .001$ ), weight for age percentile ( $R^2_{Adj.} = .10$ ,  $F(1, 71) = 8.96$ ,  $p = .004$ ), and weight for length percentile ( $R^2_{Adj.} = .06$ ,  $F(1, 69) = 5.34$ ,  $p = .024$ ) were significant. Regression coefficients for mean centered EGA were significant ( $p < .05$ ) and indicated that height ( $b = 0.96$ , 95% CI [0.71, 1.22]), length for age percentile ( $b = 4.62$ , 95% CI [2.45, 6.79]), weight ( $b = 0.18$ , 95% CI [0.09, 0.28]), and weight for age percentile ( $b = 3.38$ , 95% CI [1.13, 5.63]) significantly increased for each week increase in EGA greater than the mean. Weight for length percentile significantly decreased for each week increase in EGA greater than the mean ( $b = -3.04$ , 95% CI [-5.66, -0.42]). These findings supported the hypothesis that greater EGA had a positive relationship with body size.

Birthweight was converted from kilograms to grams prior to analyses in order to improve interpretation of the regression model. In separate regression analyses, mean centered birthweight was used to predict weight, height, length for age percentile, weight for age percentile, and weight for length percentile. Age was used as a covariate for models predicting height and weight. Mean centered birthweight was a significant predictor of height ( $R^2_{Adj.} = .77$ ,  $F(2, 68) = 117.92$ ,  $p < .001$ ), length for age percentile ( $R^2_{Adj.} = .24$ ,  $F(1, 68) = 23.08$ ,  $p < .001$ ), weight ( $R^2_{Adj.} = 0.62$ ,  $F(2, 68) = 58.12$ ,  $p < .001$ ), and weight for age percentile ( $R^2_{Adj.} = .14$ ,  $F(1, 68) = 12.39$ ,  $p = .001$ ). Regression coefficients for mean centered birthweight were significant ( $p < .05$ ) and indicated that height ( $b = 4.22$ , 95% CI [3.00, 5.44]), length for age percentile ( $b = 23.90$ , 95% CI [13.97, 33.83]), weight ( $b = 0.88$ , 95% CI [0.44, 1.33]), and weight for age percentile ( $b = 18.61$ , 95% CI [8.06, 29.16]) significantly increased for each kg increase in birthweight greater than the mean. Mean centered birthweight was not a significant predictor of weight for length percentile ( $F(1, 66) = 1.99$ ,  $p = .163$ ). These findings support the hypothesis that birthweight has a positive relationship with body size.

One-way ANOVAs were used to test for significant differences in body size between term and premature infants. Age was used as a covariate in models predicting height and weight.

Variances in height ( $F = 3.02, p = .087$ ), weight ( $F = 0.86, p = .358$ ), and weight for age percentile ( $F = 2.03, p = .159$ ) were equal across groups based on prematurity. Variances in length for age percentile ( $F = 35.04, p < .001$ ) and weight for length percentile ( $F = 5.74, p = .019$ ) were significantly different between term born and premature infants. Significant differences were indicated for height ( $F(2, 71) = 105.47, p < .001$ ), length for age percentile ( $F(1, 71) = 24.17, p < .001$ ), weight ( $F(2, 71) = 50.08, p < .001$ ), weight for age percentile ( $F(1, 71) = 7.46, p = .008$ ), and weight for length percentile ( $F(1, 69) = 5.79, p = .019$ ) based on prematurity. Examination of means indicated that body size in premature infants was significantly lower than in term infants, except in weight for length percentile. Premature infants were significantly greater than term infants in weight for length percentile. This indicated that premature infants weighed more for their length than term infants. These results supported the hypothesis that prematurity is negatively associated with body size. These findings support the hypothesis that prematurity has a negative relationship with body size.

***HYPOTHESIS 4B: SKELETAL MATURITY AT BIRTH IS SIGNIFICANTLY RELATED TO TIBIAL MEASUREMENTS.***

It was hypothesized that the tibial measurements were positively associated with birthweight and EGA. Regression analyses were used to evaluate the relationships between skeletal maturity at birth and the tibial measurements. Models using age as a covariate and EGA to predict tibial length ( $R^2_{Adj.} = .84, F(2, 70) = 183.52, p < .001$ ) and cortical thickness ( $R^2_{Adj.} = .14, F(2, 70) = 7.07, p = .002$ ) were significant. Models using age, age<sup>2</sup>, age<sup>3</sup>, and EGA to predict midshaft diameter ( $R^2_{Adj.} = .59, F(4, 68) = 26.49, p < .001$ ) and medullary cavity diameter ( $R^2_{Adj.} = .60, F(4, 68) = 27.55, p < .001$ ) were significant. Regression coefficients for EGA were significant ( $p < .05$ ) and indicated that, while holding age constant, tibial length ( $b = 1.45, 95\% \text{ CI } [1.02, 1.89]$ ), midshaft diameter ( $b = 0.13, 95\% \text{ CI } [0.07, 0.19]$ ), cortical thickness ( $b = 0.07, 95\% \text{ CI } [0.02, 0.13]$ ), and medullary cavity diameter ( $b = 0.06, 95\% \text{ CI } [0.01, 0.10]$ ) significantly increased for every 1 week increase in EGA. EGA was not a significant predictor of cortical index after accounting for age ( $p = .792$ ). Findings indicated that EGA had a positive relationship with tibial measurements, which supported the hypothesis.

Models using age as a covariate and birthweight to predict tibial length ( $F(2, 67) = 180.16, p < .001$ ) and cortical thickness ( $R^2_{Adj.} = .15, F(2, 67) = 7.25, p = .001$ ) were significant. Models

using age, age<sup>2</sup>, age<sup>3</sup>, and birthweight to predict midshaft diameter ( $R^2_{Adj.} = .60$ ,  $F(4,65) = 25.68$ ,  $p < .001$ ) and medullary cavity diameter ( $R^2_{Adj.} = .59$ ,  $F(4,65) = 26.40$ ,  $p < .001$ ) were significant. Regression coefficients for birthweight were significant ( $p < .05$ ) and indicated that, while holding age constant, tibial length ( $b = 6.62$ , 95% CI [4.56, 8.68]), midshaft diameter ( $b = 0.59$ , 95% CI [0.30, 0.88]), medullary cavity diameter ( $b = 0.25$ , 95% CI [0.05, 0.45]), and cortical thickness ( $b = 0.37$ , 95% CI [0.10, 0.63]) increased as birthweight increased. Birthweight was not a significant predictor of cortical index ( $p = .435$ ). Findings indicated that birthweight had a positive relationship with tibial measurements, which supported the hypothesis.

Chronically ill infants were excluded from the analyses to evaluate whether this influenced the above results. After chronically ill infants were excluded from analyses, models using age as a covariate and EGA to predict tibial length ( $R^2_{Adj.} = .83$ ,  $F(2, 58) = 151.39$ ,  $p < .001$ ) and cortical thickness ( $R^2_{Adj.} = .19$ ,  $F(2, 58) = 8.22$ ,  $p = .001$ ) remained significant. Models using age, age<sup>2</sup>, age<sup>3</sup>, and EGA to predict midshaft diameter were significant ( $R^2_{Adj.} = .62$ ,  $F(4, 56) = 25.45$ ,  $p < .001$ ). Regression coefficients for EGA were significant ( $p < .05$ ) and indicated that, while holding age constant, tibial length ( $b = 1.32$ , 95% CI [0.73, 1.90]), midshaft diameter ( $b = 0.16$ , 95% CI [0.08, 0.24]), and cortical thickness ( $b = 0.09$ , 95% CI [0.02, 0.17]) significantly increased for every 1 week increase in EGA. EGA was not a significant predictor of medullary cavity diameter ( $p = .090$ ) or cortical index after removing chronically ill infants from the analysis ( $p = .548$ ). Among infants without chronic illness, EGA had a positive relationship with linear and appositional growth of the tibia. These findings lend further support to hypothesis 4b.

After chronically ill infants were excluded from analyses, models using age as a covariate and birthweight to predict tibial length ( $R^2_{Adj.} = .83$ ,  $F(2, 57) = 148.88$ ,  $p < .001$ ), midshaft diameter ( $R^2_{Adj.} = .58$ ,  $F(2, 57) = 41.50$ ,  $p < .001$ ), and cortical thickness ( $R^2_{Adj.} = .18$ ,  $F(2, 57) = 7.53$ ,  $p = .001$ ) remained significant. Models using age, age<sup>2</sup>, age<sup>3</sup>, and birthweight to predict midshaft diameter were significant. Regression coefficients for birthweight were significant ( $p < .05$ ) and indicated that, while holding age constant, tibial length ( $b = 4.90$ , 95% CI [2.43, 7.38]), midshaft diameter ( $b = 0.57$ , 95% CI [0.20, 0.94]), and cortical thickness ( $b = 0.40$ , 95% CI [0.07, 0.73]) significantly increased for every 1 kg increase in birthweight. Birthweight was not a significant predictor of medullary cavity diameter ( $p = .247$ ) or cortical index after removing chronically ill infants from the analysis ( $p = .369$ ). Among infants without chronic illness, birthweight had a

positive relationship with linear and appositional growth of the tibia. These findings lend further support to hypothesis 4b.

It was hypothesized that prematurity would have a negative relationship with the tibial measurements. Regression models using age as a covariate, and prematurity to predict tibial length ( $R^2_{Adj.} = .81$ ,  $F(2, 70) = 153.53$ ,  $p < .001$ ) and cortical thickness ( $R^2_{Adj.} = .19$ ,  $F(2, 70) = 9.37$ ,  $p < .001$ ) were significant. Models using age, age<sup>2</sup>, age<sup>3</sup>, and prematurity to predict midshaft diameter ( $R^2_{Adj.} = .59$ ,  $F(4,68) = 26.70$ ,  $p < .001$ ), medullary cavity diameter ( $R^2_{Adj.} = .58$ ,  $F(4, 68) = 26.03$ ,  $p < .001$ ), and cortical thickness. The regression coefficients for prematurity indicated that tibial length ( $b = -10.40$ , 95% CI [-14.27, -6.52]), midshaft diameter ( $b = -1.06$ , 95% CI [-1.57, -0.55]), medullary cavity diameter ( $b = -0.37$ , 95% CI [-0.72, -0.02]), cortical thickness ( $b = -0.73$ , 95% CI [-1.18, -0.29]) were significantly lower in premature infants than term infants of the same chronological age. Model summaries are presented in **Table 4-27**. After accounting for age, prematurity was not a significant predictor of cortical index ( $p = .516$ ). These findings support the hypothesis that prematurity has a negative relationship with tibial measurements, but not the proportion of cortical bone relative to bone size.

#### ***HYPOTHESIS 4C: SKELETAL MATURITY AT BIRTH IS SIGNIFICANTLY RELATED TO MEASURES OF INFANT BONE HEALTH***

It was hypothesized that BMD had positive relationships with EGA and birthweight. BMD was regressed against mean centered birthweight (kg) and mean centered EGA to evaluate the effects of skeletal maturity at birth on BMD. Mean centered birthweight (kg) was a significant predictor of BMD ( $R^2_{Adj.} = .06$ ,  $F(1, 62) = 4.66$ ,  $p = .035$ ). Mean centered EGA was not a significant predictor of BMD ( $F(1, 64) = 3.90$ ,  $p = .053$ ). The regression coefficient for mean centered birthweight indicated that BMD increased by 0.11 g/cm<sup>2</sup> with each 1 kg increase in birthweight greater than the mean ( $b = 0.11$ , 95% CI [0.01, 0.22]). The model summary is presented in **Table 4-28**. These findings partially supported the hypothesis that skeletal maturity at birth is positively related to BMD.

Data from chronically ill infants were removed from the analysis to determine whether the correlation between prematurity and chronic illness caused the significant association between

**Table 4-27. Model summaries of regression analyses with age as a covariate and prematurity as the predictor variable. Tibial length is the dependent variable in Model 1. Tibial midshaft diameter is the dependent variable in Model 2. Medullary cavity diameter is the dependent variable in Model 3. Cortical thickness is the dependent variable in Model 4.**

Model		Unstandardized Coefficients		<i>t</i>	<i>p</i>	<i>F</i>	<i>df</i>	<i>p</i>	Adj. <i>R</i> <sup>2</sup>
		<i>b</i>	<i>SE</i>						
1						153.53	2,70	< .001	.81
	(Constant)	66.63	1.54	43.23	< .001				
	Age	4.19	0.27	15.81	< .001				
2	Premature	-10.40	1.94	-5.35	< .001				
						26.70	4,68	< .001	.59
	(Constant)	4.99	0.46	10.79	< .001				
	Age	1.19	0.32	3.65	< .001				
	Age <sup>2</sup>	-0.18	0.07	-2.69	.009				
3	Age <sup>3</sup>	0.009	0.004	2.52	.014				
	Premature	-1.06	0.25	-4.17	< .001				
						26.03	4,68	< .001	0.58
	(Constant)	1.49	0.32	4.67	< .001				
	Age	0.91	0.23	4.05	< .001				
4	Age <sup>2</sup>	-0.12	0.05	-2.57	.012				
	Age <sup>3</sup>	0.005	0.003	2.08	.041				
	Premature	-0.37	0.18	-2.13	.037				
						9.37	2,70	< .001	.19
	(Constant)	3.63	0.18	20.58	< .001				
	Age	0.07	0.03	2.35	.022				
	Premature	-0.73	0.22	-3.29	.002				

**Table 4-28. Results of simple linear regression analysis with BMD as the dependent variable and birthweight as the predictor.**

Model		Unstandardized Coefficients		<i>t</i>	<i>p</i>	<i>F</i>	<i>df</i>	<i>p</i>	Adj. <i>R</i> <sup>2</sup>
		<i>b</i>	<i>SE</i>						
						4.66	1,62	.035	.06
	(Constant)	0.91	0.04	23.40	< .001				
	Birthweight (kg)	0.11	0.05	2.16	.035				
a. EGA = Estimated Gestational Age									

BMD and birthweight. After removing the chronically ill infants from the analysis, there was no longer a significant relationship between BMD and mean centered birthweight ( $F(1, 53) = 1.68, p = .201$ ). The relationship between BMD and mean centered EGA remained insignificant ( $F(1, 53) = 0.94, p = .338$ ). This suggests that the chronically ill and/or premature infants in the analysis may have been responsible for the initial significant relationship between BMD and birthweight. As chronic illness and prematurity were previously found to be significantly associated in the current study sample, these findings could also suggest that birthweight is an important predictor for BMD among premature infants. Birthweight decreases as severity in prematurity and likelihood of chronic illness increases.

It was hypothesized that BMD had a negative relationship with prematurity. Results of a two-way ANOVA performed to assess the effects of chronic illness, prematurity, and whether there was an interaction effect between prematurity and chronic illness in the prediction of BMD were reported in the above section, hypothesis 3c, and will not be repeated here. Prematurity was not a significant variable in the model predicting BMD ( $p = .681$ ), which did not support the hypothesis that BMD had a negative relationship with prematurity.

SOS was hypothesized to have a positive relationship with EGA and birthweight. A model predicting SOS using age, age<sup>2</sup>, age<sup>3</sup>, and birthweight was statistically significant ( $R^2_{Adj.} = .43, F(4, 65) = 13.79, p < .001$ ). The regression coefficient for birthweight was significant ( $p = .001$ ) and indicated that, while holding age constant, for every 1 kg increase in birthweight SOS increased by ~96 m/s while holding age constant ( $b = 96.17, 95\% \text{ CI } [42.25, 150.10]$ ). A model predicting SOS using age, age<sup>2</sup>, age<sup>3</sup>, and EGA was statistically significant ( $R^2_{Adj.} = .41, F(4, 68) = 13.32, p < .001$ ) The regression coefficient for EGA was significant ( $p = .003$ ) and indicated that, while holding age constant, for every 1 week increase in EGA the mean SOS increased by ~18 m/s ( $b = 17.67, 95\% \text{ CI } [6.32, 29.03]$ ). Model summaries are provided in Models 1 and 2 of **Table 4-29**. These results supported the hypothesis that SOS was positively associated with EGA and birthweight.

After chronically ill infants were removed from analyses and using the age variables as covariates, the relationships between SOS and birthweight ( $R^2_{Adj.} = .42, F(4, 55) = 11.60, p < .001$ ), and EGA ( $R^2_{Adj.} = .40, F(4, 56) = 10.82, p < .001$ ) remained significant. The regression

**Table 4-29. Model summaries of regression analyses using the age variables as covariates and birthweight (Model 1), and EGA (Model 2) to predict SOS.**

Model	Unstandardized Coefficients		<i>t</i>	<i>p</i>	<i>F</i>	<i>df</i>	<i>p</i>	Adj. <i>R</i> <sup>2</sup>
	<i>b</i>	<i>SE</i>						
1					13.79	4,65	<.001	.43
	(Constant)	2938.50	113.78	25.83	<.001			
	Age	-227.80	59.64	-3.82	<.001			
	Age <sup>2</sup>	48.36	12.09	4.00	<.001			
	Age <sup>3</sup>	-2.50	0.69	-3.62	.001			
	Birthweight (kg)	96.17	27.00	3.56	.001			
2					13.32	4,68	<.001	.41
	(Constant)	2547.40	231.72	10.99	<.001			
	Age	-224.69	60.32	-3.73	<.001			
	Age <sup>2</sup>	46.93	12.18	3.85	<.001			
	Age <sup>3</sup>	-2.39	0.69	-3.45	.001			
	EGA <sup>a</sup>	17.67	5.69	3.11	.003			

a. EGA= Estimated Gestational Age

coefficient for birthweight was significant ( $p = .008$ ) and indicated that, while holding age constant, SOS increased by ~96 m/s with each 1 kg increase in birthweight ( $b = 95.81$ , 95% CI [26.64, 164.97]). The regression coefficient for EGA was significant ( $p < .001$ ) and indicated that, while holding age constant, SOS increased by ~18 m/s with each week increase in EGA ( $b = 18.48$ , 95% CI [2.24, 34.72]). Model summaries are provided in **Table 4-30**. After removal of premature infants from analyses and including the age variables as covariates, birthweight ( $p = .111$ ) and EGA ( $p = .799$ ) were no longer significant predictors in models predicting SOS. These findings supported the hypothesis that SOS was significantly associated with skeletal maturity at birth.

SOS was hypothesized to have a negative relationship with prematurity. ANOVAs were used to evaluate SOS readings for significant differences between term born and premature infants. Levene's test indicated variances in SOS were equal between term born and premature infants ( $F = 0.83$ ,  $p = .366$ ). Premature infants had significantly lower SOS readings than term born infants ( $F(1, 71) = 7.09$ ,  $p = .010$ ), which supported the hypothesis that SOS had a negative relationship with prematurity. Results supported the hypothesis that SOS was significantly associated with skeletal maturity at birth.



**Table 4-30. Model summaries of regression analyses using the age variables as covariates and birthweight (Model 1), and EGA (Model 2) to predict SOS, excluding chronically ill infants.**

Model	Unstandardized Coefficients		<i>t</i>	<i>p</i>	<i>F</i>	<i>df</i>	<i>p</i>	Adj. <i>R</i> <sup>2</sup>
	<i>b</i>	<i>SE</i>						
<b>1</b>					11.60	4,55	<.001	.42
	(Constant)	2888.96	144.65	19.97	<.001			
	Age	-203.42	67.86	-3.00	.004			
	Age <sup>2</sup>	45.52	13.52	3.37	.001			
	Age <sup>3</sup>	-2.40	0.76	-3.16	.003			
	Birthweight (kg)	95.81	34.51	2.78	.008			
<b>2</b>					10.82	4,56	<.001	.40
	(Constant)	2474.61	327.48	7.56	<.001			
	Age	-201.71	69.30	-2.91	.005			
	Age <sup>2</sup>	44.06	13.84	3.18	.002			
	Age <sup>3</sup>	-2.29	0.78	-2.94	.005			
	EGA <sup>a</sup>	18.48	8.11	2.28	.026			

a. EGA= Estimated Gestational Age

Qualitative radiographic score was hypothesized to have a positive relationship with prematurity. A non-parametric Mann-Whitney *U* test was performed to determine whether radiographic evaluation scores were significantly associated with prematurity. Data associated with chronically ill infants are presented in **Table A- 7**. Radiographic evaluation score was not associated with prematurity ( $U = 551.5, p = .193$ ), which did not support the hypothesis.

### **Relationships between Measures of Bone Quality**

#### ***HYPOTHESIS 5A: BMD HAS A NEGATIVE RELATIONSHIP WITH QUALITATIVE RADIOGRAPHIC SCORE.***

Regression analysis was used to evaluate whether the perceived degree of abnormal mineralization or demineralization on radiographs could be used to reliably predict BMD. The distribution of BMD estimates grouped by qualitative radiographic score is provided in **Figure 4-32**. BMD could not be reliably predicted using qualitative radiographic scores ( $F(1, 67) = 3.80, p \leq .055$ ). The relationship between BMD and radiographic score remained insignificant after chronically ill infants were removed from the analysis ( $p = .199$ ). With premature infants removed from the analysis, the relationship between BMD and radiographic score remained

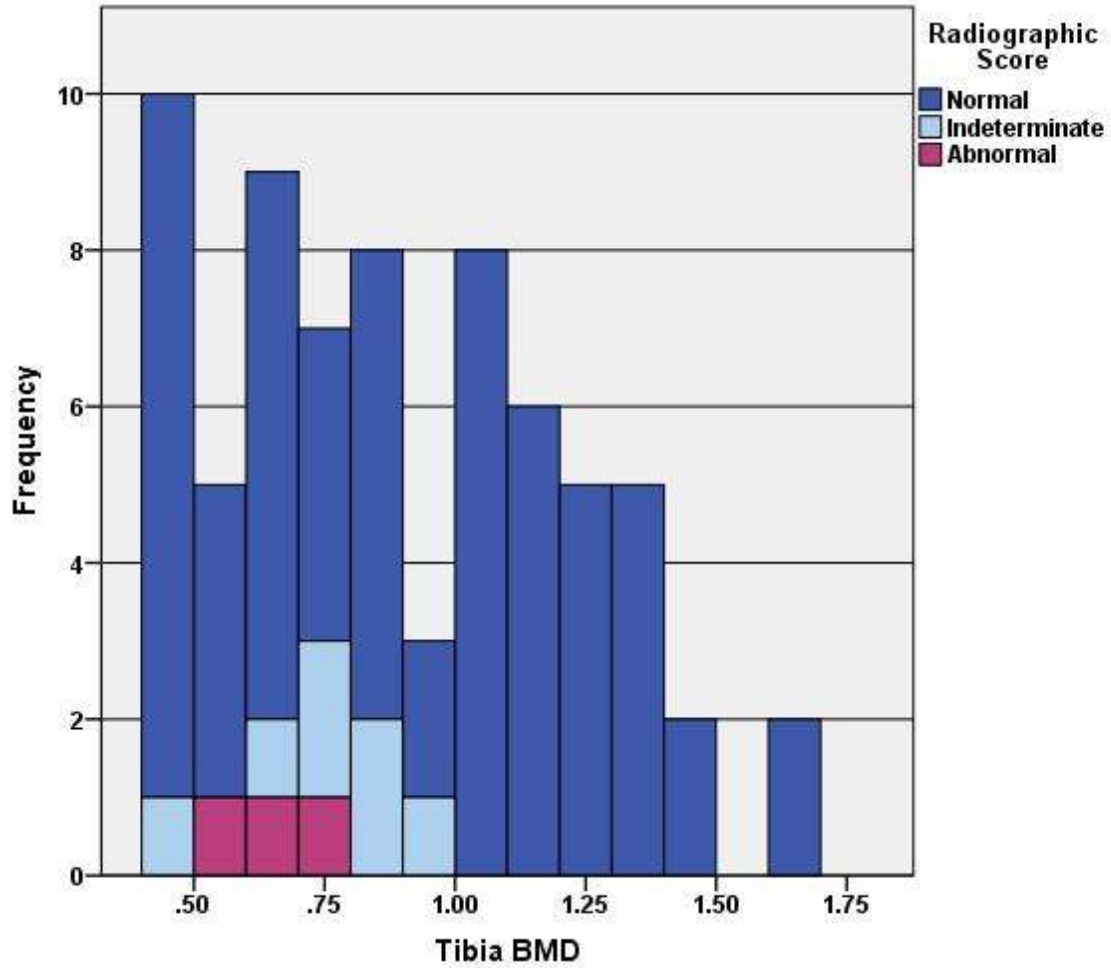


Figure 4-32. Distribution of BMD values with qualitative radiographic score specified. Dark blue represents cases classified as normally mineralized on radiographs. Light blue represents cases classified as indeterminately or slightly demineralized on radiographs. Purple represents cases classified as abnormally mineralized on radiographs.

insignificant ( $p = .057$ ). These findings did not support the hypothesis that perceived degree of abnormal mineralization or demineralization, represented by greater radiographic scores, was significantly associated with lower BMD estimates.

***HYPOTHESIS 5B: SOS HAS A SIGNIFICANT POSITIVE RELATIONSHIP WITH BMD.***

The relationships between SOS and BMD was examined using ANOVA and linear regression models. SOS estimates were not reliably predicted by BMD estimates ( $F(1, 68) = 0.24, p = .628$ ). To determine if age was acting as a suppressor variable between SOS and BMD, a model including age as a covariate and BMD as a predictor variable to predict SOS. After accounting for age, there was still no significant correlation between SOS and BMD ( $p = .668$ ). Due to their lack of significance, the relationship between SOS and BMD and qualitative radiographic scores were not explored any further using regression analyses. These findings did not support the hypothesis that SOS was positively related to BMD.

***HYPOTHESIS 5C: SOS HAS A SIGNIFICANT NEGATIVE RELATIONSHIP WITH QUALITATIVE RADIOGRAPHIC SCORE.***

The relationship between SOS and qualitative radiographic score was examined using ANOVA and linear regression analyses. There was no significant relationship between radiographic scores and SOS ( $F(1, 75) = 0.07, p = .792$ ). These findings did not support the hypothesis that lower SOS values would be associated with greater qualitative radiographic scores, which indicated perceived degree of abnormal mineralization or demineralization.

## **Summary**

Analyses indicated a significant positive association between chronic illness and prematurity among infants in the study sample. Due to this association, analyses conducted on the pooled data were repeated with chronically ill and premature infants excluded from analyses to help identify spurious relationships. Analyses indicated no association between the presence of traumatic injury and chronic illness, prematurity, body size, or indicators of bone health.

Infants with chronic illness had significantly smaller tibia lengths, midshaft diameter, and cortical thickness than infants without chronic illness. However, chronically ill infants were not significantly smaller in body size. Infants with chronic illness had significantly lower BMD, but

not SOS, than infants without chronic illness. Skeletal maturity at birth was significantly related to body size. Premature infants were significantly smaller than term born infants, except in weight for length percentile. Skeletal maturity at birth was significantly related to tibial size. Premature infants were significantly smaller in tibial size than term born infants, even after removing chronically ill infants from analyses. Prematurity was not associated with the proportion of cortical bone to cross-sectional size of the tibia. BMD and SOS were significantly related to skeletal maturity at birth. BMD was not significantly associated with prematurity, but was significantly positively associated with birthweight. SOS was positively associated with birthweight and EGA and negatively associated with prematurity. Greater qualitative radiographic score, an indication of demineralization or abnormal mineralization, was not related to prematurity.

BMD, SOS, and tibial measurements were significantly related to age. BMD significantly decreased with age. Tibial measurements significantly increased with increasing age with the exception of cortical index, which decreased. There was a cubic trend in the relationship between SOS and age. SOS decreased after birth until ~ 3 months of age and began to increase thereafter. SOS plateaued at ~9 months of age. A similar pattern was observed among premature infants, although the postnatal decrease was more severe with a prolonged recovery period relative to term infants.

Tibial size, but not the relative amount of cortical bone to cross-sectional diameter, was significantly positively related to body size. BMD was not related to body size. BMD was significantly associated with cortical index when chronically ill infants were included in the analysis, but the association was no longer significant after chronically ill infants were excluded. SOS was positively associated with body size when premature infants were included in the analysis, but not among term born infants. For the pooled data, SOS was significantly related to medullary cavity diameter and cortical index after accounting for variation due age. Among term infants, SOS was significantly associated with midshaft diameter and cortical index after accounting for age. When chronically ill infants were excluded from analyses, there was no significant relationship between tibial structure and SOS after accounting for variation due to age.

Statistical analyses were conducted to evaluate the relationship between the different measures of infant bone health. There was no significant association between BMD and SOS, BMD and qualitative radiographic score, or SOS and qualitative radiographic score.

## **CHAPTER 5 : DISCUSSION**

### **Introduction**

The purpose of this study was to evaluate factors contributing to infant bone quality that are measured by SOS. The relationship between infant bone quality and SOS was investigated through the testing of five hypotheses. Hypothesis 1: Growth-related changes in tibial structure and body size are significantly associated with each other, and both are significantly associated with age-related changes in BMD and SOS. Hypothesis 2: The presence of traumatic injury is not associated with indicators of overall health, body size, or bone health. Hypothesis 3: Chronic illness is negatively associated with growth and bone health. Hypothesis 4: Skeletal maturity at birth is positively associated with body size, bone size, and bone health. Hypothesis 5: The methods used to assess infant bone quality are significantly associated with one another. The first five sections of this chapter discuss the findings associated with each of these hypotheses. The findings associated with each of these hypotheses were used to draw conclusions that would help answer this study's major questions. Is QUS a valid tool for evaluating bone quality in infants? Can SOS be used to differentiate between infants with poor bone quality and infants with normal bone quality? And if QUS is a valid method for evaluating infant bone health, can a threshold for normal bone SOS values in infants be identified? These conclusions are addressed in the conclusion section. The final section discusses the limitations of this study.

### **Association between Growth-Related Changes in Size and Age-Related Changes in SOS and BMD**

Studies report that bone microstructural and macrostructural properties are strongly associated with SOS (Bossy et al. 2004a; Bossy et al. 2004b; Foldes et al. 1995; Greenfield et al. 1981; Guglielmi et al. 2009; Guglielmi et al. 2003; Kann et al. 1993; Kaufman and Einhorn 1993; Kohles et al. 1994; Lee et al. 1997; Njeh et al. 1997; Prevrhal et al. 2001; Raum et al. 2014; Raum et al. 2005; Sakata et al. 2004; Wuster et al. 2005). Therefore, understanding age-related changes in tibial structure is important for investigating the aspects of bone quality that are measured by SOS. Before the relationship between growth and age-related changes in SOS and BMD could be interpreted, age-related changes in bone size and its relationship with growth-related changes in body size were thoroughly assessed.

Age-related changes in tibial measurements were evaluated through regression analyses using age as the independent variable. *F* tests were performed on the  $R^2$  change to determine whether a hierarchical model (quadratic or cubic) was a better fit for the data than a linear model. Age was a significant predictor of tibial length, midshaft diameter, cortical thickness, medullary cavity diameter, and cortical index. All tibial measurements, except cortical index, significantly increased from birth to 12 months of age. The rate of increase in tibial length was greater than the rate of increase of the other tibial measurements (**Figure 4-8** to **Figure 4-12**). Overall, there was a net increase in medullary cavity diameter and midshaft diameter over the first year of life. But, the rate of increase in midshaft diameter and medullary cavity diameter fluctuated over time, resulting in curvilinear (cubic) relationships that are illustrated by the black regression lines in **Figure 4-9** and **Figure 4-10**. After birth, tibial midshaft diameter and medullary cavity diameter increased with age. At ~3-4 months of age, there was a decline in the rates of increase for the midshaft and medullary cavity diameters. At ~7-8 months of age, the rate of increase in midshaft diameter increased again and continued to increase, while the increase in medullary cavity diameter did not commence until ~8-9 months of age. The regression coefficients for the age variables indicated that periosteal expansion occurred at a slightly greater rate than expansion of the medullary cavity, which suggested a gradual increase in cortical thickness. A gradual, but significant, increase in cortical thickness with age was indicated (black regression line, **Figure 4-11**). In contrast, cortical index had a negative quadratic relationship with age. Initially, cortical index declined from birth until ~7-8 months of age at which point it began to rebound (**Figure 4-12**). Periosteal and endosteal expansion both declined a few months prior to the rebound in cortical index. The decline in endosteal expansion lasted longer than the decline in periosteal expansion, resulting in increased cortical thickness. The decline in periosteal expansion coupled with the increase in cortical thickness resulted in the increase in cortical index beginning at ~8 months of age. After ~7-8 months of age, the rate of periosteal and endosteal expansion increased again, but the rate of endosteal expansion lagged behind the rate of periosteal expansion, resulting in a continued increase in cortical thickness with age. These findings suggest that there is a decline in the amount of cortical bone relative to midshaft cross-sectional size as age increases over the first 6-7 months of life. After 6-7 months of age, the relative amount of cortical bone to midshaft cross-sectional size increases. Age-related changes in the cross-sectional tibial measurements are illustrated in **Table 5-1**.

**Table 5-1. Illustration of the age-related changes in tibial measurements and SOS during the first year of life.**

	Birth	1	2	3	4	5	6	7	8	9	10	11	12	
<b>SOS</b>		↓			→ ↑				↑					
<b>Midshaft Diameter</b>		↑			→ ↑				↑					
<b>Medullary Cavity Diameter</b>		↑			→ ↑					↑				
<b>Cortical Thickness</b>		↑			↑				↑					
<b>Cortical Index</b>		↓						→		↑				

Separate analyses were conducted on term born infants and infants without chronic illness (“healthy”) to determine if tibial growth significantly differed from results based on the pooled study sample. Age remained a significant predictor of all of the tibial measurements whether or not premature or chronically ill infants were excluded from analyses (as shown in **Table 4-7**, **Table 4-8**, and **Table 4-9**). There were no significant changes of the relationship trends between age and cortical thickness, or cortical index. Among term born infants, the relationship between age and tibial length was cubic and not linear. The rate increase in tibial length showed a slight reduction between 5-7 months of age (**Figure 4-13**). Exclusion of chronically ill infants remarkably affected relationship trends between age and, midshaft diameter and medullary cavity diameter. The relationship between age and midshaft diameter changed from cubic to linear, indicating that variability in the midshaft values of chronically ill infants caused the relationship between age and midshaft diameter to appear curvilinear for the pooled sample. Midshaft diameter showed a steady increase with age among infants without chronic illness. The relationship between age and medullary cavity diameter changed from cubic to quadratic when chronically ill infants were excluded from the analysis. Medullary cavity diameter increased with



increasing age, but the rate of increase declined towards the end of the first year of life (**Figure 4-10**).

The changes in midshaft cross-sectional geometry over the first year of life observed in the current study are consistent with growth-related changes reported in the literature. After birth, bone is redistributed from the endosteal surface to the periosteal surface of long bones. Midshaft diameter and medullary cavity diameter increase, while cortical thickness decreases, resulting in a decrease in relative cortical area (Rauch and Schoenau 2001). A study using high resolution-CT to evaluate ontogenetic changes in the cross-sectional geometry of tibias and femurs obtained from an archeological sample reported that total area, cortical area, and medullary area gradual increases with age (Gosman et al. 2013). Periosteal and endosteal expansion at the femoral and tibial midshafts were roughly equal and that cortical area was greater than medullary area (Gosman et al. 2013). Studies examining femoral growth during the first 6 months of life in more recent populations report that diaphyseal and medullary cavity diameters increase while cortical thickness slightly decreases BMD (Rauch and Schoenau 2001; Rauch and Schoenau 2002; Vinz 1970). Although cortical thickness decreases, overall bone strength increases due to the redistribution of bone mass further way from the neutral axis (Rauch and Schoenau 2001). A study on postnatal growth of the metacarpal reported that, over the first year of life, total cross-sectional area increased with age, but cortical index declined due to decreased cortical thickness (Bonnard 1968). In contrast to the previously mentioned studies, cortical thickness of the current study sample gradual increased with increasing age. However, Garn (1970) also reported a net increase in cortical thickness with increasing age. The increase in cortical thickness found in the current study sample was not sufficient enough to prevent the decline in cortical index. This finding was consistent with a previous study which reported that tibial cortical index declined until ~7 months of age (Bernard 1962). In the current study, cortical index also declined until ~7 months of age.

***HYPOTHESIS 1A: AGE-RELATED CHANGES IN TIBIAL MEASUREMENTS ARE POSITIVELY ASSOCIATED WITH VARIABLES RELATED TO BODY SIZE AND GROWTH PERCENTILES.***

The relationship between tibial size and structure and body size at time of death was assessed using height with age as a covariate, weight with age as a covariate, length for age percentile,

weight for age percentile, and weight for length percentile. Height shared significant positive relationships with all tibial measurements except cortical index. The same pattern in relationships was observed between weight and the tibial measurements. Using length for age and weight for age percentiles accounted for size differences due to age. As length for age percentile increased, tibial length, midshaft diameter, and cortical thickness significantly increased, but length for age percentile had no significant effect on medullary cavity diameter or cortical index. As weight for age percentile increased, tibial length, midshaft diameter, medullary cavity diameter, and cortical thickness significantly increased, but weight for age percentile had no significant relationship with cortical index. Weight for length percentile was not significantly associated with any of the tibial measurements.

In general, these findings support the hypothesis that age-related changes in tibial measurements are positively associated with growth-related changes in body size and growth percentiles. The relationship between age and the tibial measurements is driven by a growth-related size increase. Tibial size increased as overall body size increased, with the exception of cortical index. The increase in body size had no relationship to amount of cortical bone relative to cross-sectional size. It is not surprising that there is not association between body size and cortical index. Most of the infants in the study sample were non-ambulatory, meaning they were not mechanically loading their long bones with their body mass.

### ***HYPOTHESIS 1B: BMD AND SOS ARE SIGNFICANTLY RELATED TO AGE.***

#### ***BMD and Age***

Most studies evaluating BMD in infants report a significant association between BMC and/or BMD and age (Carrascosa et al. 1996; del Rio et al. 1994; Kalkwarf et al. 2013; Koo et al. 1995a; Koo 2000; Koo et al. 1998; Kurl et al. 2002; Prentice et al. 1990; Rauch and Schoenau 2001; Rawlings et al. 1999; Sievanen et al. 1999; Specker et al. 1997; Trotter and Hixon 1974; Yeste et al. 2004), but whether this association is positive or negative varies by study. Studies using CT to evaluate the changes in trabecular bone volume fraction in the proximal humerus and femur (Ryan and Krovitz 2006; Ryan et al. 2007) and proximal tibia (Gosman and Ketcham 2009; Gosman et al. 2011) reported that the bone volume fraction is high at birth and declines to a minimum by 1 year of age, at which point it begins to increase again. In contrast, infant total body BMC and BMD have been reported to significantly increase with postnatal age (Koo et al.

1995a; Koo et al. 1998; Rawlings et al. 1999; Specker et al. 1997). Studies of the infant lumbar spine report a positive association between BMD and postnatal age (Carrascosa et al. 1996; del Rio et al. 1994; Kalkwarf et al. 2013; Kurl et al. 2002; Yeste et al. 2004). BMC of the midshaft radius had a significant positive curvilinear relationship with age in a study evaluating British and Gambian infants (0-36 months of age) (Prentice et al. 1990). A longitudinal study of BMC and BMD at the distal forearm and forearm shaft (radius and ulna) in premature infants found a significant association between age and distal forearm BMC and BMD, but no significant association between forearm shaft and age (Sievanen et al. 1999). This suggests that the relationship between age and BMD during infancy is site-specific and depends on the proportion of cortical to trabecular bone at the evaluation site (Seeman 1997; Sievanen et al. 1999)

As was discussed previously, age-related changes in tibial structure result in increased bone strength. Therefore, it was important to test whether the indicators of bone strength used in the current study were also related to age. A significant decline in BMD with postnatal age was indicated, even after the exclusion chronically ill infants from the analysis. After chronically ill infants were excluded, BMD significantly declined with increasing age until ~9-10 months of age and increased was greater in infants 11 months of age. The decline in BMD with age is most likely associated with the age-related changes in cross-sectional geometry of the tibia.

Diaphyseal diameter and medullary cavity diameter increased significantly during the first year of life, while the increase in cortical thickness was comparatively much smaller. As a result, cortical index significantly decline until ~7 months of age at which point it gradually increased.

Other studies of the infant tibia have also reported a postnatal decline in BMD and cortical area. Trotter and Hixon (1974) reported a decline in mean percentage ash weight (a direct measure of bone density) of the tibia during infancy, while Bernard (1962) reported a decline in tibial cortical area until ~7 months of age (Bernard 1962). Studies evaluating ontogenetic changes of the infant femur report similar patterns of bone mass redistribution (Rauch and Schoenau 2001; Trotter and Hixon 1974; Vinz 1970; Vinz 1971). During the first 6 months of life, the femoral diaphyseal and medullary cavity diameters increase while cortical thickness slightly decreases (Rauch and Schoenau 2001; Rauch and Schoenau 2002; Vinz 1970). It has been reported that ~30% of total BMD is lost from the femur during infancy (Trotter 1971; Trotter and Hixon 1974; Trotter and Peterson 1970). If only cortical BMD is taken into account, the decrease in cortical

BMD is only 7% (Rauch and Schoenau 2002). The decline in femoral BMD is not only caused by a decline in relative cortical area, it is also due to a small decline in the mineral content of the cortical bone (Rauch and Schoenau 2001; Rauch and Schoenau 2002; Trotter 1971; Yiallourides et al. 2004). A study of BMD at the femoral midshaft reported a decline in the ratio of calcium to nitrogen (mineral:collagen) in femoral cortical bone that occurs between 2-4.5 months and 5-9 months of age (Dickerson 1962; Rauch and Schoenau 2001).

These findings support the hypothesis that BMD is significantly related to age. For term born, healthy infants, the postnatal decline in BMD is a physiological and not a pathological process. The decline in BMD and changes in cross-sectional geometry over the first year of life indicate a redistribution of bone mass from the endosteal surface to the periosteal surface (Rauch and Schoenau 2001; Rauch and Schoenau 2002). The redistribution of bone mass further away from the neutral axis results in a whole bone that is stronger in resistance to bending.

### ***SOS and Age***

Investigation of the relationship between SOS and age is important because it provides insight into what aspects of bone quality, such as growth-related changes in bone size and mineralization, are measured by SOS. Multiple studies have reported a significant relationship between SOS and age (Altuncu et al. 2007; Litmanovitz et al. 2003; Litmanovitz et al. 2004; McDevitt et al. 2007; Mercy et al. 2007; Nemet et al. 2001; Rack et al. 2012; Ritschl et al. 2005; Rubinacci et al. 2003; Tansug et al. 2011; Tomlinson et al. 2006; Zadik et al. 2003). However, normative SOS data for infants that are specific to age in months are still lacking. Only a handful of studies have reported SOS readings for infants older than a few months of age (Gonnelli et al. 2004; McDevitt et al. 2007; Ritschl et al. 2005; Tansug et al. 2011; Zadik et al. 2003) and even fewer studies have reported age-specific SOS data for normal term infants that are more specific than the range over the first year of life (McDevitt et al. 2007; Ritschl et al. 2005). Most studies utilizing SOS to evaluate bone quality in infants focus on preterm and term infants during the first few months of life (Ahmad et al. 2010; Altuncu et al. 2007; Litmanovitz et al. 2003; Litmanovitz et al. 2004; Littner et al. 2003; Littner et al. 2004b; Littner et al. 2005; McDevitt et al. 2005; Mercy et al. 2007; Nemet et al. 2001; Rubinacci et al. 2003; Teitelbaum et al. 2006; Tomlinson et al. 2006; van Rijn et al. 2000; Wright et al. 1987; Yiallourides et al. 2004), the majority of which report a negative correlation between SOS and postnatal age (Altuncu et al.

2007; Litmanovitz et al. 2003; Litmanovitz et al. 2004; Mercy et al. 2007; Nemet et al. 2001; Rubinacci et al. 2003; Tomlinson et al. 2006). Two studies monitoring infants over longer periods of time report an initial decrease in SOS reading with increasing postnatal age, but these studies also report that after ~6 months of age SOS begins to increase with increasing age (Ritschl et al. 2005; Tansug et al. 2011). SOS values obtained from larger pediatric study populations over broader age ranges have been published in the literature, but the age-specificity is limited to age in years (Mimouni and Littner 2004; Zadik et al. 2003).

The current study's results are consistent with the findings of these previous studies and support the hypothesis that SOS is significantly related to age. Analyses suggest a cubic trend in the relationship between age and SOS among both the pooled sample (**Figure 4-28**) and the term born infants (**Figure 4-29**). After birth, SOS readings for the pooled sample decreased over the first 3 months. After ~3 months of life, SOS readings gradually increased until ~9 months of life. After 9 months of life, SOS readings appeared to plateau. The relationship between SOS and age was similar for the term infants, but the increase in SOS appeared to occur earlier and the postnatal decline was more shallow than in the pooled sample. The relationship between SOS and age significantly differed among premature infants. The relationship between SOS and age was quadratic, showing a much more severe postnatal decline that occurred until ~5 months of age. After ~5 months of age, SOS in premature infants gradually increased. Recovery of the SOS to values approximating those seen shortly after birth appeared to occur later among the premature infants than in the term infants.

The initial decline in SOS associated with increased postnatal age reflects the physiological changes occurring in infant bone mineral metabolism that commence after birth. *In utero*, the minerals necessary for bone mineral metabolism are obtained through the active transport of calcium, phosphorus, and magnesium across the placenta (DiMeglio and Imel 2014). After birth, preterm and term infants depend on the bone mineral accumulated during the last trimester *in utero* and intestinal absorption of mineral from dietary sources to maintain mineral homeostasis. Cut off from maternal mineral sources after birth, bone resorption is triggered to release the necessary mineral into the body. As mentioned previously, research has shown that ~30% of neonatal BMD is lost and cortical area declines after birth. The decline in SOS is consistent with the decline in BMD and cortical area during the first 3-6 months of life reported by this and other

studies (Altuncu et al. 2007; Litmanovitz et al. 2003; Litmanovitz et al. 2004; Mercy et al. 2007; Nemet et al. 2001; Ritschl et al. 2005; Rubinacci et al. 2003; Tansug et al. 2011; Tomlinson et al. 2006). In term infants, the bone loss does not compromise bone structure or strength due to the skeletal mineral buildup which occurred during the last trimester (Sharp 2007).

Caution should be exercised with regard to the data from infants greater than 6 months of age. A great deal of heteroscedasticity is present in the SOS data distributed by age (**Figure 4-28**). This indicates that the variance in the SOS readings is not equal across the entire age range. Upon examination of **Figure 4-28**, it is apparent that the spread in SOS values is much greater during the first 3-4 months of age than after 4 months of age. The heteroscedasticity may be caused by the uneven age distribution of the study sample. The majority of infants in the study sample are 5 months of age or less. It also possible that there is a reduction in the variance in SOS readings as age increases. More SOS data from infants greater than 5 months age is necessary to understand if the heteroscedasticity is an artifact or a true reflection of changes in the SOS with age.

In an effort to develop more finely-grained age-specific normative data and to encourage more research in this area, means and ranges of SOS readings specific to chronological age, with premature infants included and excluded, are plotted in **Figure 4-27** and **Figure 4-29**, respectively. Relative to the data reported by Zadik and colleagues (2003) (female ( $n=590$ ):  $3012 \pm 137$  m/s; boys ( $n=485$ ):  $3000 \pm 106$  m/s), the SOS readings obtained from the current study sample fell well within the range of normative tibial SOS readings for the first year of life. However, the SOS data from this study should still be considered experimental due to the unequal and limited sample sizes of some of the age groups. More SOS data should be collected from infants before normative standards for infants specific to age in months can be developed.

***HYPOTHESIS 1C: BMD AND SOS ARE SIGNIFICANTLY RELATED TO BODY SIZE AND GROWTH PERCENTILES.***

BMD was hypothesized to have a significant positive relationship with body size and growth percentiles. This hypothesis was based on the use of an areal measurement to estimate BMD. There were no significant relationships between BMD and the body size variables or growth percentiles. It is likely that no relationship was found due the small area of bone used to calculate the BMD estimate. Although no correction for bone size was used, an area of 10 mm in height by

the width of the tibial midshaft may not be sufficient to cause a significant association with body size.

The relationship between body size and SOS was investigated for two reasons. First, a significant association between body size and SOS is suggestive of a relationship with tibial size and structure due to the correlation between body size and bone size. Secondly, studies have reported that SOS is negatively influenced by increased tissue thickness. According to the manufacturer, the MiniOmni™ Ultrasound Bone Sonometer (BeamMed Ltd, Petah Tikva, Israel) accounts for the effects of soft tissue thickness on SOS readings through proprietary algorithms. These algorithms subtract the duration of time required for the signal to travel through soft tissue (BeamMed 2010). Yet, a study examining the effects of subcutaneous fat on SOS readings found that increased subcutaneous fat significantly decreased SOS readings (Bajaj et al. 2010). Bajaj and colleagues (2010) measured the effects of subcutaneous fat on SOS readings by injecting chicken wings with lard. In addition, SOS readings obtained from large-for-gestational age (LGA) infants were compared to SOS readings from appropriate-for-gestational age (AGA) infants. SOS readings from LGA infants were significantly lower than for AGA infants. Littner and colleagues (2004) also reported that LGA infants had significantly lower SOS readings than AGA infants. These studies used QUS devices produced by the same manufacturer as the device used in the current study. The results of these studies suggest that tissue thickness continued to significantly negatively influence SOS readings despite manufacturer claims that proprietary algorithms account for tissue thickness effects.

It was hypothesized that SOS would have a significant positive association with body size and growth percentiles due to the correlation between bone size and body size. To evaluate the relationship between body size and SOS while accounting for age-related size differences, the age variables (age, age<sup>2</sup>, and age<sup>3</sup>) previously determined as significant predictors of SOS were used as covariates in models predicting SOS using the body size variables. Weight for age and length for age percentiles were not analyzed with the age variables as covariates due to the multicollinearity between the variables. Weight, weight for age percentile, height, length for age percentile, and leg circumference were significant predictors of SOS. However, after chronically ill infants were excluded from analyses only weight for age percentile, height, and length for

percentile were significant predictors of SOS. Among term infants, SOS was not significantly associated with any of the variables related to body size.

With regard to the negative influence of tissue thickness on SOS, the findings of the current study are not consistent with reports from previous studies (Bajaj et al. 2010; Littner et al. 2004b). Although tissue thickness was not directly measured in the current study, proxies for tissue thickness, such as leg circumference and weight percentile for age, were measured. In the pooled sample, SOS readings had significant positive relationships with weight for age percentile and leg circumference, suggesting that SOS increased as body mass, and presumably tissue thickness, increased. Yet, this may not be a fair comparison because weight for age percentile and leg circumference are not direct measures of tissue thickness. But, the SOS readings obtained from three LGA infants in the current study sample were also not consistent with the findings of previous studies. Only one (Case ID # 182) of the three infants born LGA had low SOS relative to the other infants of the same age (11 months). Moreover, the one LGA infant that died shortly after birth had the highest SOS reading of any infant in the study sample (Case ID # 202). SOS of the third LGA infant (Case ID # 215) was unremarkable and was in the midrange relative to other infants of similar age (3 months). More specific information pertaining to these infants is provided in **Table A- 1** to **Table A- 12** in the Appendix. Before it can be determined if tissue thickness significantly affected SOS readings in the current study, research comparing known tissue thickness at the SOS measurement site to SOS readings is necessary.

Therefore, after accounting size differences due to age and prematurity, SOS was not significantly affected by differences in body size. In contrast, analyses suggest that larger body size had positive relationship with SOS among premature infants and chronically ill infants. These findings partially support the hypothesis. SOS did not appear to be influenced by body size or tissue thickness, but is likely indirectly, significantly associated with body size through growth-related factors.

***HYPOTHESIS 1D: BMD AND SOS ARE SIGNIFICANTLY RELATED TO TIBIAL STRUCTURE.***

BMD was hypothesized to have a significant positive relationship with tibial structure due to the use of an areal measurement to estimate BMD. Cortical index was the only tibial measurement



significantly related to BMD. Among the pooled sample, there was a significant positive relationship between cortical index and BMD, which supported the hypothesis. After removal of the chronically ill infants from the analysis, there was no longer a significant association between cortical index and BMD. Although BMD was not significantly associated with tibial structure among infants without chronic illness, these findings suggest that tibial structure was significantly related to BMD in chronically ill infants. It is possible that the differences in tibial structure among the “healthy” infants were not great enough to result in a significant difference in BMD. These findings partially support the hypothesis.

To assess whether tibial macrostructure at the measurement site was significantly related to SOS, regression analyses predicting SOS from the tibial measurements while using as a covariate. Only medullary cavity diameter and cortical index were significantly correlated with SOS after accounting for variance due to age. Regression analysis indicated that SOS significantly increased as cortical index increased. Although the current study did not directly measure cortical area, it could be argued that cortical index is a measure of the relative amount of cortical bone located at the midshaft. Therefore, these results suggest that SOS in infants is significantly influenced by changes in the relative amount of cortical bone at the measurement site. Regression analysis indicated that SOS significantly decreased as medullary cavity diameter increased. After removing chronically ill infants from the analysis, there was no significant relationship between the tibial measurements and SOS after accounting for variation due to age. Among term born infants, midshaft diameter and medullary cavity diameter were significant predictors of SOS. After accounting for variance due to age, SOS decreased as medullary cavity and midshaft diameter increased. The increase in medullary cavity diameter and midshaft diameter may be suggestive of the decline in cortical index. These findings support the hypothesis that SOS is significantly associated with tibial structure. As was discussed, previously medullary cavity diameter significantly increased with age, while cortical index and SOS significantly decreased with age (**Table 5-1**). SOS may be measuring the reduction in proportion of cortical bone relative to bone size as a result of the increase in medullary cavity diameter and decrease in cortical index with increasing age.

Multiple regression analyses were conducted using stepwise variable selection to determine which factors, while controlling for age, accounted for the greatest variance in SOS. For the

pooled data, the model selected for predicting SOS included age, birthweight, height, medullary cavity diameter, cortical index, and midshaft diameter. This model accounted for ~53% of the variance in the SOS data, which accounted for quite a bit more of the variance than the hierarchical age model (35%). SOS significantly increased as birthweight increased, holding all other variables constant. Birthweight may have accounted for differences in SOS as a result of skeletal maturity reached by the time of birth. Increases in height had a positive influence on SOS, holding all other variables constant. Height is often used as an indicator of healthy development in infants and children. Pediatricians use growth percentiles for length and weight to track whether an infant appears to be growing normally. Height may have also accounted for some of the variance in SOS as a result of prematurity. Premature infants had significantly lower height measurements, but the significant relationship between height and SOS was not significant among the term born infants. After excluding chronically ill infants from analyses, age, birthweight and medullary cavity diameter were selected as significant predictors of SOS. Medullary cavity diameter, midshaft diameter, and cortical index are variables associated with bone shape and are affected by growth and health of the infant. In this model, SOS increased as medullary cavity and cortical index increased, while SOS decreased as midshaft diameter increased. Among term infants, only age and medullary cavity diameter were selected as significant predictors of SOS. As medullary cavity diameter increased SOS decreased among term born infants and infants without chronic illness. These results suggest that SOS measures skeletal changes as a result of age, skeletal maturity reached at time of birth, bone structure at the measurement site, and health factors that affect bone structure. Therefore, the multiple regression results support the hypothesis that SOS measures aspects of bone structure that are affected by growth. These results also suggest that SOS is multidimensional in the factors which influence it and supports the argument that SOS is affected by several characteristics which contribute to overall bone quality.

The negative effect on SOS with increasing medullary cavity size makes technological sense because ultrasound waves travel slower through soft tissue than through bone. The marrow within the medullary cavity would have decreased the velocity of the ultrasound signal. There was some concern that the ultrasound signal may have penetrated through the medullary cavity and into the cortex on the opposite side of the bone. Studies indicate that QUS axial measurements penetrate the periosteal/subperiosteal region by < 2 mm (Bossy et al. 2004a;

Bossy et al. 2004b). The distance between the periosteal surface adjacent the QUS probe and the endocortical wall on the opposite side of the medullary cavity was calculated for each infant. In no instance was this distance less than 2 mm, supporting the assumption that the ultrasound signal did not penetrate past the medullary cavity.

To my knowledge, the current study is the first infant study to compare SOS to bone cross-sectional measurements at the QUS measurement site. A study of older children, ranging from 3-21 years of age, compared SOS taken at the proximal phalange to bone width of the proximal phalange. The study results found that bone width had significant, but minor effects on SOS, accounting for ~6% of the variance (Baroncelli et al. 2001). Although the results of the current study seem to suggest that SOS in infants is influenced by the amount of cortical bone at the measurement site, as well as its distribution, the association between chronic illness and prematurity continue to confound the interpretation. A larger sample size of term infants without chronic illness across the entire age range (0-12 months) is needed to confirm these results.

### **Association between Traumatic Injury, Health, and Bone Health**

Results supported the hypothesis that the presence of traumatic injury is not related to indicators of overall health, body size, or bone health. Infants with traumatic injury showed no indication of compromised overall health, reduced bone mineralization, or growth deficiency. There were no infants with traumatic injury that were also chronically ill and/or premature. Infants with traumatic injury were not significantly different from those without traumatic injury in comparative analyses using BMD, SOS, or qualitative radiographic score data. Neither were there differences in body size between infants based on the presence of traumatic injury, with the exception of height. Although height was significantly different between infants with and without traumatic injury, there was no significant difference in length for age percentile. Therefore, there was no difference in body size between infants with and without traumatic injuries after accounting for variations in size due to age. The lack of any statistically significant differences between infants with and without traumatic injury suggests that the individuals who died of traumatic injury had comparable bone quality to the other infants in the study sample. These findings are important because they do not support the argument that infants with

traumatic injuries have poor bone quality or compromised bone strength which increases the risk for injury during normal handling.

### **Association between Chronic Illness, Growth, and Bone Health**

Differentiating between the effects of chronic illness on growth and bone health versus those due to prematurity was not possible due to the significant association between prematurity and chronic illness in the current study. Premature infants are at a high risk for the development of chronic illness due to immature organ systems that are not fully equipped to function in the extrauterine environment. Premature infants are at high risk for developing respiratory distress due to underdeveloped lungs. Infants in respiratory distress may require mechanical ventilation. Prolonged use of mechanical ventilation may result in the development of bronchopulmonary dysplasia, also called chronic lung disease (CLD), which is the inflammation and scarring of the lungs (Backstrom et al. 1996; Venkataraman et al. 1983). Persistent patent ductus arteriosus (PDA) is another common problem among premature infants (Hamrick and Hansmann 2010). The ductus arteriosus is a blood vessel that facilitates fetal circulation and is supposed to close after birth. When the ductus arteriosus fails to close, it is referred to as PDA. PDA has adverse effects on bone mineralization in premature infants. A study conducted on infants born at  $\leq 31$  weeks gestation found that premature infants with PDA had lower BMD than premature infants without PDA (Figueras-Aloy et al. 2014). PDA can result in low blood oxygenation, cardiomegaly (enlarged heart), and heart failure. In a multi-center study of preterm infants born at  $28 \pm 3$  mean gestational age, 31% of infants had symptomatic PDA requiring treatment or surgery (1993).

In conjunction to being born with limited nutritional stores relative to term born infants, it may be more difficult for premature infants to obtain adequate nutrition. Adequate nutrition is important for supporting bone mineral accretion. Infants born prior to 35-37 weeks gestation have difficulties with the suck-swallow-breathe pattern due to immature oral reflexes. An immature gastrointestinal (GI) tract hinders the ability to obtain adequate nutrition to support sufficient bone mineralization. Intestinal absorption of fat, calcium, and vitamin D is lower in preterm infants than term infants (King and Tavener 2014; Senterre and Salle 1982; Shaw 1976). Implementing enteral feeds before the GI system is mature enough can result in necrotizing

enterocolitis, intestinal tissue death (King and Tavener 2014). Infants that cannot feed normally require intravenous feeding or enteral feeding facilitated through a gastric tube (King and Tavener 2014). Intravenous feeding is called total parental nutrition (TPN). Long-term use of TPN is associated with reduced bone mineralization due to limits on the concentration of calcium and phosphorus (Figueras-Aloy et al. 2014). At high concentrations, the calcium and phosphorus will precipitate out of the solution. Maintaining adequate enteral or parenteral nutrition is complicated several other factors. Fluid intake is limited by the size of the infant and intake may be restricted as a treatment for other illnesses. Over intake of fluid is also problematic for infants with immature renal systems.

Therapeutic interventions used to treat chronic illnesses, including those associated with prematurity, may increase the risk for developing low BMD (Rigo and De Curtis 2006). As mentioned previously, respiratory distress may require mechanical ventilation. Diuretics are often used in combination with mechanical ventilation to decrease fluid buildup in the lungs. Diuretics cause increased urinary excretion of calcium, negatively affecting bone mineral metabolism (Venkataraman et al. 1983). Additionally, mechanical ventilation may require immobilization, increasing the risk of bone loss due to disuse (Backstrom et al. 1996). Glucocorticoids are used to reduce the inflammation caused by CLD, but prolonged and excessive use of glucocorticoids is detrimental to bone mineral metabolism by increasing bone resorption and decreasing bone formation (Canalis and Delany 2002; Kurl et al. 2000; Weiler et al. 1995). Infants with CLD have higher energy requirements due to the increased respiratory rate that results in higher energy expenditures (de Meer et al. 1997; Greer and McCormick 1986). Fluid restriction is used as a treatment to prevent pulmonary hypertension in infants with PDA (De Buyst et al. 2012). Pulmonary hypertension may result in permanent lung damage. However, the fluid restriction prevents maximum nutrient intake (Itabashi et al. 1999).

In the current study sample, there were 13 infants identified as chronically ill. Most of these infants were undergoing medical treatment or at least monitoring for their illness. Seven of the 13 chronically ill infants were premature (**Figure 4-3**). Of the premature infants with chronic illness, two had heart disease and one had heart disease and chronic lung disease. The heart disease was unknown prior to death in only one of these cases, and this infant died before 1 month of age. The other infants with heart disease were born extremely premature (25 weeks

EGA) and had been undergoing medical treatment/monitoring of their conditions. There were three premature infants with genetic disorders, all of which had been undergoing medical treatment/monitoring for their conditions. One of the infants had Trisomy 21 with associated congenital heart disease and was receiving TPN. Trisomy 21 has been associated with low BMD and reduced growth velocity between 3-6 months of age (Brook and Brown 2008c) One of the infants had Prader-Willi syndrome and was deficient in human growth hormone (HGH), but was undergoing HGH replacement therapy. HGH stimulates growth and influences the conversion of food into energy. HGH is produced by the pituitary gland. It has been reported HGH deficiency adversely affects bone mineralization and growth velocity (Bachrach 2001). Children with HGH deficiency have been found to have low areal (Saggese et al. 1993) and volumetric (Högler et al. 2005) lumbar spine BMD prior to therapy. Six months of GH replacement therapy positively affected growth velocity and 12 months positively affected BMD (Saggese et al. 1993). The third infant with a genetic disorder had Campomelic dysplasia which is caused by a gene mutation in Sox9. Sox9 is important in skeletal development (Bi et al. 2001). This infant had bowing of the long bones and clubbed feet. One of the premature infants had a seizure disorder that was treated with anticonvulsants since 3 weeks of age. Long-term anticonvulsant use is associated with reduced BMD (Sheth 2004).

Five term born infants were classified as chronically ill and one infant with an unknown EGA was classified as chronically ill. Two of the term born, chronically ill infants had heart disease. One of these infants had cardiomegaly with a widely patent foramen ovale. The second infant with heart disease had fibromuscular dysplasia resulting in subtotal occlusion of the coronary arteries. These conditions were not diagnosed prior to autopsy, so neither of these infants had been undergoing medical treatment/monitoring of their conditions. One of the term born infants had multiple congenital abnormalities that affected the heart, lungs, and liver. This infant had been undergoing medical treatment/monitoring prior to death. One of the term born, chronically ill infants had mitochondrial myopathy. Mitochondrial myopathy is a disease of the muscle mitochondria (DiMauro et al. 1985). Complications of mitochondrial myopathy are heart defects, diabetes, and stunted growth (Muscular Dystrophy Association Inc. 2015). This infant had a prolonged hospitalization due to their illness prior to death. One of the infants had a collagen 4A1 (COL4A1) disorder, cerebral palsy, and severe seizure disorder. This infant had been undergoing medical treatment/monitoring and was treated with anticonvulsants since birth.

COL4A1 disorder affects the type 4 collagen  $\alpha 1$  chain, which is an important component of vasculature, renal glomeruli, and ocular membranes (Vahedi and Alamowitch 2011). This infant was 9 months of age at the time of death. The chronically ill infant in which EGA was unknown had a seizure disorder since 1 month of age that was treated with anticonvulsants. This infant was 5 months of age at time of death.

***HYPOTHESIS 3A: CHRONIC ILLNESS IS NEGATIVELY ASSOCIATED WITH VARIABLES RELATED TO BODY SIZE.***

Although it was not possible to differentiate the effects of chronic illness on growth and bone health from those due to prematurity, the differences between infants with and without chronic illness were evaluated. Due to the detrimental effects on bone mineral metabolism and higher energy expenditure associated with chronic illness, it was hypothesized that chronic illness would be negatively associated with variables related to body size. Results did not support this hypothesis. There were no significant relationships between chronic illness and the variables associated with body size, even after accounting for variation due to age.

***HYPOTHESIS 3B: CHRONIC ILLNESS IS NEGATIVELY ASSOCIATED WITH TIBIAL GROWTH.***

It was also hypothesized that chronic illness would be negatively associated with tibial growth. More specifically, it was hypothesized that chronic illness would be negatively associated tibial length, midshaft diameter, cortical thickness, and cortical index. Medullary cavity diameter was hypothesized to be positively associated with medullary cavity diameter due to increased endocortical resorption. After accounting for variation due to age, infants with chronic illness had significantly lower tibial length, midshaft diameter, and cortical thickness. This is illustrated by comparing the light blue regression lines to the dark blue regression lines in **Figure 4-8**, **Figure 4-9**, and **Figure 4-11**. There was no significant association between chronic illness and medullary cavity diameter or cortical index.

The regression lines in **Figure 4-8** suggest that chronically ill infants began to catch up in tibial length to infants without chronic illness by ~8 months of life. Tibial midshaft diameter and cortical thickness remained significantly lower in chronically ill infants than infants without chronic illness, regardless of age. The relationship between age and midshaft diameter was more variable among chronically ill infants than infants without chronic illness. Tibial midshaft

diameter increased after birth, but the rate of increase sharply declined by ~3 months of birth and appeared to decrease until ~8 months of age, which may indicate growth disturbance in periosteal expansion among the older chronically ill infants (**Figure 4-9**). Tibial midshaft diameter appeared to increase after 8 months of age, but remained lower than in the infants without chronic illness. Interestingly, there appeared to be no significant relationship between cortical thickness and age among the chronically ill infants, further suggesting a growth disturbance not observed among infants without chronic illness. Expansion of the medullary cavity appeared to occur at reduced rate in chronically ill infants relative to infants without chronic illness (**Figure 4-10**). Cortical index tended to be lower in chronically ill infants than infants without chronic illness (**Figure 4-12**), but this difference was not significant.

In general, these results support the hypothesis that chronic illness is negatively associated with tibial growth. Linear growth of the tibia occurred at a significantly lower rate in chronically ill infants than infants without chronic illness, but appeared to catch up in tibial length by the end of the first year of life. Midshaft diameter and cortical thickness remained significantly lower in chronically ill infants throughout the first year of life. Medullary cavity diameter was insignificantly smaller in chronically ill infants. Significantly smaller midshaft diameters without significant differences in medullary cavity diameters resulted in significantly lower cortical thickness in chronically ill infants. Another important observation was the lack of a relationship between cortical thickness and age among chronically ill infants (**Figure 4-11**), suggestive of a growth disturbance. It should be kept in mind that there were only five term infants with chronic illness. Therefore, these results may not be representative of term born infants with chronic illness.

***HYPOTHESIS 3C: CHRONIC ILLNESS IS SIGNIFICANTLY RELATED TO MEASURES OF INFANT BONE HEALTH.***

Once evidence of the detrimental effect of chronic illness on tibial growth was obtained, analyses were conducted to determine whether the detrimental effects of chronic illness on tibial growth were also reflected by indicators of tibial bone health, such as SOS, BMD, and qualitative radiographic evaluation. There was no significant association between chronic illness and SOS, but there were significant associations between chronic illness and BMD, as well as radiographic score. Chronically ill infants had significantly lower BMD estimates and greater qualitative



radiographic scores (indicative of demineralization or abnormal mineralization) than infants without chronic illness. These findings indicate that the chronically ill infants in the current study sample experienced a significant degree of macroscopic bone loss, which supports the hypothesis that chronic illness is negatively associated with indicators of bone health.

There is a large body of literature on the effects of chronic illness on BMD (Bachrach 2001; Binkovitz et al. 2007; Brook and Brown 2008a; Done 2012; Koo 1996; Sheth 2004; Specker et al. 2001). The degree to which chronic illness affects BMD depends on disease duration and severity (Bachrach 2001). Chronic illness can affect bone mineralization directly, as in osteogenesis imperfecta, or secondarily through complicating factors such as malnutrition, immobilization or decreased physical activity, and medications with adverse effects on bone mineral metabolism. A large number of chronic illnesses are associated with reduced BMD. Some broad categories of chronic illnesses that are associated with low BMD include specific genetic disorders, liver disease, renal disease, congenital heart disease, malabsorption disorders, lung disease, neurological disease, and endocrine disorders (Bachrach 2001; Binkovitz and Henwood 2007; Binkovitz et al. 2007; Brook and Brown 2008a; Brook and Brown 2008b; Brook and Brown 2008c; Carrascosa et al. 1996; Done 2012; Holm 2007; Koo 1996; Rigo and De Curtis 2006; Specker et al. 2001; Specker and Schoenau 2005). There were 13 chronically ill infants in the current study sample. These chronic illnesses have already been described in **Table 4-3**. For information on the specifics of each chronically ill infant see **Table A- 2** and **Table A- 7** in the Appendix.

Although there was a significant relationship between qualitative radiographic score and chronic illness, evaluation of the qualitative radiographic scores for the chronically ill infants highlights the large degree of error associated with this method. There were two cases of chronically ill infants with abnormally mineralized bone and three cases with indeterminate bone loss on radiographs (**Table A- 5**). There were also three chronically ill infants that were classified as completely normal radiographically. However, these three infants were 1 month of age or less. It is possible that these three infants died before the sequelae of their chronic illness/disease became overtly manifest at the macroscopic level. In normal term infants, it is rare for rickets or osteomalacia to be observed in infants before 4 months of age and is most commonly observed in infants at least 6 months of age due to the increased accretion of bone mineral that occurs during

the last trimester of gestation (Imel et al. 2014). These three infants reached 36 weeks gestation at time of birth, which is one week shy of being considered full term. It is possible that the infants were able to maintain sufficient metabolic function with the available stores of bone mineral that built up during the last trimester of gestation. This may suggest that, in term infants, bone is more resistant to insult during the first months of life than previously assumed.

While chronically illness had a significant negative relationship with bone mineralization, the relationship between SOS and chronic illness did not mirror this finding. Chronic illness had no significant effect on SOS, even after premature infants were removed from the analysis. This result did not support the hypothesis that SOS was significantly negatively associated and chronic illness and is contradictory to other pediatric studies. Studies have found that duration of total parenteral nutrition (McDevitt et al. 2007; Rack et al. 2012; Tansug et al. 2011; Tomlinson et al. 2006; Yiallourides et al. 2004), mechanical ventilation, and treatment with corticosteroids or diuretics were inversely related to SOS (Rack et al. 2012). A longitudinal study which followed preterm infants up to 35-37 weeks corrected gestational age reported no significant difference between infants with or without chronic lung disease, but the few infants that developed necrotizing enterocolitis had some of the lowest SOS measurements in the study sample. Pediatric studies of older children with chronic illnesses, such as Crohn's disease, rheumatic diseases, Type 1 diabetes, and illnesses resulting in severe handicaps, report that chronically ill children had significantly lower SOS than children without chronic illness (Damilakis et al. 2004; Hartman et al. 2004a; Hartman et al. 2004b; Hartman et al. 2004c; Levine et al. 2002; Zadik et al. 2005). The current study may have found no significant differences between infants with and without chronic illness due to possible confounding effect of the association between prematurity and chronic illness. Another possible explanation is that duration of chronic illness in these infants was not long enough to have a significant effect on SOS. However, this seems unlikely due to the significant effect of chronic illness on BMD among the infants in the current study.

## **Association between Skeletal Maturity at Birth, Body Size, Tibial Structure, and Bone Health**

### ***HYPOTHESIS 4A: SKELETAL MATURITY AT BIRTH IS SIGNIFICANTLY RELATED TO BODY SIZE.***

Skeletal maturity at birth was hypothesized to be significantly related to body size during the first year of life. The reasoning behind this hypothesis was that longer gestation times result in larger body sizes at birth and that body size continues to be larger throughout the first year of life. Additionally, the likelihood of chronic illness and metabolic disturbance as gestational age at birth decreases for reasons that were previously discussed.

To determine whether increased skeletal maturity at birth had positive effects on variables related to body size, regression analyses were conducted which predicted the body size variables using mean centered EGA and mean centered birthweight. Age was used as a covariate in models predicting height and weight. Analyses indicated that height, length for age percentile, weight, and weight for age percentile significantly increased for each week increase in EGA greater than the mean. The same results were obtained for each kg increase in birthweight greater than the mean. Weight for length percentile significantly decreased for each week increase in EGA greater than the mean. These findings supported the hypothesis that greater skeletal maturity at birth is related to greater body size in infants.

To confirm that prematurity had a significant negative relationship with body size during the first year of life, one-way ANOVAs were used to test for significant differences in body size between term and premature infants. Age was used as a covariate in models predicting height and weight. Infants that were born prematurely were significantly smaller in height, length for age percentile, weight, and weight for age percentile than term born infants. Weight for length percentile was significantly greater among infants born prematurely. This indicated a significant difference in fat distribution between premature and term born infants. These results support the hypothesis that prematurity is negatively associated with body size.

***HYPOTHESIS 4B: SKELETAL MATURITY AT BIRTH IS SIGNIFICANTLY RELATED TO TIBIAL MEASUREMENTS.***

Prematurity is widely reported to have adverse effects on skeletal health (Barltrop et al. 1977; Done 2012; Imel et al. 2014; Ortner 2003b; Senterre and Salle 1982; Shaw 1976). The degree of adverse effect on skeletal health depends on severity of associated chronic illness and degree of prematurity. Based on detrimental effects of prematurity on skeletal health, it was hypothesized that the tibial measurements would be positively associated with increased birthweight and EGA. Regression analyses were used to evaluate the relationships between skeletal maturity at birth and the tibial measurements. Age was used as a covariate in all analyses. Analyses indicated that as EGA and birthweight increased tibial length, cortical thickness, midshaft diameter, and medullary cavity diameter significantly increased. There was no relationship between cortical index and EGA or birthweight. Analyses were repeated with chronically ill infants excluded from the analysis to determine if the significant relationship between skeletal maturity at birth and tibial size were due to the chronically ill infants in the analyses. After exclusion of chronically ill infants from analyses, EGA and birthweight remained significant predictors of tibial length, midshaft diameter, and cortical thickness, even after accounting for variation due to age. EGA and birthweight were no longer significant predictors of medullary cavity diameter. Therefore, EGA and birthweight had positive relationships with linear and appositional growth of the tibia among infants without chronic illness. These findings support the hypothesis that increased skeletal maturity at birth resulted in greater tibial size, even after accounting for variation due to age and chronic illness. However, increased skeletal maturity at birth had no relationship with the amount of cortical bone relative to cross-sectional size.

To determine if prematurity significantly affected skeletal health in the current study sample, one-way ANOVAs were conducted. Analyses indicated that premature infants had significantly lower tibial length, midshaft diameter, and cortical thickness, and medullary cavity diameter than term born infants even after accounting for variation due to age. These findings support the hypothesis that prematurity has a significant negative relationship with tibial size, but not the relative amount of cortical bone to bone size.

Due to the significant association between chronic illness and prematurity in the current study, the detrimental effects of these factors cannot be entirely separated. However, the separation of

the effects of prematurity from chronic illness may not be necessary. Whether the metabolic disturbance is caused by chronic illness or nutritional deficiency is of little consequence due to bone's limited response to illness and/or nutritional deficiencies. Bone responds to these stresses by altering bone deposition (decrease or increase), resorption (decrease or increase), or through a combination of altered deposition and resorption (Salter 1999b). The effects of chronic illness and prematurity on growth of the tibia in the current study are consistent with the negative effects of metabolic disturbance on skeletal growth reported in the clinical and anthropological literature. The presence of skeletal lesions has been used in anthropological studies as an indicator of metabolic stress due to disease load and/or nutritional deficiency. Eleazer (2013) used a subadult cemetery sample to evaluate the effects of metabolic stress and mechanical loading on cross-sectional geometry of the rib, femur, and humerus during growth. The subadult sample was divided into lesion/no-lesion groups to differentiate between chronically stressed and acutely/non-stressed subadults, respectively. Long bone lengths did not significantly differ between stress groups, but long bone lengths tended to be lower among subadults between 1 and 7 years of age with lesions than subadults with no lesions. Medullary area was non-significantly greater in the elements of lesion group than the no lesion group. Relative cortical area tended to be lower in all three elements of the lesion group, while total area was slightly non-significantly greater in the lesion group. This suggested that the lesion group experienced greater endosteal resorption than the no-lesion group due to metabolic disturbance, but that the lesion group also experienced mechanical compensation for the loss of cortical bone through slightly greater periosteal expansion. In the lesion group, the femur showed the greatest reduction in relative cortical area elements, but the least amount of mechanical compensation through periosteal expansion. Even with the lower degree of compensation through periosteal expansion, the femur remained non-significantly stronger in bending rigidity relative to the humerus. Eleazer (2013) concluded that the non-significant reduction in cortical bone in the lesion group did not result in decreased bone rigidity. Compensation through periosteal expansion resulted in non-significantly greater bending rigidity in the elements of the lesion group than the no-lesion group. Therefore, chronic metabolic stress reduced macroscopic bone mass, but mechanical compensation through diaphyseal expansion increased the strength properties in the same bone (Eleazer 2013). Skeletal elements responded to metabolic bone loss by maintaining relative resistances to mechanical loading through periosteal expansion (Eleazer 2013).

Eleazer (2013) also reported that chronic metabolic stress was associated with microscopic bone loss, but not in the same pattern between the stress groups. In the no-lesion group, more cortical bone (microscopic bone loss) was removed from the femur during remodeling, as was expected for a highly loaded bone. In the lesion group, microscopic bone loss preferentially occurred in the humerus and did not occur in the femur or rib. The femur and rib of the lesion group showed the greatest reductions in relative cortical area in comparison to the no-lesion group. The humerus showed the least amount of reduction in relative cortical area for the lesion group, but was the only element with microscopic bone mass reduction in the lesion group. This suggested that metabolic stress disrupts the effects of mechanical loading on cortical bone, as indicated by the microscopic resorption observed in the humerus of the lesion group and not the femur. Additionally, this suggests that, under chronic stress, microscopic bone mass in highly loaded elements is conserved.

The findings of Eleazer (2013) are consistent with the finding of significantly lower tibial length and cortical thickness among the chronically ill and premature infants in the current study sample. Differences in cortical index were not statistically significant, but cortical index tended to be lower among premature and chronically ill infants. Tibial midshaft diameter was not significantly greater among the premature and chronically ill infants as was observed by Eleazer (2013), but this is likely due to the younger age group and the associated limited degree of mechanical loading in the current study sample. In contrast, midshaft diameter was significantly lower among chronically ill and premature infants. Mechanical compensation by periosteal expansion would not be expected in infants that are non-ambulatory, which made up the largest proportion of the current study sample.

Mensforth (1985) conducted a study comparing two archeological samples with exposure to differing levels of environmental stress also found significant differences in skeletal growth. Degree of environmental stress was inferred from second year death rates and the frequency of periosteal reactions for each age cohort of each population sample. Tibial length was comparable between the two groups for the first six months of life. After 6 months of life, diaphyseal growth of the tibia was delayed in the sample which experienced greater environmental stress. The greatest degree of growth delay occurred between 6 and 24 months of age (Mensforth 1985). The differences between groups were not statistically significant, but the lack of significance may

have been due to small sample sizes. In contrast to Mensforth (1985), the current study did not find comparable tibial lengths during the first 6 months of life between infants with and without chronic illness. The significant differences in tibial length based on chronic illness during the first six months of life may have been caused by the association between prematurity and chronic illness in the current sample, which was not a likely factor in the archeological groups.

***HYPOTHESIS 4C: SKELETAL MATURITY AT BIRTH IS SIGNIFICANTLY RELATED TO MEASURES OF INFANT BONE HEALTH***

Due to the previously discussed negative effects of prematurity on skeletal health, skeletal maturity at birth was hypothesized to be significantly related to BMD, qualitative radiographic score, and SOS. Regression analyses were conducted using mean centered EGA and mean centered birthweight to predict BMD and SOS. One-way ANOVAs were conducted to evaluate whether there were significant differences in BMD, SOS, and qualitative radiographic score between premature and term born infants.

Mean centered birthweight was a significant predictor of BMD, but mean centered EGA was not. After exclusion of chronically ill infants from the analyses, BMD was no longer significantly related to birthweight. These findings may suggest that birthweight is an important predictor of BMD among chronically ill and possibly premature infants, as prematurity and chronic illness were significantly associated in the current sample. There was no significant difference in BMD between term born and premature infants. These findings only partially support the hypothesis that BMD is significantly related to skeletal maturity at birth. Birthweight was a significant predictor of BMD, but this may have been related to the chronically ill or premature infants in the sample. BMD was not significantly associated with prematurity, but this result cannot be stated with confidence due to the significant relationship between BMD and chronic illness and the significant association between prematurity and chronic illness in the current study.

It is well documented that, relative to term infants, preterm infants have lower mineral stores at birth and reduced calcium and vitamin D absorption, resulting reduced BMD (Senterre and Salle 1982). There are numerous DXA studies which excluded infants with chronic illness that report a positive association between BMC and/or BMD measurements and gestational age at birth (Ahmad et al. 2010; Atkinson and Randall-Simpson 2000; Hayashi et al. 1996; James et al.

1986; Koo et al. 2002; Koo and Hockman 2000; Koo et al. 1996; Kurl et al. 2000; Rigo et al. 1998; Sievanen et al. 1999; Vyhmeister et al. 1987). It was not likely that the age of the infants played a role in the inconsistency between the current study's findings and other studies, as all premature infants without chronic illness ranged from 2-4 months of age. The small sample size of premature infants with associated BMD data, and without chronic illness ( $n = 5$ ) may be responsible for the contrasting findings. EGA ranged from 26-36 weeks gestation among these infants. Significant differences may not have been detected due to the combination of small sample size and large range in EGA.

A large number of infant QUS studies have evaluated the effects of skeletal maturity at birth on SOS. Based on these studies, it was hypothesized that SOS would be significantly related to skeletal maturity at birth. Regression analyses were used to test this hypothesis and age was used as a covariate. In the current study, EGA and birthweight were significant positive predictors of SOS. These findings are consistent with reports from other studies (Chen et al. 2012; Littner et al. 2003; McDevitt et al. 2007; Nemet et al. 2001; Pereda et al. 2003; Rack et al. 2012; Rubinacci et al. 2003; Tansug et al. 2011; Teitelbaum et al. 2006; Tomlinson et al. 2006). These studies propose that maturity at time of birth is the main factor influencing SOS and not overall body size at birth. The findings of the current study support this proposal. While holding age constant, SOS increased by 96 m/s with every 1 kg increase in birthweight. With every 1 week increase in EGA, SOS increased by 18 m/s. This is similar to the increase in SOS reported by the manufacturer for each week gain in EGA between 26-40 weeks gestation, 15 m/s (Littner et al. 2003; Zadik et al. 2003). After chronically ill infants were excluded from the analyses, EGA and birthweight remained significant predictors of SOS in the current study. However, once premature infants were excluded from the analysis, EGA and birthweight were no longer significant predictors of SOS. This suggests that gains in birthweight and EGA after reaching term age ( $\geq 37$  weeks gestation) resulted in no statistically significant gains in SOS. These findings support the hypothesis and indicate that the detrimental effects on bone health and structure due to prematurity effect measures of SOS.

For premature infants, postnatal bone loss can be detrimental to the skeleton. Premature infants either do not have the opportunity to experience or complete the skeletal mineral accretion that should have occurred during the last trimester *in utero*, resulting in adverse effects on the infant



skeleton. Studies comparing SOS between newborn term and premature infants report that preterm infants had significantly lower SOS than term infants (Chen et al. 2012). It has been reported that premature infants reaching term age continued to have significantly lower SOS than newborn term infants (Altuncu et al. 2007; Nemet et al. 2001; Rack et al. 2012). In the current study, it was hypothesized that prematurity would have a significant negative relationship with SOS. One-way ANOVA was used to predict SOS using prematurity as the dependent variable. Results indicated that premature infants had significantly lower SOS than term infants. While the removal of premature infants from the regression analysis had limited effect on the relationship between age and SOS, the relationship between SOS and age among premature infants was substantially different from relationships based on the pooled data or the term infants. As was discussed previously, reanalysis of the data using only the term infants revealed a cubic trend between age and SOS that was similar to the analysis using the pooled data, but with slopes that were slightly more shallow (**Table 4-14, Figure 4-30**). A quadratic trend was observed for the relationship between age and SOS among the premature infants (**Table 4-17**). The difference in severity of postnatal decline in SOS with increasing age is reflected in **Figure 4-32**. Among premature infants, SOS steeply declined until ~4-5 months of age, at which point it increased with age. The slope for age indicated that the postnatal decline in SOS was much more severe in premature infants than term infants. In addition, the subsequent increase in SOS appeared to commence later in premature infants, after 5 months of age, than term infants, a gradual increase after 3 months of age. The increase in SOS data from premature infants greater than 5 months of age is suggestive of the recovery in BMD which reportedly occurs in preterm infants between 6-12 months of age (Lapillonne et al. 1994; Specker et al. 2001; Wauben et al. 1998). However, too much weight should not be given to the preterm data due to the limited number of preterm infants greater than 5 months old ( $n = 4$ ).

The greater severity of the initial postnatal decline in SOS among premature infants, relative to term infants, is consistent with reports from other studies (McDevitt et al. 2007; Ritschl et al. 2005; Tansug et al. 2011; Tomlinson et al. 2006). Reportedly, the decline in SOS is the most severe for the most premature infants (24-27 weeks EGA) (Tomlinson et al. 2006). A longitudinal study of preterm infants reported that preterm infants tended to reach their lowest SOS at ~3 months of age while term infants tended to reach their lowest SOS by 6 months of age (Ritschl et al. 2005). In the current study, the lowest SOS tended to occur at 4-5 months of age in

premature infants and 2-3 months of age in term infants. Differences in age at nadir may have resulted from comparing a longitudinal study to a cross-sectional study. Inclusion of chronically ill infants in the analysis may be another explanation for the difference, as this likely increased the variation in SOS among both the term and premature infants.

## **Relationships between Measures of Bone Quality**

### ***HYPOTHESIS 5A: BMD HAS A NEGATIVE RELATIONSHIP WITH QUALITATIVE RADIOGRAPHIC SCORE.***

Qualitative evaluation of radiographs is a common practice for screening infants at high risk for osteopenia due to prematurity and/or chronic illness. If perceived degree of bone mineralization on radiographs is a true reflection of BMD, there should be a significant relationship between qualitative radiographic scores and the BMD estimates. It was hypothesized that BMD would have a negative relationship with greater radiographic scores. Regression analysis was used to evaluate the relationship between qualitative radiographic score and BMD. No statistically significant relationship was found between BMD and qualitative radiographic evaluation scores. Upon examination of the distribution of BMD data by radiographic mineralization score (**Figure 4-32**), the lack of association between these indicators of bone quality becomes clear. Many of the infants with normal radiographic evaluation scores had low BMD values. These results did not change after exclusion of chronically ill infants or premature infants from the analyses. Although no significant association was found between BMD and qualitative radiographic score, both BMD and qualitative radiographic score was significantly related to chronic illness, as was discussed above. In conjunction, these findings lend partial support to the hypothesis that qualitative radiographic score is significantly negatively related to BMD. There may be no significant relationship among infants without chronic illness, but there does seem to be a relationship among chronically ill infants.

The insignificant results indicate there is a large degree of error associated the qualitative assessment of bone mineralization from radiographs. Although BMD estimates were on the low end of the continuum, mineralization appeared normal on radiographs. These findings are consistent with previous studies that compared rickets diagnoses made from qualitative assessment of radiographs to diagnoses based on measurements of BMD or biochemical analyses

(Fraser et al. 1967; James et al. 1986; Kruse 1995; Mulugeta et al. 2011). James and colleagues (1986) report a weak but significant correlation between radiographic appearance and bone mineral content. However, at 40 weeks postconceptual age, four of the six preterm infants with normal radiographic scores had BMC measurements that were 3.7 to 6.5 *SDs* below the mean for infants born at term (James et al. 1986). A pediatric study evaluating the biochemical characterization of the three stages of vitamin D deficiency reported that radiographic indicators of rickets remained mild during the first stage of rickets and did not become moderate to severe till the disease progressed to stages 2 and 3 (Kruse 1995). If the radiographic indicators of rickets do not become moderate or severe until stage 2 or 3, it is conceivable that demineralization of bone, indicated by low BMD values, could be missed during qualitative radiographic evaluation. Another pediatric study reported that radiographic indicators of rickets were minimal in infants during the first stage of vitamin D deficiency (Fraser et al. 1967). As with the previously mentioned study, stage of vitamin D deficiency was assessed using biochemical analyses. The results of these previous studies were consistent with studies that report a large amount of BMD must be lost (reports vary between 30-40%) before osteopenia/osteoporosis is reliably identified on radiograph (Bachrach et al. 2007; Barden and Mazess 1988; Done 2012; Sievanen et al. 2001). A study examined inter-observer agreement of osteopenia/osteoporosis diagnosis based on qualitative radiographic evaluation (Mulugeta et al. 2011). Correct diagnosis of osteopenia was determined by DXA Z-score values of lumbar BMD measurements. Inter-observer agreement was 71% for normal bone mineralization, 25% for severe demineralization, and 0% for mild demineralization. Determination of normal bone mineralization was adequate, but the diagnosis of osteopenia/osteoporosis in children based on radiographs of the appendicular skeleton had low sensitivity and poor inter-observer agreement. The results also indicated that the reliability of the diagnosis improved with increasing severity of the BMD loss (Mulugeta et al. 2011), which is consistent the finding of a significant relationship between chronic illness and both BMD and qualitative radiographic score.

***HYPOTHESIS 5B: SOS HAS A SIGNIFICANT POSITIVE RELATIONSHIP WITH BMD.***

BMD was an indicator of bone quality in the current study. A significant relationship between BMD and SOS would be indicative that SOS is influenced by a significant component of bone quality. As such and based on previous studies, it was hypothesized that SOS would have a

significant positive relationship with BMD. Regression analyses indicated no significant relationship between SOS and BMD, even after accounting for age and excluding chronically ill and premature infants from analyses. These findings did not support the hypothesis and were quite unexpected. Previous pediatric studies reported low but significant correlation between SOS readings and BMD or bone mineral content measured by DXA or ashing (Ahmad et al. 2010; Fielding et al. 2003; Jaworski et al. 1995; Sundberg et al. 1998; van Rijn et al. 2000; Wright et al. 1987). Differences in age distribution between the study samples utilized by these studies and the current study sample may have resulted in the lack of correlation between BMD and SOS. These other studies examined term infants within a few days of birth, premature infants up to 3 months of age, or children older than 5 years of age, while the current study sample included preterm and term infants which ranged from birth to 12 months. It is possible that the broad age span of our study sample may have suppressed any statistically significant relationship between SOS and BMD. The first year of life is a period of remarkable growth and development. As age increases, the relationship between SOS and BMD may change as a consequence of growth, suppressing associations between the variables by increasing the overall variance in the data. Another possible explanation is that the significant correlation between BMD and SOS develops at some point after the first year of life, since SOS and BMD are significantly correlated in adults and some pediatric studies. It cannot be known whether SOS and BMD values are unrelated during the first year of life until volumetric BMD obtained from the SOS measurement site is compared SOS measurements collected from a larger sample of healthy and chronically ill infants that includes both term born and premature infants.

Although there was no significant relationship between SOS and BMD, SOS and BMD appear to be affected by similar factors. After birth, both BMD and SOS decline with increasing age. It is possible that the factors influencing the postnatal decline in SOS and BMD are inter-related but different factors. For instance, BMD was significantly affected by chronic illness, but was not significantly affected by prematurity after accounting for chronic illness. In contrast, SOS was significantly affected by prematurity and not chronic illness. Yet, chronic illness and prematurity were significantly associated in the current study sample. Another possibility is that the small sample size of chronically ill term born, infants ( $n = 5$ ) may have prevented any statistically meaningful comparison. Numerous studies on older children have found chronically ill infants have significantly lower SOS than infants without chronic illness (Damilakis et al. 2004;

Hartman et al. 2004a; Hartman et al. 2004b; Hartman et al. 2004c; Levine et al. 2002; Zadik et al. 2005). It is also possible that the adverse effects of chronic illness on SOS develop some time after the first year of life, but this seems unlikely since chronic illness had already manifested negative effects on BMD in the current study sample.

Researchers have suggested that SOS and BMD measure overlapping but not identical properties of bone related to bone quality (Baroncelli et al. 2001; Fricke et al. 2005). A study of healthy children aged 11 to 16 years lends support to this argument. In this study, the lowest quartiles for SOS and BMD did not contain the same individuals from the study sample (Sundberg et al. 1998). Consistent with the findings of the current study, a study of 10-12 year old healthy children found no significant correlation between BMD and SOS (Rebocho et al. 2014). The study also reported that there was only a 36.3% overlap among individuals in the lowest tertiles of SOS and BMD. An important finding of Rebocho and colleagues (2014) was that radial SOS, and not BMD, was the only significant variable which predicted past fracture (Rebocho et al. 2014); supporting the argument that SOS and BMD measure different aspects of bone quality. Findings of the current study also support this argument by showing that prematurity had a greater influence on SOS while BMD was more greatly influenced by chronic illness. More research with finer grained measurements of bone properties is necessary to test this hypothesis.

***HYPOTHESIS 5C: SOS HAS A SIGNIFICANT NEGATIVE RELATIONSHIP WITH QUALITATIVE RADIOGRAPHIC SCORE.***

To determine whether degree of perceived mineralization was significantly associated with SOS readings, the relationship between qualitative radiographic evaluation scores and SOS was evaluated using regression analyses. It was hypothesized that SOS would have a significant negative relationship with increased radiographic scores. The reasoning behind this hypothesis was that increased radiographic evaluation scores indicated demineralization or abnormal mineralization, which has negative effects on bone quality. These negative effects on bone quality would be reflected by lower values of SOS. Analyses indicated no significant relationship with SOS. Results remained the same for term born infants and after the exclusion of chronically ill infants. This finding was not unexpected since qualitative radiographic score was not significantly related to BMD during direct comparisons of these variables. Additionally, the large

degree of error associated with the qualitative radiographic method may have introduced a large amount of statistical noise into the analysis.

### **Limitations**

The current study has several limitations. The use of a cadaver study sample limited the extrapolation findings to living infants. An assumption of this study was that the infants without significant biological findings at autopsy, to explain death, were “healthy” or in “normal” health at the time of death and would have bone quality comparable to living infants of the same age. Since truly healthy infants do not die without biological cause, this assumption may not be accurate. There may have been yet unknown factors, which influenced the likelihood of death for the infants versus those infants that continued to live. These unknown factors may have also influenced infant bone quality, limiting the applicability to living infants. Another limitation was the number of chronically ill ( $n = 13$ ) infants. The low number of these types of cases limited the statistical analyses performed on the study sample data, and therefore the conclusions that could be drawn.

Although there is no way of knowing if the infants in the study sample have comparable bone quality to living infants, tibial measurements in the current study did not appear to be significantly different from measurements of living infants reported in the literature. The range of tibial length from birth to 12 months of age among term born infants in the current study was consistent with previous studies (Anderson et al. 1964; Gindhart 1973; Maresh 1970; Stuart et al. 1940; Trotter and Peterson 1969). With the exception of the Trotter and Peterson (1969), all measurements were taken on living, healthy infants in these previous studies. The consistency between tibial lengths of the current study sample and those reported in the literature suggests that linear growth in the current study sample was at least comparable to linear growth in living infants. As with tibial length, midshaft diameter was comparable between the current sample and studies evaluating healthy, living infants (Maresh 1970; Stuart et al. 1940). The similarities in the ranges of tibial midshaft diameter between the current study sample and diameters reported in the literature support the argument that growth in the current study sample was at least comparable to growth in healthy, living infants

Classifying bone as either normal or abnormal is a difficult task due to the numerous factors contributing to bone's ability to function as a mineral reservoir as well as resist fracture. At the outset of this research, it was planned to use histological evaluation as the gold standard for determining bone health status. Cellular functioning is a very important building block for overall bone health, but no standards have been developed for the evaluation of bone health in infants. Results from histological evaluation could not be validated and were excluded from analyses. Clearly there is a relationship between bone's ability to function as an organ maintaining mineral homeostasis and its ability to resist fracture, but much more remains to be elucidated about this relationship and how it changes as a result of growth during infancy.

The limited number of influential factors on SOS evaluated in the current study relative to the complexity of the topic of bone quality may be considered another limitation. This study evaluated growth and environmental factors that may have influenced SOS such as body size, tibial structure, chronic illness, and skeletal maturity at birth. There are many more factors that need to be evaluated as possible influential factors on SOS. For instance, prenatal factors such as maternal tobacco and illicit drug use may have adversely affected SOS. Cross-sectional properties of the tibial midshaft were not calculated because radiographs were only taken in the anterior-posterior plane. Calculation of cross-sectional properties would have required an assumption of a circular cross-section, which may not be a valid assumption for the tibia. Therefore, cross-sectional properties which are correlated with strength in bending were not evaluated. Additionally, the effects of bone micro-architectural and tissue-level properties on SOS were not evaluated. However, it is not possible to account for every environmental and biological factor that may have affected SOS. More research on cross-sectional, micro-structural, and tissue-level properties of infant bone is needed as these properties remain poorly understood for infants, as well as the relationship between these properties and SOS during infancy.

The low resolution technology used to obtain the BMD data was another limitation. Units of x-ray attenuation from digital radiographs may not be sensitive enough (i.e. too low in resolution) to adequately measure BMD in low density bone. A study evaluating the correlation between ash weight of defatted bone and bone mineral density calculated using the x-ray attenuation method (radiographic absorptiometry) reported a significant decrease in accuracy when the bones are covered by soft tissue (Baker et al. 1959). In adults, this method can determine bone loss within

broad limits (10-20%) (Mimouni and Littner 2004). Partial volume effect is an inherent limitation in the use of x-ray attenuation units to calculate BMD (Schönau 1998). Partial volume effect occurs when a pixel only contains a portion of the bone image, such as the periosteal or endosteal edges of a bone. The density of the bone that is captured in a single pixel is average out over the entire pixel causing the mean density of that pixel to be lower than the actual density of the portion of bone. In infants, this is especially problematic because they have relatively thin cortical walls causing a greater number of pixels to be partially filled. The greater number of partially filled pixels results causes an artificial reduction in the mean density calculated for the entire bone (Schönau 1998). The difference between the actual bone density of a bone and the measured bone density is referred to as the measurement error. In the current study, there may have been increased measurement error introduced by partial volume effect. Partial volume effect cannot be avoided, but it can be reduced by using a higher resolution technology to measure BMD. Additionally, higher resolution technologies, such as DXA or CT, would be able to detect smaller differences in BMD that is possible through the use of x-ray attenuation.

The utilization of a study sample from the medical examiner's setting may have also affected the relationship between SOS and BMD measurements. The majority of infants in our study sample were considered in "normal" health at the time of death because the cause of death for most of the infants was SUID or Undetermined (co-sleeping). These classifications for cause of death are applied to infants in whom there are no physiological findings at autopsy that explain the death. But, with the exception of accidental deaths, these infants cannot actually be considered completely normal because it seems unlikely that infants in completely normal health die without a physiological cause. At time of death, over 40% of the study sample fell below the 25<sup>th</sup> percentile for height and weight. This may indicate differences in growth between living and deceased infants, but growth percentiles are meant to track growth and not meant to be used to evaluate growth at a single point in time. The large proportion of infants in the current study sample that were below the 25<sup>th</sup> percentile at their time of death may be coincidental. This possibility is supported by the comparable tibial lengths and widths reported in the current study sample in relation to those reported by studies of living, healthy infants. The possible difference in growth is simply meant to illustrate that there may be a number of unidentified, environmental and/or biological factors that predisposed these infants to death. These unidentified factors may or may not have also affected BMD of the study sample. If so, SOS and BMD of deceased



infants may not exhibit the same association as has been reported for *in vivo* population samples. To our knowledge, only one other study has used a cadaveric sample to determine whether SOS could be used to assess bone status in infants (Wright et al. 1987). Wright and colleagues (1987) reported a significant positive correlation between BMD and SOS measurements obtained from the distal radius and ulna of 13 deceased newborn infants.

## CHAPTER 6 : CONCLUSIONS AND RECOMMENDATIONS

Age-related changes in tibial measurements were significantly related to growth-related changes in body size as was hypothesized. Tibial size increased as overall body size increased, with the exception of cortical index. These results suggest that increased body size for age is associated with greater overall tibia size, but not necessary a more robust structure as the proportion of cortical thickness to midshaft diameter did not significantly differ based on body size. The lack of association between cortical index and body size is likely due to the reduced amount of mechanical loading in the study sample. Most of the infants in the study sample were non-ambulatory.

SOS and BMD were both significantly related to age as was hypothesized. BMD showed a significant postnatal decline. The postnatal decline in BMD is consistent with studies that report BMD and cortical area decline during the first 3-6 months of life (Altuncu et al. 2007; Litmanovitz et al. 2003; Litmanovitz et al. 2004; Mercy et al. 2007; Nemet et al. 2001; Ritschl et al. 2005; Rubinacci et al. 2003; Tansug et al. 2011; Tomlinson et al. 2006). SOS also showed a significant postnatal decline, but the relationship between SOS and age became more complicated as age increased. Relative to the other investigated variables, age accounted for the largest proportion of variance in SOS (33%) among term born infants. Among term born infants, SOS had a curvilinear (cubic) relationship with age during the first year of life. SOS declined over the first 2-3 months of life followed by a gradual increase that plateaued as age approached 12 months. The early postnatal decline in SOS is consistent with the postnatal decline observed in bone mass. These findings suggest that SOS measures age-related changes at the measurement site.

BMD and SOS were hypothesized to be positively related to body size. It was hypothesized that BMD would be positively associated with body size due to the use of an areal measurement to estimate BMD, which does not account for differences in body size. SOS was hypothesized to be positively associated with body size due to the correlation between body size and bone size and the reported negative effect of increased tissue thickness on SOS. There was no significant relationship between BMD and body size, which is likely due to the small area of bone used to estimate BMD. After accounting size differences due to age and prematurity, SOS was not significantly related to body size. In contrast, analyses suggest that larger body size had positive

relationship with SOS among premature infants and chronically ill infants. Therefore, SOS was not influenced by body size or tissue thickness, but is likely indirectly, significantly associated with body size through growth-related factors affecting bone size.

BMD was hypothesized to be positively associated with tibial size and structure. BMD was significantly associated with the proportion of cortical bone relative to cross-sectional size of the midshaft. There was no longer significant after chronically ill infants were excluded from analyses. These findings did not support the hypothesis. One explanation for these findings is that the differences in tibial size after accounting for variation due to age were too small to result in a significant relationship between BMD and tibial structure among infants without chronic illness. The method used to measure BMD may be another explanation for the insignificant relationship between BMD and the tibial measurements. Although the method used to estimate BMD captured the postnatal decline in BMD and the reduction in BMD due to chronic illness, radiographic absorptiometry may not have the sensitivity necessary to detect small differences in low density bone. Detecting small differences in BMD may be essential for infants due to the postnatal loss of bone mass. Higher resolution techniques may be necessary to achieve greater precision in BMD estimates obtained from infants.

SOS was hypothesized to be positively associated with tibial size and structure. SOS did have a significant association with tibial structure after accounting variation due to age. In the pooled sample and among term born infants, SOS was significantly and negatively related to medullary cavity diameter, as was hypothesized. SOS was also significantly related to cortical index in the pooled sample and midshaft diameter among the term born infants. Additionally, age-related changes in SOS appear to correspond to growth-related changes in cortical index. These findings support the hypothesis that SOS is significantly associated with bone structure at the measurement site.

At the outset of this research, the presence of traumatic injury was hypothesized to have no association with indicators of overall health, bone structure, or bone health. Results support this hypothesis. Infants with skeletal fractures as a result of traumatic injury were not significantly different from the other infants in the study sample in terms of body size and growth percentiles. Additionally, there were no significant associations between traumatic injury and chronic illness

or prematurity. Therefore, neither skeletal fragility nor bone disease was a contributing factor in fracture occurrence for infants whose deaths were attributed to traumatic injury. These findings do not support common arguments made by the legal defense during adjudication of child abuse cases that bone fragility is a common contributing factor to skeletal injuries in infants.

Chronic illness was hypothesized to be negatively associated with growth and bone health, which would be reflected in BMD and qualitative radiographic evaluation scores. Chronic illness was not related to body size but was significantly related to tibial size. Linear and appositional growth of the tibia were negatively affected by chronic illness, but medullary cavity diameter nor the proportion of cortical bone to midshaft cross-sectional size were significantly affected. This finding supported the hypothesis that chronic illness was negatively associated with bone health in the current study sample. Chronically ill infants had significantly lower BMD than infants without chronic illness. Due to the reported negative effect of chronic illness on BMD, qualitative radiographic evaluation scores were also hypothesized to be positively associated with chronic illness. Results supported this hypothesis. Chronically ill infants had significantly greater qualitative radiographic scores. Therefore, chronic illness in the current study sample had significant negative effects on mineralization in the current study sample.

Studies have reported that chronically ill children have significantly lower SOS than healthy children (Damilakis et al. 2004; Hartman et al. 2004a; Hartman et al. 2004b; Hartman et al. 2004c; Levine et al. 2002; Zadik et al. 2005). Based on these studies it was hypothesized that chronic illness would be negatively related to SOS. However, there was no significant relationship between SOS and chronic illness in the current study. The insignificant finding may have resulted from the small sample size of chronically ill infants ( $n = 13$ ). A larger sample size of chronically ill infants is needed to further investigate the relationship between chronic illness and SOS. The proposed hypothesis that SOS is significantly influenced by chronic illness was not supported by results, but this finding cannot be interpreted due to the significant association between chronic illness and prematurity in the current study sample.

Skeletal maturity at birth was hypothesized to be significantly positively related to body size. Increased skeletal maturity at birth, as assessed by birthweight and EGA, was significantly related to increased body size, even after accounting for variation due to age. Prematurity had a

significant negative relationship with all measures of body size except for weight for length percentile, which was significantly greater among premature infants. This difference suggests that fat distribution is different between term born and premature infants. These findings support the hypothesis that increased skeletal maturity at birth is significantly related to greater body size during the first year of life.

Skeletal maturity at birth was also hypothesized to have a positive relationship with the tibial size, while prematurity was hypothesized to have a negative relationship with tibial size. The influence of skeletal maturity at birth on tibial size and structure were evaluated by comparing tibial measurements to EGA and birthweight. In the pooled sample, all of the tibial measurements except for cortical index were positively associated with EGA and birthweight. After the exclusion of chronically ill infants from the analysis, EGA and birthweight remained significant predictors of tibia length, midshaft diameter, and cortical thickness. Prematurity was hypothesized to be negatively associated with all tibial measurements. After accounting for age-related size differences, premature infants were significantly smaller in all tibial measurements except for cortical index. These findings support the hypothesis that skeletal maturity at birth is significantly associated with tibial size, during the first year of life. Therefore, infants with greater skeletal maturity at birth have larger tibias than infants that are less skeletally mature at birth, but the proportion of cortical bone to midshaft cross-sectional size was not affected.

The absence of a significant relationship between cortical index and both chronic illness and prematurity was an interesting finding. These findings indicate that chronic illness and prematurity had significant negative effects on linear and appositional growth of the tibia, but endocortical resorption was not significantly increased among these infants. It is possible that resorption of the endocortical surface may have been prevented by increased strain produced by the combination of thinner cortices and smaller midshaft diameter. Although most of the infants in the study sample were non-ambulatory, mechanical strain produced by muscles contractions may have been sufficient to prevent significant endocortical resorption. Bone responds to increased strain by depositing bone on the periosteal surface, but metabolic disturbance may have impaired this response in the chronically ill and premature infants. This explanation is consistent with mechanostat theory (Frost 1996; Frost 2001) in biomechanics and the non-mechanical factors that influence how bone adapts to strains (Frost 2003a; Martin et al. 1998b).

Due to the detrimental effects of prematurity on bone health and bone size, BMD was hypothesized to be negatively associated with prematurity and positively associated with increased skeletal maturity at birth. BMD was significantly associated with EGA and birthweight in the pooled sample, but was no longer significantly related when chronically ill infants were excluded from analyses. Therefore, increased skeletal maturity at birth had no relationship with BMD among infants without chronic illness. Analyses also indicated no significant relationship between prematurity and BMD, which did not support the hypothesis. The negative relationship between BMD and prematurity is well documented in the literature. It is possibly that this insignificant relationship was produced by the low resolution method used to estimate BMD, which lacks precision.

Studies report that premature infants have significantly lower SOS than term born infants (Altuncu et al. 2007; Nemet et al. 2001; Rack et al. 2012). Due to the significant negative influence of prematurity on SOS reported by other studies (McDevitt et al. 2007; Ritschl et al. 2005; Tansug et al. 2011; Tomlinson et al. 2006), it was hypothesized that SOS would have a significant positive relationship with EGA and birthweight. Results indicated that EGA and birthweight had significant positive relationships with SOS. When premature infants were excluded from analyses, EGA and birthweight no longer had a significant relationship with SOS. Analyses also indicated that premature infants had significantly lower SOS values than term born infants. The difference in the relationship between age and SOS among term and premature infants lends further support to the hypothesis that SOS measures characteristics of bone that are related to bone health and structure. Among premature infants, the postnatal decline in SOS was more severe and lasted until ~4-5 months of age (**Figure 4-30**). Additionally, the recovery of SOS to neonatal levels occurred later in premature infants than term infants. Not only does SOS capture age-related changes at the measurement site, it is also influenced by degree of skeletal maturity at birth which can adversely affect bone health.

Relationships between measurements of bone quality were also explored. BMD and qualitative radiographic score were hypothesized to be significantly related because both of these variables are measures of bone mineralization. Analyses indicated no significant relationship between BMD and qualitative radiographic score in the current study. This was an unexpected finding since both BMD and qualitative radiographic score were significantly related to chronic illness.

However, there is a large degree of error was also associated with the qualitative radiographic method. Examination of **Figure 4-32** illustrates the number of infants with low BMD estimates that were classified as having normal mineralization according to qualitative radiographic evaluation. The error associated with this method may have introduced a large degree of statistical noise which prevented the detection of a significant association.

To further investigate what other factors may be influencing SOS, the relationships between SOS and the other bone health indicators were investigated. Previous studies reported low but significant, positive correlations between SOS and BMD in children (Ahmad et al. 2010; Fielding et al. 2003; Jaworski et al. 1995; Sundberg et al. 1998; van Rijn et al. 2000; Wright et al. 1987). In accordance with these reports, SOS was hypothesized to be positively associated with BMD. It was also hypothesized that SOS would have a significant negative relationship with qualitative radiographic evaluation score. Neither of these hypotheses was supported by results. SOS had no significant associations with BMD or qualitative radiographic evaluation score. However, age-related changes in SOS suggest that SOS was influenced by the postnatal decline in bone mass. There are several explanations for the insignificant relationship between BMD and SOS. SOS is reportedly influenced by more than one aspect of bone quality, while BMD only measures bone quantity. It is possible that bone quantity is influential during early postnatal life, while other factors become more influential on SOS later in postnatal life. The low resolution method used to obtain BMD estimates may be another explanation. The low resolution of the method produced BMD estimates with low precision. The low precision of the BMD estimates may have introduced error into the analysis preventing the detection of a significant relationship between BMD and SOS. The use of areal BMD as opposed to a volumetric BMD may have also decreased the precision of the BMD estimates. A final possibility is that there is no relationship between BMD and SOS during the first year of life. This relationship may not develop until after the first year of life. Before it can be determined whether SOS is significantly influenced by BMD during infancy, comparison of SOS to volumetric BMD measurements obtained with a high-resolution imaging technology is necessary.

Multiple regression analyses indicated that SOS was significantly influenced by skeletal maturity at birth and at time of measurement, as well as by bone structure at the measurement site. Fifty-three percent of the variance in SOS was accounted for by a model including age, birthweight,

height, medullary cavity diameter, midshaft diameter, and cortical index. Height, cortical index, and midshaft diameter were excluded from the model after chronically ill infants were removed from the analysis. Reanalysis using only the term born infants resulted in a model that only included age and medullary cavity diameter as significant predictors of SOS. These results support the hypotheses that SOS measures aspects of bone quality associated with skeletal maturity and bone structure. Another implication of the regression analyses is that there is a large proportion of variance in SOS that is not accounted for by skeletal maturity and bone structure, and more research is necessary to investigate these factors.

Bone quality is a complex multidimensional concept that is influenced by environment, genetics, and biology. This research has produced many questions. It is known that bone mass declines for several months after birth, but it remains unknown how the loss of bone mass influences infant bone strength. If postnatal bone loss is a normal physiological process, are BMD measurements informative for determining if infant bone is abnormal or compromised? It is reported that infant bone strength is not compromised by the decline in bone mass due to the redistribution of bone mass further away from the neutral axis, resulting in an increase in bending strength (Rauch and Schoenau 2001; Rauch and Schoenau 2002). Although this possibility is likely because skeletal fractures in infants are not a common occurrence, this hypothesis has not been formally tested. The point at which postnatal bone loss becomes abnormal or leads to compromised bone strength also remains unknown. More research is needed to gain an understanding of age-specific changes in BMD during infancy and how this may differ by skeletal element. With the exception of Ahmad and colleagues (2010), age-specific BMD values for the infant tibia have not been reported in the literature. Most studies report values for whole body BMD or BMD of the lumbar vertebrae measured using DXA. It also needs to be investigated whether aspects of bone quality other than BMD are more informative for evaluating bone strength during infancy. To encourage future research in the area of infant bone health and bone quality, this study contributes age-specific SOS and BMD values which can be found in **Table A- 12** of the Appendix.

Two major conclusions can be drawn from this research. First, traumatic injury in infants is not associated with increased bone fragility. Secondly, bone macrostructure and factors detrimental to growth and bone health, such as prematurity and possibly chronic illness, influence SOS measurements. QUS remains a promising technology for evaluating infant bone quality, but



more research is necessary. Studies comparing SOS to finer-grained measurements of various aspects of bone quality are necessary before it can be determined whether QUS can be used as a diagnostic tool to evaluate infant bone quality. These fine-grained measurements can be obtained using high-resolution technologies such as micro-CT and Raman spectroscopy. Comparison of SOS with measurements of bone strength obtained from biomechanical testing is also necessary. As the next step of this research, a study incorporating these technologies will be conducted to evaluate the relationship between bone strength and SOS and to investigate which aspects of bone quality are measured by SOS.

## **REFERENCES**

1981. Vitamin D metabolism in the rickets of very-low-birth-weight, premature infants. *Nutrition Reviews* 39(6):234-236.
1993. The Vermont-Oxford trials network: very low birth weight outcomes for 1990. *Pediatrics* 91(3):540.
- Abendschein W, and Hyatt GW. 1970. Ultrasonics and selected physical properties of bone. *Clinical Orthopaedics and Related Research*(69):294-&.
- Adams J, and Bishop N. 2009. DXA in adults and children. *Primer on the Metabolic Bone Diseases and Disorders of Mineral Metabolism: John Wiley & Sons, Inc.* p 151-158.
- Adams J, and Shaw N. 2004. *A practical guide to bone densitometry in children.* Camerton, Bath, UK: National Osteoporosis Society.
- Ahmad I, Nemet D, Eliakim A, Koeppel R, Grochow D, Coussens M, Gallitto S, Rich J, Pontello A, Leu SY et al. . 2010. Body composition and its components in preterm and term newborns: a cross-sectional, multimodal investigation. *Am J Hum Biol* 22(1):69-75.
- Akikusa J, Garrick D, and Nash M. 2003. Scurvy: forgotten but not gone. *Journal of paediatrics and child health* 39(1):75-77.
- Alini M, Marriott A, Chen T, Abe S, and Poole AR. 1996. A novel angiogenic molecule produced at the time of chondrocyte hypertrophy during endochondral bone formation. *Developmental Biology* 176(1):124-132.
- Allen M, Hock J, and Burr D. 2004. Periosteum: biology, regulation, and response to osteoporosis therapies. *Bone* 35:1003-1012.
- Allen MR, and Burr DB. 2014a. Bone modeling and remodeling. In: Burr DB, and Allen MR, editors. *Basic and Applied Bone Biology.* Amsterdam: Elsevier/Academic Press. p 75-90.
- Allen MR, and Burr DB. 2014b. Techniques in histomorphometry. In: Burr DB, and Allen MR, editors. *Basic and Applied Bone Biology.* San Diego: Academic Press. p 131-148.
- Allen MR, and Krohn K. 2014. Skeletal imaging. In: Burr DB, and Allen MR, editors. *Basic and Applied Bone Biology.* San Diego: Academic Press. p 93-113.
- Allgrove J. 2009. *The parathyroid and disorders of calcium and bone metabolism: Wiley-Blackwell.* 374-427 p.
- Altuncu E, Akman I, Yurdakul Z, Ozdogan T, Solakoglu M, Selim N, Bilgen H, Ozek E, and Bereket A. 2007. Quantitative ultrasound and biochemical parameters for the assessment of osteopenia in preterm infants. *Journal of Maternal-Fetal & Neonatal Medicine* 20(5):401-405.
- Amprino R, and Engstrom A. 1952. Studies on x-ray absorption and diffraction of bone tissue. *Acta Anatomica* 15(1-2):1-22.
- Anderson HC, and Morris DC. 1993. Mineralization. In: Abou-Samra AB, Mundy GR, and Martin TJ, editors. *Physiology and pharmacology of bone.* Berlin: New York. p 267-298.
- Anderson HC, and Shapiro IM. 2010. The epiphyseal growth plate. In: Bonner F, Farach-Carson MC, and Roach HI, editors. *Bone and Development.* London: Springer. p 39-64.
- Anderson M, Messner MB, and Green WT. 1964. Distribution of lengths of the normal femur and tibia in children from one to eighteen years of age. *Journal of Bone and Joint Surgery* 46(6):1197-1202.

- Arcy LB. 1965. The skeletal system. *Developmental Anatomy A textbook and Laboratory Manual of Embryology*. 7 ed. Philadelphia: W. B. Saunders. p 396-425.
- Ardran GM. 1951. Bone destruction not demonstrable by radiography. *British Journal of Radiology* 24(278):107-109.
- Arsenault AL. 1989. A comparative electron-microscopic study of apatite crystals in collagen fibrils of rat bone, dentin and calcified turkey leg tendons. *Bone and Mineral* 6(2):165-177.
- Ashman RB, Corin JD, and Turner CH. 1987. Elastic properties of cancellous bone - measurement by an ultrasonic technique. *J Biomech* 20(10):979-986.
- Ashman RB, and Rho JY. 1988. Elastic-modulus of trabecular bone material. *J Biomech* 21(3):177-181.
- Atkinson SA, and Randall-Simpson J. 2000. Factors influencing body composition of premature infants at term-adjusted age. *Annals of the New York Academy of Sciences* 904(1):393-399.
- Aufderheide AC, and Rodriguez-Martin C. 1998. *The Cambridge Encyclopedia of Human Paleopathology*. Cambridge: Cambridge University Press.
- Augat P, Reeb H, and Claes LE. 1996. Prediction of fracture load at different skeletal sites by geometric properties of the cortical shell. *Journal of Bone and Mineral Research* 11(9):1356-1363.
- Bachrach L, Levine M, Cowell C, and Shaw N. 2007. Clinical indications for the use of dxa in pediatrics. In: Sawyer A, Bachrach L, and Fung E, editors. *Bone Densitometry in Growing Patients: Humana Press*. p 59-72.
- Bachrach LK. 2001. Osteoporosis in childhood and adolescence. In: Kelsey RMF, editor. *Osteoporosis (Second Edition)*. San Diego: Academic Press. p 151-167.
- Backstrom M, Kuusela A-L, and Maki R. 1996. Metabolic bone disease of prematurity. *Annals of Medicine* 28(4):275-282.
- Bajaj M, Koo W, Hammami M, and Hockman EM. 2010. Effect of subcutaneous fat on quantitative bone ultrasound in chicken and neonates. *Pediatr Res* 68(1):81-83.
- Baker PT, Schraer H, and Yalman RG. 1959. The accuracy of human bone composition determined from roentgenograms. *Photogrammetric Engineering* 25:455-460.
- Banse X. 2002. When density fails to predict bone strength. *Acta Orthopaedica Scandinavica* 73:2-57.
- Barden HS, and Mazess RB. 1988. Bone densitometry in infants. *J Pediatr* 113(1 Pt 2):172-177.
- Barkmann R, Kantorovich E, Singal C, Hans D, Genant HK, Heller M, and Glüer C-C. 2000. A new method for quantitative ultrasound measurements at multiple skeletal sites: first results of precision and fracture discrimination. *Journal of Clinical Densitometry* 3(1):1-7.
- Barltrop D, Mole R, and Sutton A. 1977. Absorption and endogenous faecal excretion of calcium by low birthweight infants on feeds with varying contents of calcium and phosphate. *Archives of disease in childhood* 52(1):41-49.
- Baron R. 1999. Anatomy and ultrastructure of bone. In: Favus MJ, editor. *Primer on the metabolic bone diseases and disorders of mineral metabolism*. Fourth ed. Philadelphia: Lippincott William & Wilkins. p 3-10.
- Baron R, Neff L, Louvard D, and Courtoy PJ. 1985. Cell-mediated extracellular acidification and bone-resorption - evidence for a low pH in resorbing lacunae and localization of a 100-kd lysosomal membrane-protein at the osteoclast ruffled border. *Journal of Cell Biology* 101(6):2210-2222.

- Baroncelli GI, Federico G, Bertelloni S, De Terlizzi F, Cadossi R, and Saggese G. 2001. Bone quality assessment by quantitative ultrasound of proximal phalanxes of the hand in healthy subjects aged 3-21 years. *Pediatric Research* 49(5):713-718.
- Bartl R, Frisch B, and Bartl C. 2009. Biology of bone. In: Bartl R, and Frisch B, editors. *Osteoporosis : diagnosis, prevention, therapy*. 2nd rev. ed. Berlin: Springer. p 7-28.
- Bauer DC, Gluer CC, Cauley JA, Vogt TM, Ensrud KE, Genant HK, and Black DM. 1997. Broadband ultrasound attenuation predicts fractures strongly and independently of densitometry in older women - A prospective study. *Archives of Internal Medicine* 157(6):629-634.
- BeamMed. 2010. Sunlight MiniOmni Bone Sonometer User Guide. US Version 1.0 ed. Petah Tikva, Israel: BeamMed.
- Bell NH. 1985. Vitamin D-endocrine system. *Journal of Clinical Investigation* 76(1):1.
- Bellido T, and Hill Gallant KM. 2014. Hormonal effects on bone cells. In: Burr DB, and Allen MR, editors. *Basic and Applied Bone Biology*. San Diego: Academic Press. p 299-314.
- Bellido T, Plotkin LI, and Bruzzaniti. 2013. Bone cells. In: Burr DB, and Allen MR, editors. *Basic and applied bone biology*. Amsterdam: Elsevier/Academic Press. p 27-45.
- Benmalek A, and Sabatier J-P. 1998. Comparison and cross-calibration of DXA systems: ODX-240 and Sophos L-XRA versus Hologic QDR-4500, for spinal bone mineral measurement. Translation of a reference database. *Osteoporosis international* 8(6):570-577.
- Beresford JN. 1989. Osteogenic stem-cells and the stromal system of bone and marrow. *Clinical Orthopaedics and Related Research*(240):270-280.
- Bernard J. 1962. Le rapport cortico-diaphysaire tibial pendant la croissance. *Archives Francaises De Pediatrie* 19(6):805-&.
- Berry JL, Davies M, and Mee AP. 2002. Vitamin D metabolism, rickets, and osteomalacia. *Seminars in musculoskeletal radiology*: Thieme Medical Publishers, Inc. p 173-182.
- Bi W, Huang W, Whitworth DJ, Deng JM, Zhang Z, Behringer RR, and de Crombrughe B. 2001. Haploinsufficiency of Sox9 results in defective cartilage primordia and premature skeletal mineralization. *Proceedings of the National Academy of Sciences* 98(12):6698-6703.
- Bilezikian J. 1999. Primary hyperparathyroidism. In: Favus MJ, editor. *Primer on the metabolic bone diseases and disorders of mineral metabolism*. 4th ed. Philadelphia: Lippincott William & Wilkins. p 187-192.
- Bingham PJ, Brazell IA, and Owen M. 1969. The effect of parathyroid extract on cellular activity and plasma calcium levels in vivo. *Journal of Endocrinology* 45(3):387-400.
- Binkley TL, and Specker BL. 2000. pQCT measurement of bone parameters in young children: validation of technique. *Journal of Clinical Densitometry* 3(1):9-14.
- Binkovitz LA, and Henwood MJ. 2007. Pediatric DXA: technique and interpretation. *Pediatric Radiology* 37(1):21-31.
- Binkovitz LA, Sparke P, and Henwood MJ. 2007. Pediatric DXA: clinical applications. *Pediatric Radiology* 37(7):625-635.

- Bishop N, Dahlenburg S, Fewtrell M, Morley R, and Lucas A. 1996. Early diet of preterm infants and bone mineralization at age five years. *Acta Pædiatrica* 85(2):230-236.
- Black DM, Cummings SR, Genant HK, Nevitt MC, Palermo L, and Browner W. 1992. Axial and appendicular bone density predict fractures in older women. *Journal of bone and mineral research* 7(6):633-638.
- Bodine PV, and Komm BS. 2006. Wnt signaling and osteoblastogenesis. *Reviews in endocrine & metabolic disorders* 7(1-2):33-39.
- Bonnard GD. 1968. Cortical thickness and diaphyseal diameter of the metacarpal bones from the age of three months to eleven years. *Helvetica Paediatrica Acta* 23(5):445-463.
- Bordier P, Matrajt H, Hioco D, Hepner G, Thompson G, and Booth C. 1968. Subclinical Vitamin-D deficiency following gastric surgery histological evidence in bone. *The Lancet* 291(7540):437-440.
- Bossy E, Talmant M, and Laugier P. 2004a. Three-dimensional simulations of ultrasonic axial transmission velocity measurement on cortical bone models. *Journal of the Acoustical Society of America* 115(5):2314-2324.
- Bossy E, Talmant M, Peyrin F, Akrouf L, Cloetens P, and Laugier P. 2004b. An in vitro study of the ultrasonic axial transmission technique at the radius: 1-mhz velocity measurements are sensitive to both mineralization and intracortical porosity. *Journal of Bone and Mineral Research* 19(9):1548-1556.
- Bourne G. 1942. The effect of graded doses of vitamin C upon the regeneration of bone in guinea-pigs on a scorbutic diet. *The Journal of physiology* 101(3):327-336.
- Bouxsein ML. 2003. Bone quality: where do we go from here? *Osteoporosis International* 14:S118-S127.
- Bouxsein ML, Boardman KC, Pinilla TP, and Myers ER. 1995. Ability of bone properties at the femur, forearm, and calcaneus to predict the structural capacity of the proximal femur during a sideways fall. *Journal of Bone and Mineral Research* 10:S178-S178.
- Bouxsein ML, Coan BS, and Lee SC. 1999. Prediction of the strength of the elderly proximal femur by bone mineral density and quantitative ultrasound measurements of the heel and tibia. *Bone* 25(1):49-54.
- Boyce T, and Bloebaum R. 1993. Cortical aging differences and fracture implications for the human femoral neck. *Bone* 14(5):769-778.
- Brickley M, and Ives R. 2006. Skeletal manifestations of infantile scurvy. *American Journal of Physical Anthropology* 129(2):163-172.
- Brickley M, and Ives R. 2008a. Miscellaneous conditions. In: Brickley M, and Rachel I, editors. *The Bioarchaeology of Metabolic Bone Disease*. San Diego: Academic Press. p 241-260.
- Brickley M, and Ives R. 2008b. Vitamin C deficiency scurvy. *The bioarchaeology of metabolic bone disease*. Oxford: Academic Press. p 41-74.
- Brickley M, and Ives R. 2008c. Vitamin D deficiency. In: Brickley M, and Rachel I, editors. *The Bioarchaeology of Metabolic Bone Disease*. San Diego: Academic Press. p 75-150.
- Brook CGD, and Brown RS. 2008a. Disorders of calcium and bone metabolism. In: Brook CGD, and Brown RS, editors. *Handbook of Clinical Pediatric Endocrinology*. 1 ed: Blackwell Publishing Ltd. p 33-58.
- Brook CGD, and Brown RS. 2008b. The endocrine problems of infancy. In: Brook CGD, and Brown RS, editors. *Handbook of Clinical Pediatric Endocrinology*. 1 ed: Blackwell Publishing Ltd. p 14-32.

- Brook CGD, and Brown RS. 2008c. Problems of growth in childhood. In: Brook CGD, and Brown RS, editors. *Handbook of Clinical Pediatric Endocrinology*. 1 ed: Blackwell Publishing Ltd. p 123-145.
- Brooke OG, and Lucas A. 1985. Metabolic bone-disease in preterm infants. *Archives of Disease in Childhood* 60(7):682-685.
- Browne JG, Mesallati T, Picard C, Reeve-Arnold K, Reilly PO, Daly JS, Casey MC, Walsh JB, and Taylor D. 2010. Investigating bone quality in patients with hip fractures using newer bioengineering techniques. *Bone* 47, Supplement 1(0):S80-S81.
- Bruder SP, and Caplan AI. 1989. Cellular and molecular events during embryonic bone-development. *Connective Tissue Research* 20(1-4):65-71.
- Brunton JA, Bayley HS, and Atkinson SA. 1993. Validation and application of dual-energy x-ray absorptiometry to measure bone mass and body composition in small infants. *The American journal of clinical nutrition* 58(6):839-845.
- Buckwalter JA. 1994. Musculoskeletal tissues and the musculoskeletal system. In: Weinstein SL, and Buckwalter JA, editors. *Turek's Orthopaedics: Principles and their Application*. 5 ed. Philadelphia: J. B. Lippincott. p 13-67.
- Buckwalter JA, and Cooper RR. 1987. Bone structure and function. *Instructional Course Lectures, The American Academy of Orthopaedic Surgeons Park Ridge, Illinois: The American Academy of Orthopaedic Surgeons*. p 27-48.
- Buckwalter JA, Glimcher MJ, Cooper RR, and Recker R. 1995a. Bone Biology .1. Structure, blood-supply, cells, matrix, and mineralization. *Journal of Bone and Joint Surgery-American Volume* 77A(8):1256-1275.
- Buckwalter JA, Glimcher MJ, Cooper RR, and Recker R. 1995b. Bone Biology .2. Formation, form, modeling, remodeling, and regulation of cell-function. *Journal of Bone and Joint Surgery-American Volume* 77A(8):1276-1289.
- Burr DB, and Akkus O. 2013. Bone morphology and organization. In: Burr DB, and Allen MR, editors. *Basic and applied bone biology*. Amsterdam: Elsevier/Academic Press. p 3-25.
- Burr DB, Hirano T, Turner CH, Hotchkiss C, Brommage R, and Hock JM. 2001. Intermittently administered human parathyroid hormone(1-34) treatment increases intracortical bone turnover and porosity without reducing bone strength in the humerus of ovariectomized cynomolgus monkeys. *Journal of Bone and Mineral Research* 16(1):157-165.
- Burstein AH, Zika JM, Heiple KG, and Klein L. 1975. Contribution of collagen and mineral to elastic-plastic properties of bone. *Journal of Bone and Joint Surgery-American Volume* 57(7):956-961.
- Cabin RJ, and Mitchell RJ. 2000. To Bonferroni or Not to Bonferroni: When and How Are the Questions. *Bulletin of the Ecological Society of America* 81(3):246-248.
- Canalis E. 2009. Growth factor control of bone mass. *Journal of Cellular Biochemistry* 108(4):769-777.
- Canalis E, and Delany AM. 2002. Mechanisms of glucocorticoid action in bone. *Ann N Y Acad Sci* 966:73-81.
- Carrascosa A, Gussinyé M, Yeste D, Del Río L, Audí L, Enrubia M, and Vargas D. 1996. Skeletal mineralization during infancy, childhood and adolescence in the normal population and in populations with nutritional and hormonal disorders. Dual X-ray absorptiometry (DEXA) evaluation. *Paediatric Osteology New developments in diagnosis and therapy* Amsterdam: Elsevier Science:93-102.

- Chan GM. 1992. Performance of dual-energy X-ray absorptiometry in evaluating bone, lean body mass, and fat in pediatric subjects. *Journal of Bone and Mineral Research* 7(4):369-374.
- Chanavaz M. 1995. Anatomy and histophysiology of the periosteum: quantification of the periosteal blood supply to the adjacent bone with <sup>85</sup>Sr and gamma spectrometry. *Journal of Oral Implantology* 21:214-219.
- Chang MK, Raggatt LJ, Alexander KA, Kuliwaba JS, Fazzalari NL, Schroder K, Maylin ER, Ripoll VM, Hume DA, and Pettit AR. 2008. Osteal tissue macrophages are intercalated throughout human and mouse bone lining tissues and regulate osteoblast function in vitro and in vivo. *J Immunol* 181(2):1232-1244.
- Chatproedprai S, and Wananukul S. 2001. Scurvy: a case report. *Journal of the Medical Association of Thailand= Chotmaihet thangphaet* 84:S106-110.
- Chen H, Hewison M, and Adams JS. 2006. Functional characterization of heterogeneous nuclear ribonuclear protein C1/C2 in vitamin D resistance: A novel response element-binding protein. *Journal of Biological Chemistry* 281(51):39114-39120.
- Chen HL, Tseng HI, Yang SN, and Yang RC. 2012. Bone status and associated factors measured by quantitative ultrasound in preterm and full-term newborn infants. *Early Hum Dev* 88(8):617-622.
- Chen T, Chen PJ, Fung CS, Lin CJ, and Yao WJ. 2004. Quantitative assessment of osteoporosis from the tibia shaft by ultrasound techniques. *Med Eng Phys* 26(2):141-145.
- Civitelli R, Ziambaras K, and Leelawattana R. 1998. Pathophysiology of calcium, phosphate and magnesium absorption. *Metabolic Bone Disease* Louis V Avioli, Stephen M Krane (eds) Academic Press, San Diego:165-208.
- Compagni A, Logan M, Klein R, and Adams RH. 2003. Control of skeletal patterning by EphrinB1-EphB interactions. *Developmental Cell* 5(2):217-230.
- Cooper RR, Milgram JW, and Robinson RA. 1966. Morphology of the osteon. An electron microscope study. *Journal of Bone and Joint Surgery* 48-A:1239-1271.
- Cooper RR, and Misol S. 1970. Tendon and ligament insertion: a light and electron microscopy study. *Journal of Bone and Joint Surgery* 52-A:1-20.
- Cosman F, Herrington B, Himmelstein S, and Lindsay R. 1991. Radiographic absorptiometry: a simple method for determination of bone mass. *Osteoporosis International* 2(1):34-38.
- Cullinane DM, and Einhorn TA. 2002. Biomechanics of bone. In: Bilezikian JP, Raisz LG, and Rodan GA, editors. *Principles of Bone Biology* Second ed. San Diego: Academic Press. p 17-32.
- Cummings SR, Browner W, Cummings S, Black D, Nevitt M, Browner W, Genant H, Cauley J, Ensrud K, and Scott J. 1993. Bone density at various sites for prediction of hip fractures. *The Lancet* 341(8837):72-75.
- Currey JD. 1984. *The mechanical adaptations of bones*. Princeton: Princeton University Press.
- Currey JD. 2002. The structure of bone tissue. *Bones : structure and mechanics*. Princeton, NJ: Princeton University Press. p 3-26.
- Currey JD. 2006. The adaptation of mechanical properties to different functions. *Bones: Structure and Mechanics*. Princeton: Princeton University Press.
- Currey JD, and Butler G. 1975. The mechanical properties of bone tissue in children. *The Journal of bone and joint surgery American volume* 57(6):810-814.



- Dai JC, He P, Chen X, and Greenfield EM. 2006. TNF $\alpha$  and PTH utilize distinct mechanisms to induce IL-6 and RANKL expression with markedly different kinetics. *Bone* 38(4):509-520.
- Damilakis J, Galanakis E, Mamoulakis D, Sbyrakis S, and Gourtsoyiannis N. 2004. Quantitative ultrasound measurements in children and adolescents with type 1 diabetes. *Calcif Tissue Int* 74(5):424-428.
- Darby MK, and Loughead JL. 1996. Neonatal nutritional requirements and formula composition: A review. *Journal of Obstetric, Gynecologic, & Neonatal Nursing* 25(3):209-220.
- De Buyst J, Rakza T, Pennaforte T, Johansson A-B, and Storme L. 2012. Hemodynamic effects of fluid restriction in preterm infants with significant patent ductus arteriosus. *The Journal of pediatrics* 161(3):404-408.
- de Meer K, Westerterp KR, Houwen RHJ, Brouwers HAA, Berger R, and Okken A. 1997. Total energy expenditure in infants with bronchopulmonary dysplasia is associated with respiratory status. *European Journal of Pediatrics* 156(4):299-304.
- del Rio L, Carrascosa A, Pons F, Gusinye M, Yeste D, and Domenech FM. 1994. Bone mineral density of the lumbar spine in white Mediterranean Spanish children and adolescents: changes related to age, sex, and puberty. *Pediatr Res* 35(3):362-366.
- DeLuca HF, and Schnoes HK. 1976. Metabolism and mechanism of action of vitamin D. *Annual review of biochemistry* 45(1):631-666.
- Dempster DW, Cosman F, Kurland ES, Zhou H, Nieves J, Woelfert L, Shane E, Plavetic K, Muller R, Bilezikian J et al. . 2001. Effects of daily treatment with parathyroid hormone on bone microarchitecture and turnover in patients with osteoporosis: A paired biopsy study. *Journal of Bone and Mineral Research* 16(10):1846-1853.
- Department of Family and Protective Services. 2014. DFPS 2013 Data Book. [http://www.dfps.state.tx.us/documents/about/Data\\_Books\\_and\\_Annual\\_Reports/2013/DataBook13All.pdf](http://www.dfps.state.tx.us/documents/about/Data_Books_and_Annual_Reports/2013/DataBook13All.pdf).
- Dickerson JWT. 1962. Changes in composition of human femur during growth. *Biochemical Journal* 82(1):56-&.
- Dietrich JW, Canalis EM, Maina DM, and Raisz LG. 1976. Hormonal control of bone collagen synthesis in vitro: effects of parathyroid hormone and calcitonin. *Endocrinology* 98(4):943-949.
- DiMauro S, Bonilla E, Zeviani M, Nakagawa M, and DeVivo DC. 1985. Mitochondrial myopathies. *Annals of Neurology* 17(6):521-538.
- DiMeglio LA, and Imel EA. 2014. Calcium and phosphate: Hormonal regulation and metabolism. In: Burr DB, and Allen MR, editors. *Basic and Applied Bone Biology*. San Diego: Academic Press. p 261-282.
- Done S. 2012. Fetal and neonatal bone health: update on bone growth and manifestations in health and disease. *Pediatric Radiology* 42(1):158-176.
- Downey P, and Siegel M. 2006. Bone Biology and the clinical implications for osteoporosis. *Physical Therapy* 86:77-91.
- Drozdowska B, and Pluskiewicz W. 2001. Quantitative ultrasound at the calcaneus in premenopausal women and their postmenopausal mothers. *Bone* 29(1):79-83.
- Dyson ED, and Whitehouse WJ. 1968. Composition of trabecular bone in children and its relation to radiation dosimetry. *Nature* 217(5128):576-578.
- Eanes ED, and Hailer AW. 1985. Liposome-mediated calcium-phosphate formation in metastable solutions. *Calcified Tissue Int* 37(4):390-394.

- Eleazer CD. 2013. The interaction of mechanical loading and metabolic stress on human cortical bone: testing anthropological assumptions using cross-sectional geometry and histomorphology [Dissertation]. Knoxville: The University of Tennessee.
- Ellender G, Feik S, and Carach B. 1988. Periosteal structure and development in a rat caudal vertebra. *Journal of Anatomy* 158:173-187.
- Enlow DHA. 1963. Principles of bone remodeling. Springfield: Ch C Thomas. 1 vol. (x-131 p.) p.
- Epstein DM, Dalinka MK, Kaplan FS, Aronchick JM, Marinelli DL, and Kundel HL. 1986. Observer variation in the detection of osteopenia. *Skeletal Radiology* 15(5):347-349.
- Epstein S, Inzerillo AM, Caminis J, and Zaidi M. 2003. Disorders associated with acute rapid and severe bone loss. *Journal of Bone and Mineral Research* 18(12):2083-2094.
- Everts V, Delaisse JM, Korper W, Jansen DC, Tigchelaar-Gutter W, Saftig P, and Beertsen W. 2002. The bone lining cell: Its role in cleaning Howship's lacunae and initiating bone formation. *Journal of Bone and Mineral Research* 17(1):77-90.
- Fain O. 2005. Musculoskeletal manifestations of scurvy. *Joint Bone Spine* 72(2):124-128.
- Fielding KT, Nix DA, and Bachrach LK. 2003. Comparison of calcaneus ultrasound and dual X-ray absorptiometry in children at risk of osteopenia. *Journal of Clinical Densitometry* 6(1):7-15.
- Figueras-Aloy J, Álvarez-Domínguez E, Pérez-Fernández JM, Moretones-Suñol G, Vidal-Sicart S, and Botet-Mussons F. 2014. Metabolic bone disease and bone mineral density in very preterm infants. *The Journal of Pediatrics* 164(3):499-504.
- Foldes AJ, Rimon A, Keinan DD, and Popovtzer MM. 1995. Quantitative ultrasound of the tibia - a novel-approach for assessment of bone status. *Bone* 17(4):363-367.
- Follis R, Park E, and Jackson D. 1950. The prevalence of scurvy at autopsy during the first two years of age. *Bulletin of the Johns Hopkins Hospital* 87:569-592.
- Follis RH. 1948. Pathology of nutritional disease. Springfield, IL: Thomas.
- Fraenkel E. 1929. Infantiler Skorbut (Möller-Barlow sche Krankheit). Knochen· Muskeln Sehnen· Sehnenscheiden Schleimbeutel: Springer. p 222-239.
- Francis RM, and Selby PL. 1997. Osteomalacia. *Bailliere's clinical endocrinology and metabolism* 11(1):145-163.
- Fraser D, Kooh SW, and Scriver CR. 1967. Hyperparathyroidism as the cause of hyperaminoaciduria and phosphaturia in human vitamin D deficiency. *Pediatr Res* 1(6):425-435.
- Fricke O, Tutlewski B, Schwahn B, and Schoenau E. 2005. Speed of sound: Relation to geometric characteristics of bone in children, adolescents, and adults. *Journal of Pediatrics* 146(6):764-768.
- Friedman J, AU WYW, and Raisz LG. 1968. Responses of fetal rat bone to thyrocalcitonin in tissue culture. *Endocrinology* 82(1):149-156.
- Friedman J, and Raisz LG. 1965. Thyrocalcitonin: Inhibitor of bone resorption in tissue culture. *Science* 150(3702):1465-1467.
- Frost H. 2003a. On changing views about age-related bone loss. In: Agarwal S, and Stout S, editors. *Bone Loss and Osteoporosis*: Springer US. p 19-31.

- Frost HM. 1996. Perspectives: a proposed general model of the "mechanostat" (suggestions from a new skeletal-biologic paradigm). *Anat Rec* 244(2):139-147.
- Frost HM. 2001. From Wolff's law to the Utah paradigm: Insights about bone physiology and its clinical applications. *The Anatomical Record* 262(4):398-419.
- Frost HM. 2003b. Bone's mechanostat: A 2003 update. *Anatomical Record Part a-Discoveries in Molecular Cellular and Evolutionary Biology* 275A(2):1081-1101.
- Gafni RI, and Baron J. 2004. Overdiagnosis of osteoporosis in children due to misinterpretation of dual-energy x-ray absorptiometry (DEXA). *The Journal of pediatrics* 144(2):253-257.
- Gaillard P. 1966. Bone culture studies. *J Bone & Joint Surg B* 48:386.
- Gärdsell P, Johnell O, Nilsson BE, and Gullberg B. 1993. Predicting various fragility fractures in women by forearm bone densitometry: a follow-up study. *Calcified Tissue Int* 52(5):348-353.
- Genant HK, Engelke K, Fuerst T, Glüer CC, Grampp S, Harris ST, Jergas M, Lang T, Lu Y, and Majumdar S. 1996. Noninvasive assessment of bone mineral and structure: state of the art. *Journal of Bone and Mineral Research* 11(6):707-730.
- Gilsanz V. 1998. Bone density in children: a review of the available techniques and indications. *European journal of radiology* 26(2):177-182.
- Gilsanz V, Kovanlikaya A, Costin G, Roe TF, Sayre J, and Kaufman F. 1997. Differential effect of gender on the sizes of the bones in the axial and appendicular skeletons 1. *The Journal of Clinical Endocrinology & Metabolism* 82(5):1603-1607.
- Gindhart PS. 1973. Growth standards for the tibia and radius in children aged one month through eighteen years. *American Journal of Physical Anthropology* 39(1):41-48.
- Glimcher MJ. 1992. The nature of the mineral component of bone and the mechanisms of calcification. In: Coe FL, and Favus MJ, editors. *Disorders of bone and mineral metabolism*. New York: Raven Press. p 265-286.
- Glorieux FH, Pettifor JM, and Jüppner H. 2003. Fetal mineral homeostasis. In: Kovacs CS, editor. *Pediatric Bone: Biology and Diseases*. San Diego: Academic Press. p 271-302.
- Glüer CC. 2009. Quantitative computed tomography in children and adults. *Primer on the Metabolic Bone Diseases and Disorders of Mineral Metabolism: John Wiley & Sons, Inc.* p 158-163.
- Gluer CC, Cummings SR, Bauer DC, Stone K, Pressman A, Mathur A, and Genant HK. 1996. Osteoporosis: Association of recent fractures with quantitative US findings. *Radiology* 199(3):725-732.
- Godfrey K, Walker-Bone K, Robinson S, Taylor P, Shore S, Wheeler T, and Cooper C. 2001. Neonatal bone mass: Influence of parental birthweight, maternal smoking, body composition, and activity during pregnancy. *Journal of Bone and Mineral Research* 16(9):1694-1703.
- Goldstein SA. 1987. The mechanical-properties of trabecular bone - dependence on anatomic location and function. *J Biomech* 20(11-12):1055-1061.
- Gong JK, Arnold JS, and Cohn SH. 1964. Composition of trabecular + cortical bone. *Anatomical Record* 149(3):325-&.

- Gonnelli S, Montagnani A, Gennari L, Martini S, Merlotti D, Cepollaro C, Perrone S, Buonocore G, and Nuti R. 2004. Feasibility of quantitative ultrasound measurements on the humerus of newborn infants for the assessment of the skeletal status. *Osteoporosis International* 15(7):541-546.
- Goshima J, Goldberg VM, and Caplan AI. 1991. The osteogenic potential of culture-expanded rat marrow mesenchymal cells assayed *in vivo* in calcium-phosphate ceramic blocks. *Clinical Orthopaedics and Related Research*(262):298-311.
- Gosman JH, Hubbell ZR, Shaw CN, and Ryan TM. 2013. Development of cortical bone geometry in the human femoral and tibial diaphysis. *Anatomical record (Hoboken, NJ : 2007)* 296(5):774-787.
- Gosman JH, and Ketcham RA. 2009. Patterns in ontogeny of human trabecular bone from Sunwatch Village in the prehistoric Ohio valley: General features of microarchitectural change. *American Journal of Physical Anthropology* 138(3):318-332.
- Gosman JH, Stout SD, and Larsen CS. 2011. Skeletal biology over the life span: A view from the surfaces. *Yearbook of Physical Anthropology* 54:86-98.
- Grech P, Martin TJ, Barrington NA, and Ell PJ. 1985. *Diagnosis of metabolic bone disease*. London: Chapman & Hall Medical.
- Greenfield EM, Gornik SA, Horowitz MC, Donahue HJ, and Shaw SM. 1993. Regulation of cytokine expression in osteoblasts by parathyroid hormone: Rapid stimulation of interleukin-6 and leukemia inhibitory factor mRNA. *Journal of Bone and Mineral Research* 8(10):1163-1171.
- Greenfield GB. 1990. *Radiology of bone diseases*: Lippincott Williams and Wilkins.
- Greenfield MA, Craven JD, Huddleston A, Kehrer ML, Wishko D, and Stern R. 1981. Measurement Of The Velocity Of Ultrasound In Human Cortical Bone *In vivo* - Estimation Of Its Potential Value In The Diagnosis Of Osteoporosis And Metabolic Bone-Disease. *Radiology* 138(3):701-710.
- Greer FR, and McCormick A. 1986. Bone growth with low bone mineral content in very low birth weight premature infants. *Pediatr Res* 20(10):925-928.
- Gregg EW, Kriska AM, Salamone LM, Roberts MM, Aderson SJ, Ferrell RE, Kuller LH, and Cauley JA. 1997. The epidemiology of quantitative ultrasound: A review of the relationships with bone mass, osteoporosis and fracture risk. *Osteoporosis International* 7(2):89-99.
- Grewar D. 1965. Infantile scurvy. *Clinical pediatrics* 4(2):82-89.
- Grinspoon SK, Baum H, Kim V, Coggins C, and Klibanski A. 1995. Decreased bone formation and increased mineral dissolution during acute fasting in young women. *The Journal of clinical endocrinology and metabolism* 80(12):3628-3633.
- Griscom NT, and Jaramillo D. 2000. "Osteoporosis", "Osteomalacia", and "Osteopenia": Proper terminology in Childhood. *Am J Roentgenol* 175(1):267-268.
- Guan CC, Yan M, Jiang XQ, Zhang P, Zhang XL, Li J, Ye DX, and Zhang FQ. 2009. Sonic hedgehog alleviates the inhibitory effects of high glucose on the osteoblastic differentiation of bone marrow stromal cells. *Bone* 45(6):1146-1152.
- Guglielmi G, Adams J, and Link TM. 2009. Quantitative ultrasound in the assessment of skeletal status. *European Radiology* 19(8):1837-1848.

- Guglielmi G, Njeh CF, Terlizzi F, Serio DA, Scillitani A, Cammisia M, Fan B, Lu Y, and Genant HK. 2003. Phalangeal quantitative ultrasound, phalangeal morphometric variables, and vertebral fracture discrimination. *Calcified Tissue Int* 72(4):469-477.
- Gursoy T, Yurdakok M, Hayran M, Korkmaz A, Yigit S, and Tekinalp G. 2008. Bone speed of sound curves of twin and singleton neonates. *Journal of Pediatric Endocrinology and Metabolism* 21(11):1065-1072.
- Hall BK, and Miyake T. 1992. The membranous skeleton: the roll of cell condensations in vertebrate skeletogenesis. *Anatomy and Embryology* 186:107-124.
- Hamrick SEG, and Hansmann G. 2010. Patent ductus arteriosus of the preterm infant. *Pediatrics* 125(5):1020-1030.
- Hans D, DargentMolina P, Schott AM, Sebert JL, Cormier C, Kotzki PO, Delmas PD, Pouilles JM, Breart G, and Meunier PJ. 1996. Ultrasonographic heel measurements to predict hip fracture in elderly women: The EPIDOS prospective study. *Lancet* 348(9026):511-514.
- Hans D, Fuerst T, and Duboeuf F. 1997. Quantitative ultrasound bone measurement. *European radiology* 7(2):S43.
- Hans D, Srivastav S, Singal C, Barkmann R, Njeh C, Kantorovich E, Glüer C, and Genant H. 1999. Does combining the results from multiple bone sites measured by a new quantitative ultrasound device improve discrimination of hip fracture? *Journal of Bone and Mineral Research* 14(4):644-651.
- Harris County Institute of Forensic Sciences. 2014. Harris County Institute of Forensic Sciences Annual Report 2013. [http://www.harriscountytexas.gov/CmpDocuments/114/Articles/14-0912\\_FINAL\\_Annual\\_Report\\_2013.pdf](http://www.harriscountytexas.gov/CmpDocuments/114/Articles/14-0912_FINAL_Annual_Report_2013.pdf).
- Hartl F, Tyndall A, Kraenzlin M, Bachmeier C, Gückel C, Senn U, Hans D, and Theiler R. 2002. Discriminatory ability of quantitative ultrasound parameters and bone mineral density in a population-based sample of postmenopausal women with vertebral fractures: Results of the Basel osteoporosis study. *Journal of Bone and Mineral Research* 17(2):321-330.
- Hartman C, Brik R, Tamir A, Merrick J, and Shamir R. 2004a. Bone quantitative ultrasound and nutritional status in severely handicapped institutionalized children and adolescents. *Clinical Nutrition* 23(1):89-98.
- Hartman C, Hino B, Lerner A, Eshach-Adiv O, Berkowitz D, Shaoul R, Pacht A, Rozenthal E, Tamir A, Shamaly H et al. . 2004b. Bone quantitative ultrasound and bone mineral density in children with celiac disease. *Journal of Pediatric Gastroenterology and Nutrition* 39(5):504-510.
- Hartman C, Shamir R, Eshach-Adiv O, Iosilevsky G, and Brik R. 2004c. Assessment of osteoporosis by quantitative ultrasound versus dual energy X-ray absorptiometry in children with chronic rheumatic diseases. *The Journal of Rheumatology* 31(5):981-985.
- Hauge EM, Qvesel D, Eriksen EF, Mosekilde L, and Melsen F. 2001. Cancellous bone remodeling occurs in specialized compartments lined by cells expressing osteoblastic markers. *Journal of Bone and Mineral Research* 16(9):1575-1582.
- Hayashi T, Satoh H, Soga T, Tanaka D, Itabashi K, and Okuyama K. 1996. Evaluation of bone density in newborn infants by computed X-ray densitometry. *Journal of pediatric gastroenterology and nutrition* 23(2):130-134.
- Haynesworth SE, Goshima J, Goldberg VM, and Caplan AI. 1992. Characterization of cells with osteogenic potential from human marrow. *Bone* 13(1):81-88.
- Heaney RP. 1997. Vitamin D: Role in the calcium economy. In: Feldman D, Glorieux FH, and Pike J, editors. *Vitamin D*. San Diego: Academic Press. p 485-497.
- Hess AF. 1930. Rickets, including osteomalacia and tetany. London: Henry Kimpton.

- Hirsch PF, and Munson PL. 1969. Thyrocalcitonin. *Journal Article* 49(3):548-622.
- Hochberg Z. 2003. Rickets--past and present. Introduction. In: Hochberg Ze, editor. *Vitamin D and Rickets*. 2003/09/11 ed. Basel: Karger. p 1-13.
- Hodges R. 1980. Vitamin C. In: Alfin-Slater R, and Kritchevsky D, editors. *Nutrition and the Adult: Springer US*. p 73-96.
- Hodgkinson R, Njeh CF, Currey JD, and Langton CM. 1997. The ability of ultrasound velocity to predict the stiffness of cancellous bone in vitro. *Bone* 21(2):183-190.
- Högler W, Briody J, Moore B, Lu PW, and Cowell CT. 2005. Effect of growth hormone therapy and puberty on bone and body composition in children with idiopathic short stature and growth hormone deficiency. *Bone* 37(5):642-650.
- Högler W, Schmid A, Raber G, Sölder E, Eibl G, Heinz-Erian P, and Kapelari K. 2003. Perinatal bone turnover in term human neonates and the influence of maternal smoking. *Pediatric research* 53(5):817-822.
- Holick MF. 2003. Vitamin D: A millenium perspective. *J Cell Biochem* 88(2):296-307.
- Holick MF, and Adams JS. 1990. Vitamin D metabolism and biological function. *Metabolic bone disease and Clinically Related Disorders*. 2 ed. Philadelphia: : W. B. Saunders. p 155-195.
- Holm IA. 2007. *Disorders of bone metabolism: Blackwell Publishing Ltd*. 280-292 p.
- Hong J, Hipp J, Mulkern R, Jaramillo D, and Snyder B. 2000. Magnetic resonance imaging measurements of bone density and cross-sectional geometry. *Calcified Tissue Int* 66(1):74-78.
- Huang C, Ross PD, Yates AJ, Walker RE, Imose K, Emi K, and Wasnich RD. 1998. Prediction of fracture risk by radiographic absorptiometry and quantitative ultrasound: A prospective study. *Calcified Tissue Int* 63(5):380-384.
- Hui SL, Slemenda CW, and Johnston CC. 1989. Baseline measurement of bone mass predicts fracture in white women. *Annals of internal medicine* 111(5):355-361.
- Hunziker EB. 1994. Mechanism of longitudinal bone-growth and its regulation by growth-plate chondrocytes. *Microscopy Research and Technique* 28(6):505-519.
- Ibbotson KJ, Roodman GD, McManus LM, and Mundy GR. 1984. Identification and characterization of osteoclast-like cells and their progenitors in cultures of feline marrow mononuclear cells. *The Journal of Cell Biology* 99(2):471-480.
- Imel EA, DiMeglio LA, and Burr DB. 2014. Metabolic bone diseases. In: Burr DB, and Allen MR, editors. *Basic and Applied Bone Biology*. San Diego: Academic Press. p 317-344.
- Itabashi K, Miura A, Okuyama K, Takeuchi T, and Kitazawa S. 1999. Estimated nutritional intake based on the reference growth curves for extremely low birthweight infants. *Pediatrics International* 41(1):70-77.
- Jaffe HL. 1972. *Metabolic, degenerative, and inflammatory diseases of bones and joints: Lea & Febiger*.
- James J, Congdon P, Truscott J, Horsman A, and Arthur R. 1986. Osteopenia of prematurity. *Archives of disease in childhood* 61(9):871-876.
- Jande S. 1972. Effects of parathormone on osteocytes and their surrounding bone matrix. *ZZellforsch* 130(4):463-470.

- Javaid MK, and Cooper C. 2002. Prenatal and childhood influences on osteoporosis. *Best Practice & Research Clinical Endocrinology & Metabolism* 16(2):349-367.
- Jaworski M, Lebedowski M, Lorenc RS, and Trempe J. 1995. Ultrasound bone measurement in pediatric subjects. *Calcif Tissue Int* 56(5):368-371.
- Jaworski Z. 1972. Pathophysiology, diagnosis and treatment of osteomalacia. *The Orthopedic Clinics of North America* 3(3):623-652.
- Jaworski ZFG. 1983. Histomorphometric characteristics of metabolic bone disease. In: Recker RR, editor. *Bone histomorphometry: techniques and interpretation*. Boca Raton: CRC Press. p 241-263.
- Jaworski ZFG, Duck B, and Sekaly G. 1981. Kinetics of osteoclasts and their nuclei in evolving secondary haversian systems. *Journal of Anatomy* 133(OCT):397-405.
- Jaworski ZFG, Kimmel DB, and Jee WSS. 1983. Cell kinetics underlying skeletal growth and bone tissue turnover. In: Recker RR, editor. *Bone Histomorphometry: Techniques and Interpretation*. Boca Raton, FL: CRC Press. p 225-239.
- Jenny Kiratli B. 2001. Immobilization osteopenia. In: Marcus R, Feldman D, and Kelsey J, editors. *Osteoporosis (Second Edition)*. 2nd ed. San Diego: Academic Press. p 207-227.
- Johnson CB. 1991. Neonatal rickets: metabolic bone disease of prematurity. *Neonatal network : NN* 9(7):13-17.
- Jones HE, and Balster RL. 1998. Inhalant abuse in pregnancy. *Obstetrics and gynecology clinics of North America* 25(1):153-167.
- Jones S, and Boyde A. 1978. Scanning electron microscopy of bone cells in culture. *Endocrinology of calcium metabolism Excerpta Medica, Amsterdam* 97.
- Jüppner H, and Kronenberg H. 1999. Parathyroid hormone. *Primer on Metabolic Bone Diseases and Disorders of Mineral Metabolism*, Fifth ed edited by FAVUS, MJ, Washington, American Society for Bone and Mineral Research:117-124.
- Kalkwarf HJ, Zemel BS, Yolton K, and Heubi JE. 2013. Bone mineral content and density of the lumbar spine of infants and toddlers: influence of age, sex, race, growth, and human milk feeding. *Journal of Bone and Mineral Research* 28(1):206-212.
- Kang C, and Speller R. 1998. Comparison of ultrasound and dual energy X-ray absorptiometry measurements in the calcaneus. *The British journal of radiology* 71(848):861-867.
- Kann P, Schulz U, Nink M, Pfützner A, Schrezenmeir J, and Beyer J. 1993. Architecture in cortical bone and ultrasound transmission velocity. *Clin Rheumatol* 12(3):364-367.
- Kaufman JJ, and Einhorn TA. 1993. Perspectives - Ultrasound assessment of bone. *Journal of Bone and Mineral Research* 8(5):517-525.
- Keila S, Kelner A, and Weinreb M. 2001. Systemic prostaglandin E2 increases cancellous bone formation and mass in aging rats and stimulates their bone marrow osteogenic capacity in vivo and in vitro. *Journal of Endocrinology* 168:131-139.
- Kemp AM. 2008. Fractures in physical child abuse. *Paediatrics and Child Health* 18(12):550-553.
- Kemp AM, Dunstan F, Harrison S, Morris S, Mann M, Rolfe K, Datta S, Thomas DP, Sibert JR, and Maguire S. 2008. Patterns of skeletal fractures in child abuse: systematic review. *BMJ* 337.

- Keshawaraz NM, and Recker RR. 1984. Expansion of the medullary cavity at the expense of cortex in postmenopausal osteoporosis. *Metabolic Bone Disease & Related Research* 5(5):223-228.
- King C. 2008. *Preterm infants*: Blackwell Publishing Ltd. 73-89 p.
- King C, and Tavener K. 2014. *Preterm infants*. *Clinical Paediatric Dietetics*: John Wiley & Sons, Ltd. p 81-103.
- Kleerekoper M, Nelson DA, Flynn MJ, Pawluszka AS, Jacobsen G, and Peterson EL. 1994. Comparison of radiographic absorptiometry with dual-energy X-ray absorptiometry and quantitative computed tomography in normal older white and black women. *Journal of Bone and Mineral Research* 9(11):1745-1749.
- Kohles S, Vanderby Jr R, Ashman R, Manley P, Markel M, and Heiner J. 1994. Ultrasonically determined elasticity and cortical density in canine femora after hip arthroplasty. *J Biomech* 27(2):137-144.
- Koo B, Walters J, Hockman E, and Koo W. 2002. Body composition of newborn twins: inpair differences. *J Am Coll Nutr* 21(3):245-249.
- Koo W, Walters J, and Carlson S. 1995a. Postnatal changes in bone mineralization for infants born at term. *Journal of Bone and Mineral Research*: BLACKWELL SCIENCE PUBL INC CAMBRIDGE 238 MAIN ST, CAMBRIDGE, MA 02142. p S295-S295.
- Koo WW. 2000. Body composition measurements during infancy. *Ann N Y Acad Sci* 904:383-392.
- Koo WW, Bush AJ, Walters J, and Carlson SE. 1998. Postnatal development of bone mineral status during infancy. *J Am Coll Nutr* 17(1):65-70.
- Koo WW, and Hockman EM. 2000. Physiologic predictors of lumbar spine bone mass in neonates. *Pediatr Res* 48(4):485-489.
- Koo WW, Walters J, and Bush AJ. 1995b. Technical considerations of dual-energy X-ray absorptiometry-based bone mineral measurements for pediatric studies. *Journal of Bone and Mineral Research* 10(12):1998-2004.
- Koo WWK. 1996. Laboratory assessment of nutritional metabolic bone disease in infants. *Clinical Biochemistry* 29(5):429-438.
- Koo WWK, Bajaj M, Mosely M, and Hammami M. 2008. Quantitative bone US measurements in neonates and their mothers. *Pediatric Radiology* 38(12):1323-1329.
- Koo WWK, Walters J, Bush AJ, Chesney RW, and Carlson SE. 1996. Dual-energy X-ray absorptiometry studies of bone mineral status in newborn infants. *Journal of Bone and Mineral Research* 11(7):997-1002.
- Kovacs CS, and Kronenberg HM. 1997. Maternal-fetal calcium and bone metabolism during pregnancy, puerperium, and lactation *Endocrine reviews* 18(6):832-872.
- Kovacs CS, and Rosen C. 2008. Fetal calcium metabolism. In: Rosen CJ, editor. *Primer on the Metabolic Bone Diseases and Disorders of Mineral Metabolism*. 7 ed. Washington D. C.: ASBMR. p 108-112.
- Kovanlikaya A, Loro ML, Hangartner TN, Reynolds RA, Roe TF, and Gilsanz V. 1996. Osteopenia in children: CT assessment. *Radiology* 198(3):781-784.
- Kruse K. 1995. Pathophysiology of calcium metabolism in children with vitamin D-deficiency rickets. *J Pediatr* 126(5 Pt 1):736-741.



- Kurl S, Heinonen K, Jurvelin JS, and Länsimies E. 2002. Lumbar bone mineral content and density measured using a Lunar DPX densitometer in healthy full-term infants during the first year of life. *Clinical Physiology and Functional Imaging* 22(3):222-225.
- Kurl S, Heinonen K, and Länsimies E. 2000. Effects of prematurity, intrauterine growth status, and early dexamethasone treatment on postnatal bone mineralisation. *Archives of Disease in Childhood Fetal and Neonatal Edition* 83(2):F109-F111.
- Lachman E. 1955. Osteoporosis-the potentialities and limitations of its roentgenologic diagnosis. *Am J Roentgenol* 74:712-713.
- Landis WJ. 1995. The strength of a calcified tissue depends in part on the molecular-structure and organization of its constituent mineral crystals in their organic matrix. *Bone* 16(5):533-544.
- Lanham-New SA, Thompson RL, More J, Brooke-Wavell K, Hunking P, and Medici E. 2007. Importance of vitamin D, calcium and exercise to bone health with specific reference to children and adolescents. *Nutrition Bulletin* 32(4):364-377.
- Lapillonne AA, Glorieux FH, Salle BL, Braillon PM, Chambon M, Rigo J, Putet G, and Senterre J. 1994. Mineral balance and whole body bone mineral content in very low-birth-weight infants. *Acta Paediatr Suppl* 405:117-122.
- Laskey MA. 1996. Dual-energy X-ray absorptiometry and body composition. *Nutrition* 12(1):45-51.
- Laugier P. 2011. Quantitative ultrasound instrumentation for bone in vivo characterization. In: Laugier P, and Häät G, editors. *Bone Quantitative Ultrasound*: Springer Netherlands. p 47-71.
- Lee ER, Lamplugh L, Shepard NL, and Mort JS. 1995. The Septoclast, a cathepsin B-rich cell involved in the resorption of growth-plate cartilage. *J Histochem Cytochem* 43(5):525-536.
- Lee SC, Coan BS, and Bouxsein ML. 1997. Tibial ultrasound velocity measured in situ predicts the material properties of tibial cortical bone. *Bone* 21(1):119-125.
- Leonard MB, Propert KJ, Zemel BS, Stallings VA, and Feldman HI. 1999. Discrepancies in pediatric bone mineral density reference data: potential for misdiagnosis of osteopenia. *The Journal of pediatrics* 135(2):182-188.
- Levine A, Mishna L, Ballin A, Givoni S, Dinari G, Hartman C, and Shamir R. 2002. Use of quantitative ultrasound to assess osteopenia in children with Crohn disease. *Journal of Pediatric Gastroenterology and Nutrition* 35(2):169-172.
- Lewis M, Blake G, and Fogelman I. 1994. Patient dose in dual x-ray absorptiometry. *Osteoporosis International* 4(1):11-15.
- Lindsay R, Zhou H, Cosman F, Nieves J, Dempster DW, and Hodsmann AB. 2007. Effects of a one-month treatment with PTH(1-34) on bone formation on cancellous, endocortical, and periosteal surfaces of the human ilium. *Journal of Bone and Mineral Research* 22(4):495-502.
- Litmanovitz I, Dolfen T, Friedland O, Arnon S, Regev R, Shaikin-Kestenbaum R, Lis M, and Eliakim A. 2003. Early physical activity intervention prevents decrease of bone strength in very low birth weight infants. *Pediatrics* 112(1):15-19.
- Litmanovitz I, Dolfen T, Regev R, Arnon S, Friedland O, Shaikin-Kestenbaum R, Lis M, and Eliakim A. 2004. Bone turnover markers and bone strength during the first weeks of life in very low birth weight premature infants. *Journal of Perinatal Medicine* 32(1):58-61.

- Littner Y, Mandel D, Cohen S, Mimouni FB, and Dollberg S. 2004a. Bone ultrasound velocity of appropriately grown for gestational age concordant twins. *American Journal of Perinatology* 21(5):269-273.
- Littner Y, Mandel D, Mimouni FB, and Dollberg S. 2003. Bone ultrasound velocity curves of newly born term and preterm infants. *Journal of Pediatric Endocrinology & Metabolism* 16(1):43-47.
- Littner Y, Mandel D, Mimouni FB, and Dollberg S. 2004b. Decreased bone ultrasound velocity in large-for-gestational-age infants. *J Perinatol* 24(1):21-23.
- Littner Y, Mandel D, Mimouni FB, and Dollberg S. 2005. Bone ultrasound velocity of infants born small for gestational age. *Journal of Pediatric Endocrinology & Metabolism* 18(8):793-797.
- Locklin RM, Khosla S, Turner RT, and Riggs BL. 2003. Mediators of the biphasic responses of bone to intermittent and continuously administered parathyroid hormone. *Journal of Cellular Biochemistry* 89(1):180-190.
- Loridan L, and Senior B. 1969. Cushing's syndrome in infancy. *The Journal of Pediatrics* 75(3):349-359.
- Love JC, and Sanchez LA. 2009. Recognition of skeletal fractures in infants: An autopsy technique. *Journal of Forensic Sciences* 54(6):1443-1446.
- Lukaski HC. 1993. Soft tissue composition and bone mineral status: evaluation by dual-energy X-ray absorptiometry. *The Journal of nutrition* 123(2 Suppl):438-443.
- Mack PB, and Vogt FB. 1971. Roentgenographic bone density changes in astronauts during representative Apollo space flight. *Am J Roentgenol* 113(4):621-633.
- Maeda Y, Nakamura E, Nguyen MT, Suva LJ, Swain FL, Razzaque MS, Mackem S, and Lanske B. 2007. Indian Hedgehog produced by postnatal chondrocytes is essential for maintaining a growth plate and trabecular bone. *P Natl Acad Sci USA* 104(15):6382-6387.
- Maierhofer WJ, Gray RW, Cheung HS, and Lemann Jr J. 1983. Bone resorption stimulated by elevated serum 1, 25-(OH) 2-vitamin D concentrations in healthy men. *Kidney Int* 24(4).
- Malloy PJ, and Feldman D. 2010. Genetic disorders and defects in vitamin D action. *Endocrinology and Metabolism Clinics of North America* 39(2):333-346.
- Mankin HJ. 1974. Review article, rickets, osteomalacia, and renal osteodystrophy Part 1. *The Journal of Bone & Joint Surgery* 56(1):101-128.
- Maresh MM. 1970. Human growth and development. In: McCammon RW, editor. *Human growth and development*. Springfield, IL: C. C. Thomas. p 157-200.
- Marks SC, and Odgren PR. 2002. Structure and Development of the skeleton. In: Bilezikian JP, Raisz LG, and Rodan GA, editors. *The Principles of Bone Biology*. 2 ed. San Diego: Academic Press. p 3-15.
- Marshall D, Johnell O, and Wedel H. 1996. Meta-analysis of how well measures of bone mineral density predict occurrence of osteoporotic fractures. *British Medical Journal* 312(7041):1254-1259.
- Martin RB, Burr D, and Sharkey N. 1998a. Mechanical properties of bone. *Skeletal Tissue Mechanics*: Springer New York. p 127-180.
- Martin RB, Burr DB, and Sharkey NA. 1998b. Mechanical adaptability of the skeleton. *Skeletal tissue mechanics*. New York: Springer.

- Martin RB, Burr DB, and Sharkey NA. 1998c. Skeletal biology. *Skeletal Tissue Mechanics*. New York: Springer. p 29-78.
- Martin RB, and Ishida J. 1989. The relative effects of collagen fiber orientation, porosity, density, and mineralization on bone strength. *J Biomech* 22(5):419-426.
- Martin SC. 1990. Calcitonin. In: Avioli LV, and Krane SM, editors. *Metabolic Bone Disease and Clinically Related Disorders*. 2 ed. Philadelphia: W. B. Saunders. p 131-154.
- Martin TJ, Robinson CJ, and Macintyre I. 1966. The mode of action of thyrocalcitonin. *The Lancet* 287(7443):900-902.
- Matthews JL. 1980. Bone structure and ultrastructure. In: Urist MR, editor. *Fundamental and Clinical Bone Physiology*. Philadelphia: J. B. Lippincott. p 4-44.
- Mayne PD, and Kovar IZ. 1991. Calcium and phosphorus metabolism in the premature infant. *Annals of clinical biochemistry* 28:131-142.
- Mays S. 2006. Age-related cortical bone loss in women from a 3rd–4th century AD population from England. *American journal of physical anthropology* 129(4):518-528.
- Mays S, Brickley M, and Ives R. 2007. Skeletal evidence for hyperparathyroidism in a 19th century child with rickets. *Int J Osteoarchaeol* 17(1):73-81.
- Mays S, Rogers J, and Watt I. 2001. A possible case of hyperparathyroidism in a burial of 15–17th century AD date from Wharram Percy, England. *Int J Osteoarchaeol* 11(5):329-335.
- Mazess RB, and Cameron JR. 1972. Growth of bone in school children: comparison of radiographic morphometry and photon absorptiometry. *Growth* 36(1):77-92.
- McCann P. 1962. The incidence and value of radiological signs in scurvy. *The British journal of radiology* 35(418):683-686.
- McDevitt H, Tomlinson C, White MP, and Ahmed SF. 2005. Quantitative ultrasound assessment of bone in preterm and term neonates. *Archives of Disease in Childhood-Fetal and Neonatal Edition* 90(4):F341-F342.
- McDevitt H, Tomlinson C, White MP, and Ahmed SF. 2007. Changes in quantitative ultrasound in infants born at less than 32 weeks' gestation over the first 2 years of life: Influence of clinical and biochemical changes. *Calcified Tissue Int* 81(4):263-269.
- McKenzie JA, and Silva MJ. 2011. Comparing histological, vascular and molecular responses associated with woven and lamellar bone formation induced by mechanical loading in the rat ulna. *Bone* 48:250-258.
- Melsen F, and Leif M. 1978. Dynamic studies of trabecular bone formation and osteoid maturation in normal and certain pathological conditions. *Metabolic Bone Disease and Related Research* 1(1):45-48.
- Melton LJ, Atkinson EJ, O'Fallon WM, Wahner HW, and Riggs BL. 1993. Long-term fracture prediction by bone mineral assessed at different skeletal sites. *Journal of Bone and Mineral Research* 8(10):1227-1233.
- Mensforth RP. 1985. Relative tibia long bone growth in the Libben and Bt-5 prehistoric skeletal populations. *Am J Phys Anthropol* 68(2):247-262.
- Mercy J, Dillon B, Morris J, Emmerson AJ, and Mughal MZ. 2007. Relationship of tibial speed of sound and lower limb length to nutrient intake in preterm infants. *Archives of Disease in Childhood-Fetal and Neonatal Edition* 92(5):381-385.

- Meunier P, Courpron P, Edouard C, Bernard J, Bringuier J, and Vignon G. 1973. Physiological senile involution and pathological rarefaction of bone: quantitative and comparative histological data. *Clinics in endocrinology and metabolism* 2(2):239-256.
- Milgram JW. 1990. Radiologic and histologic pathology of nontumorous diseases of bones and joints: Northbrook Pub. Co.
- Miller ME, and Hangartner TN. 1999. Temporary brittle bone disease: Association with decreased fetal movement and osteopenia. *Calcified Tissue Int* 64(2):137-143.
- Miller P. 2000. Controversies in bone mineral density diagnostic classifications. *Calcified Tissue Int* 66(5):317-319.
- Mimouni F, and Littner Y. 2004. Bone mass evaluation in children-comparison between methods. *Pediatric endocrinology reviews: PER* 1(3):320-330.
- Mokkink L, van der Lee J, Grootenhuys M, Offringa M, and Heymans HA. 2008. Defining chronic diseases and health conditions in childhood (0–18 years of age): national consensus in the Netherlands. *European Journal of Pediatrics* 167(12):1441-1447.
- Moran MD. 2003. Arguments for Rejecting the Sequential Bonferroni in Ecological Studies. *Oikos* 100(2):403-405.
- Mosekilde L, and Melsen F. 1976. Anticonvulsant osteomalacia determined by quantitative analysis of bone changes. *Acta Medica Scandinavica* 199(1-6):349-356.
- Mulugeta PG, Jordanov M, Hernanz-Schulman M, Yu C, and Kan JH. 2011. Determination of osteopenia in children on digital radiography compared with a DEXA reference standard. *Academic radiology* 18(6):722-725.
- Mundy G, and Roodman G. 1987. Osteoclast ontogeny and function. *Bone and mineral research* 5:209-279.
- Muscular Dystrophy Association Inc. 2015. Mitochondrial myopathies: Overview. <http://www.mda.org>.
- Nakagawa S. 2004. A farewell to Bonferroni: the problems of low statistical power and publication bias. *Behavioral Ecology* 15(6):1044-1045.
- Nakahara H, Bruder SP, Goldberg VM, and Caplan AI. 1990. In vivo osteochondrogenic potential of cultured-cells derived from the periosteum. *Clinical Orthopaedics and Related Research*(259):223-232.
- Nakahara H, Goldberg VM, and Caplan AI. 1991. Culture-expanded human periosteal-derived cells exhibit osteochondral potential in vivo. *Journal of Orthopaedic Research* 9(4):465-476.
- Nemet D, Dolfin T, Wolach B, and Eliakim A. 2001. Quantitative ultrasound measurements of bone speed of sound in premature infants. *European Journal of Pediatrics* 160(12):736-740.
- Neuman WF, and Neuman MW. 1953. The nature of the mineral phase of bone. *Chem Rev* 53(1):1-45.
- Nguyen T, Sambrook P, Kelly P, Jones G, Lord S, Freund J, and Eisman J. 1993. Prediction of osteoporotic fractures by postural instability and bone density. *BMJ: British Medical Journal*:1111-1115.
- Nicholson PHF, Lowet G, Cheng XG, Boonen S, vanderPerre G, and Dequeker J. 1997. Assessment of the strength of the proximal femur in vitro: Relationship with ultrasonic measurements of the calcaneus. *Bone* 20(3):219-224.
- Nilsson A, Ohlsson C, Isaksson OGP, Lindahl A, and Isgaard J. 1994. Hormonal-regulation of longitudinal bone-growth. *European Journal of Clinical Nutrition* 48:S150-S160.

- Njeh C, Hans D, Wu C, Kantorovich E, Sister M, Fuerst T, and Genant H. 1999. An in vitro investigation of the dependence on sample thickness of the speed of sound along the specimen. *Med Eng Phys* 21(9):651-659.
- Njeh C, Wu C, Fan B, Hans D, Fuerst T, He Y, and Genant H. 2000. Estimation of wrist fracture load using phalangeal speed of sound: an in vitro study. *Ultrasound in medicine & biology* 26(9):1517-1523.
- Njeh CF, Boivin CM, and Langton CM. 1997. The role of ultrasound in the assessment of osteoporosis: A review. *Osteoporosis International* 7(1):7-22.
- Njeh CF, Saeed I, Grigorian M, Kendler DL, Fan B, Shepherd J, McClung M, Drake WM, and Genant HK. 2001. Assessment of bone status using speed of sound at multiple anatomical sites. *Ultrasound in Medicine and Biology* 27(10):1337-1345.
- Norrdin R, Phemister R, Jaenke R, and Presti CL. 1977. Density and composition of trabecular and cortical bone in perinatally irradiated beagles with chronic renal failure. *Calcified tissue research* 24(1):99-104.
- Nuzzo S, Meneghini C, Braillon P, Bouvier R, Mobilio S, and Peyrin F. 2003. Microarchitectural and physical changes during fetal growth in human vertebral bone. *Journal of Bone and Mineral Research* 18(4):760-768.
- Ogden JA. 1979. The development and growth of the musculo-skeletal system. In: Albright JA, and Brands R, editors. *Scientific Basis of Orthopaedics*. New York: Appleton-Century-Crofts. p 41-103.
- Orden A, Oyhenart E, Cesani M, Zucchi M, Mune M, Villanueva M, Rodriguez R, Pons E, and Pucciarelli H. 2002. Effect of moderate undernutrition on the functional components of the axial skeleton. *American Journal of Physical Anthropology: WILEY-LISS DIV JOHN WILEY & SONS INC, 605 THIRD AVE, NEW YORK, NY 10158-0012 USA*. p 120-120.
- Ortner DJ. 2003a. Endocrine disturbances. In: Ortner DJ, editor. *Identification of Pathological Conditions in Human Skeletal Remains (Second Edition)*. 2nd ed. San Diego: Academic Press. p 419-433.
- Ortner DJ. 2003b. *Identification of pathological conditions in human skeletal remains*. Academic Press.
- Ortner DJ. 2003c. Metabolic disorders. In: Ortner DJ, editor. *Identification of Pathological Conditions in Human Skeletal Remains (Second Edition)*. Second ed. San Diego: Academic Press. p 383-418.
- Ortner DJ. 2008. The background to bone biology and mineral metabolism. In: Brickley M, and Rachel I, editors. *The bioarchaeology of metabolic bone disease*. 1st ed. Amsterdam: Boston. p 21-40.
- Ortner DJ, Butler W, Cafarella J, and Milligan L. 2001. Evidence of probable scurvy in subadults from archeological sites in North America. *American Journal of Physical Anthropology* 114(4):343-351.
- Ortner DJ, and Ericksen MF. 1997. Bone changes in the human skull probably resulting from scurvy in infancy and childhood. *Int J Osteoarchaeol* 7(3):212-220.
- Ortner DJ, Kimmerle EH, and Diez M. 1999. Probable evidence of scurvy in subadults from archeological sites in Peru. *American Journal of Physical Anthropology* 108(3):321-331.
- Ortner DJ, and Mays S. 1998. Dry-bone manifestations of rickets in infancy and early childhood. *Int J Osteoarchaeol* 8(1):45-55.
- Ortner DJ, and Turner-Walker G. 2003. The biology of skeletal tissues. In: Ortner DJ, editor. *Identification of Pathological Conditions in Human Skeletal Remains*. 2nd ed. London: Academic Press. p 11-35.

- Paic F, Igwe JC, Nori R, Kronenberg MS, Franceschetti T, Harrington P, Kuo L, Shin D-G, Rowe DW, Harris SE et al. . 2009. Identification of differentially expressed genes between osteoblasts and osteocytes. *Bone* 45(4):682-692.
- Paley D, Young MC, Wiley AM, Fornasier VL, and Jackson RW. 1986. Percutaneous bone-marrow grafting of fractures and bony defects - an experimental-study in rabbits. *Clinical Orthopaedics and Related Research*(208):300-312.
- Pande K, Bernard J, McCloskey E, De Takats D, and Kanis J. 2000. Ultrasound velocity and dual-energy X-ray absorptiometry in normal and pagetic bone. *Bone* 26(5):525-528.
- Parfitt AM. 1988. Bone remodeling. *Henry Ford Hospital medical journal* 36(3):143-144.
- Parfitt AM. 1994. Osteonal and hemi-osteonal remodeling - the spatial and temporal framework for signal traffic in adult human bone. *Journal of Cellular Biochemistry* 55(3):273-286.
- Parfitt AM. 2000. The mechanism of coupling: A role for the vasculature. *Bone* 26(4):319-323.
- Parfitt AM. 2003. New concepts of bone remodeling: A unified spatial and temporal model with physiologic and pathophysiologic implications. In: Agarwal S, and Stout S, editors. *Bone Loss and Osteoporosis: Springer US*. p 3-17.
- Paterson CR. 2009. Vitamin D deficiency rickets and allegations of non-accidental injury. *Acta Pædiatrica* 98(12):2008-2012.
- Pearce S, Hurtig M, Runciman J, and Dickey J. 2000. Effect of age, anatomic site and soft tissue on quantitative ultrasound. *Journal Of Bone And Mineral Research* 15:SU315-SU315.
- Peck W, and Woods W. 1988. The cells of bone. *Osteoporosis: etiology, diagnosis and management Raven Press, New York*:17-19.
- Pereda L, Ashmeade T, Zaritt J, and Carver JD. 2003. The use of quantitative ultrasound in assessing bone status in newborn preterm infants. *J Perinatol* 23(8):655-659.
- Perez-Rossello JM, Feldman HA, Kleinman PK, Connolly SA, Fair RA, Myers RM, and Gordon CM. 2012. Rachitic changes, demineralization, and fracture risk in healthy infants and toddlers with vitamin D deficiency. *Radiology* 262(1):234-241.
- Perrin EC, Newacheck P, Pless IB, Drotar D, Gortmaker SL, Leventhal J, Perrin JM, Stein RE, Walker DK, and Weitzman M. 1993. Issues involved in the definition and classification of chronic health conditions. *Pediatrics* 91(4):787-793.
- Petrtyl M, Hert J, and Fiala P. 1996. Spatial organization of the haversian bone in man. *J Biomech* 29(2):161-&.
- Pettifor JM. 2003. Nutritional rickets. In: Glorieux FH, Pettifor JM, and Jüppner H, editors. *Pediatric Bone First ed. San Diego: Academic Press*. p 541-565.
- Pettifor JM, and Daniels ED. 1997. Vitamin D deficiency and nutritional rickets in children. In: Feldman D, Glorieux FH, and Pike J, editors. *Vitamin D. San Diego: Academic Press*. p 663-679.
- Pettit AR, Chang MK, Hume DA, and Raggatt LJ. 2008. Osteal macrophages: A new twist on coupling during bone dynamics. *Bone* 43(6):976-982.
- Pimentel L. 2003. Scurvy: historical review and current diagnostic approach. *The American journal of emergency medicine* 21(4):328-332.

- Pitt M. 1988. Rickets and osteomalacia. In: Resnick D, and Niwayama G, editors. *Diagnosis of bone and joint disorders*. 2nd ed. Philadelphia: WB Saunders. p 2086-2119.
- Pitt M. 1995. Rickets and osteomalacia. In: Resnick D, editor. *Diagnosis of Bone and Joint Disorders*. 3rd ed. Philadelphia: Saunders. p 1885-1922.
- Polig E, and Jee WSS. 1990. A model of osteon closure in cortical bone. *Calcified Tissue Int* 47(5):261-269.
- Portigliatti Barbos M, Bianco P, Ascenzi A, and Boyde A. 1984. Collagen orientation in compact bone: II. Distribution of lamellae in the whole of the human femoral shaft with reference to its mechanical properties. *Metabolic Bone Disease and Related Research* 5(6):309-315.
- Potts JT. 1998. Primary hyperparathyroidism. In: Avioli LV, and Krane SM, editors. *Metabolic Bone Disease and Clinically Related Disorders (Third Edition)*. San Diego: Academic Press. p 411-442.
- Prentice A, Laskey MA, Shaw J, Cole TJ, and Fraser DR. 1990. Bone mineral content of Gambian and British children aged 0-36 months. *Bone Miner* 10(3):211-224.
- Prevrhal S, Fuerst T, Fan B, Njeh C, Hans D, Uffmann M, Srivastav S, and Genant HK. 2001. Quantitative ultrasound of the tibia depends on both cortical density and thickness. *Osteoporosis International* 12(1):28-34.
- Price JS, Oyajobi BO, and Russell RGG. 1994. The cell biology of bone-growth. *European Journal of Clinical Nutrition* 48:S131-S131.
- Prins S, Jorgensen H, Jorgensen L, and Hassager C. 1997. The role of quantitative ultrasound in the assessment of bone: a review. *Clin Physiol*.
- Rack B, Lochmuller EM, Janni W, Lipowsky G, Engelsberger I, Friese K, and Kuster H. 2012. Ultrasound for the assessment of bone quality in preterm and term infants. *Journal of Perinatology* 32(3):218-226.
- Raisz L, Kream B, Smith M, and Simmons H. 1980. Comparison of the effects of vitamin D metabolites on collagen synthesis and resorption of fetal rat bone in organ culture. *Calcified Tissue Int* 32(1):135-138.
- Raisz LG. 1965. Bone resorption in tissue culture. Factors influencing the response to parathyroid hormone. *Journal of Clinical Investigation* 44(1):103.
- Raisz LG. 1999. Physiology and pathophysiology of bone remodeling. *Clinical Chemistry* 45(8):1353-1358.
- Raisz LG, and Kream BE. 1983. Regulation of bone formation (second of two parts). *The New England journal of medicine* 309(2):83-89.
- Raisz LG, and Rodan GA. 1990. Cellular basis for bone turnover. In: Avioli LV, and Krane SM, editors. *Metabolic Bone Disease and Clinically Related Disorders*. 2 ed. Philadelphia: W. B. Saunders. p 1-41.
- Rang M, and ed. 1969. *The Growth plate and its disorders*. Edinburgh: London, E & S Livingstone. xi, 203 p.
- Rasband WS. 1997-2014. *ImageJ*. Bethesda, Maryland, USA: U. S. National Institute of Health.
- Rathbun J. 1948. "Hypophosphatasia" A new developmental anomaly. *Archives of Pediatrics & Adolescent Medicine* 75(6):822.
- Rauch F, and Schoenau E. 2001. Changes in bone density during childhood and adolescence: An approach based on bone's biological organization. *Journal of Bone and Mineral Research* 16(4):597-604.

- Rauch F, and Schoenau E. 2002. Skeletal development in premature infants: A review of bone physiology beyond nutritional aspects. *Archives of Disease in Childhood* 86:F82-F85.
- Raum K, Grimal Q, Varga P, Barkmann R, Gluer CC, and Laugier P. 2014. Ultrasound to assess bone quality. *Curr Osteoporos Rep* 12(2):154-162.
- Raum K, Leguerney I, Chandelier F, Bossy E, Talmant M, Saïed A, Peyrin F, and Laugier P. 2005. Bone microstructure and elastic tissue properties are reflected in QUS axial transmission measurements. *Ultrasound in medicine & biology* 31(9):1225-1235.
- Rauner M, Stein N, and Hofbauer LC. 2012. Basics of bone biology. In: Pietschmann P, editor. *Principles of osteoimmunology : molecular mechanisms and clinical applications*. New York: Springer-Verlag. p 1-26.
- Raux P, Townsend PR, Miegel R, Rose RM, and Radin EL. 1975. Trabecular Architecture Of Human Patella. *J Biomech* 8(1):1-7.
- Ravichandiran N, Schuh S, Bejuk M, Al-Harthy N, Shouldice M, Au H, and Boutis K. 2010. Delayed identification of pediatric abuse-related fractures. *Pediatrics* 125(1):60-66.
- Rawlings DJ, Cooke RJ, McCormick K, Griffin IJ, Faulkner K, Wells JCK, Smith JS, and Robinson SJ. 1999. Body composition of preterm infants during infancy. *Archives of Disease in Childhood - Fetal and Neonatal Edition* 80(3):F188-F191.
- Rebocho LM, Cardadeiro G, Zymbal V, Goncalves EM, Sardinha LB, and Baptista F. 2014. Measurement properties of radial and tibial speed of sound for screening bone fragility in 10- to 12-year-old boys and girls. *Journal of clinical densitometry : the official journal of the International Society for Clinical Densitometry* 17(4):528-533.
- Recker RR. 1992. Embryology, anatomy, and microstructure of bone. In: Coe FL, and Favus MJ, editors. *Disorders of Bone Mineral Metabolism*. New York: Raven Press. p 219-240.
- Resnick D. 1995. Thyroid disorders. In: Resnick D, editor. *Diagnosis of Bone and Joint Disorders*. Third ed. Philadelphia: W B Saunders. p 1995-2011.
- Resnick D, and Niwayama G. 1988. *Diagnosis of Bone and Joint Disorders*. Philadelphia: W. B. Saunders.
- Reynolds W, and Karo J. 1972. Radiologic diagnosis of metabolic bone disease. *The Orthopedic clinics of North America* 3(3):521.
- Riggs BL, Khosla S, and Melton LJ. 1999. The assembly of the adult skeleton during growth and maturation: implications for senile osteoporosis. *Journal of Clinical Investigation* 104(6):671-672.
- Rigo J, and De Curtis M. 2006. Disorders of calcium, phosphorus and magnesium metabolism. In: Martin RJ, Fanaroff AA, and C. WM, editors. *Fanaroff & Martin's Neonatal-Perinatal Medicine: Diseases of the Fetus and Infant*. 8 ed. Philadelphia, PA: Mosby-Elsevier. p 1491-1523.
- Rigo J, Nyamugabo K, Picaud JC, Gerard P, Pieltain C, and De Curtis M. 1998. Reference values of body composition obtained by dual energy X-ray absorptiometry in preterm and term neonates. *J Pediatr Gastroenterol Nutr* 27(2):184-190.
- Ritschl E, Wehmeijer K, De Terlizzi F, Wipfler E, Cadossi R, Douma D, Urlesberger B, and Muller W. 2005. Assessment of skeletal development in preterm and term infants by quantitative ultrasound. *Pediatric Research* 58(2):341-346.



- Rizzoli R, and Bonjour JP. 2004. Dietary protein and bone health. *Journal of bone and mineral research* 19(4):527-531.
- Robling AG, Castillo AB, and Turner CH. 2006. Biomechanical and molecular regulation of bone remodeling. *Annual Review of Biomedical Engineering* 8:449-455.
- Rodan GA. 1992. Introduction to bone biology. *Bone* 13:S3-S6.
- Rodan GA, and Martin TJ. 1981. Role of osteoblasts in hormonal-control of bone-resorption - a hypothesis. *Calcified Tissue Int* 33(4):349-351.
- Roodman GD, Ibbotson KJ, MacDonald BR, Kuehl TJ, and Mundy GR. 1985. 1,25-Dihydroxyvitamin D3 causes formation of multinucleated cells with several osteoclast characteristics in cultures of primate marrow. *Proceedings of the National Academy of Sciences* 82(23):8213-8217.
- Ross DS. 1998. Bone Disease in Hyperthyroidism. In: Avioli LV, and Krane SM, editors. *Metabolic bone disease and clinically related disorders* 3ed. San Diego: Academic Press. p 531-544.
- Ross P, Huang C, Davis J, Imose K, Yates J, Vogel J, and Wasnich R. 1995. Predicting vertebral deformity using bone densitometry at various skeletal sites and calcaneus ultrasound. *Bone* 16(3):325-332.
- Ross PD, Davis JW, Epstein RS, and Wasnich RD. 1991. Preexisting fractures and bone mass predict vertebral fracture incidence in women. *Annals of Internal Medicine* 114(11):919-923.
- Rubinacci A, Moro GE, Boehm G, de Terlizzi F, Moro GL, and Cadossi R. 2003. Quantitative ultrasound for the assessment of osteopenia in preterm infants. *European Journal of Endocrinology* 149(4):307-315.
- Ruff C, and Hayes W. 1982. Subperiosteal expansion and cortical remodeling of the human femur and tibia with aging. *Science* 217(4563):945-948.
- Russell R, Bunning R, Hughes D, and Gowen M. 1990. Humoral and local factors affecting bone formation and resorption. *New techniques in metabolic bone disease* Butterworth, London:1-20.
- Ryan TM, and Krovitz GE. 2006. Trabecular bone ontogeny in the human proximal femur. *J Hum Evol* 51(6):591-602.
- Ryan TM, Van Rietbergen B, and Krovitz GE. 2007. Mechanical adaptation of trabecular bone in the growing human femur and humerus. *American Journal of Physical Anthropology* 132(S44):205.
- Saggese G, Baroncelli GI, Bertelloni S, Cinquanta L, and Di Nero G. 1993. Effects of long-term treatment with growth hormone on bone and mineral metabolism in children with growth hormone deficiency. *J Pediatr* 122(1):37-45.
- Sakata S, Barkmann R, Lochmüller E-M, Heller M, and Glüer C-C. 2004. Assessing bone status beyond bmd: Evaluation of bone geometry and porosity by quantitative ultrasound of human finger phalanges. *Journal of Bone and Mineral Research* 19(6):924-930.
- Salle BL, Rauch F, Travers R, Bouvier R, and Glorieux FH. 2002. Human fetal bone development: histomorphometric evaluation of the proximal femoral metaphysis. *Bone* 30(6):823-828.
- Salter RB. 1999a. Normal structure and function of the musculoskeletal tissues. In: Salter RB, editor. *Textbook of Disorders and Injuries of the Musculoskeletal System*. Third ed. Baltimore: Williams & Wilkins. p 7-28.
- Salter RB. 1999b. Reactions of musculoskeletal tissues to disorders and injuries. In: Salter RB, editor. *Textbook of disorders and injuries of the musculoskeletal system: An introduction to orthopaedics, fractures, and joint*

- injuries, rheumatology, metabolic bone disease, and rehabilitation. Third ed. Baltimore: Lippincott Williams & Wilkins. p 29-49.
- Sartoris D, and Resnick D. 1989. Dual-energy radiographic absorptiometry for bone densitometry: current status and perspective. *Am J Roentgenol* 152(2):241-246.
- Scherl SA. 2006. Orthopaedic injuries in child abuse. *Current Paediatrics* 16(3):199-204.
- Scheuer L, and Black S. 2000a. Bone development. In: Scheuer L, and Black S, editors. *Developmental Juvenile Osteology*. Amsterdam: Elsevier/Academic Press. p 18-31.
- Scheuer L, and Black S. 2000b. Development and ageing of the juvenile skeleton. In: Cox M, and Mays S, editors. *Human osteology in archaeology and forensic science*. New York: Cambridge University Press. p 9-22.
- Schmidt-Nielsen K. 1984. *The strength of bones and skeletons. Scaling: Why animal size is so important?* Cambridge: Cambridge University Press.
- Schmidt M. 1929. *Rhachitis und osteomalazie. Knochen· Muskeln Sehnen· Sehnenscheiden Schleimbeutel*: Springer. p 1-165.
- Schoenau E, Land C, Stabrey A, Remer T, and Kroke A. 2004. The bone mass concept: problems in short stature. *European journal of endocrinology* 151(Suppl 1):S87-S91.
- Schönau E. 1998. Problems of bone analysis in childhood and adolescence. *Pediatric Nephrology* 12(5):420-429.
- Schuit SCE, van der Klift M, Weel A, de Laet C, Burger H, Seeman E, Hofman A, Uitterlinden AG, van Leeuwen J, and Pols HAP. 2004. Fracture incidence and association with bone mineral density in elderly men and women: the Rotterdam Study. *Bone* 34(1):195-202.
- Seeman E. 1997. From density to structure: Growing up and growing old on the surfaces of bone. *Journal of Bone and Mineral Research* 12(4):509-521.
- Seeman E. 2008. Bone quality: the material and structural basis of bone strength. *Journal of bone and mineral metabolism* 26(1):1-8.
- Seeman E, and Delmas PD. 2006. Bone Quality — The material and structural basis of bone strength and fragility. *New England Journal of Medicine* 354(21):2250-2261.
- Senterre J, and Salle B. 1982. Calcium and phosphorus economy of the preterm infant and its interaction with vitamin D and its metabolites. *Acta Pædiatrica* 71:85-92.
- Sevitt S. 1981. *Bone repair and fracture healing in man*. Edinburgh: New York. 315 p. p.
- Sharp M. 2007. Bone disease of prematurity. *Early human development* 83(10):653.
- Shaw J. 1976. Evidence for defective skeletal mineralization in low-birthweight infants: the absorption of calcium and fat. *Pediatrics* 57(1):16-25.
- Shaw J. 1982. Trace metal requirements of preterm infants. *Acta Pædiatrica* 71:93-100.
- Shaw JH. 1955. Effect of nutritional factors on bones and teeth. *Annals of the New York Academy of Sciences* 60(5):733-762.
- Sheth RD. 2004. Bone health in pediatric epilepsy. *Epilepsy & Behavior* 5, Supplement 2:30-35.

- Shires R, Avioli LV, Bergfeld MA, Fallon MD, Slatopolsky E, and Teitelbaum SL. 1980. Effects of semistarvation on skeletal homeostasis. *Endocrinology* 107(5):1530-1535.
- Shore EM, Xu MQ, Feldman GJ, Fenstermacher DA, Brown MA, Kaplan FS, and Consortium FOPIR. 2006. A recurrent mutation in the BMP type I receptor ACVR1 causes inherited and sporadic fibrodysplasia ossificans progressiva. *Nat Genet* 38(5):525-527.
- Shore RM, and Poznanski AK. 1999. Radiologic evaluation of bone mineral in children. In: Favus MJ, editor. *Primer on the metabolic bone diseases and disorders of mineral metabolism*. 4th ed. Philadelphia: Lippincott Williams & Wilkins. p 134-146.
- Sievanen H, Backstrom MC, Kuusela A-L, Ikonen RS, and Maki M. 1999. Dual energy X-ray absorptiometry of the forearm in preterm and term infants: Evaluation of the methodology. *Pediatr Res* 45(1):100-105.
- Sievanen H, Cheng S, Ollikainen S, and Uusi-Rasi K. 2001. Ultrasound velocity and cortical bone characteristics in vivo. *Osteoporos Int* 12(5):399-405.
- Silver IA, Murrills RJ, and Etherington DJ. 1988. Microelectrode studies on the acid environment beneath adherent macrophages and osteoclasts. *Experimental Cell Research* 175:266-276.
- Silverman FN. 1985. *Caffey's pediatric X-ray diagnosis: an integrated imaging approach*. Chicago: Year Book Medical Publishers.
- Sissons H. 1956. The osteoporosis of Cushing's syndrome. *Journal of Bone & Joint Surgery, British Volume* 38(1):418-433.
- Sloan B, Kulwin DR, and Kersten RC. 1999. Scurvy causing bilateral orbital hemorrhage. *Archives of ophthalmology* 117(6):842-843.
- Sommerfeldt DW, and Rubin CT. 2001. Biology of bone and how it orchestrates the form and function of the skeleton. *Eur Spine J* 10:S86-S95.
- Specker BL, Beck A, Kalkwarf H, and Ho M. 1997. Randomized trial of varying mineral intake on total body bone mineral accretion during the first year of life. *Pediatrics* 99(6):E12.
- Specker BL, Namgung R, and Tsang RC. 2001. Bone mineral acquisition *in utero*, during infancy, and throughout childhood. In: Marcus R, Feldman D, and Kelsey J, editors. *Osteoporosis*. 2nd ed. San Diego: Academic Press. p 599-620.
- Specker BL, and Schoenau E. 2005. Quantitative bone analysis in children: current methods and recommendations. *The Journal of pediatrics* 146(6):726-731.
- St-Arnaud R, and Glorieux FH. 1997. Vitamin D and bone development. In: Feldman D, Glorieux FH, and Pike JW, editors. *Vitamin D*. San Diego: Academic Press. p 293-303.
- Stein RE, Bauman LJ, Westbrook LE, Coupey SM, and Ireys HT. 1993. Framework for identifying children who have chronic conditions: the case for a new definition. *J Pediatr* 122(3):342-347.
- Stern PH. 1980. The D vitamins and bone. *Pharmacological Reviews* 32(1):47-80.
- Stickens D, Behonick DJ, Ortega N, Heyer B, Hartenstein B, Yu Y, Fosang AJ, Schorpp-Kistner M, Angel P, and Werb Z. 2004. Altered endochondral bone development in matrix metalloproteinase 13-deficient mice. *Development* 131(23):5883-5895.

- Storm EE, and Kingsley DM. 1999. GDF5 coordinates bone and joint formation during digit development. *Developmental Biology* 209(1):11-27.
- Streeter GL. 1949. Developmental horizons in human embryos (4th issue) - A review of the histogenesis of cartilage and bone. *Contributions to Embryology* 33(220):151-&.
- Stuart HC, Hill P, and Shaw C. 1940. The growth of bone, muscle and overlying tissues as revealed by studies of roentgenograms of the leg area. *Monographs of the Society for Research and Child Development* 5(3):1-190.
- Sundberg M, Gardsell P, Johnell O, Ornstein E, and Sernbo I. 1998. Comparison of quantitative ultrasound measurements in calcaneus with DXA and SXA at other skeletal sites: a population-based study on 280 children aged 11-16 years. *Osteoporos Int* 8(5):410-417.
- Swezey R, Draper D, and Swezey A. 1996. Bone densitometry: comparison of dual energy x-ray absorptiometry to radiographic absorptiometry. *The Journal of rheumatology* 23(10):1734-1738.
- Takada M, Engelke K, Hagiwara S, Grampp S, Jergas M, Glüer CC, and Genant HK. 1997. Assessment of osteoporosis: comparison of radiographic absorptiometry of the phalanges and dual X-ray absorptiometry of the radius and lumbar spine. *Radiology* 202(3):759-763.
- Talmant M, Kolta S, Roux C, Haguenaer D, Vedel I, Cassou B, Bossy E, and Laugier P. 2009. *In vivo* performance evaluation of bi-directional ultrasonic axial transmission for cortical bone assessment. *Ultrasound in medicine & biology* 35(6):912-919.
- Tamura Y, Welch DC, Zic JA, Cooper WO, Stein SM, and Hummell DS. 2000. Scurvy presenting as painful gait with bruising in a young boy. *Archives of pediatrics & adolescent medicine* 154(7):732-735.
- Tansug N, Yildirim SA, Canda E, Ozalp D, Yilmaz O, Taneli F, and Ersoy B. 2011. Changes in quantitative ultrasound in preterm and term infants during the first year of life. *European Journal of Radiology* 79(3):428-431.
- Taylor J. 1992. The periosteum and bone growth. In: Hall B, editor. *Bone growth*. Boca Raton: CRC Press. p 21-52.
- Teitelbaum JE, Rodriguez RJ, Ashmeade TL, Yaniv I, Osuntokun BO, Hudome S, and Fanaroff A. 2006. Quantitative ultrasound in the evaluation of bone status in premature and full-term infants. *Journal of Clinical Densitometry* 9(3):358-362.
- Teitelbaum SL. 2000. Bone resorption by osteoclasts. *Science* 289(5484):1504-1508.
- Thompson PW, Taylor J, Oliver R, and Fisher A. 1998. Quantitative ultrasound (QUS) of the heel predicts wrist and osteoporosis-related fractures in women age 45-75 years. *Journal of Clinical Densitometry* 1(3):219-225.
- Tomlinson C, McDevitt H, Ahmed SF, and White MP. 2006. Longitudinal changes in bone health as assessed by the speed of sound in very low birth weight preterm infants. *Journal of Pediatrics* 148(4):450-455.
- Torzilli PA, Burstein AH, Takebe K, Zika JC, and Heiple KG. 1981. The mechanical and structural properties of maturing bone. In: Cowen SC, editor. *Mechanical properties of Bone*. New York: American Society of Mechanical Engineers. p 145-161.
- Townsend PR, Rose RM, and Radin EL. 1975. Buckling studies of single human trabeculae. *J Biomech* 8(3-4):199-&.
- Töyräs J, Kröger H, and Jurvelin J. 1999. Bone properties as estimated by mineral density, ultrasound attenuation, and velocity. *Bone* 25(6):725-731.

- Trotter M. 1971. The density of bones in the young skeleton. *Growth* 35(3):221-231.
- Trotter M, and Hixon B. 1974. Sequential changes in weight, density, and percentage ash weight of human skeletons from an early fetal period through old age. *Anatomical Record* 179:1-18.
- Trotter M, and Peterson RR. 1969. Weight of bone during the fetal period. *Growth* 33(2):167-184.
- Trotter M, and Peterson RR. 1970. The density of bones in the fetal skeleton. *Growth* 34:283-292.
- Turner CH, and Burr DB. 1993. Basic biomechanical measurements of bone - a tutorial. *Bone* 14(4):595-608.
- Turner CH, and Robling AG. 2004. Mechanical loading and bone formation. *IBMS BoneKEy* 1(9):15-23.
- Vahedi K, and Alamowitch S. 2011. Clinical spectrum of type IV collagen (COL4A1) mutations: a novel genetic multisystem disease. *Current Opinion in Neurology* 24(1):63-68.
- van der Lee JH, Mokkink LB, Grootenhuys MA, Heymans HS, and Offringa M. 2007. Definitions and measurement of chronic health conditions in childhood: a systematic review. *Jama* 297(24):2741-2751.
- van der Meulen MCH, Jepsen KJ, and Mikic B. 2001. Understanding bone strength: Size isn't everything. *Bone* 29(2):101-104.
- van Rijn RR, van der Sluis IM, Lequin MH, Robben SG, de Muinck Keizer-Schrama SM, Hop WC, and van Kuijk C. 2000. Tibial quantitative ultrasound versus whole-body and lumbar spine DXA in a Dutch pediatric and adolescent population. *Invest Radiol* 35(9):548-552.
- Venkataraman PS, Han BK, Tsang RC, and Daugherty CC. 1983. Secondary hyperparathyroidism and bone disease in infants receiving long-term furosemide therapy. *Am J Dis Child* 137(12):1157-1161.
- Vinz H. 1970. Studies on density, water and mineral contents of compact human bone tissue depending on age. *Gegenbaurs Morphol Jahrb* 115:273-283.
- Vinz H. 1971. [Degree of mineralization depending on the age of compact bone substance]. *Z Alternsforsch* 23(4):353-359.
- Vose GP. 1969. Estimation of changes in bone calcium content by radiographic densitometry 1. *Radiology* 93(4):841-844.
- Vose GP, and Kubala AL. 1959. Bone strength—its relationship to x-ray-determined ash content. *Hum Biol*:261-270.
- Vyhmeister NR, Linkhart TA, Hay S, Baylink DJ, and Ghosh B. 1987. Measurement of bone mineral content in the term and preterm infant. *American journal of diseases of children (1960)* 141(5):506-510.
- Wallace JM. 2014. Skeletal hard tissue biomechanics. In: Burr DB, and Allen MR, editors. *Basic and Applied Bone Biology*. San Diego: Academic Press. p 115-130.
- Ward KA, Mughal Z, and Adams JE. 2007. Tools for measuring bone in children and adolescents. In: Sawyer A, Bachrach L, and Fung E, editors. *Bone Densitometry in Growing Patients*: Humana Press. p 15-40.
- Wasserman R. 1997. *Vitamin D and the intestinal absorption of calcium and phosphorus*. Academic Press. San Diego.

- Wauben IP, Atkinson SA, Grad TL, Shah JK, and Paes B. 1998. Moderate nutrient supplementation of mother's milk for preterm infants supports adequate bone mass and short-term growth: a randomized, controlled trial. *Am J Clin Nutr* 67(3):465-472.
- Wear KA. 2000. Measurements of phase velocity and group velocity in human calcaneus. *Ultrasound in medicine & biology* 26(4):641-646.
- Weaver CM, and Fuchs RK. 2014. Skeletal growth and development. In: Burr DB, and Allen MR, editors. *Basic and Applied Bone Biology*. San Diego: Academic Press. p 245-260.
- Weaver CM, and Gallant KMH. 2014. Nutrition. In: Burr DB, and Allen MR, editors. *Basic and Applied Bone Biology*. San Diego: Academic Press. p 283-297.
- Weiler HA, Wang Z, and Atkinson SA. 1995. Dexamethasone treatment impairs calcium regulation and reduces bone mineralization in infant pigs. *Am J Clin Nutr* 61(4):805-811.
- Weinmann JPSH. 1947. *Bone and bones; fundamentals of bone biology*. St. Louis: Mosby. 464 p.
- Weiss M, Ben-Shlomo A, Hagag P, and Ish-Shalom S. 2000. Discrimination of proximal hip fracture by quantitative ultrasound measurement at the radius. *Osteoporosis International* 11(5):411-416.
- Whiteside L. 1983. Circulation in bone. In: McCollister Evarts C, editor. *Surgery of the Musculoskeletal System*. New York: Churchill Livingstone. p 51-63.
- WHO Multicentre Growth Reference Study Group. 2006. WHO Child Growth Standards: Length/height-for-age, weight-for-age, weight-for-length, weight-for-height and body mass index-for-age: Methods and development. Geneva: World Health Organization. p 312.
- Widdowson EM, Southgate DAT, and Hey E. 1988. Fetal growth and body composition. In: Landblad BS, editor. *Perinatal nutrition*. New York: Academic Press.
- Widdowson EM, and Spray CM. 1951. Chemical development *in utero*. *Archives of disease in childhood* 26(127):205-214.
- Wilkins L. 1950. *The diagnosis and treatment of endocrine disorders in childhood and adolescence*: Thomas.
- Wimberger H. 1925. Klinisch-radiologische Diagnostik von Rachitis, Skorbut und Lues congenita im Kindesalter. In: Kraus F, Meyer E, Minkowski O, Müller F, Sahli H, Schittenhelm A, Czerny A, Heubner O, and Langstein L, editors. *Ergebnisse der Inneren Medizin und Kinderheilkunde*: Springer Berlin Heidelberg. p 264-370.
- Worlock P, Stower M, and Barbor P. 1986. Patterns of fractures in accidental and non-accidental injury in children: A comparative study. *British Medical Journal (Clinical Research Edition)* 293(6539):100-102.
- Wren TA, Liu X, Pitukcheewanont P, and Gilsanz V. 2005. Bone densitometry in pediatric populations: discrepancies in the diagnosis of osteoporosis by DXA and CT. *The Journal of pediatrics* 146(6):776-779.
- Wright LL, Glade MJ, and Gopal J. 1987. The use of transmission ultrasonics to assess bone status in the human newborn. *Pediatric Research* 22(5):541-544.
- Wu XB, Li YN, Schneider A, Yu WQ, Rajendren G, Iqbal J, Yamamoto M, Alam M, Brunet LJ, Blair HC et al. . 2003. Impaired osteoblastic differentiation, reduced bone formation, and severe osteoporosis in noggin-overexpressing mice. *Journal of Clinical Investigation* 112(6):924-934.
- Wuster C, de Terlizzi F, Becker S, Cadossi M, Cadossi R, and Muller R. 2005. Usefulness of quantitative ultrasound in evaluating structural and mechanical properties of bone: comparison of ultrasound, dual-energy X-ray

- absorptiometry, micro-computed tomography, and mechanical testing of human phalanges in vitro. *Technol Health Care* 13(6):497-510.
- Wuster C, Scheidt C, Bergman M, Braudt K, and Ziegler R. 1992. Bone density measurement of calcaneus with ultrasound: A new precision procedure with good agreement to vertebral measurement. *Osteoporosis* 1:237-242.
- Wutzl A, Rauner M, Seemann R, Millesi W, Krepler P, Pietschmann P, and Ewers R. 2010. Bone morphogenetic proteins 2, 5, and 6 in combination stimulate osteoblasts but not osteoclasts in vitro. *Journal of Orthopaedic Research* 28(11):1431-1439.
- Yates AJ, Ross PD, Lydick E, and Epstein RS. 1995. Radiographic absorptiometry in the diagnosis of osteoporosis. *The American journal of medicine* 98(2):41S-47S.
- Yeste D, Almar J, Clemente M, Gussinye M, Audi L, and Carrascosa A. 2004. Areal bone mineral density of the lumbar spine in 80 premature newborns: a prospective and longitudinal study. *J Pediatr Endocrinol Metab* 17(7):959-966.
- Yiallourides M, Savoia M, May J, Emmerson AJ, and Mughal MZ. 2004. Tibial speed of sound in term and preterm infants. *Biology of the Neonate* 85(4):225-228.
- Yoon HS, and Katz JL. 1976a. Ultrasonic wave-propagation in human cortical bone .1. Theoretical considerations for hexagonal symmetry. *J Biomech* 9(6):407-412.
- Yoon HS, and Katz JL. 1976b. Ultrasonic wave-propagation in human cortical bone .2. Measurements of elastic properties and microhardness. *J Biomech* 9(7):459-&.
- Zadik Z, Price D, and Diamond G. 2003. Pediatric reference curves for multi-site quantitative ultrasound and its modulators. *Osteoporosis International* 14(10):857-862.
- Zadik Z, Sinai T, Borondukov E, Zung A, Yaniv I, and Reifen R. 2005. Longitudinal monitoring of bone accretion measured by quantitative multi-site ultrasound (QUS) of bones in patients with delayed puberty (a pilot study). *Osteoporosis International* 16(9):1036-1041.

## **APPENDICES**



## *Infant Injury Database*

### *Database Variable Definitions and Data Entry Protocol*

The purpose of this database is to describe pathology/trauma found in infants. The database is constructed into 11 tabs. The main headings of each section below correspond to the tab titles within the database. The listed variables within each section correspond to the variables found within the corresponding tab of the database. Database variables are underlined and definitions or descriptions of each variable follow. In some cases, clarification on how some data should be categorized or entered is also provided.

#### **Case Stats**

- Fractures-Anthropology: Number of fractures observed by the forensic anthropologist. This number is automatically generated by the database from the information entered in the Fxs\_Anthro tab.
- Fractures-Pathology: Number of fractures observed by the forensic anthropologist. This number is automatically generated by the database from the information entered in the Fxs\_Path tab.
- Fractures-Radiology: Number of fractures observed by the radiologist. This number is automatically generated by the database from the information entered in the Fxs\_Radiol tab.
- Pathology-External: Number of areas with external trauma. This number is automatically generated by the database from information entered in the Pathology tab.
- Pathology-Organs: Number of organs with pathology/trauma. This number is automatically generated by the database from information entered in the Pathology tab.
- Pathology-ICH: Number of intracranial hemorrhages. This number is automatically generated by the database from information entered in the Pathology tab.
- Case Number: Unique agency/hospital case number assigned to every reported case
- Last Log date: Date and time data was last entered for the case, expressed in month/day/year and hours:minutes:seconds
- Initials: Initials of last individual to enter data regarding the case
- Case Status: Case status marked complete indicates that all information for this case has been entered and is complete. Case status marked incomplete indicates that data entry for this case has yet to be completed.
- Change Case Status: To change case status or upon starting data entry for a case, enter your initials into this box and select change case status. Pop-up box will ask you to select No if the case is to remain incomplete and yes if you want to change the case status to complete.

#### **Presentation**

- Study ID: Random index number assigned to each case by the database software for tracking purposes
- CaseNumber: unique agency/hospital case number assigned to every reported case
- Case ID: Random number assigned to the CaseNumber to anonymize the cases

- Date of death: Date the infant was declared dead by medical personnel, expressed in month/day/year
- Time of death: Time the infant was declared dead by medical personnel, expressed in hours:minutes
- Date of birth: Date the infant was born, expressed in month/day/year
- Race: The biological ancestry or ethnic affiliation of the infant, expressed as Black, White, Hispanic, or Asian.
- Gender: The biological sex of the infant
- Manner appears: An estimated preliminary manner of death listed in the Forensic Investigator's Scene Report based on death scene information
- TraumaType: Injuries to the infant documented by the Forensic Investigator based on preliminary examination at the death scene
- TraumaCausedBy: Possible mechanism of injury as documented by the Forensic Investigator based on preliminary death scene investigation
- Cause of Trauma: Categorize cause of trauma as No trauma, (BA/BF/SF/TH), or Undetermined. BA/BF/SF/TH indicates ballistic, blunt force, sharp force, or thermal trauma is present. Undetermined should be selected when trauma is present but the cause cannot be determined.
- Cause Category: Categorize cause of death as Asphyxia/Drowning, Co-sleeping, Infectious, Other, SUID, Trauma, or Undetermined based on the finalized classification made by the Medical examiner regarding the cause of the infant's death.
- Cause of Death: The finalized classification made by the Medical Examiner regarding the cause of the infant's death
- Manner: The finalized classification made by the Medical Examiner regarding the manner of the infant's death
- InjuryZip: The postal zip code of the location where the infant was injured or became unresponsive
- Place of Death: The location or facility where the infant died, such as hospital or residence.
- DeathZip: The postal zip code of the location where the infant's death occurred
- Found in location: The location where the infant was found, such as the crib or an adult bed.
- Discovered by: What is the relationship between the infant and the person who found the infant? Such as mother, father, etc.
- Transport pending: Was the infant transported to a hospital? yes or no
- Transport preference: If the infant was transported to a hospital, what was the means of transport or the relationship of the individual transporting? Such as private vehicle or the emergency medical service (EMS).
- TransportFrom: If the infant was transported to a hospital, what was the location where transport began? Such as residence or father's residence.
- Duration of Transport: Duration of time it took to transport the infant to the hospital, expressed in minutes.
- Time EMS at scene: Time EMS arrived at the scene, expressed in hours:minutes
- Time to hospital 1: Arrival time at first hospital, expressed in hours:minutes

- Time to hospital 2: If transported to second hospital for different treatment, arrival time at second hospital, expressed in hours:minutes
- Autopsy performed: If full autopsy performed by Medical Examiner, enter autopsy into the free text box, otherwise specify the type of autopsy.
- Bone quality in situ: How was the bone quality as assessed by anthropologist during the autopsy? Select Good, Indeterminate, Poor, or Unknown.
- Bone quality after processing: If bone specimens were removed and processed, how was the bone quality as assessed by the anthropologist after removal and processing? Select Good, Indeterminate, Poor, or Unknown.
- Path reviewed: Did the anthropologist review the pathological findings or discuss the findings with the pathologist prior to the anthropological examination? Select yes, no or unknown
- Full skeletal exam: Was a full pediatric skeletal exam (PSE) performed by an anthropologist? Select yes, no, or unknown.
- Pathologist: The name of pathologist who completed the postmortem examination
- Pathologist (if additional): Name of pathologist supervising the pathology fellow (if the fellow has conducted the autopsy) or name of pathologist that reviewed and co-signed the case

### **Clinical\_HX**

- CC: Infant's chief health complaint or symptoms documented in perimortem period
- Current height: Height of infant at time of death, expressed in cm.
- Current Weight: Weight of infant at time of death, expressed in kg.
- Found Down: Was the infant found unconscious or unresponsive? Select yes, no, or unknown.
- How Long: If found down, how long was the infant down? Expressed in minutes or hours and minutes
- Movement: Upon discovery of infant unresponsive or in distress, was movement noted? Select yes, no, or unknown.
- Seizures: Upon discovery of infant unresponsive or in distress, were seizures noted? Select yes, no, or unknown.
- Breathing: Upon discovery of infant unresponsive or in distress, was the infant breathing? Select yes, no, or unknown.
- Pulse palpated: Upon discovery of infant unresponsive or in distress, when checked, was a pulse palpated? Select yes, no, or unknown.
- Vomiting: Upon discovery of infant unresponsive or in distress, was vomit noted? Select yes, no, or unknown.
- Co-sleeping: Upon discovery of infant unresponsive or in distress, was the infant sleeping in the same bed with another individual (co-sleeping)? Select yes, no, or unknown.
- Co-sleeping with: If the infant was co-sleeping, what is the relationship of the infant to the other individual(s) in the bed? Such as mother, father, brother, etc.
- Weight: The corresponding weight of the other individual(s) co-sleeping with the infant, expressed in pounds.

- Person(s) impaired: Were the co-sleeping individuals impaired by a substance(s)? Select yes, no, or unknown.
- Last feeding: What was the range of time from the most recent feeding to the time the infant became or was discovered unresponsive? Select <= 30 minutes, 30-60 minutes, 60-90 minutes, 90 minutes to 2 hours, 2-4 hours, 4-6 hours, >6 hours, or unknown.
- CPR performed: Was cardiopulmonary resuscitation performed? Select yes, no, or unknown.
- By whom: Who performed the CPR? Select Medical personnel, layperson, or mixture. Mixture should be selected if laypersons and medical personnel both performed CPR.
- Where performed: Where was the CPR performed? Such as hospital or residence.
- CPR technique: What CPR technique was used? Select 2-thumb, anterior, both or unknown. CPR performed by medical personnel should be classified as 2-thumb. CPR performed by laypersons, including that instructed by emergency dispatcher, should be classified as anterior, unless documented otherwise. CPR performed by mixture of laypersons and medical personnel should be classified as both.
- CPR technique verified: Was the technique verified by another witness? Select yes, no, or unknown.
- Clinical Dx: If a clinician made a documented diagnosis related to the infant's death, this diagnosis is entered here
- L retinal hemorrhages: Were retinal hemorrhages noted in the left eye? Select traumatic, nontraumatic, or unknown. Select traumatic if they were noted and caused by traumatic injury. If not present or caused by mechanisms other than traumatic injury, select nontraumatic.
- R retinal hemorrhages: Were retinal hemorrhages noted in the right eye? Select traumatic, nontraumatic, or unknown. Select traumatic if they were noted and caused by traumatic injury. If not present or caused by mechanisms other than traumatic injury, select nontraumatic.
- Notes: Free text box for additional notes regarding the circumstances surrounding the infant's death.

### **Medical\_Hx**

- EGA (weeks): Estimated gestational age of the infant at birth, expressed in weeks
- Birth weight: Weight at birth, expressed in grams
- Prenatal Care?: Did the mother receive prenatal care? Select yes, no, or unknown
- Date of most recent hospitalization: Date of the most recent hospitalization, expressed in month/day/year. Date of birth should be excluded. If it was a delayed hospital death, the date of admission prior to death should be entered here.
- Normal at last visit: Was the infant normal at the last pediatric check-up? Select yes, no, or unknown
- Chronic medical condition: Did the infant have a chronic medical condition? Select yes, no, or unknown
- If so, type of condition: If infant had a chronic medical condition(s), list any chronic medical conditions here
- Developmental disability: Did the infant have a developmental disability? Select yes, no, or unknown

- If so, type of disability: If the infant had a developmental disability, list any developmental disabilities here.
- Normal gross motor development: Were the infant's motor skills developing normally? Select yes, no, or unknown
- GM stage: Select gross motor development stage the infant had progressed to prior to death, such as non-ambulatory, crawling, cruising, walking, or unknown. Cruising is defined as walking with the aid of objects or persons to maintain balance.
- Additional medical information: List additional relevant medical information here, such as prior medical history.
- Current medications: List any medication the infant was being given in the perimortem period here
- Previous medications: List any medication previously administered to the infant here
- Formula fed: Was the infant formula fed? Select yes, no, or unknown
- Breast fed: Was the infant breast fed? Select yes, no, or unknown
- Fed solid foods: Was the infant eating solid foods? Select yes, no, or unknown
- Known solid food: If the infant was eating solid foods, list all known solid foods here
- Special diet: Was the infant on a special diet? Select yes, no, or unknown. Examples of special diets include vegetarian, vegan, gluten free, etc.
- Dietary restrictions: Were there any medical dietary restrictions? Select yes, no, unknown
- Rickets: Had the infant ever been diagnosed with rickets? Select yes, no, or unknown
- Family history bone disease: Was there a family history of bone disease? Select yes, no, or unknown
- Full sibling: Was a full sibling diagnosed with bone disease? Select yes, no, or unknown
- Type of Bone Disease: If there was a family history of bone disease, list the disease(s) here
- Genetic Condition: Did the infant have an underlying genetic condition? Select yes, no, or unknown
- Prior Infant Deaths: Were there any prior infant (birth to 1 year of age) deaths in the immediate family? Select yes, no, or unknown
- Infant age at death: If there were prior infant deaths in the immediate family, enter the age of the infant's infant relative at death here, expressed in months
- Relationship to case: Identify the relationship of the deceased infant to the target decedent here, such as brother, step brother, uncle, etc.
- Cause of death: Enter the cause of death of the infant's infant relative here
- Prior Child Deaths: Were there any prior childhood (>1 year of age) deaths in the immediate family? Select yes, no, or unknown
- Child age at death: Age of the infant's child relative at death, expressed in years
- Relationship to case: Identify the relationship of the deceased child to the target decedent here, such as brother, cousin, uncle, etc.
- Cause of death: Enter the cause of death of the infant's child relative

### **Fxs\_Anthro**

List all fractures/bony defects for each bone as indicated by the forensic anthropologist, including multiple fractures/defects of the same bone

- Bone: Select type of bone injured or cranial suture with injury
- Rib number: If injured bone is a rib, select the corresponding rib number. This option is only available for the rib.
- Side: Select the side of the injured bone, such as left or right. This option may not be available for some types of injured bone
- Fracture location: Select specific location of the injury on the bone, eg: anterior, posterior, suture, etc. Options for specific location depend on the type of injured bone selected
- Fracture type: Select type of fracture observed for the injured bone. Options for type of fracture depend on the type of injured bone selected.
- Fracture healing: Identify the stage of healing. Options for the fracture healing will depend on the type of injured bone selected. Selections include no healing, initial response, soft callus, hard callus, reducing callus, unspecified healing, or tissue bridging (skull only). CML fractures with healing and areas of subperiosteal new bone formation (SPNBF) unassociated with a fracture should be categorized as unspecified healing.

### **Fxs\_Path**

List all fractures/bony defects for each bone as indicated by the forensic pathologist, including multiple fractures/defects of the same bone

- Same list as the “ANTHROPOLOGY FRACTURE” tab

### **Fxs\_Radiol**

List all fractures/bony defects for each bone as indicated by the radiologist, including multiple fractures/defects of the same bone

- Same list as the “ANTHROPOLOGY FRACTURE” tab

### **Pathology**

#### **External Path**

- Cutaneous injuries: If cutaneous injuries present, select cutaneous and all areas with cutaneous injuries identified by the pathologist during the autopsy. The options are listed below.
  - Cutaneous
  - Mouth
  - Face
  - Scalp
  - Subscalpular hemorrhage
  - Neck
  - Ear
  - Back
  - Chest
  - Cutaneous rib outline
  - Buttocks
  - Ventral Abdomen
  - Anal-Genital

#### External Path- Extremities

- R upper arm

- R forearm
- R hand
- L upper arm
- L forearm
- L hand
- R upper leg
- R lower leg
- R foot
- L upper leg
- L lower leg
- L foot
- Other soft tissue injuries

**Abnormal Organ Pathologies**

- Injury internal organs: Select all organs with abnormal findings (pathological and traumatic). Categorize organs with petechiae as pathological. Organ tissue congestion should not be categorized as pathological or traumatic. Options for organ selection or listed below.

- Heart
- L lung
- R lung
- Esophagus
- Thymus
- Adrenal
- Bladder
- Gallbladder
- Large intestine
- Small intestine
- Peritoneum
- Kidney
- Liver
- Pancreas
- Spleen
- Stomach
- Ovaries
- Uterus

**Intracerebral hemorrhage types**

- Intracranial hemorrhage: If present, select the type of hemorrhage(s). Options for selection are listed below.

- Subdural (SDH)
- Subarachnoid (SAH)
- Extra-dural (EDH)
- Intraventricular (IVH)
- Parenchymal-Contusion
- Parenchymal-Intraparenchymal
- Unknown.

## Notes

- None/Path refer to: Enter the specific soft tissue, organ or area with pathology/trauma to be described in the corresponding “notes” column
- Notes: Corresponding to the specific soft tissue, organ or area listed in the adjacent “None/Path refer to” column, enter a detailed description of the pathology/injuries observed

## Bone Density Study PT 1

### Tibia SOS Measurements

- Side analyzed: Which tibia was measured? Select left or right
- SOS measurement: SOS value measured with MiniOmni QUS, expressed in m/s
- Leg side: Which leg was measured for circumference? Select left or right
- Leg circumference: Leg circumference at the tibial midshaft, expressed in mm
- Arm side: Which arm was measured for circumference? Select left or right
- Arm circumference: Arm circumference at radial midshaft, expressed in mm

### Radiology Data

- Date: Date radiographs analyzed, expressed as month/day/year
- Observer: Name of analyst
- Bone: Which bones were analyzed by the radiologist? Select tibia/fibula or radius/ulna
- Adequate Radiograph?: Was the radiograph adequate for analysis? Select yes or no
- Rachitic Changes Present: Were rachitic changes present? Select present or absent
- If so, check all that apply: If present, select all characteristics from drop down menu that apply. Options include cupping, irregular/fraying margins, and widened metaphyses
- Demineralization score: Demineralization score assigned by radiologist, 0 (normal), 1 (indeterminate), or 2 (abnormal).
- If so, check all that apply: If demineralization score is greater than 0, select characteristics that apply from drop down menu. Options include general translucency, thinning cortices, and thinning trabeculae
- Notes: Any additional notes provided by the radiologist

## Bone Density Study PT 2

### Histology

- Date: Date slide analyzed by bone pathologist, expressed in month/day/year
- Observer: Name of analyst
- Bone: Select bone analyzed by bone pathologist. Select rib or iliac crest
- Adequate Specimen?: Was the specimen adequate for analysis? Select yes or no
- Current Vasculature: Enter score for current vasculature assigned by bone pathologist. Options are 0 (normal), 1 (indeterminate), or 2 (abnormal).



- Current Mineralization: Enter score for current mineralization assigned by bone pathologist. Options are 0 (normal), 1 (indeterminate), or 2 (abnormal).
- Current Volume: Enter score for current volume assigned by bone pathologist. Options are 0 (normal), 1 (indeterminate), or 2 (abnormal).
- Current Formation: Enter score for current formation assigned by bone pathologist. Options are 0 (normal), 1 (indeterminate), or 2 (abnormal).
- Current Resorption: Enter score for current resorption assigned by bone pathologist. Options are 0 (normal), 1 (indeterminate), or 2 (abnormal).
- Composite Score: Summation current variable scores. This variation is automatically generated by the database.
- Native Collagen: Enter score for native collagen assigned by bone pathologist. Options are 0 (normal), 1 (indeterminate), or 2 (abnormal).
- Native Mineralization: Enter score for native mineralization assigned by bone pathologist. Options are 0 (normal), 1 (indeterminate), or 2 (abnormal).
- Abnormal?: Was the native bone abnormal? Select yes, no, or N/A
- If abnormal: If native bone was abnormal, describe type of native bone abnormalities noted by the bone pathologist.
- Notes: Enter any additional notes provided by the bone pathologist here.

#### **Bone Mineral Content**

- Date: Date radiograph analyzed, expressed in month/day/year
- Observer: Name of analyst
- Bone: Which bone was bone analyzed for bone mineral content (BMC). Select radius or ulna
- Adequate Specimen?: Was the radiograph adequate for analysis? Select yes or no
- BMC Value: Enter BMC value estimated by analyst from radiograph
- Side: Which bone side was analyzed for BMC? Select left or right
- BMD Value: Enter BMD value estimated by analyst from the radiograph
- Side: Which bone side was analyzed for BMD? Select left or right

**Figure A- 1. Data recorded for each infant in the Infant Injury Database and associated variable definitions.**

TCH Case ID #  Autopsy Date  Date of Admission to Hospital

Date of Birth  Date of Death  Gestational Age at Birth  weeks

Sex  Race  Residence Zip Code

Birth weight  kg Current Weight  kg Current Length  cm

Cause of Death

Prenatal Care  Normal Gross Motor Development

Chronic Illness Diagnosed (including genetic abnormalities)  If yes, describe:

Family History of Genetic Disorder  If yes, describe:

Prior History of Infant/Child Death in Family  If yes, Age of Infant/Child at Death:

Acute Illness Diagnosed  If yes, describe:

Figure A-2. Page 1 of form completed by TCH pathologist for each decedent.

Normal Dietary Intake  If yes, check all that apply:  breast milk  
 formula  
 baby food (including rice cereal and/or purees)  
 table food

If no, check all that apply:  TPN  
 vegan diet  
 nut milk  
 goat milk  
 cow milk  
 other

History of Steroid Use  History of Anti-Convulsant Drugs

History of Indomethacin Use

Other Medications  If yes, describe:

\*If no history of medications documented in chart then assumed "none"

CPR Fractures  If yes, list rib number, side, and location:

CPR Fractures  Acute  Remote

Acute fractures  If yes, describe:

Remote fractures  If yes, describe:

Additional Notes:

Figure A-3. Page 2 of form completed by TCH pathologist for each decedent

**Table A- 1. Demographic and autopsy findings of each infant in the study sample.**

Case ID #	Sex <sup>a</sup>	Race <sup>b</sup>	Age <sup>c</sup> (wks.)	Age <sup>d</sup> (mos.)	Exact Age	EGA <sup>e</sup>	T-C Age <sup>f</sup> (wks.)	T-C Age <sup>g</sup> (mos.)	Prem. <sup>h</sup>	BW. <sup>i</sup> (g)	GMD Stage <sup>j</sup>	Hospital Delay <sup>k</sup> (days)	Traumatic Injury? <sup>l</sup>	Trauma Type <sup>m</sup>
152	M	B	12	2	2.8912	40	12	3	N		Non-amb.	0	N	NA
153	F	H	13	3	3.1541	40	13	3	N	2920	Non-amb.	5	N	NA
154	M	B	14	3	3.0883	37	11	2	N	3010	Non-amb.	0	N	NA
155	F	H	49	11	11.3347	37	46	11	N	2690	Crawl-ing	0	N	NA
156	F	H	12	2	2.8583	40	12	3	N	3150	Non-amb.	0	N	NA
157	F	B	39	9	9.0349	38	37	9	N	2540	Non-amb.	0	N	NA
158	F	B	13	3	3.0226	38	11	2	N	2980	Unk.	0	N	NA
159	F	H	8	2	2.3326	33	1	0	Y	1361	Non-amb.	0	N	NA
160	M	B	8	1	1.8398	40	8	2	N	3266	Non-amb.	25	N	NA
161	F	H	3	0	.7556	39	2	0	N	3037	Non-amb.	0	Y	Blunt Force
162	F	H	23	5	5.4209	38	21	5	N	3294	Non-amb.	0	Y	Blunt Force
163	F	B	11	2	2.6940	36	7	1	Y	2595	Non-amb.	0	N	NA
164	M	B	30	7	7.0637	40	30	7	N	2840	Crawl-ing	0	N	NA
165	M	B	47	10	10.9076	39	46	11	N	2850	Walk-ing	0	Y	Blunt Force
166	M	B	29	6	6.7680	36	25	6	Y	2210	Unk.	0	N	NA
167	F	H	21	5	5.0267	40	21	5	N	2977	Non-amb.	0	N	NA
168	F	W	17	3	3.9754	40	17	4	N	3540	Non-amb.	0	N	NA
169	M	H	10	2	2.3984	38	8	2	N	2750	Non-amb.	0	N	NA
170	M	B	5	1	1.2156	40	5	1	N	2268	Non-amb.	0	N	NA
171	F	H	31	7	7.2608	36	27	6	Y	2406	Unk.	0	N	NA
172	F	B	21	5	5.0267	25	6	1	Y	540	Non-amb.	0	N	NA
173	F	B	13	3	3.0226	30	3	0	Y	1542	Non-amb.	0	N	NA
174	F	B	29	6	6.8665	36	25	6	Y	2520	Non-amb.	0	N	NA
175	M	B	25	5	5.7495	40	25	6	N	3572	Non-amb.	0	N	NA
176	M	H	11	2	2.9240	40	11	2	N	3690	Non-amb.	0	N	NA
177	M	B	24	5	5.6838	43	27	6	N		Non-amb.	3	Y	Blunt Force
178	M	H	18	4	4.1725	25	3	0	Y	737	Non-amb.	0	N	NA
179	F	H	6	1	1.5770	37	3	0	N	3090	Non-amb.	0	N	NA
180	F	H	16	3	3.8439	39	15	3	N	3565	Non-amb.	0	N	NA
181	M	W	43	9	9.9877	39	42	10	N	2980	Non-amb.	0	N	NA
182	F	H	50	11	11.5647	39	49	12	N	4000	Non-amb.	0	N	NA
183	M	B	49	11	11.3676	39	48	12	N	2695	Walk-ing	0	Y	Blunt Force
184	M	B	15	3	3.4498	35	10	2	Y	2125	Non-amb.	0	N	NA
185	F	B	9	2	2.1684	31	0	0	Y	1450	Non-amb.	0	N	NA
186	M	H	8	1	1.8727	37	5	1	N	3070	Non-amb.	0	N	NA
187	F	B	39	9	9.1663	38	37	9	N	2690	Crawl-ing	0	N	NA
188	M	B	7	1	1.6756	40	7	1	N	3236	Non-amb.	0	N	Blunt Force
189	F	B	10	2	2.4312	40	10	2	N	2552	Non-amb.	0	N	NA

**Table A- 1. Continued**

Case ID #	Sex <sup>a</sup>	Race <sup>b</sup>	Age <sup>c</sup> (wks.)	Age <sup>d</sup> (mos.)	Exact Age	EGA <sup>e</sup>	T-C Age <sup>f</sup> (wks.)	T-C Age <sup>g</sup> (mos.)	Prem. <sup>h</sup>	BW. <sup>i</sup> (g)	GMD Stage <sup>j</sup>	Hospital Delay <sup>k</sup> (days)	Traumatic Injury? <sup>l</sup>	Trauma Type <sup>m</sup>
190	F	W	22	5	5.1910	37	19	4	N	2880	Non-amb.	0	N	NA
191	F	A	37	8	8.6078	30	27	6	Y	1320	Unk.	2	N	NA
192	F	B	6	1	1.4784	37	3	0	N	2590	Non-amb.	0	N	NA
193	M	H	20	4	4.5997	38	18	4	N	3470	Non-amb.	0	N	NA
194	F	H	17	4	3.9754	40	17	4	N	3175	Non-amb.	0	N	NA
195	M	H	17	3	3.9097	39	16	4	N	3370	Non-amb.	0	N	NA
196	F	W	35	8	8.1150	39	34	8	N	2766	Unk.	0	N	NA
197	M	B	27	6	6.4066	38	25	6	N	3118	Non-amb.	2	N	NA
198	M	B	12	2	2.8583	37	9	2	N	2830	Non-amb.	0	N	NA
199	F	H	9	2	2.1684	39	8	2	N	3485	Non-amb.	0	N	NA
200	F	W	17	4	4.0739	38	15	3	N	2948	Crawl-ing	0	N	NA
201	F	B	8	2	2.0370	35	3	0	Y	2220	Non-amb.	0	N	NA
202	M	W	0	0	.0000	38	0	0	N	4050	Non-amb.	0	N	NA
203	F	W	23	5	5.2895		23				Unk.	0	N	NA
204	F	W	18	4	4.3039	40	18	4	N	3685	Non-amb.	43	Y	Blunt Force
205	M	B	26	6	6.0452	40	26	6	N	2582	Non-amb.	0	N	NA
206	M	B	21	5	5.0267		21			2380	Unk.	0	N	NA
207	M	B	23	5	5.2896	39	22	5	N	2401	Non-amb.	0	N	NA
208	M	H	12	2	2.7598	26	0	0	Y	886	Non-amb.	0	N	NA
209	F	B	46	10	10.7762		46				Unk.	0	Y	Blunt Force
210	M	H	45	10	10.4476	38	43	10	N	2610	Cruis-ing	0	N	NA
211	M	W	8	1	1.9055	32	0	0	Y		Non-amb.	3	N	NA
212	M	H	22	5	5.2567		22				Non-amb.	0	N	NA
213	M	H	12	2	2.8583	37	9	2	N		Non-amb.	6	N	NA
214	M	B	32	7	7.3593	40	32	8	N	3236	Unk.	0	N	NA
215	M	H	16	3	3.8768	40	16	4	N	3875	Non-amb.	0	N	NA
216	M	W	41	9	9.4949	39	40	10	N	3150	Unk.	0	N	NA
217	F	W	14	3	3.2854	37	11	2	N	2095	Non-amb.	4	N	NA
218	F	H	5	1	1.1499	36	1	0	Y	2060	Non-amb.	33	N	NA
219	M	B	49	11	11.3347	38	47	11	N	3365	Walk-ing	0	N	NA
220	F	H	16	3	3.7782	40	16	4	N	3710	Non-amb.	0	N	NA
221	M	B	4	1	1.0842	38	2	0	N	2620	Non-amb.	0	N	NA
222	F	A	5	1	1.2813	36	1	0	Y	2549	Non-amb.	0	N	NA
223	M	B	9	2	2.1355	40	9	2	N	3182	Non-amb.	0	N	NA
224	F	B	21	4	4.8624	39	20	5	N	3665	Non-amb.	4	Y	Blunt Force
225	M	H	1	0	.3285	36	0	0	Y	2520	Non-amb.	0	N	NA
226	F	B	14	3	3.3511	40	14	3	N	2790	Non-amb.	0	N	NA
227	F	W	3	0	.8871	41	4	1	N	3650	Non-amb.	2	N	NA

**Table A- 1. Continued**

Case ID #	Sex <sup>a</sup>	Race <sup>b</sup>	Age <sup>c</sup> (wks.)	Age <sup>d</sup> (mos.)	Exact Age	EGA <sup>e</sup>	T-C Age <sup>f</sup> (wks.)	T-C Age <sup>g</sup> (mos.)	Prem. <sup>h</sup>	BW. <sup>i</sup> (g)	GMD Stage <sup>j</sup>	Hospital Delay <sup>k</sup> (days)	Traumatic Injury? <sup>l</sup>	Trauma Type <sup>m</sup>
228	M	B	11	2	2.6940	39	10	2	N	3710	Non-amb.	2	Y	Blunt Force
229	F	W	5	1	1.2813	39	4	1	N	3010	Non-amb.	0	N	NA
<p>a. Sex: M = Male, F = Female                      b. Race: B = black, H = Hispanic, W = white, A = Asian                      c. Chronological age in weeks                      d. Chronological age in months                      e. Estimated Gestational Age                      f. Term-Corrected age in weeks                      g. Term-Corrected age in months                      h. Premature: Y = Yes, N = No                      i. Birthweight in grams                      j. Gross Motor Development Stage: Non-amb. = Non-ambulatory, Unk. = Unknown                      k. Hospital Delayed Death: number of days between arrival to hospital and death                      l. Traumatic Injury Present: Y = Yes, N = No                      m. Trauma Type: NA = Not Applicable</p>														

**Table A- 2. Chronic illness and autopsy classifications**

Case ID #	Chronically Ill <sup>a</sup>	MOD <sup>b</sup>	COD <sup>c</sup>	COD Category <sup>d</sup>
152	Y	Undetermined	Undetermined (co-sleeping)	Co-sleeping
153	0	Natural	Hypoxic encephalopathy and multi-organ failure complicating Sudden Infant Death Syndrome	Other
154	0	Natural	Sudden Infant Death Syndrome	SUID
155	0	Natural	Small bowel infarction due to intestinal volvulus	Other
156	N	Natural	Sudden Infant Death Syndrome	SUID
157	0	Natural	Sudden Infant Death Syndrome	SUID
158	N	Natural	Acute bronchopneumonia due to bacterial Streptococcus pneumonia infection complicating respiratory bronchiolitis and idiopathic pulmonary hemosiderosis	Infectious
159	N	Undetermined	Undetermined (co-sleeping)	Co-sleeping
160	N	Undetermined	Undetermined	Undetermined
161	0	Homicide	Blunt trauma of head, torso and extremities	Trauma
162	N	Homicide	Blunt trauma with subdural hematoma	Trauma
163	N	Accident	Asphyxia due to overlay	Asphyxia/Drowning
164	N	Natural	Sudden Infant Death Syndrome	SUID
165	N	Homicide	Blunt trauma of the head	Trauma
166	N	Natural	Sudden Infant Death Syndrome (SUID)	SUID
167	0	Undetermined	Undetermined (co-sleeping)	Co-sleeping
168	N	Undetermined	Undetermined	Undetermined
169	0	Undetermined	Undetermined (co-sleeping)	Co-sleeping
170	N	Undetermined	Undetermined (co-sleeping)	Co-sleeping
171	N	Undetermined	Undetermined (co-sleeping)	Co-sleeping
172	Y	Natural	Complications of extreme prematurity	Other
173	N	Undetermined	Undetermined (co-sleeping)	Co-sleeping
174	Y	Natural	Complications of Group B strep Meningitis	Infectious
175	N	Natural	Sudden Infant Death Syndrome	SUID
176	0	Undetermined	Undetermined	Undetermined
177	N	Homicide	Subdural and subarachnoid hemorrhage due to blunt force head injuries	Trauma
178	Y	Natural	Complications of prematurity with neonatal lung disease and cardiomegaly	Other
179	N	Natural	Acute Bacterial Pneumonia (Haemophilus influenzae)	Infectious
180	N	Natural	Sudden Infant Death Syndrome	SUID
181	Y	Natural	Complications of intrauterine hypoxic neurologic events (cerebral palsy)	Other
182	N	Undetermined	Undetermined	Undetermined
183	N	Homicide	Blunt head trauma	Trauma
184	N	Undetermined	Undetermined (co-sleeping)	Co-sleeping
185	N	Undetermined	Undetermined	Undetermined
186	N	Natural	Sudden Infant Death Syndrome	SUID
187	N	Natural	Sudden Infant Death Syndrome	SUID

**Table A- 2. Continued.**

Case ID #	Chronically Ill <sup>a</sup>	MOD <sup>b</sup>	COD <sup>c</sup>	COD Category <sup>d</sup>
188	0	Undetermined	Undetermined	Undetermined
189	N	Undetermined	Undetermined	Undetermined
190	0	Natural	Sudden Infant Death Syndrome	SUID
191	Y	Undetermined	Undetermined	Undetermined
192	0	Undetermined	Undetermined (co-sleeping)	Co-sleeping
193	N	Undetermined	Undetermined	Undetermined
194	0	Undetermined	Undetermined (co-sleeping)	Co-sleeping
195	N	Undetermined	Undetermined (co-sleeping)	Co-sleeping
196	N	Undetermined	Undetermined	Undetermined
197	0	Accident	Positional asphyxia	Asphyxia/Drowning
198	N	Undetermined	Undetermined (co-sleeping)	Co-sleeping
199	N	Undetermined	Undetermined (co-sleeping)	Co-sleeping
200	N	Natural	Sudden infant death syndrome	SUID
201	N	Natural	Bacterial pneumonia and sepsis due to Staphylococcus aureus infection	Infectious
202	N	Natural	Extensive remote Central Nervous System injury- congenital viral infection vs. hypoxic ischemia	Other
203	0	Natural	Sudden Infant Death Syndrome	SUID
204	N	Homicide	Complications following blunt force head trauma	Trauma
205	Y	Natural	Congenital diaphragmatic hernia	Other
206	0	Accident	Overlay	Asphyxia/Drowning
207	N	Undetermined	Undetermined (co-sleeping)	Co-sleeping
208	N	Undetermined	Undetermined (co-sleeping)	Co-sleeping
209	0	Accident - MVA	Blunt trauma of head and torso	Trauma
210	0	Accident	Asphyxia due to compression of neck	Asphyxia/Drowning
211	N	Undetermined	Undetermined (co-sleeping)	Co-sleeping
212	Y	Undetermined	Undetermined	Undetermined
213	Y	Natural	Mitochondrial myopathy	Other
214	0	Homicide	Toxic effects of diphenhydramine	Other
215	Y	Natural	Myocardial ischemia and infarction due to fibromuscular dysplasia of coronary arteries	Other
216	0	Accident	Suffocation	Asphyxia/Drowning
217	0	Natural	Sudden Infant Death Syndrome	SUID
218	Y	Natural	Multiorgan failure with hemorrhagic coagulopathy secondary to neonatal hemochromatosis	Other
219	0	Undetermined	Drowning	Asphyxia/Drowning
220	0	Undetermined	Undetermined (co-sleeping)	Co-sleeping
221	0	Natural	Sudden Infant Death Syndrome	SUID
222	Y	Natural	Complications of Campomelic dysplasia	Other
223	0	Natural	Sudden Infant Death Syndrome	SUID



**Table A- 2. Continued.**

Case ID #	Chronically Ill <sup>a</sup>	MOD <sup>b</sup>	COD <sup>c</sup>	COD Category <sup>d</sup>
224	0	Homicide	Blunt force injuries of head	Trauma
225	Y	Natural	Patent ductus arteriosus with persistent fetal circulation	Other
226	0	Natural	Volvulus of sigmoid colon	Other
227	0	Natural	Near sudden infant death syndrome	SUID
228	N	Homicide	Multiple blunt force injuries with skull and rib fractures, subdural and subarachnoid hemorrhage and hepatic lacerations	Trauma
229	N	Accident	Asphyxia due to overlay	Asphyxia/Drowning

a. Chronically ill: Y = Yes, N = No  
b. Manner of Death  
c. Cause of Death  
d. Cause of Death Category: SUID = Sudden Unexplained Infant Death

Submit by Email

Print Form

### Bone Density Study: Radiology Scoring Form

Observer

Case Number

Date of Analysis

Radius/Ulna Adequate Radiograph to Interpret

Rachitic Changes

Check all that apply:

- widened metaphysis
- cupping
- irregular/fraying margins

Demineralization

Check all that apply:

- thinning trabeculae
- thinning cortices
- general translucency

Demineralization Score Key  
0 = Normal  
1 = Indeterminate  
2 = Abnormal

Comments:

Tibia/Fibula Adequate Radiograph to Interpret

Rachitic Changes

Check all that apply:

- widened metaphysis
- cupping
- irregular/fraying margins

Demineralization

Check all that apply:

- thinning trabeculae
- thinning cortices
- general translucency

Demineralization Score Key  
0 = Normal  
1 = Indeterminate  
2 = Abnormal

Comments:

Figure A-4. Qualitative radiography evaluation score form.

Submit by Email

Print Form

### Bone Density Project: Histology Form

Observer

Case Number

Date of Analysis

Iliac Crest Sample Adequate Sample to Evaluate

Current Vasculature

Current Mineralization

Current Volume

Current Formation

Current Resorption

**Iliac Crest Composite Score**

Score Key  
0 = Normal  
1 = Indeterminate  
2 = Abnormal

Native Collagen

Abnormal?

If Abnormal,

Native Mineralization

Comments

Rib Sample Adequate Sample to Evaluate

Current Vasculature

Current Mineralization

Current Volume

Current Formation

Current Resorption

**Rib Composite Score**

Score Key  
0 = Normal  
1 = Indeterminate  
2 = Abnormal

Native Collagen

Abnormal?

If Abnormal,

Native Mineralization

Comments

Figure A-5. Qualitative histological evaluation score form.

**Table A- 3. Description of infants with traumatic injuries.**

Trauma Cases								
Case ID	Age <sup>a</sup>	Sex	Race	EGA <sup>b</sup>	Weight (kg)	SOS (m/s)	BMD (g/cm <sup>2</sup> )	Radiographic Score <sup>d</sup>
161	0	F	H	39	2.67	2843	1.14	0
228	2	M	B	39	6.8	3053	1.06	1
204	4	M	W	40	4.59	3189	1.26	0
224	4	F	B	39	8	2899	0.71	1
162	5	F	H	38	6.69	3115	0.69	0
177	5	F	B	43	10	3173	0.92	0
165	10	M	B	39	8.91	3331	0.85	0
209	10	M	B	Unk. <sup>c</sup>	10.9	3376	0.45	0
183	11	F	B	39	9.07	3106	1.18	0

a. Chronological age in months  
b. EGA = Estimated gestational age  
c. Unk. = Unknown  
d. Qualitative radiographic evaluation score: 0 = normal, 1 = indeterminate, 2 = abnormal mineralization

**Table A- 4. Qualitative Radiographic Evaluation Results**

		Count	Variable %
<b>Rachitic Changes</b>	Absent	78	100
	Present	0	0
	Total	78	100
<b>Radial Mineralization Score</b>	Normal	64	83
	Indeterminate	10	13
	Abnormal Mineralization	3	4
	Total	77	100
<b>Tibial Mineralization Score</b>	Normal	65	83
	Indeterminate	10	13
	Abnormal Mineralization	3	4
	Total	78	100

**Table A- 5. Description of infants with abnormally mineralized bone on radiographs.**

Abnormally Mineralized Cases										
Case ID	Age <sup>a</sup>	Sex	Race	EGA <sup>b</sup>	Wt. (kg)	SOS	BMD (g/cm <sup>2</sup> )	MOD <sup>c</sup>	COD <sup>d</sup>	Radiography Notes <sup>e</sup>
170	1	M	B	40	4	2666	0.77	Und. <sup>f</sup>	Und. <sup>g</sup> (co-sleeping)	radioluscent metaphyseal bands, thinning cortices
213	2	M	H	37	6.64	2971	0.53	Nat. <sup>g</sup>	Mitochondrial myopathy	thinning cortices, thinning trabeculae
215	3	M	H	40	5.21	3155	0.63	Nat. <sup>g</sup>	Myocardial ischemia and infarction due to fibromuscular dysplasia of coronary arteries	thinning cortices, thinning trabeculae
<p>a. Chronological age in months                      b. EGA = Estimated gestational age                      c. MOD = Manner of death                      d. COD = Cause of death                      e. Notes from qualitative radiographic evaluation                      f. Und. = Undetermined                      g. Nat. = Natural</p>										

**Table A- 6. Descriptive statistics of bone measurements, BMD, and SOS data.**

<b>Study Sample: Bone Measurements</b>			
	<i>N</i>	<b>Mean</b>	<i>SD</i>
Tibial Length (mm)	77	83.58	15.62
Tibial Midshaft Diameter (mm)	77	7.20	0.16
Medullary Cavity Diameter (mm)	77	3.38	0.11
Cortical Index <sup>a</sup>	77	0.53	0.010
		<b>Median</b>	<b>Inter-Quartile Range</b>
Cortical Thickness (mm)	77	3.75	3.09-4.43
<b>Bone Mineral Density (g/cm<sup>2</sup>)</b>			
Radial midshaft BMD	48	0.40	0.30-0.58
Tibial midshaft BMD	70	0.86	0.62-1.15
<b>Quantitative Ultrasound</b>			
		<b>Mean</b>	<i>SD</i>
Tibial midshaft SOS (m/s)	77	3010.75	213.12 m/s
a. Cortical Index = Total Cortical Thickness/Tibial Midshaft Diameter			

**Table A- 7. Data associated with chronically ill infants.**

<b>Case ID</b>	<b>SOS (m/s)</b>	<b>BMD (g/cm<sup>2</sup>)</b>	<b>Radiographic Score<sup>a</sup></b>	<b>Description of Chronic Illness</b>
225	3163	0.82	0	see <b>Table 4-3</b>
218	3307	<sup>b</sup>	0	see <b>Table 4-3</b>
222	2822	0.59	0	see <b>Table 4-3</b>
213	2971	0.53	2	see <b>Table 4-3</b>
152	2688	0.42	0	see <b>Table 4-3</b>
178	2595	0.49	0	see <b>Table 4-3</b>
215	3155	0.63	2	see <b>Table 4-3</b>
172	2740	0.79	0	see <b>Table 4-3</b>
212	2822	0.45	0	see <b>Table 4-3</b>
205	2907	0.93	1	see <b>Table 4-3</b>
174	2940	0.51	0	see <b>Table 4-3</b>
191	3219	0.41	1	see <b>Table 4-3</b>
181	3194	0.62	1	see <b>Table 4-3</b>
a. Qualitative radiographic evaluation score: 0 = normal, 1 = indeterminate, 2 = abnormal mineralization				
b. BMD could not be calculated				

**Table A- 8. Results of Qualitative Radiographic Evaluation for each infant.**

Case ID #	Radius Rachitic Score <sup>a</sup>	Tibia Rachitic Score <sup>a</sup>	Radius Mineralization Score <sup>a</sup>	Tibia Mineralization Score <sup>a</sup>	Overall Mineralization Score <sup>a</sup>	Demineralization Characteristics	Radiography Notes
152	0	0	0	0	0		
153	0	0	0	0	0		
154	0	0	0	0	0		Focal irregularity of trabecular pattern mid tibia, but this cannot be characterized further without
155	0	0	1	1	1	Thinning cortices	
156	0	0	0	0	0		
157	0	0	1	1	1	Thinning trabeculae	Tibia cortex is maintained but the trabecular pattern looks a little indistinct
158	0	0	0	0	0		
159	0	0	0	0	0		
160	0	0	0	0	0		
161	0	0	0	0	0		
162	0	0	0	0	0		
163	0	0	0	0	0		
164	0	0	0	0	0		
165	0	0	0	0	0		
166	0	0	0	0	0		
167	0	0	0	0	0		
168	0	0	0	0	0		
169	0	0	0	0	0		
170	0	0	2	2	2	Thinning cortices	Radiolucent metaphyseal bands
171		0		0	0		No arm radiograph
172	0	0	1	1	1	Thinning cortices	
173	0	0	0	0	0		
174	0	0	0	0	0		
175	0	0	0	0	0		
176	0	0	0	0	0		
177	0	0	0	0	0		
178	0	0	1	1	1	Thinning cortices	
179	0	0	0	0	0		
180	0	0	0	0	0		
181	0	0	0	0	0		
182	0	0	0	0	0		
183	0	0	0	0	0		
184	0	0	0	0	0		

**Table A- 8. Continued**

Case ID #	Radius Rachitic Score <sup>a</sup>	Tibia Rachitic Score <sup>a</sup>	Radius Mineralization Score <sup>a</sup>	Tibia Mineralization Score <sup>a</sup>	Overall Mineralization Score <sup>a</sup>	Demineralization Characteristics	Radiography Notes
185	0	0	1	1	1	General translucency	Radiograph of left leg; this is a small infant, but the general bone density seems slightly decreased
186	0	0	0	0	0		
187	0	0	0	0	0		
188	0	0	0	0	0		
189	0	0	0	0	0		
190	0	0	0	0	0		
191	0	0	0	0	0		
192	0	0	0	0	0		
193	0	0	0	0	0		
194	0	0	0	0	0		
195	0	0	0	0	0		
196	0	0	0	0	0		
197	0	0	0	0	0		
198	0	0	0	0	0		
199	0	0	0	0	0		
200	0	0	0	0	0		
201	0	0	0	0	0		
202	0	0	0	0	0		
203	0	0	0	0	0		
204	0	0	0	0	0		
205	0	0	1	1	1	General translucency	
206	0	0	0	0	0		
207	0	0	0	0	0		
208	0	0	0	0	0		
209	0	0	0	0	0		
210	0	0	0	0	0		
211	0	0	0	0	0		Trophic bands present at wrist
212	0	0	0	0	0		Trophic bands at wrist
213	0	0	2	2	2	Thinning cortices, Thinning trabeculae	
214	0	0	0	0	0		
215	0	0	2	2	2	Thinning cortices, Thinning trabeculae	
216	0	0	0	0	0		
217	0	0	0	0	0		
218	0	0	1	1	1	General translucency	



**Table A- 8. Continued.**

Case ID #	Radius Rachitic Score <sup>a</sup>	Tibia Rachitic Score <sup>a</sup>	Radius Mineralization Score <sup>a</sup>	Tibia Mineralization Score <sup>a</sup>	Overall Mineralization Score <sup>a</sup>	Demineralization Characteristics	Radiography Notes
219	0	0	0	0	0		
220	0	0	0	0	0		
221	0	0	0	0	0		
222	0	0	0	0	0		Radius-small and bowed, but mineralization looks within normal limits; Tibia-same as above with deformities
223	0	0	1	1	1	General translucency	
224	0	0	1	1	1	Thinning cortices	
225	0	0	1	1	1	General translucency	
226	0	0	0	0	0		
227	0	0	0	0	0		Trophic bands in metaphyses
228	0	0	0	0	0		
229	0	0	0	0	0		

a. Score: 0 = Normal, 1 = Indeterminate/Slight Demineralization, 2 = Abnormal Mineralization

**Table A- 9. Results of Qualitative Histological Evaluation of the costochondral rib section for each infant.**

Case ID #	Rib Side <sup>a</sup>	Rib # <sup>b</sup>	Rib Vasc. <sup>cd</sup>	Rib Mineralization <sup>d</sup>	Rib Volume <sup>d</sup>	Rib Formation <sup>d</sup>	Rib Resorption <sup>d</sup>	Rib Native Mineralization <sup>d</sup>	Rib Native Collagen <sup>d</sup>	Rib Normal? <sup>e</sup>	Rib Notes
152	R	4	1	1	1	1	1	0	0	Y	increased periosteal inflammation
153	L	4	2	1	2	2	2	1	1	N	way too many vessels and resorption
154	L	6	1	0	0	0	1	0	0	Y	marrow in several of the vessels
155	L	4	1	0	0	0	1	0	0	Y	
156	L	4	0	0	0	0	0	0	0	Y	
157	R	4	1	0	1	0	2	0	0	Y	way too much resorption
158	R	6	1	0	0	1	2	0	0	Y	increased resorption
159	R	4	1	0	1	1	2	0	0	Y	
160	L	4	2	0	1	2	2	0	0	Y	Increased periosteal new bone formation
161	L	9	0	0	0	0	0	0	0	Y	
162	L	7	1	0	0	0	1	0	0	Y	? Normal growth
163	L	4	0	0	0	0	1	0	0	Y	
164	L	6	0	0	0	0	0	0	0	Y	
165	R	4	0	0	0	0	1	0	0	Y	
166	L	6	1	0	1	1	2	0	0	Y	
167	R	5	1	0	0	1	2	0	0	Y	
168	R	6	2	0	1	1	1	0	0	Y	increased vasculature
169	L	4	1	1	0	0	1	0	0	Y	too much woven bone in the cortex
170	L	4	0	0	0	0	0	0	0	Y	
171	L	4	2	0	1	2	2	0	1	Y	significant issues with the periosteum and growth plate
172	L	4	2	0	2	2	2	0	1	Y	significant cortical disruption
173	R	5	2	1	2	2	2	0	1	Y	very increased vessels and resorption
174	L	4	0	0	1	1	2	0	0	Y	small cortical defect
175	R	5	1	0	1	1	1	0	0	Y	low bone volume
176	R	5	2	0	0	1	2	0	0	Y	
177	R	4	0	0	0	0	0	0	0	Y	
178	R	4	1	1	0	0	0	1	2	Y	extensive cortical woven bone

**Table A- 9. Continued.**

Case ID #	Rib Side <sup>a</sup>	Rib # <sup>b</sup>	Rib Vasc. <sup>cd</sup>	Rib Mineralization <sup>d</sup>	Rib Volume <sup>d</sup>	Rib Formation <sup>d</sup>	Rib Resorption <sup>d</sup>	Rib Native Mineralization <sup>d</sup>	Rib Native Collagen <sup>d</sup>	Rib Normal? <sup>e</sup>	Rib Notes
179	R	4	2	0	0	1	2	0	0	Y	
180	R	6	0	0	0	0	0	0	0	Y	
181	L	4	1	0	0	1	1	0	2	Y	
182	L	4	0	0	1	1	1	0	0	Y	
183	R	4	1	0	0	1	1	0	0	Y	
184	L	6	2	1	1	1	2	0	0	Y	
185	L	7	0	0	0	0	0	0	0	Y	
186	L	4	2	0	0	1	2	0	1	Y	increased resorption
187	L	4	1	0	0	1	1	0	0	Y	
188	R	4	1	0	0	0	1	1	1	N	thinned cortex and growth plate disturbance
189	R	4	0	0	0	0	0	0	0	Y	
190	R	4	0	0	0	1	2	0	0	Y	Increased formation and resorption
191	R	4	0	0	0	0	0	0	0	Y	
192	L	4	1	0	2	0	2	0	0	Y	increased resorption and splinters of resorbing bone
193	L	4	0	0	2	1	2	0	2	N	not sure how to classify this... most of the cortex is missing...collagen seems weak in formation
194	L	4	0	0	0	0	1	0	0	Y	gaps in the cortices
195	L	6	0	0	0	0	1	0	0	Y	mildly increased resorption
196	L	4	0	0	0	0	0	0	0	Y	relatively normal
197	L	4	0	0	0	1	2	0	0	Y	increased resorption with fragmentation and subperiosteal new bone formation
198	L	3	0	0	0	0	0	0	0	Y	relatively normal
199	L	4	1	0	0	1	2	0	0	Y	subperiosteal fibrosis and remodeling
200	L	4	0	0	0	0	0	0	0	Y	relatively normal
201	L	4	0	0	0	0	2	0	1	Y	increased endosteal resorption

**Table A- 9. Continued.**

Case ID #	Rib Side <sup>a</sup>	Rib # <sup>b</sup>	Rib Vasc. <sup>cd</sup>	Rib Mineralization <sup>d</sup>	Rib Volume <sup>d</sup>	Rib Formation <sup>d</sup>	Rib Resorption <sup>d</sup>	Rib Native Mineralization <sup>d</sup>	Rib Native Collagen <sup>d</sup>	Rib Normal? <sup>e</sup>	Rib Notes
202	L	4	2	0	0	1	2	0	0	Y	increased cortical resorption
203	L	4	0	0	0	0	2	0	0	Y	increased subperiosteal resorption
204	L	4	0	0	0	0	0	0	0	Y	relatively normal
205	R	4	0	0	0	0	0	0	0	Y	relatively normal
206	R	4	1	0	1	1	1	0	0	Y	thinned cortex and trabecular architecture
207	R	6	0	0	0	0	0	0	0	Y	relatively normal
208	R	4	0	0	0	0	0	0	0	Y	relatively normal
209	L	5	0	0	0	0	0	0	0	Y	relatively normal
210	R	3	0	0	0	0	0	0	0	Y	relatively normal
211	L	4	0	0	2	1	1	0	1	Y	markedly thinned bone and increased resorption, new subchondral bone formation
212	R	3	0	0	2	0	1	0	1	Y	markedly thinned bone and increased resorption
213	L	4	0	0	1	0	2	0	0	Y	thinned bone with increased resorption
214	L	6	0	0	0	0	1	0	1	Y	mildly increased resorption in the rib
215	L	4	0	1	0	0	0	0	1	Y	discordant rib and iliac samples
216	L	5	1	0	1	1	1	0	0	Y	gap in cortex with remodeling
217	R	6	0	0	0	0	2	0	0	Y	extensive cortical resorption
218	L	4	0	0	0	0	0	0	0	Y	
219	L	7	0	0	0	0	2	0	0	Y	extensive subperiosteal resorption
220	L	5	0	0	0	0	1	0	0	Y	
221	L	4	0	0	0	1	1	0	0	Y	subperiosteal new bone formation
222	L	4	0	0	0	0	0	0	0	Y	
223	L	4	0	0	0	0	1	0	0	Y	
224	R	4	0	0	0	0	0	0	0	Y	
225	L	4	0	0	0	0	0	0	0	Y	

**Table A- 9. Continued.**

Case ID #	Rib Side <sup>a</sup>	Rib # <sup>b</sup>	Rib Vasc. <sup>cd</sup>	Rib Mineralization <sup>d</sup>	Rib Volume <sup>d</sup>	Rib Formation <sup>d</sup>	Rib Resorption <sup>d</sup>	Rib Native Mineralization <sup>d</sup>	Rib Native Collagen <sup>d</sup>	Rib Normal? <sup>e</sup>	Rib Notes
226	L	6	0	0	0	0	1	0	0	Y	
227	L	4	0	0	0	0	0	0	0	Y	
228	R	9	0	0	0	0	0	0	0	Y	
229	L	7	0	0	0	0	0	0	0	Y	

a. Side of body: L = left, R = right  
 b. Rib number in series of 1 – 12  
 c. Rib Vasculature  
 d. Qualitative evaluation score: 0 = normal, 1 = Indeterminate, 2 = Abnormal  
 e. Rib classified normal: Y = yes, N = no

**Table A- 10. Results of Qualitative Histological Evaluation of the iliac crest section for each infant.**

Case ID #	Iliac Side <sup>a</sup>	Iliac Vasc. <sup>bc</sup>	Iliac Mineralization <sup>c</sup>	Iliac Volume <sup>c</sup>	Iliac Formation <sup>c</sup>	Iliac Resorption <sup>c</sup>	Iliac Native Mineralization <sup>c</sup>	Iliac Native Collagen <sup>c</sup>	Iliac Normal? <sup>d</sup>	Iliac Notes
152	L	0	0	0	0	0	0	0	Y	
153	L	0	0	0	0	1	0	0	Y	rib and iliac crest do not match biology
154	L	1	1	0	2	2	0	0	Y	? Normal growth
155	L	0	1	0	1	2	0	0	Y	current resorption out of balance with formation
156	L	1	0	1	0	1	0	0	Y	increased subperiosteal resorption
157	L	0	0	0	0	1	0	0	Y	
158	L	0	0	1	0	0	0	0	Y	too much periosteum
159	L	0	0	0	1	1	0	0	Y	
160	L	0	0	0	0	1	0	0	Y	
161	L	0	0	0	0	0	0	0	Y	
162	L	1	0	0	0	1	0	0	Y	
163	L	0	0	0	0	1	0	0	Y	
164	L	0	0	0	0	0	0	0	Y	
165	L	0	0	0	0	2	0	0	Y	increased resorption
166	L	1	1	0	1	2	0	0	Y	
167	L	1	0	0	1	2	0	0	Y	periosteum too big
168	L	1	2	1	1	2	0	0	Y	? Normal growth
169	L	2	1	1	2	1	0	0	Y	too much periosteum
170	L	0	0	0	0	1	0	0	Y	
171	L	1	0	1	1	1	0	0	Y	
172	L	1	0	0	0	1	0	0	Y	
173	L	1	0	2	0	1	0	1	Y	low bone volume
174	L	0	0	0	0	1	0	0	Y	
175	L	0	0	1	1	2	0	0	Y	
176	L	0	0	0	0	0	0	0	Y	
177	L	0	0	0	0	1	0	0	Y	
178	L	0	0	0	0	0	0	0	Y	mismatch in rib and iliac crest biology
179	L	1	0	0	0	1	0	0	Y	
180	R	0	0	0	0	0	0	0	Y	
181	L	0	0	0	0	1	0	0	Y	mismatch in rib and iliac crest biology
182	L	1	0	0	0	1	0	0	Y	
183	L	0	0	0	1	2	0	0	Y	
184	L	2	1	0	1	2	0	2	N	trabeculae are deformed

**Table A- 10. Continued**

Case ID #	Iliac Side <sup>a</sup>	Iliac Vasc. <sup>bc</sup>	Iliac Mineralization <sup>c</sup>	Iliac Volume <sup>c</sup>	Iliac Formation <sup>c</sup>	Iliac Resorption <sup>c</sup>	Iliac Native Mineralization <sup>c</sup>	Iliac Native Collagen <sup>c</sup>	Iliac Normal? <sup>d</sup>	Iliac Notes
185	R	2	0	0	2	1	0	0	Y	Increased cortical vessels and periosteal new bone
186	L	0	0	0	0	0	0	0	Y	
187	L	1	0	0	1	1	0	0	Y	
188	L	0	0	0	0	0	0	0	Y	
189	L	0	0	0	0	1	0	0	Y	
190	L	1	0	0	0	2	0	0	Y	extensive resorption noted
191	L	0	0	0	0	0	0	0	Y	
192	L	0	0	1	0	1	0	0	Y	thinned bone and increased resorption
193	L	0	0	0	0	2	0	0	Y	increased subperiosteal resorption and loss of trabecular integrity
194	L	0	0	0	0	1	0	0	Y	relatively normal with mild remodeling
195	L	0	0	0	0	0	0	0	Y	relatively normal
196	L	0	0	0	0	0	0	0	Y	relatively normal
197	L	0	0	0	0	0	0	0	Y	relatively normal
198	L	1	0	0	0	2	0	0	Y	increased subperiosteal resorption
199	L	0	0	0	0	0	0	0	Y	relatively normal
200	L	0	0	0	0	0	0	0	Y	relatively normal
201	L	0	0	2	2	0	0	0	Y	there is extensive new formation and resorption along one cortex
202	L	2	0	2	1	2	0	0	Y	significant cortical loss, hemorrhage, and inflammation
203	L	0	0	0	0	2	0	0	Y	increased subperiosteal resorption
204	L	0	0	0	0	0	0	0	Y	relatively normal
205	L	0	0	0	0	1	0	0	Y	relatively normal
206	L	2	0	0	0	1	0	0	Y	increased subperiosteal vascularization
207	L	1	2	2	0	1	0	2	N	problems with growth plate and primary spongiosa
208	L	0	0	0	0	0	0	0	Y	relatively normal

**Table A- 10. Continued.**

Case ID #	Iliac Side <sup>a</sup>	Iliac Vasc. <sup>bc</sup>	Iliac Mineralization <sup>c</sup>	Iliac Volume <sup>c</sup>	Iliac Formation <sup>c</sup>	Iliac Resorption <sup>c</sup>	Iliac Native Mineralization <sup>c</sup>	Iliac Native Collagen <sup>c</sup>	Iliac Normal? <sup>d</sup>	Iliac Notes
209	L	0	0	0	0	0	0	0	Y	relatively normal
210	L	0	0	0	0	0	0	0	Y	relatively normal
211	L	1	0	2	2	0	0	0	Y	this is new bone formation near one of the cortices and it is unclear why
212	L	0	0	1	0	2	0	0	Y	extensive resorption along the subperiosteal space
213	L	0	0	1	0	2	0	0	Y	extensive resorption
214	L	0	0	1	0	1	1	0	Y	mild bone loss
215	L	0	1	2	1	1	1	0	Y	low bone and disorganization ...etiology unclear
216	L	0	0	0	0	1	0	0	Y	mildly increased remodeling subperiosteally
217	L	0	0	0	0	0	0	0	Y	
218	L	0	0	0	0	0	0	0	Y	
219	L	0	0	0	0	1	0	0	Y	
220	L	0	0	0	0	0	0	0	Y	
221	L	0	0	0	0	0	0	0	Y	
222	L	0	0	0	0	0	0	0	Y	
223	L	0	0	0	0	0	0	0	Y	
224	L	0	0	0	0	0	0	0	Y	
225	L	0	0	0	0	0	0	0	Y	
226	L	0	0	0	0	0	0	0	Y	
227	L	0	0	0	0	0	0	0	Y	
228	L	0	0	0	0	0	0	0	Y	
229	L	0	0	0	0	0	0	0	Y	

a. Side of body: L = left, R = right  
b. Iliac Vasculature  
c. Qualitative evaluation score: 0 = normal, 1 = Indeterminate, 2 = Abnormal  
d. Iliac classified normal: Y = yes, N = no



**Table A- 11. Body size, growth percentiles, and tibia measurements for each infant.**

Case ID #	Body Size Measurements			Growth Percentiles			Tibia Measurements				
	Leg Circumference (mm)	Height (cm)	Weight (kg)	Length for Age	Weight for Age	Weight for Length	Tibia Length (mm)	Midshaft Diameter (mm)	Medullary Cavity Diameter (mm)	Total Cortical Thickness <sup>a</sup> (mm)	Cortical Index <sup>b</sup>
152	144	65.00	7.30	96.4	89.1	52.4	81.028	8.136	3.602	4.534	.557
153	169	62.00	8.84	79.4	99.9	100.0	80.104	8.165	4.354	3.811	.467
154	166	66.50	7.20	98.5	83.0	24.2	90.527	7.396	3.360	4.036	.546
155	150	72.00	8.84	32.4	51.6	63.3	98.256	7.607	4.264	3.343	.439
156	156	60.96	5.07	74.6	17.6	1.7	79.074	5.781	3.021	2.760	.477
157	143	63.50	5.90	0.3	0.3	6.9	88.693	7.391	3.501	3.890	.526
158	127	60.96	4.99	69.9	10.4	1.0	82.300	7.630	3.926	3.704	.485
159	129	54.00	4.08	4.5	2.8	29.1	67.528	5.421	2.892	2.529	.467
160	110	62.00	3.96	96.9	3.3	0.0	74.229	6.319	2.572	3.747	.593
161	82	52.00	2.67	37.5	2.4	0.0	63.652	5.884	2.293	3.591	.610
162	166	60.50	6.69	3.7	33.3	87.7	83.232	7.238	3.395	3.843	.531
163	135	54.61	4.53	3.9	6.8	57.9	69.711	5.803	3.321	2.482	.428
164	154	68.58	6.35	38.0	0.7	0.1	95.571	8.059	2.915	5.144	.638
165	167	77.00	8.91	86.4	31.7	9.9	116.558	9.156	3.967	5.189	.567
166	164	66.04	7.80	11.1	32.2	67.5	94.804	7.547	3.268	4.279	.567
167	144	63.50	6.31	39.8	22.9	23.6	86.883	6.559	3.627	2.932	.447
168	147	63.50	5.92	74.7	26.1	7.5	87.087	6.698	3.060	3.638	.543
169	138	60.96	5.73	70.2	42.8	14.3	76.590	7.522	3.486	4.036	.537
170	113	55.00	4.00	44.5	16.3	6.3	67.196	5.682	2.795	2.887	.508
171	160	66.00	8.46	24.5	77.0	94.1	94.319	8.163	5.362	2.801	.343
172	116	48.00	3.85	0.0	0.0	99.7	65.430	6.012	3.080	2.932	.488
173	120	51.50	3.72	0.0	0.0	55.2	71.781	6.275	3.253	3.022	.482
174	158	62.00	6.40	1.6	8.0	51.6	90.065	5.870	3.356	2.514	.428
175	179	69.50	9.31	84.7	94.1	91.3	96.879	9.654	4.394	5.260	.545
176	134	59.00	5.37	15.4	9.8	23.3	80.574	6.994	2.843	4.151	.594
177	145	71.30	10.00	96.9	98.8	94.8	92.452	7.991	4.272	3.719	.465
178	135	52.00	4.77	0.0	0.0	99.5	62.112	7.487	3.091	4.396	.587
179	113	57.00	4.00	68.6	17.4	0.3	66.635	6.332	2.467	3.865	.610
180	155	63.00	6.74	70.5	68.6	58.3	91.152	7.082	3.283	3.799	.536
181	190	78.00	10.10	98.1	81.7	50.8	115.962	7.553	3.984	3.569	.473
182	173	76.20	10.90	85.0	95.2	94.8	111.842	10.451	5.607	4.844	.463
183	161	73.66	9.07	29.2	33.8	41.9	118.208	9.340	4.750	4.590	.491
184	135	57.00	5.71	0.8	11.4	89.4	85.228	6.758	2.116	4.642	.687
185		48.50	3.38	0.0	0.1	85.8					
186	144	57.00	5.36	32.1	44.7	69.8	74.515	7.169	3.045	4.124	.575
187	169	66.04	7.98	3.9	38.6	82.5	101.502	7.573	3.851	3.722	.491

**Table A- 11. Continued**

Case ID #	Body Size Measurements			Growth Percentiles			Tibia Measurements				
	Leg Circumference (mm)	Height (cm)	Weight (kg)	Length for Age	Weight for Age	Weight for Length	Tibia Length (mm)	Midshaft Diameter (mm)	Medullary Cavity Diameter (mm)	Total Cortical Thickness <sup>a</sup> (mm)	Cortical Index <sup>b</sup>
188	132	54.00	4.55	12.5	21.7	76.7	69.047	6.205	2.784	3.421	.551
189	124	54.00	4.29	3.9	5.3	50.4	76.418	8.225	2.959	5.266	.640
190	152	61.00	5.78	7.3	6.5	25.8	84.278	6.686	3.566	3.120	.467
191	175	68.58	8.48	34.2	63.9	79.2	95.253	6.593	3.874	2.719	.412
192	118	57.50	3.88	78.8	16.0	0.0	73.036	6.712	2.322	4.390	.654
193	157	61.00	7.05	2.5	38.1	91.9	91.839	8.526	3.640	4.886	.573
194	170	62.00	8.00	49.4	96.2	99.1	89.743	8.071	3.650	4.421	.548
195	160	61.00	6.79	11.3	42.2	83.1	83.105	7.952	4.759	3.193	.402
196	146	66.68	6.79	17.6	9.0	14.7	89.553	6.881	3.746	3.135	.456
197	190	71.12	13.60	89.5	100.0	100.0	100.121	8.296	4.191	4.105	.495
198	134	64.00	6.50	91.1	61.1	16.9	83.117	7.090	2.646	4.444	.627
199	155	55.88	5.44	23.9	61.2	91.5	74.297	6.057	2.846	3.211	.530
200	150	61.00	5.66	29.2	14.7	18.9	75.183	7.108	3.782	3.326	.468
201	131	53.34	4.20	3.2	6.2	58.4	74.422	7.225	2.917	4.308	.596
202	106	55.50	3.96	100.0	93.2	2.9	63.482	5.439	1.516	3.923	.721
203	147	65.50	5.99	66.3	10.4	1.9	82.554	6.989	2.718	4.271	.611
204	125	60.50	4.59	3.8	0.2	0.1	82.871	6.563	3.357	3.206	.488
205	101	58.00	4.18	0.0	0.0	0.1	88.993	6.474	3.744	2.730	.422
206	161	66.04	8.85	52.0	93.1	97.3	88.440	7.531	4.503	3.028	.402
207	141	66.00	6.80	43.5	15.7	11.1	97.116	8.799	5.656	3.143	.357
208	101	42.00	2.53	0.0	0.0		59.000	4.486	2.011	2.475	.552
209	176	76.20	10.90	92.6	96.7	94.8	114.824	11.210	4.522	6.688	.597
210	177	64.00	8.70	0.0	28.0	99.4	102.579	9.101	3.392	5.709	.627
211	110	49.00	3.56	0.0	0.5	91.9	55.253	4.680	1.902	2.778	.594
212	156	60.00	6.90	0.2	19.3	95.1	75.380	6.822	3.579	3.243	.475
213	143	59.00	6.64	18.8	67.8	96.1	83.523	6.016	3.465	2.551	.424
214	165	76.00	9.16	99.7	78.2	24.2	105.704	10.049	4.986	5.063	.504
215	106	63.50	5.21	47.7	1.0	0.0	90.376	7.348	4.281	3.067	.417
216	173	72.00	9.08	39.7	51.8	61.0	103.035	8.999	4.499	4.500	.500
217	159	62.00	6.25	74.6	61.9	41.3	69.822	7.008	2.650	4.358	.622
218	175	51.50	6.13	11.2	98.6	100.0	52.778	4.095	1.492	2.603	.636
219	190	76.00	11.00	67.1	91.2	93.1	117.431	11.304	5.471	5.833	.516
220	177	66.00	7.90	97.2	96.1	80.0	84.964	7.673	2.901	4.772	.622
221	120	51.00	3.70	2.6	7.7	69.1	65.896	5.470	2.677	2.793	.511
222	109	42.50	3.06	0.0	0.9		50.111	5.463	2.786	2.677	.490
223	142	57.00	5.31	20.9	31.3	65.9	83.469	7.529	2.784	4.745	.630

**Table A- 11. Continued**

Case ID #	Body Size Measurements			Growth Percentiles			Tibia Measurements				
	Leg Circumference (mm)	Height (cm)	Weight (kg)	Length for Age	Weight for Age	Weight for Length	Tibia Length (mm)	Midshaft Diameter (mm)	Medullary Cavity Diameter (mm)	Total Cortical Thickness <sup>a</sup> (mm)	Cortical Index <sup>b</sup>
224	156	69.00	8.00	93.8	89.6	52.4	96.757	7.286	4.174	3.112	.427
225	99	50.00	2.66	35.4	4.4	0.4	61.905	4.990	1.473	3.517	.705
226	132	59.00	5.89	25.5	42.5	69.8	81.127	7.066	1.992	5.074	.718
227	146	55.88	6.76	88.3	100.0	100.0	66.573	5.377	1.892	3.485	.648
228	147	56.00	6.80				82.512	8.121	3.344	4.777	.588
229	113	54.00	3.87	42.3	20.9	12.5	68.059	6.490	2.736	3.754	.578

a. Total cortical thickness at midshaft  
b. Cortical Index = Total cortical thickness/ midshaft diameter

**Table A- 12. SOS and BMD measurements for each infants.**

Case ID #	Quantitative Ultrasound				Radiographic Absorptiometry	
	SOS <sup>a</sup> 1 (m/s)	SOS <sup>a</sup> 2 (m/s)	SOS <sup>a</sup> 3 (m/s)	Avg. SOS <sup>a</sup> (m/s)	Tibia BMD (g/cm <sup>2</sup> )	Radius BMD (g/cm <sup>2</sup> )
152	2851	2534	2679	2688	0.41786	
153	3184	3241	3249	3224.67	0.46701	
154	3077	3112	3126	3105	0.66124	0.28368
155	3524	3509	3508	3513.67		
156	3184	3176	3180	3180	1.3197	0.57633
157	3135	3231	3272	3212.67	0.83905	
158	2824	2841	2827	2830.67	1.1487	0.60934
159	2761	2794	2848	2801	0.5506	0.28394
160	3170	3089	3038	3099	0.66878	0.32536
161	2860	2835	2835	2843.33	1.1432	
162	3067	3180	3097	3114.67	0.69363	0.40636
163	2718	2867	2816	2800.33		
164	3360	3364	3363	3362.33	0.63448	0.29715
165	3342	3329	3322	3331	0.84716	0.44895
166	3074	3056	2958	3029.33	0.86517	0.35268
167	2890	2931	2949	2923.33	0.43649	0.28055
168	2730	2747	2750	2742.33	1.0264	0.52945
169	2928	2952	2950	2943.33	0.87218	0.26217
170	2696	2621	2682	2666.33	0.76629	0.3583
171	2983	3002	3088	3024.33		
172	2741	2767	2713	2740.33	0.78603	0.56035
173	2667	2678	2650	2665	1.0126	0.3621
174	2918	2958	2944	2940	0.50731	0.29014
175	2873	2893	2879	2881.67	0.59804	0.40222
176	2879	2846	3017	2914	0.71679	0.2811
177	3161	3169	3190	3173.33	0.92445	0.33676
178	2622	2574	2589	2595	0.48637	0.27195
179	2922	2864	2848	2878	1.3102	0.57633
180	3062	2958		3010	1.169	0.40537
181	3108	3195	3278	3193.67	0.62066	0.47806
182	3142	3100	3134	3125.33		0.50421
183	3111	3114	3094	3106.33	1.1795	0.35257
184	2973	3013	3015	3000.33	1.2561	0.82565
185						
186	2864	2778	2784	2808.67	0.90007	0.32423
187	3271	3295	3295	3287	0.78767	0.60731
188	3014	3062	3051	3042.33	1.1853	0.23335
189	2516	2562	2497	2525	1.3707	0.58785
190	2868	2886	2880	2878	1.0315	
191	3206	3233	3217	3218.67	0.40879	
192	2863	2891	2858	2870.67		0.23236
193	2981	2955	2883	2939.67	0.45695	1.4788
194	2842	2822	2816	2826.67	1.4945	
195	2962	2813	2834	2869.67	1.0677	0.50586
196	3360	3345	3328	3344.33	0.7193	0.36148
197	3104	3051	3106	3087	0.88199	0.25178
198	3166	3164	3169	3166.33	1.4595	0.39916
199	2930	2846	2945	2907	1.3101	0.83212
200	2992	3011	3020	3007.67	1.2092	0.65703
201	2433	2463	2461	2452.33	1.0381	0.51429

**Table A- 12. Continued.**

Case ID #	Quantitative Ultrasound				Radiographic Absorptiometry	
	SOS <sup>a</sup> 1 (m/s)	SOS <sup>a</sup> 2 (m/s)	SOS <sup>a</sup> 3 (m/s)	Avg. SOS <sup>a</sup> (m/s)	Tibia BMD (g/cm <sup>2</sup> )	Radius BMD (g/cm <sup>2</sup> )
202	3572	3472	3478	3507.33	1.0133	0.68064
203	2845	2884	2915	2881.33	1.2201	0.51007
204	3156	3195	3215	3188.67	1.2606	0.33227
205	2911	2899	2911	2907	0.93144	0.60989
206	3104	2961	3040	3035	1.0784	0.30774
207	3027	3018	3036	3027	1.1138	0.39144
208	2751	2721	2724	2732	0.63602	0.23529
209	3387	3365	3377	3376.33	0.45361	
210	3284	3264	3283	3277	0.47127	
211	2834	2924	2996	2918		
212	2761	2914	2792	2822.33	0.44535	
213	2996	2963	2953	2970.67	0.53267	
214	3088	3084	3094	3088.67	0.68128	
215	3151	3140	3173	3154.67	0.62527	
216	3194	3245	3281	3240	0.8057	
217	3019	2955	2931	2968.33	0.70265	
218	3406	3270	3246	3307.33		
219	3161	3070	3141	3124	1.2782	
220	3150	3142	3143	3145	0.87401	
221	2985	3094	3114	3064.33	0.46738	
222	2822	2822	2822	2822	0.58747	
223	3006	2984	2954	2981.33	0.61827	
224	2696	2979	3022	2899	0.71026	
225	3178	3169	3143	3163.33	0.81694	
226	3009	2937	3020	2988.67	1.3421	
227	3083	3095	3055	3077.67	1.682	
228	3090	3006	3062	3052.67	1.0621	0.73991
229	3132	3134	3131	3132.33	1.6129	0.6818

a. a. SOS = Speed of Sound

## VITA

Miriam Elizabeth Soto Martinez was born in Houston, TX to parents Rita and Natividad Soto, Jr. She received a B.S. in Anthropology with a minor in biology from the University of Houston in 2004. She attended the University of Tennessee, Knoxville to further her education in biological anthropology and pursue a career in forensic anthropology. Miriam received her M.A. in Biological Anthropology from the University of Tennessee, Knoxville in 2008 and was the first in her family to earn an advanced degree. She continued her graduate education and received her Ph.D. in Biological Anthropology in 2015. During her time in graduate school, Miriam was a graduate teaching assistant in introductory biology and osteology. She was also a research assistant for Dr. Nicholas Herrmann and Dr. Jennifer Love. She is currently employed by the Harris County Institute of Forensic Sciences as a post-doctoral forensic anthropology research fellow.